Percolation, statistical topography, and transport in random media

M. B. Isichenko

Institute for Fusion Studies, The University of Texas at Austin, Austin, Texas 78712
and Kurchatov Institute of Atomic Energy, 123182 Moscow, Russia

A review of classical percolation theory is presented, with an emphasis on novel applications to statistical topography, turbulent diffusion, and heterogeneous media. Statistical topography involves the geometrical properties of the isosets (contour lines or surfaces) of a random potential $\psi(\mathbf{x})$. For rapidly decaying correlations of ψ, the isopotentials fall into the same universality class as the perimeters of percolation clusters. The topography of long-range correlated potentials involves many length scales and is associated either with the correlated percolation problem or with Mandelbrot's fractional Brownian reliefs. In all cases, the concept of fractal dimension is particularly fruitful in characterizing the geometry of random fields. The physical applications of statistical topography include diffusion in random velocity fields, heat and particle transport in turbulent plasmas, quantum Hall effect, magnetoresistance in inhomogeneous conductors with the classical Hall effect, and many others where random isopotentials are relevant. A geometrical approach to studying transport in random media, which captures essential qualitative features of the described phenomena, is advocated.

CONTENTS

I. INTRODUCTION

A. General

The percolation problem describes the simplest possible phase transition with nontrivial critical behavior. The pure geometrical nature of this transition and its compelling application to diverse physical problems have drawn the attention of many researchers, and the percolation theory is well reviewed (Shante and Kirkpatrick, 1971; Essam, 1972; Kirkpatrick, 1973; Stauffer, 1979; Essam, 1980; Kesten, 1982; Deutscher *et al.*, 1983; Zallen, 1983; Shklovskii and Efros, 1984; Stauffer, 1985; Sokolov, 1986). The general formulation of the percolation problem is concerned with elementary geometrical objects (spheres, sticks, sites, bonds, etc.) placed at random in a d-dimensional lattice or continuum. The objects have a well-defined connectivity radius λ_0, and two objects are said to communicate if the distance between them is less than λ_0. One is interested in how many objects can form a cluster of communication and, especially, when and how the clusters become infinite. The control parameter is evidently the density n_0 of the objects (their average number per unit volume), or the dimensionless filling factor $\eta = n_0 \lambda_0^d$. The *percolation threshold*, $\eta = \eta_c$, corresponds to the minimum concentration at which an *infinite cluster* spans the space. Thus the percolation model exhibits two essential features: critical behavior and long-range correlations near the critical value of the

control parameter η.

This model is relevant for a number of transport problems in disordered media exhibiting critical behavior, such as electron localization (Anderson, 1958; Ziman, 1969) and hopping conduction in amorphous solids (Zallen, 1983; Shklovskii and Efros, 1984). Other applications of percolation theory may concern the spreading of disease in a garden or, say, the critical concentration of bribe takers to impede the normal functioning of a government.

Not only critical phenomena can be associated with the percolation model. Consider, for example, the diffusion of a passive tracer in a two-dimensional, steady, incompressible random flow

$$\mathbf{v}(x,y)=\nabla\psi(x,y)\times\hat{\mathbf{z}}\ , \tag{1.1}$$

where $\psi(x,y)$ is a random stream function. The streamlines of this flow are the contours of ψ. The geometry of the streamlines is associated with the geometry of percolation clusters as follows. Let us call "objects" the regions where $\psi(x,y)$ is less than a specified constant level h. If $z=\psi(x,y)$ is imagined to be the elevation of a random landscape and h designates the level of flooding, then the objects are the lakes. Two neighboring lakes "communicate" if they merge into a bigger lake, which is a "cluster." So the contours $\psi(x,y)=h$ present the coastlines of the lakes, that is, the envelopes of the clusters. The control parameter of this percolation problem is the level h such that at some critical level, $h=h_c$, the lakes form an infinite ocean and among the contours $\psi(x,y)=h_c$ there is at least one infinitely long.

Flow (1.1), however, includes streamlines lying at all levels, and its transport properties show no critical behavior in the only relevant control parameter (Péclet number)

$$P=\frac{\psi_0}{D_0}\ , \tag{1.2}$$

which is the ratio of the root-mean-square stream function ψ_0 and the molecular diffusivity D_0 of the tracer. Nevertheless, if the Péclet number is large, $P\gg1$, the transport shows long correlation because the tracer particles advected along very large streamlines diffuse very slowly from these lines to more typical short closed lines and hence provide a significant *coherent* contribution to the turbulent diffusivity D^*. The larger the Péclet number, the longer and narrower the bundles of streamlines that dominate the effective transport in the considered flow. Under certain constraints, the effective diffusivity scales as (Isichenko *et al.*, 1989)

$$D^*\simeq D_0P^{10/13},\quad P\gg1\ , \tag{1.3}$$

where the exponent 10/13 is expressible in terms of the critical exponents of two-dimensional percolation theory (Sec. IV.A.3).

The effective diffusion in a random flow presents an example of a long-range correlated phenomenon without critical behavior. The critical exponents of the percolation transition enter the result because the large value of the control parameter ($P\gg1$) picks up a near-critical (in the sense of the contour percolation) set of streamlines dominating the effective transport. Unlike the transport processes occurring *on* the percolation clusters (Aharony, 1984; Orbach, 1984; Rammal, 1984; O'Shaughnessy and Procaccia, 1985a, 1985b; Hans and Kehr, 1987; Harris, 1987; Havlin and Ben-Avraham, 1987), the motion along incompressible streamlines represents transport *around* the percolation clusters.

The appearance of formula (1.3) leaves little hope for its derivation using a regular perturbation-theory method in solving the advection-diffusion equation

$$\frac{\partial n}{\partial t}+\mathbf{v}\cdot\nabla n=D_0\nabla^2n \tag{1.4}$$

for the tracer density n. Instead, geometrical arguments can be used to reduce the advective-diffusive problem to the problem of random contours, whose critical behavior is not amenable to any kind of a perturbation analysis but is well described in terms of percolation theory.

The problem of critical phenomena (cf. Domb *et al.* 1972–1988) is among the most difficult in nonlinear physics. This is well manifested by the fact that several decades separate the Boltzmann-Gibbs statistical mechanics and the first solution of the Ising model by Onsager (1944). After Wilson (1971a, 1971b, 1975) introduced the renormalization-group technique to the theory of phase transitions, the number of solvable critical models rapidly increased (Ma, 1976; Baxter, 1982). Some of the analytical results on percolation criticality were obtained relatively recently (den Nijs, 1979; Saleur and Duplantier, 1987).

The value of the available results on critical behaviors is grossly increased by the *universality of critical exponents* describing the behavior of the order parameter and of other physical quantities near the critical point (Sec. II.C). Universality implies that the set of critical exponents is structurally stable—that is, it does not change under a small perturbation of the model itself, provided that the perturbation does not introduce long correlations that decay slower than certain algebraic functions. This universality leads to the possibility of new applications of critical phenomena theory that might go far beyond the phase-transition problems in statistical physics.

There exists a class of problems of transport in random and disordered media that can be reduced to the statistical properties of contours (isolines or isosurfaces) of random potentials. The geometrical properties of random isosets are studied in the framework of *statistical topography* (Ziman, 1979; Isichenko and Kalda, 1991b). In the simplest case of a potential characterized by a single scale of length and a rapidly decaying correlation function, the statistical topography problem can be mapped onto the standard percolation problem, where the random contours are associated with percolation perimeters (Secs. II.E and III.C). In two dimensions the basic percolation

exponents are known exactly (Sec. II.A), thereby presenting all necessary characteristics of the long-range contour behavior. For the case of algebraic behavior in the random potential correlator, the topography involves essentially many length scales, but still can be studied using the formalism of *fractional Brownian functions* (Sec. III.B), the long-range correlated percolation problem (Sec. II.D), or a renormalization-group-style technique of the *separation of scales* (Sec. III.E) built on the knowledge of the monoscale percolation exponents.

The paper concentrates on various physical applications of percolation theory and statistical topography, such as the quantized Hall conductance (Secs. III.D and III.E.4) and the processes of transport in classical random media, including advection-diffusion transport (Sec. IV.A) or inhomogeneous conductors (Sec. IV.B). The flows discussed in the context of advection-diffusion are not necessarily of hydrodynamic origin. The focus of Secs. IV.A.4 and IV.A.5 is primarily on transport in turbulent plasmas, including the diffusion of stochastic magnetic-field lines and charged particles, whereas Sec. IV.B.3.b deals with an electrostatic potential advected by abstract (nonphysical) flows, a problem arising when the effective conductivity of inhomogeneous media (polycrystals, for example) in a strong magnetic field is calculated.

The outline of the paper is presented by the table of contents, and so is not repeated here. Two remarks regarding the organization of the review are in order, however. Section I.B serves as a terse introduction to the fractal geometry that is heavily used throughout the paper. Those readers who are familiar with fractals may wish to skip this discussion. It is included here, since in certain quarters—for example, in the plasma physics community—fractals are, regrettably, scarcely used and the necessity to refer to the original texts would make this paper difficult to read. Secondly, it should be noted that Sec. II adds to the existing excellent reviews of percolation theory (Stauffer, 1979; Essam, 1980; Deutscher *et al.*, 1983; Zallen, 1983; Shklovskii and Efros, 1984; Stauffer, 1985) only a moderate amount of new discussion regarding the problems of correlated percolation (Sec. II.D) and continuum percolation (Sec. II.E). Readers familiar with percolation theory may wish to begin with Sec. III.

B. Fractals

An essentially geometrical approach to studying transport processes requires a concise characterization of random fields. The fractal dimension serves such a purpose. Introduced originally by Hausdorff (1918) and Besicovitch (1929), the concept of fractional, or generalized, dimension was first used in fairly abstract mathematical studies on number theory (Besicovitch, 1935a, 1935b; Good, 1941). The fractal dimension was introduced in a physical context by Mandelbrot (1975a, 1977, 1982, 1983), whose works generated a widespread interest in fractal geometry (Pietronero and Tosatti, 1986; Paladin and Vulpiani, 1987; Feder, 1988; Peitgen and Saupe, 1988; Voss, 1989). Fractal dimensions were reported for numerous environmental data (Burrough, 1981) and even for space-time (Zeilinger and Svozil, 1985). The most sensible physical applications of fractals are concerned with fluid turbulence (Mandelbrot, 1975b; Procacia, 1984; Sreenivasan and Meneveau, 1986; Benzi *et al.*, 1991; Constantin *et al.*, 1991), chaotic attractors (Kaplan and Yorke, 1979; Mori, 1980; Farmer *et al.*, 1983; Grassberger and Procaccia, 1983), electron localization (Lévy and Souillard, 1987), and critical phenomena (Suzuki, 1983), including the transition to chaos in classical systems (Jensen *et al.*, 1985). Of course, there are many others (Mandelbrot, 1983; Feder, 1988; Falconer, 1990; Bunde and Havlin, 1991).

We begin our discussion of fractals with somewhat abstract mathematical definitions to be followed by more specific physical examples. The original Hausdorff-Besicovitch definition of the "dimensional number" D of a set of points F embedded in a d-dimensional space is as follows. Let F be covered by the "boxes" $U_1, U_2, \ldots$ (meaning $F \subset U_1 \cup U_2 \cup \ldots$) having the diameters (maximum linear size measured in the d space) $\lambda_1, \lambda_2, \ldots$, respectively. Denote by $U(F,\lambda)$ the set of all possible coverings of F with $\lambda_i \leq \lambda$. Then the "exterior s-dimensional measure" $M_s(F)$ is defined as

$$M_s(F) = \lim_{\lambda \to +0} \inf_{U(F,\lambda)} \sum_i \lambda_i^s \ . \tag{1.5}$$

Finally, if $M_s(F)=0$ for $s > D_H$, and $M_s(F)=\infty$ for $s < D_H$, then D_H is the "dimensional number," or the Hausdorff dimension, of F:

$$D_H = \inf\{s: M_s(F)=0\} = \sup\{s: M_s(F)=\infty\} \ . \tag{1.6}$$

Another definition of dimension, which is due to Kolmogorov (1958; see also Kolmogorov and Tikhomirov, 1959) and also known as *capacity*, is

$$D_K = -\lim_{\lambda \to +0} \frac{\log N_\lambda}{\log \lambda} \ , \tag{1.7}$$

where the *covering number* N_λ is the minimum number of d-dimensional hypercubes of side λ needed to cover the set F. Due to the presence of *infimum* in formula (1.5) over all possible coverings with variable box sizes, the Hausdorff dimension is generally not greater than the Kolmogorov capacity (Ruelle, 1989): $D_H \leq D_K$. The Hausdorff and Kolmogorov dimensions are usually equivalent, $D_H = D_K \equiv D$ (Young, 1982, 1984), except for somewhat pathological cases. An interesting example of an object with different Hausdorff and Kolmogorov dimensions is presented by the algebraic spiral $r(\phi) = \phi^{-\alpha}$, $\alpha > 0$, where r and ϕ are the polar radius and angle, respectively (Vassilicos and Hunt, 1991). Being clearly different from conventional fractals (and thereby motivating the term "K fractal" as opposed to standard "H fractals"), such a spiral still has the nontrivial Kolmogorov capacity,

$$D_K = \max\left[1, \frac{2}{1+\alpha}\right], \tag{1.8}$$

associated with a single accumulation point at the origin. However, for any $\epsilon > 0$, a variable-size covering (with the box sizes λ, depending algebraically on ϕ) can be found such that the sum of $\lambda_i^{1+\epsilon}$ tends to zero as $\lambda \to 0$. That is, the Hausdorff dimension of the spiral is unity: $D_H = 1$. The pathology of this example extends to the violation of cross-section rule (1.15).

For "well-behaved" sets, both the Hausdorff dimension D_H and the capacity D_K are equal to the topological dimension E, which is an integer, such as $E = 0$ (a set of isolated points), $E = 1$ (a curve), $E = 2$ (a surface), and $E = 3$ (a region of finite volume). It is believed (Vassilicos and Hunt, 1991), though not proved in general, that whenever $D_H > E$, the Hausdorff and the Kolmogorov dimensions are the same, $D_H = D_K = D$. The generalized dimension D of a set F satisfies the evident inequalities $E(F) \le D(F) \le d$ and $D(F') \le D(F)$, if $F' \subset F$, and can in principle take on arbitrary fractional (and even irrational) value, such as $\log 8/\log 3 = 1.893\ldots$ for the Sierpinski carpet shown in Fig. 1. Mandelbrot (1982) proposed the term *fractals* for the sets whose dimensional number D is greater than the topological dimension E. For this case, Mandelbrot coined the term *fractal dimension* for D. The rigorous theory of fractal sets can be found in the books of Falconer (1985, 1990). In what follows, we restrict ourselves to a more qualitative discussion.

The most appealing property of fractals is their self-similarity, or scaling, meaning that some parts of a whole are similar, after rescaling, to the whole. For example, the upper-left square comprising one-ninth the area of the Sierpinski carpet (Fig. 1) can be magnified 3 times to reproduce the original carpet. This is an example of exact self-similarity. Exactly self-similar structures can be of two distinct kinds: the ones with global self-similarity (like the Sierpinski carpet) and locally self-similar sets,

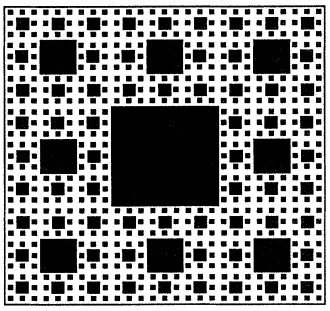

FIG. 1. Sierpinski carpet produced by removing from a square its central part with the size one-third the square edge. Then the procedure is repeated with each of the eight remaining parts, and so on *ad infinitum*. At the nth step of the procedure, it takes $N_n = 8^n$ squares of the size $\lambda_n = 3^{-n}$ to cover the remaining set, leading to the fractal dimension $D = -\log N_n / \log \lambda_n = \log_3 8$.

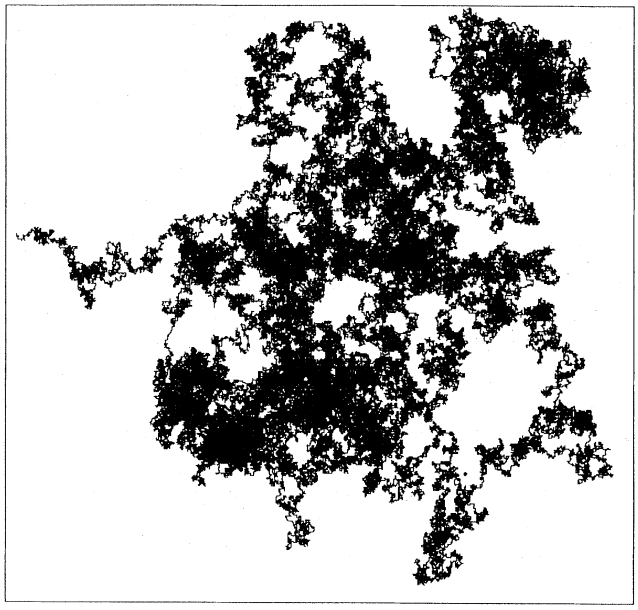

FIG. 2. Computer-generated trail of a Brownian particle. At any resolution of the trajectory, it asymptotically covers a finite area on the plane, because the fractal dimension $D = 2$.

whose accumulation points are isolated. The algebraic spiral $r(\phi) = \phi^{-\alpha}$ (which is not a fractal in Mandelbrot's sense) is an example of local self-similarity with respect to only its center.

For fractals involving random element, one speaks about a statistical self-similarity, meaning equivalent, after the proper rescaling, statistical distributions characterizing the geometry of a part and of the whole fractal. Examples of random fractals are the trajectory of a particle pursuing Brownian motion ($E = 1, D = 2$; see Fig. 2) and the infinite cluster near the percolation threshold ($E = 1$ and $D = 91/48$ for $d = 2$ and $\simeq 2.50$ for $d = 3$).

It is important to note that virtually no physical object in real space qualifies for the formal definition of a fractal involving a nontrivial (i.e., $D > E$) Hausdorff-Besicovitch dimension (1.6), because each physical model has certain limits of applicability expressed in the length scales involved. Instead, *physical fractals* are defined as geometrical objects having sufficiently wide *scaling range* $[\lambda_{\min}, \lambda_{\max}]$ specifying the length scales of self-similar behavior. As soon as the ratio $\lambda_{\max}/\lambda_{\min}$ becomes *a large parameter*, one can spead about a fractal. Specifically, in the scaling range the covering number N_λ is proportional to λ^{-D}. If one restricts oneself to the region of the size $\lambda_{\max}$ (the upper limit of the scaling range), then the covering number $N_{\lambda_{\max}}$ is clearly 1; hence

$$N_\lambda \simeq \left[\frac{\lambda_{\max}}{\lambda}\right]^D, \quad \lambda_{\min} < \lambda < \lambda_{\max}. \tag{1.9}$$

Expression (1.9) replaces the more mathematical definition (1.7) of the fractal dimension D and is actually

used in the computation of D using box-counting algorithms (Feder, 1988). Furthermore, definition (1.9) generalizes the Hausdorff-Besicovitch-Kolmogorov definitions (which all correspond to the limiting case $\lambda_{\min}=0$) in that the fractal dimension can also characterize the long-scale behavior. For example, an infinite percolation cluster at the percolation threshold is statistically self-similar in the scaling range of $[\lambda_0, \infty]$, where λ_0 is the size of communicating objects (Kapitulnik *et al.*, 1984). In fact, a percolation cluster is one of the most popular models of a fractal. The long-range correlations in virtually all critical phenomena imply statistical self-similarity in a diverging scaling range, which makes fractal geometry quite a suitable language to describe the geometrical aspects of phase transitions (Gefen *et al.*, 1980; Suzuki, 1986).

In general, $\lambda_{\max}$ in (1.9) can be replaced by a smaller variable radius, $a \le \lambda_{\max}$, and, putting $\lambda=\lambda_{\min}$, we obtain the *radius-mass relation*

$$M(a) \simeq \left[\frac{a}{\lambda_{\min}}\right]^D, \quad a > \lambda_{\min} , \tag{1.10}$$

expressing the suitably normalized "mass" (for the number of points, curve length, or other natural measure) inside a circle of radius a whose center lies on the fractal.

Using formula (1.9), one can measure the fractal dimension of curves (topological dimension $E=1$) by a compass. Let λ be the compass step. Then the measured length is

$$L(\lambda)=\lambda N_\lambda \simeq \lambda \left[\frac{\lambda_{\max}}{\lambda}\right]^D \propto \lambda^{1-D} . \tag{1.11}$$

The observation that there is no "actual" length of a coastline, meaning that the result of measurement algebraically depends on the accuracy of λ, became one of the stimuli for introducing the concept of fractals (Mandelbrot, 1967, 1975b).

Normally, different measurements of the fractal dimension yield the same result. One, however, should be cautious when dealing with *self-affine* fractals, that is, with those reproducing themselves after rescalings that are different in different directions. Usually, the distance in such objects is measured in different directions by quantities of different physical dimensionality, such as time and length. For the fractal dimension to be meaningful, one has to switch to nondimensional variables, a procedure involving certain units of measure (seconds, centimeters, etc.). Hence the scaling range of self-affine fractals may depend on the units used. A pitfall is that, for self-affine fractals, the "box-counting dimension" [Eq. (1.9)] and the "compass dimension" [Eq. (1.11)] may be different (Mandelbrot, 1985). An example of a self-affine fractal is the graph $\{t, B_H(t)\}$ of a fractional Brownian function $B_H(t)$, whose definition and properties are discussed in Sec. III.B. While the box-counting (Hausdorff or Kolmogorov) dimension of the fractional Brownian graph equals $2-H (0<H<1)$, its compass dimension is surprisingly different and equals $1/H$ for $1/2<H<1$, due to the impact of the fractal anisotropy on the compass measuring (Mandelbrot, 1985).

In Table I we tabulate the fractal dimensions and scaling ranges of some geometrical objects discussed in this paper. Notice that the same objects can have different values of fractal dimension in different scaling ranges.

To calculate the fractal dimension of more complicated objects involving cross sections of fractals by a plane, a line, or the intersection of several fractals, a simple formula can be used. Consider two fractals, F_1 and F_2, with the fractal dimensions D_1 and D_2, respectively, in a d-dimensional cube with the edge a. According to Eq. (1.9), the covering number of F_i is $N_\lambda(F_i) \simeq (a/\lambda)^{D_i}$. If the cube is divided into boxes with size λ, then F_i will intersect the following fraction of boxes:

$$p_\lambda(F_i)=N_\lambda(F_i)\left[\frac{\lambda}{a}\right]^d \simeq \left[\frac{\lambda}{a}\right]^{d-D_i} . \tag{1.12}$$

Suppose that there is no specific correlation in the position of F_1 and F_2. Then we would find the fraction $p_\lambda(F)$ of λ foxes covering the intersection $F=F_1 \cap F_2$ as

$$p_\lambda(F)=p_\lambda(F_1)p_\lambda(F_2) \simeq \left[\frac{\lambda}{a}\right]^{2d-D_1-D_2} . \tag{1.13}$$

Comparing (1.13) with the relation $p_\lambda(F)=N_\lambda(F)(\lambda/a)^d \propto (\lambda/a)^{d-D}$, we find the fractal dimension of the intersection (Mandelbrot, 1984)

$$D=D_1+D_2-d . \tag{1.14}$$

A corollary of the intersection rule (1.14) concerns the cross sections of fractals by regular shapes. Let $D_2=E_2=d-1$ be the dimension of a plane in the space ($d=3$) or of a line in the plane ($d=2$). Then the fractal dimension of the cross section is 1 less than that of the fractal F_1:

$$D=D_1-1 . \tag{1.15}$$

A generalization of the intersection rule (1.14) for the case of N independent intersecting fractals reads

$$D=D_1+\cdots+D_N-(N-1)d . \tag{1.16}$$

Of course, formulas (1.14)–(1.16) are valid as long as $D>0$; otherwise, the intersection is essentially empty. Mandelbrot (1984) suggests to use negative D's as the measure of *how empty* the intersection is, meaning how fast the expected measure of the intersection vanishes as the lower limit $\lambda_{\min}$ of the scaling range approaches zero. The scaling range of the intersection of several fractals is the intersection of individual scaling ranges, unless one of the fractals is self-affine. For example, the self-affinity of the fractional Brownian graph ($D=2-H$) leads to an upper bound on its scaling range (see Table I) that depends on the units of measure. This bound can be lifted by taking a cross section: The fractional Brownian zero-

set ($D=1-H$) is a self-similar fractal in an unbounded scaling range.

For regular shapes (K fractals) such as the spiral $r(\phi)=\phi^{-\alpha}$, the argument of "no specific correlation" breaks down, leading to the violation of the cross-section rule (1.15): One can easily check that the Kolmogorov capacity of the spiral's linear cross section $\{x_n=(2\pi n)^{-\alpha},\ n=1,2,\ldots\}$ equals (Vassilicos and Hunt, 1991) $D_K'=1/(1+\alpha)$, differing from D_K-1, where D_K is determined by formula (1.8).

TABLE I. Fractal dimensions and scaling ranges of some geometrical sets.

Object	Fractal dimension	Scaling range	Section
Fractional Brownian hypersurface* $\{\mathbf{x},B_H(\mathbf{x})\}$ in a $(d+1)$ space, $\langle[B_H(\mathbf{x}_1)-B_H(\mathbf{x}_2)]^2\rangle^{1/2}=b\lvert\mathbf{x}_1-\mathbf{x}_2\rvert^H$, $0<H<1$	$d+1-H$ d	$[0,b^{1/(1-H)}]$ $[b^{1/(1-H)},\infty]$	III.B
Fractional Brownian trail $\{\mathbf{x}(t)=\mathbf{B}_H(t)\}$ in d dimensions	$\min(1/H,d)$	$[0,\infty]$	III.B
Zero-set of the fractional Brownian function: $\{\mathbf{x}: B_H(\mathbf{x})=0\}$	$d-H$	$[0,\infty]$	III.B
Connected piece of the above isoset with the diameter a	$\begin{cases}(10-3H)/7, & d=2\\ d-H, & d\geq 3\end{cases}$	$[0,a]$	III.E
Connected contour piece (diameter a) of a monoscale (λ_0) random potential $\psi(x,y)$	$\frac{7}{4}$	$[\lambda_0,a]$	III.C
Same for a multiscale potential $\psi_\lambda\propto\lambda^H$, $\lambda_0<\lambda<\lambda_m$, $-\frac{3}{4}<H<1$	$(10-3H)/7$ $\frac{7}{4}$	$[\lambda_0,\lambda_m]$ $[\lambda_m,a]$	III.E
Finite percolation cluster ($a\gg\lambda_0$) on a lattice with the period λ_0 in d dimensions	$d-\frac{\beta}{\nu}=\begin{cases}\frac{91}{48}, & d=2\\ \simeq 2.50, & d=3\end{cases}$	$[\lambda_0,a]$	II.A
Infinite cluster near the percolation threshold with the correlation length $\xi\gg\lambda_0$	$d-\beta/\nu$ d	$[\lambda_0,\xi]$ $[\xi,\infty]$	II.A
Backbone of an infinite cluster	$\simeq\begin{cases}1.6, & d=2\\ 1.7, & d=3\end{cases}$	$[\lambda_0,\xi]$	II.A
External hull of a finite percolation cluster	$\begin{cases}\frac{7}{4}, & d=2\\ d-\beta/\nu, & d\geq 3\end{cases}$	$[\lambda_0,a]$	II.A
Red bonds of an incipient ($\xi=\infty$) infinite cluster	$1/\nu$	$[\lambda_0,\infty]$	II.A
Infinite self-avoiding random walk (SAW) on a 2D lattice with the period λ_0	$\frac{4}{3}$	$[\lambda_0,\infty]$	II.A
Infinite smart kinetic walk (SKW) on the same lattice	$\frac{7}{4}$	$[\lambda_0,\infty]$	II.A
Correlated percolation cluster ($-1/\nu<H<0$) with the diameter a	$d+\beta H$	$[\lambda_0,a]$	II.D
External hull of a correlated percolation cluster ($-1/\nu<H<0$)	$\begin{cases}(10-3H/7, & d=2\\ d+\beta H, & d\geq 3\end{cases}$	$[\lambda_0,a]$	II.D
Chaotic attractor (size a) of a three-dimensional dynamical system with Lyapunov exponents $-\Lambda_3>\Lambda_1>\Lambda_2=0$	$2+\Lambda_1/\lvert\Lambda_3\rvert$	$[0,a]$	I.B, IV.B.2

*Self-affine fractal. The box-counting dimension is shown.

Among the most intensively studied fractal objects are chaotic, or "strange," attractors that present a generic invariant set for dissipative dynamical systems with the phase-space dimension $d \geq 3$ (Ott, 1981; Lichtenberg and Lieberman, 1983; Eckmann and Ruelle, 1985; Ruelle, 1989). The first example of such an attractor was studied by Lorenz (1963). The motion on the attractor is characterized by (a) the sensitivity to the initial conditions, that is, exponentially diverging neighboring orbits, and (b) exponentially shrinking phase-space volume. In terms of the characteristic Lyapunov exponents, $\Lambda_1 \geq \Lambda_2 \geq \cdots \geq \Lambda_d$, describing the eigenvalue growth rates of the edges of an infinitesimal phase-space hypercube, this means that $\Lambda_1 > 0$, whereas $\sum_{i=1}^{d} \Lambda_i < 0$. Kaplan and Yorke (1979) conjectured that the fractal dimension of a chaotic attractor be given by the simple formula

$$D = j + \sum_{i=1}^{j} \Lambda_i / |\Lambda_{j+1}| , \tag{1.17}$$

where j is the maximum integer for which $\sum_{i=1}^{j} \Lambda_i > 0$. Young (1982) showed that formula (1.17) is exact for $d = 3$. [The Mori (1980) formula for D coincides with (1.17) for $d = 3$, but is incorrect in higher dimensions.] Notice that one of the Lyapunov exponents of a continuous-time dynamical system is necessarily zero (in the direction of the phase-space flow unless the orbit terminates in a fixed point). This leads to further simplification of the Kaplan-Yorke formula for $d = 3$ ($\Lambda_1 > 0 = \Lambda_2 > \Lambda_3$; $|\Lambda_3| > \Lambda_1$):

$$D = 2 + \Lambda_1 / |\Lambda_3| . \tag{1.18}$$

Thus the fractal dimension of a chaotic attractor in a three-dimensional phase space lies between 2 and 3, because the chaotic behavior ($\Lambda_1 > 0$) of self-avoiding orbits is not possible on manifolds with dimension 2 or less. We shall encounter somewhat unusual application of strange attractors and the formula (1.18) to the problem of effective conductivity of polycrystals (Sec. IV.B.2.a).

The concept of fractal dimension describes only geometrical or static properties of self-similar objects. The characterization of dynamical properties of fractals, such as the fraction of time spent by a particle in a given subset of an attractor (Grassberger, 1983b), the relative intensity of energy dissipation in turbulence (Frisch and Parisi, 1985), or the relative intensity of passive scalar gradients or frozen-in vector fields in chaotic advection (Ott and Antonsen, 1988, 1989), involves a continuous family of exponents (Hentschel and Procaccia, 1983b)

$$D_q(F) = \frac{1}{q-1} \lim_{\lambda \to 0} \frac{\log \sum_{i=1}^{N_\lambda} p_i^q}{\log \lambda} . \tag{1.19}$$

Here $p_i (\sum_{i=1}^{N_\lambda} p_i = 1)$ is the corresponding "relative importance," also called probability measure or mass density, of the subset $U_i(\lambda) \subset F$ contained inside the ith covering box with the edge λ. In the limit $q \to 0$ Eq. (1.19) becomes the fractal dimension (1.7). For $q' > q$ one has $D_{q'} \leq D_q$. For a "homogeneous fractal," whose parts are equally important, the probability measure is constant, $p_i \equiv N_\lambda^{-1}$, and the generalized dimension D_q equals the fractal dimension $D(F)$ for all q.

The set F can be represented as a union of a continuous family of subsets F_α, each being a fractal of the fractal dimension $f(\alpha) \leq D(F)$ and characterized by the algebraic singularity in the probability measure, $p_i(\lambda) \propto \lambda^\alpha$. The generalized dimension D_q is related to the α-singularity dimension $f(\alpha)$ as (Jensen *et al.*, 1985; Halsey *et al.*, 1986)

$$D_q(F) = \frac{1}{q-1} \min_\alpha [q\alpha - f(\alpha)] . \tag{1.20}$$

The continuously changed generalized dimension D_q and the corresponding "spectrum of singularities" $f(\alpha)$ present the mathematical formalism of the theory of *multifractals* (Paladin and Vulpiani, 1987; Feder, 1988; Mandelbrot, 1990, 1991; Aharony and Harris, 1992). The self-similarity property of multifractals is more complicated than that of homogeneous fractals and is describes in terms of *multiscaling* (Jensen *et al.*, 1991).

In this paper, we are primarily concerned with homogeneous fractals, such as percolating streamlines of an incompressible random flow. For the purpose of advective transport, the streamlines are homogeneous fractals due to the Liouville theorem applied to the Hamiltonian equations of tracer particle motion. That is, the probability of the particle presence in different equally sized boxes covering the particle orbit is approximately the same.

II. PERCOLATION

In this section a brief review is given of lattice and continuum percolation theories with an emphasis on the universality of critical behavior. In the long run, this universality enables the success in applying percolation theory to a number of problems that seem to be very far from the origin one introduced by Broadbent and Hammersley (1957). An incomplete list of problems to which percolation theory has been applied includes hopping conduction in semiconductors (Seager and Pike, 1974; Shklovskii and Efros, 1984), gelation in polymers (de Gennes, 1979a; Family, 1984), electron localization in disordered potentials (Ziman, 1969, 1979; Thouless, 1974), the quantum Hall effect (Trugman, 1983), flux vortex motion (Trugman and Doniach, 1982) and intergrain Josephson contacts (Gurevich *et al.*, 1988) in superconductors, the gas-liquid transition in colloids (Safran *et al.*, 1985), permeability of porous rocks (Sahimi, 1987; Thompson *et al.*, 1987) and of fractured hard rocks (Balberg *et al.*, 1991), plasma transport in stochastic magnetic fields (Kadomtsev and Pogutse, 1979; Yushmanov, 1990b; Isichenko, 1991b), turbulent diffusion (Gruzinov *et al.*, 1990), epidemic processes (Grassberger, 1983a), and forest fires (MacKay and Jan, 1984).

The goal of this section is not to compete with major reviews on percolation theory (Shante and Kirkpatrick, 1971; Essam, 1972, 1980; Kirkpatrick, 1973; Stauffer, 1979, 1985; Deutscher *et al.*, 1983; Zallen, 1983; Shklovskii and Efros, 1984; Sokolov, 1986), but rather to serve as a precursor to further discussion. We also supplement earlier review articles by covering recent analytical and numerical results related to hull exponents, correlated percolation, and continuum percolation. We adopt a qualitative physical approach, appealing to heuristic arguments rather than to rigorous mathematical proofs. Those who are interested in the mathematical foundations of percolation theory are referred to the monographs by Kesten (1982) and Grimmett (1989).

In this section, we focus primarily on the geometrical properties of percolation clusters that are described by the so-called *static* exponents. A variety of *dynamic* properties of percolation clusters, including conduction and random walks on clusters, their elastic properties, etc., are given lesser discussion. Review of the dynamics of percolation clusters and of other fractals is given by Aharony (1984), Orbach (1984), Rammal (1984), Havlin and Ben-Avraham (1987), Hans and Kehr (1987), Harris (1987), Harris, Meir, and Aharony (1987), and Bouchaud and Georges (1990).

In Sec. II.A the simplest conceptual problem of random percolation on a periodic lattice is discussed, and a review of the exponents of critical behavior near the percolation threshold is given. The scaling theory of percolation clusters, which relates different percolation exponents, is outlined in Sec. II.B. The universality of critical exponents—that is, their insensitivity to the geometry of the underlying lattice—is discussed in Sec. II.C. Correlated percolation is reviewed in Sec. II.D. In Sec. II.E we discuss various formulations of the continuum percolation problem that are free from lattice constraints.

A. Lattice percolation and the geometry of clusters

This new kind of mathematical problem grew out of the question of percolation of a fluid through a porous medium or a maze, thus resulting in the term "percolation problem." Broadbent and Hammersley, the founders of the percolation theory, coined the term "percolation" as opposed to the term "diffusion." According to Broadbent and Hammersley (1957), if diffusive processes involve a random walk of a particle in a regular medium, then percolation processes involve a regular motion (e.g., fluid or electric current flow) through a random medium. The simplest problem of this kind can be formulated as follows. Given a periodic lattice embedded in a d-dimensional space and the probability p for each site of the lattice to be "occupied" (and hence with the probability $1-p$ to be "empty"), what is the distribution of resulting clusters over sizes and other geometrical parameters? A cluster means (by definition) a conglomerate of occupied s sites, which communicate via the nearest-neighbor

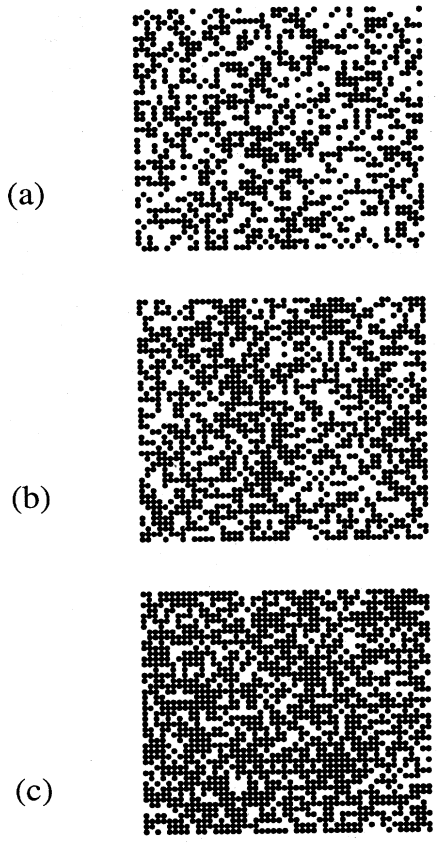

FIG. 3. Site percolation clusters on a 2D square lattice at $p=0.45$ (a), $p=0.5927=p_c$ (b), and $p=0.7$ (c).

rule (Fig. 3). In percolation theory special attention is given to the *percolation threshold*, $p=p_c$, at which an *infinite cluster* spans the lattice. Besides this *site percolation*, one can introduce the idea of *bond percolation*, with clusters of connected conducting bonds (Fig. 4). The bonds are conducting with the probability p and, correspondingly, blocked with the probability $1-p$. The site and the bond percolation problems are very similar to each other. There also exists a hybrid site-bond formulation of the percolation problem (Heermann and Stauffer, 1981). To be specific, we discuss lattice percolation mainly with the example of the site problem.

Statistically, one can describe the cluster distribution by the cluster density $n_s(p)$, which is the number of clusters including exactly s occupied sites per unit volume. It is convenient to choose the unit volume corresponding to one site of the lattice. For sufficiently small s, the density $n_s(p)$ can be calculated in a straightforward way by simply counting the number of permissible configurations ("lattice animals") of a cluster (de Gennes *et al.*, 1959; Sykes and Essam, 1964a; Sykes and Glen, 1976; Sykes *et al.*, 1976a, 1976b, 1976c; Essam, 1980). These expressions for $n_s(p)$ are polynomial functions of p. For example, a cluster consisting of a single site on a two-dimensional square lattice means the occupancy of the

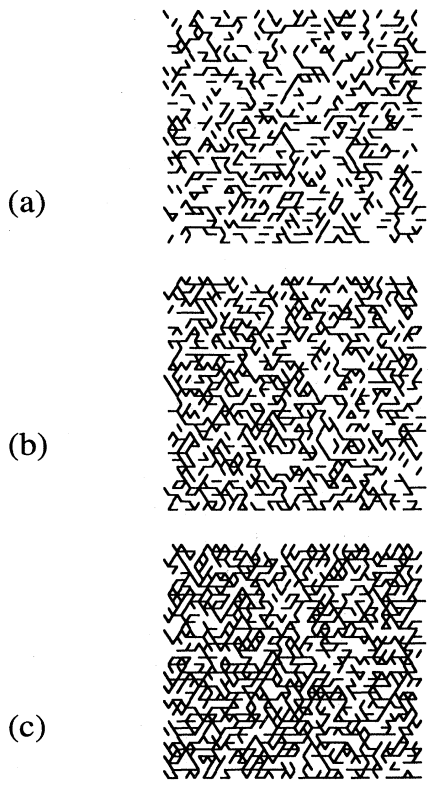

FIG. 4. Bond percolation clusters on a 2D triangular lattice at $p=0.25$ (a), $p=0.3473=p_c$ (b), and $p=0.45$ (c).

site (probability p) and the emptiness of the four nearest neighbors [probability $(1-p)^4$]. Hence $n_1(p)=p(1-p)^4$. Analogously, $n_2(p)=2p^2(1-p)^6$, $n_3(p)=2p^3(1-p)^8+4p^3(1-p)^6$, etc. For higher s, the calculation of $n_s(p)$ becomes increasingly cumbersome and is best performed by computer (Martin, 1974).

The percolation problem would be somewhat tedious were the cluster distribution a smooth function of the probability p, as suggested by the above series expansions for finite s. The central point of the theory is that, for each lattice, there exists a *critical probability* p_c, $0<p_c<1$, at which an infinite cluster definitely (i.e., with the probability 1) appears. The existence of this critical transition—the percolation threshold—is heuristically evident from the following argument. For $p=1-\varepsilon$, $0<\varepsilon\ll 1$, the percolation to infinity through occupied sites cannot be destroyed by removing a small fraction ε of sites [Fig. 3(c)]. On the other hand, for small $p\ll 1$, it is clearly exponentially improbable to percolate to a large distance a through occupied sites; hence, for $a\to\infty$, the probability of finding such a cluster tends to zero. Thus, for $p\ll 1$ there is no infinite cluster [Fig. 3(a)]. This indicates the existence of a critical probability p_c [Fig. 3(b)], which, roughly speaking, is " of the order of 1/2."

The value of the critical probability p_c depends on the dimension of space d, the kind of problem (site or bond), and the type of lattice. In two dimensions, p_c can be calculated exactly in some cases due to the fact that critical probabilities of certain lattices can be simply related to each other (Sykes and Essam, 1963, 1964b). Suppose there exists a one-to-one correspondence between the bonds of two lattices A and B. Suppose further that, if a bond on lattice A is conducting, then the corresponding bond on lattice B is blocked, and vice versa. If, under such a convention, the percolation through lattices A and B is mutually exclusive, then these two lattices are said to be *matching*, or *dual*: $A=B^*$. Geometrically, the corresponding bonds of matching lattices "cut each other" (see Fig. 5). The simplest examples of matching lattices are triangular (T) and honeycomb (H); the square lattice (S) is self-matching: $S=S^*$. The critical probabilities of matching lattices are complementary:

$$p_c(A,b)+p_c(A^*,b)=1\ , \tag{2.1}$$

where b means the bond problem. It immediately follows that the critical probability for the two-dimensional square lattice is

$$p_c(S,b)=\tfrac{1}{2}\ . \tag{2.2}$$

One can similarly introduce matching between bond and site lattices. For example, the sites of the triangular lattice match the bonds of the square lattice [Fig. 5(c)];

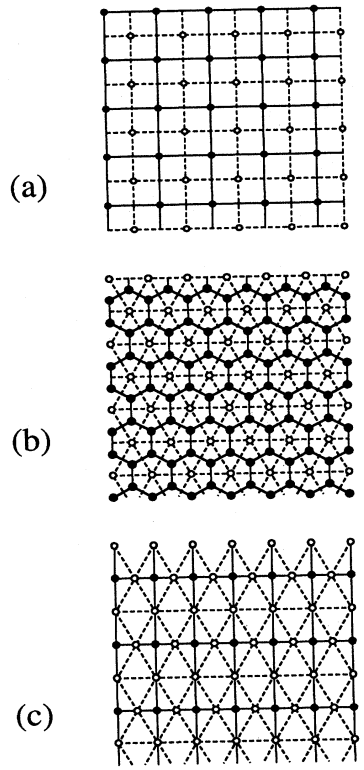

FIG. 5. Pairs of two-dimensional matching lattices, one shown by solid lines (for bonds) and filled circles (for sites) and the other by dashed lines and empty circles: (a) square-lattice bond problem is self-matching; (b) honeycomb and triangular lattices are bond matching; (c) square bonds match triangular sites.

TABLE II. Percolation thresholds for some lattices.

d	Lattice	Bond	Site
2	Square	$0.50^{1(a)}$	$0.590\pm0.010^{2(a)}$
		$1/2^{3(c)}$	$0.591\pm0.005^{4(b)}$
		$0.499\pm0.004^{4(b)}$	$0.53\pm0.002^{5(a)}$
		$0.499^{6(b)}$	$0.5927\pm0.000\,03^{7(b)}$
			$0.59273(6)^{8(b)}$
	Triangular	$0.33^{1(a)}$	$1/2^{3(c)}$
		$2\sin(\pi/18)=0.347\,296^{3(c)}$	$0.500\pm0.005^{4(b)}$
	Honeycomb	$0.66^{1(a)}$	$0.70\pm0.01^{2(a)}$
		$1-2\sin(\pi/18)=0.652\,701\,4^{3(c)}$	$0.697\pm0.004^{4(b)}$
			$0.698\pm0.003^{5(a)}$
3	Simple Cubic	$0.24^{1(a)}$	$0.307\pm0.010^{2(a)}$
		$0.247\pm0.005^{2(a)}$	$0.320\pm0.004^{4(b)}$
		$0.248\pm0.001^{9(b)}$	$0.318\pm0.002^{10(b)}$
		$0.2479\pm0.004^{11(a)}$	$0.3117\pm0.000\,3^{9,13(b),11(a)}$
		$0.2488\pm0.000\,2^{12(a)}$	
	Body-centered cubic	$0.178\pm0.005^{2(a)}$	$0.243\pm0.010^{2(a)}$
		$0.1795\pm0.000\,3^{11(a)}$	$0.254\pm0.004^{4(b)}$
		$0.18025\pm0.000\,15^{12(a)}$	$0.2464\pm0.000\,7^{11(a)}$
	Face-centered cubic	$0.119\pm0.002^{2(a)}$	$0.195\pm0.005^{2(a)}$
		$0.1190\pm0.000\,5^{14(a)}$	$0.208\pm0.003\,5^{4(b)}$
		$0.1198\pm0.000\,3^{11(a)}$	$0.1998\pm0.000\,6^{11(a)}$
	Diamond	$0.388\pm0.05^{2(a)}$	$0.425\pm0.012^{2(a)}$
		$0.3886\pm0.000\,5^{11(a)}$	$0.4299\pm0.000\,8^{11(a)}$

[1]Domb and Sykes (1060).
[2]Sykes and Essam (1964a).
[3]Sykes and Essam (1963, 1964b).
[4]Dean and Bird (1967).
[5]Sykes *et al.* (1976a, 1976b, 1976c).
[6]Fogelholm (1980).
[7]Ziff (1986).
[8]Kertész (1986).
[9]Heermann and Stauffer (1981).
[10]Onizuka (1975).
[11]Gaunt and Sykes (1983).
[12]Adler *et al.* (1990).
[13]Kertész *et al.* (1982).
[14]Dunn *et al.* (1975).

[(a)]From series expansion.
[(b)]Monte Carlo simulation.
[(c)]Exact.

hence

$$p_c(T,s)=1-p_c(S,b)=\tfrac{1}{2}\ . \tag{2.3}$$

For matching bond problems on triangular and honeycomb lattices, Sykes and Essam (1963, 1964b) found an additional exact relation for critical probabilities that yields

$$1-3p_c(T,b)+p_c^3(T,b)=0\ ; \tag{2.4}$$

hence

$$p_c(T,b)=1-p_c(H,b)=2\sin(\pi/18)\ . \tag{2.5}$$

In the three-dimensional case, no percolation threshold is known exactly; only numerical data are available. Table II shows the values of p_c for the simplest lattices. At first glance, there is no apparent rule describing the values of the critical probabilities p_c for different lattices. An approximate rule, however, was found by Scher and Zallen (1970), who noticed that for each dimension there exists an invariant that is almost independent of the type of lattice. This invariant, $\phi_c=fp_c$, is the critical fraction of space occupied by spheres (discs in 2D) of the bond-length diameter, positioned in the occupied sites of the lattice. The quantity f is called the "filling factor" of the lattice and denotes the volume fraction occupied by mutually touching spheres positioned at each site. The critical space occupation probability equals $\phi_c=0.44\pm0.02$ in two dimensions; $\phi_c=0.154\pm0.005$ in three dimensions.

The decrease in critical probability with increasing dimension d is well understood. For example, 2D bond clusters on a square lattice (S) are nothing more than a planar cross section of 3D bond clusters on a simple cubic lattice (SC) at the same probability p. Even though all 2D clusters are finite ($p<p_c(\mathrm{S},b)=0.5$), they can be-

long to an infinite 3D cluster communicating via the third dimension ($p > p_c(\mathrm{SC}, b) \simeq 0.248$). The lattice filling factor f is also smaller for higher dimensions: $f(\mathrm{S}) = \pi/4$, $f(\mathrm{SC}) = \pi/8$.

A more fundamental difference between two- and three-dimensional percolation is that in 3D one can introduce two nontrivial critical probabilities, $p_c \equiv p_{c1} < p_{c2}$. Following the original motivation of Broadbent and Hammersley (1957), let us call the clusters of occupied sites (or conducting bonds) "wet." The second critical probability p_{c2} specifies the threshold of percolation through "dry" clusters of vacant sites (or blocked bonds) corresponding to the occurrence probability $1-p$. Since the wet and the dry percolation problems are identical, we conclude that $p_{c2} = 1 - p_{c1}$.

In two dimensions, simultaneous percolation through both wet and dry clusters is impossible unless these clusters cross each other (as is the case for bonds on a triangular lattice). This well manifests itself by the fact that the critical percolation probabilities p_c are not less than $\frac{1}{2}$ (with the mentioned exception for the triangle bonds; see Table II). For $p_c > \frac{1}{2}$ (square sites, honeycomb sites, and bonds) and $1 - p_c < p < p_c$, there is percolation through neither wet nor dry clusters.

In three dimensions, one generally has $p_c < \frac{1}{2}$ (see Table II) so that $p_{c1} < p_{c2}$. The presence for $p_{c1} < p < p_{c2}$ of both wet and dry infinite clusters reflects the existence of different nonintersecting, isotropic paths to infinity. (This is why freeway overpasses are made three dimensional.) The difference between two and three dimensions becomes especially distinct for percolation in the continuum (Sec. II.E), where the image of "wet" and "dry" areas may be given a more literal sense by considering coastlines arising during the flooding of a random relief $z = \psi(\mathbf{x})$. This issue will be given further discussion in the context of statistical topography (Sec. III).

The cluster density $n_s(p)$ accounts only for finite-size clusters. The infinite cluster is characterized by the density $P_\infty(p)$, which denotes the probability for a given site to belong to the infinite cluster. [Sometimes $P_\infty(p)$ is defined as the conditional probability for a given *occupied* site to belong to the infinite cluster. These two definitions of $P_\infty(p)$ differ by the factor of p, which is unimportant for the critical behavior near $p = p_c$.] It can be shown (Kikuchi, 1970; Newman and Schulman, 1981) that, in two or three dimensions, there exists either exactly one (for $p \geq p_c$) or no (for $p < p_c$) infinite cluster. The sum of all the probabilities that a given site belongs to either a finite-size cluster or the infinite cluster must equal p (the probability to be simply occupied):

$$\sum_{s=1}^{\infty} s n_s(p) + P_\infty(p) = p \ . \tag{2.6}$$

In the subcritical case, $p < p_c$, $P_\infty(p)$ is identically zero. For $p > p_c$, $P_\infty(p)$ is positive; consequently, in the vicinity of the percolation threshold, the function $P_\infty(p)$ is nonanalytic. There is extensive numerical evidence for the power dependence

$$P_\infty(p) \propto (p - p_c)^\beta \theta(p - p_c), \quad |p - p_c| \ll 1 \ , \tag{2.7}$$

where $\theta(x)$ is the Heaviside step function. The exponent β is one of the standard set of *critical exponents* $\alpha, \beta, \gamma, \ldots$ (Domb *et al.*, 1972–1988) that govern the behavior of different quantities near the critical point:

$$\hat{S}_p \sum_{s=1}^{\infty} n_s(p) \propto |p - p_c|^{2-\alpha} \ , \tag{2.8a}$$

$$\hat{S}_p \sum_{s=1}^{\infty} s n_s(p) \propto (p - p_c)^\beta \ , \tag{2.8b}$$

$$\hat{S}_p \sum_{s=1}^{\infty} s^2 n_s(p) \propto |p - p_c|^{-\gamma} \ , \tag{2.8c}$$

$$\hat{S}_H \sum_{s=1}^{\infty} s n_s(p_c) e^{-Hs} \propto H^{1/\delta} \ , \tag{2.8d}$$

$$\xi(p) \propto |p - p_c|^{-\nu} \ . \tag{2.8e}$$

In Eqs.(2.8), the operator $\hat{S}_x$ denotes the main singular (as a function of x) part of the subsequent expression. Specifically, this operator yields zero when applied to an analytic function. "Singular" in this context means a function that is either discontinuous or has a discontinuous derivative of some order at $p = p_c$. All expressions (2.8) assume $|p - p_c| \ll 1$, $0 < H \ll 1$. Equation (2.8b) is a direct consequence of Eqs. (2.6) and (2.7). The quantity $\xi(p)$ in Eq. (2.8e) is the so-called *correlation*, or *coherence length*, which is a characteristic size of the cluster distribution (see Sec. II.B). This is not an average radius of percolation clusters (the average linear size is of the order of the lattice period, as small clusters still dominate), but is rather a maximum size above which the clusters are exponentially scarce. The correlation length $\xi(p)$ is also the upper bound of the scaling range where percolation clusters behave self-similarly and hence may be characterized by a fractal dimension (Stanley, 1977, 1984; Margolina *et al.*, 1982; Kapitulnik *et al.*, 1984). Equivalently, the correlation length separates an algebraic behavior of a cluster correlation function (Shklovskii and Efros, 1984) from its exponential decay.

Table III summarizes the percolation critical exponents. These exponents depend only on the dimension of the space and not on the type of lattice or the kind of percolation problem (see Sec. II.C). As discussed in Sec. II.B, phenomenological (scaling) arguments can be used to derive relations between the critical exponents entering Eqs. (2.8), so that only two of them are left to be calculated from first principles. The choice of these two "basic" exponents is relative; to be specific, we consider the correlation length exponent ν and the infinite cluster density exponent β as the basic percolation exponents. In two dimensions ($d = 2$), these indices are known analytically (den Nijs, 1979; Pearson, 1980; Baxter, 1982), namely, $\nu = 4/3$ and $\beta = 5/36$. For $d = 3$, only numerical estimates are available: $\nu \simeq 0.90$ and $\beta \simeq 0.40$ (see Table III).

In the analogy that can be drawn between the percola-

TABLE III. Percolation critical exponents.

Exponent	$d=2$	$d=3$
$\alpha=2-\nu d$	$-2/3$[d,e]	-0.64 ± 0.05[4(a)]
β	$5/36=0.138\,88$[1,2,3(d)] 0.15 ± 0.03[5(e)] 0.138 ± 0.007[6(a)] 0.14 ± 0.02[8(c)]	0.39 ± 0.07[5(e)] 0.454 ± 0.008[4(a)] 0.45 ± 0.2[7(c)] 0.43 ± 0.04[9(b)] 0.405 ± 0.025[10(a)]
$\gamma=\nu d-2\beta$	$43/18=2.388\,8$[1,2,3(d)] 2.38 ± 0.02[5(a)] 2.43 ± 0.03[6(a)] 2.43 ± 0.04[8(c)] 2.39 ± 0.02[11(c)]	1.70 ± 0.11[5(a)] 1.73 ± 0.03[4(a)] 1.63 ± 0.2[7(c)] 1.91 ± 0.01[11(c)] 1.805 ± 0.02[10(a)] 1.77 ± 0.02[12(b)]
$\delta=\nu d/\beta-1$	$91/5=18.2$[d,e]	4.81 ± 0.14[4(e)]
ν	$4/3$[1,2,3(d)] 1.34 ± 0.02[5(a)] 1.343 ± 0.019[8(c)] 1.33 ± 0.07[15(c)] 1.35 ± 0.03[14(b)] 1.35 ± 0.06[16(b)] $1.333\,0(7)$[17(b)]	0.82 ± 0.05[5(a)] 0.89 ± 0.01[13(b)] 0.91 ± 0.08[14(b)] 0.88 ± 0.02[4(e)] 0.94 ± 0.02[7(c)] 0.88 ± 0.05[9(b)] 0.905 ± 0.023[10(e)]
μ	1.25 ± 0.05[18(b)] 1.10 ± 0.05[18(b)] 1.30[21(f)] 1.25 ± 0.1[23(f)] 1.28 ± 0.03[24(b)] 1.27 ± 0.04[25(b)] 1.31 ± 0.04[26(b)] 1.22 ± 0.08[16(b)] $\nu=4/3$[27(g)] 1.24 ± 0.05[28(b)] 1.32 ± 0.05[28(c)]	1.6 ± 0.1[19(b)] 1.725 ± 0.005[20(b)] 1.4[22(c)] 1.70 ± 0.05[18(b)] 1.75 ± 0.1[18(b)] 1.50 ± 0.10[23(f)] $9\nu/4\simeq2.00$[27(g)] 2.46 ± 0.1[28(c)] 1.95 ± 0.1[28(b)]
$\tau=(2\nu d-\beta)/(\nu d-\beta)$	$187/91=2.054\,9$[d,e] 2.0 ± 0.1[8(c)]	2.19 ± 0.01[12(b)]
$d_c=d-\beta/\nu$	$91/48=1.895\,83$[d,e] 1.88 ± 0.02[29(b)] $91/48\pm1\%$[30(b)]	2.484 ± 0.012[4(e)] 2.51 ± 0.025[9(b)] 2.5 ± 0.05[31(b)] 2.529 ± 0.016[12(b)] 2.49[30(b)]
d_h	$7/4=1.75$[32(d)] 1.75 ± 0.05[34(b)] 1.74 ± 0.02[35(b)] 1.76 ± 0.01[35(b)] 1.751 ± 0.002[37(b)] 1.750 ± 0.002[38(b)]	$d_h=d_c$[33,30,12(d)] 2.548 ± 0.014[12(b)]
d_b	1.60 ± 0.05[39(b)] 1.62 ± 0.02[40,28(b)] 1.61 ± 0.01[41(b)]	1.77 ± 0.07[39(b)] 1.74 ± 0.04[40(b)]
$d_{rb}=1/\nu$[42]	$d_{rb}=3/4$[(d)] 0.75 ± 0.01[29(b)] 0.75 ± 0.07[43(b)]	

TABLE III. (*Continued*).

Exponent	$d=2$	$d=3$
$d_{\min}$	1.18 ± 0.08[44(b)] 1.17 ± 0.015[43(b)] 1.10 ± 0.05[39(b)] 1.132 ± 0.003[46(b)] 1.021 ± 0.005[45(b)] 1.15 ± 0.02[41(b)]	1.35 ± 0.05[39(b)] 1.26 ± 0.06[45(b)]

[1]den Nijs (1979).
[2]Pearson (1980).
[3]Nienhuis (1982).
[4]Gaunt and Sykes (1983).
[5]Dunn *et al.* (1975).
[6]Sykes *et al.* (1976a, 1976b, 1976c).
[7]Elan *et al.* (1984).
[8]Gawlinski and Stanley (1977).
[9]Grassberger (1986a).
[10]Adler *et al.* (1990).
[11]Lee (1990).
[12]Strenski *et al.* (1991).
[13]Heermann and Stauffer (1981).
[14]Kertész *et al.* (1982).
[15]Vicsek and Kertész (1981).
[16]Mitescu *et al.* (1982).
[17]Kertész (1986).
[18]Straley (1977).
[19]Kirkpatrick (1973).
[20]Onizuka (1975).
[21]Smith and Lobb (1979).
[22]Webman *et al.* (1976).
[23]Clerc *et al.* (1980).
[24]Derrida and Vannimenus (1982).
[25]Li and Strieder (1982).
[26]Fogelholm (1980).
[27]Family and Coniglio (1985).
[28]Murat *et al.* (1986).
[29]Nagatani (1986).
[30]Margolina *et al.* (1982).
[31]Gouyet *et al.* (1988).
[32]Saleur and Duplantier (1987).
[33]Stauffer (1979).
[34]MacKay and Jan (1984).
[35]Voss (1984).
[36]Grossman and Aharony (1986).
[37]Ziff (1986).
[38]Grassberger (1986b).
[39]Herrmann *et al.* (1984).
[40]Herrmann and Stanley (1984).
[41]Laidlaw *et al.* (1987).
[42]Coniglio (1981).
[43]Pike and Stanley (1981).
[44]Alexandrowicz (1980).
[45]Edwards and Kerstein (1985).
[46]Grassberger (1985).

[a]From series expansion.
[b]Monte Carlo lattice simulation.
[c]Monte Carlo continuum simulation.
[d]Exact.
[e]From scaling relations.
[f]Experiment.
[g]Flory (1969) approximation.

tion problem and magnetic phase transitions (Stauffer, 1979), the sums on the left-hand sides of Eqs. (2.8) can be regarded as free energy (2.8a), spontaneous magnetization (2.8b), susceptibility (2.8c), and magnetization (2.8d) in the external field H. In these terms, the probability difference $p-p_c$ corresponds to the temperature difference T_c-T, so that subcritical (finite) clusters present a high-temperature (disordered) phase, and the supercritical infinite cluster spans the space to form a low-temperature (ordered) phase. Hence the infinite cluster density $P_\infty(p)$ plays the role of the order parameter of the percolation phase transition (Kikuchi, 1970).

The lattice percolation problem can be placed among other discrete lattice phase-transition models, such as the Ising (1925) model, the q-state Potts model (Potts, 1952; Nienhuis *et al.*, 1979), the n-vector model $O(n)$ (Stanley, 1968; Nienhuis, 1982), and others (Baxter, 1982). The Ising model, which was historically the first analytically solved phase-transition model, is the particular case of $O(n)$ for $n=1$ and also of the q-state Potts model for $q=2$. The percolation problem corresponds to a proper limit of the Potts model for $q\to1$ (Fortuin and Kasteleyn, 1972). Trugman (1986) suggested a maximum-entropy method to define a generalized inhomogeneous-system model incorporating percolation and other models as special cases.

In two dimensions, there is a powerful technique for the calculation of various critical exponents. This technique is based on the representation of Coulomb gas introduced, in its most convenient form, by Kadanoff (1978). A review of the results obtained by this method can be found in Nienhuis (1984).

Another approach for possibly exact evaluation of critical exponents in two dimensions is based on the conformal invariance technique (Polyakov, 1970; Belavin *et al.*, 1984; Dotsenko and Fateev, 1984; Saleur, 1987). This method predicts a discrete series of "permissible" fractal dimensions (Kac, 1979; Larsson, 1987),

$$d_f=(100-x^2)/48\ , \tag{2.9}$$

where x is an integer. Speculating on the correspondence between various objects (e.g., clusters and their subsets) and conformal fields, one can pick a conformal dimension (2.9) closest to a numerical value and claim an exact result (Larsson, 1987). All analytically known fractal dimensions associated with 2D percolation clusters and random walks belong to this list of "magic numbers" (see Table IV).

When analytical results were not available, the most accurate estimates for critical probabilities and critical exponents were obtained using the series-expansion method (Sykes and Essam, 1964a; Sykes *et al.*, 1976a, 1976b, 1976c; Adler *et al.*, 1990). The idea of the method (Domb and Sykes, 1960) is to represent diverging sums, such as the one in Eq. (2.8c), in the form of series in p (low-density expansion) or $1-p$ (high-density expansion) using the lattice animal enumeration. The critical behavior is then studied by locating the nearest singular point of the series on the real positive axis of p, using low-order Padé approximants (cf. Baker and Graves-Monris, 1981).

The critical exponents introduced above are referred to as *static* exponents because they characterize only the geometry and distribution of clusters. Percolation clusters are usually used for modeling such physical objects as amorphous solids (Zallen, 1983), composite materials (Garland and Tanner, 1978), porous rock (Thompson *et al.*, 1987), polymers (de Gennes, 1979b; Family, 1984), etc. In studying various physical properties of disordered media (conductivity, elasticity, permeability, etc.), the corresponding properties of percolation networks are described in terms of *dynamic* exponents. The simplest problem of this kind, associated with the appearance of an infinite cluster, is the problem of long-range conductance in a random resistor network (Kirkpatrick, 1973; Skal and Shklovskii, 1974; Shklovskii and Efros, 1984; Harris, 1987; Havlin and Ben-Avraham, 1987). For bond percolation where each "conducting" bond has a fixed resistance of 1, while "blocked" bonds have an infinite resistance, the large-scale behavior of the system undergoes a sharp transition from an insulator ($p<p_c$) to a conductor ($p>p_c$). Near the percolation threshold, the long-range direct-current conductivity σ_{dc} has a singularity of the form

$$\sigma_{dc} \propto (p-p_c)^{\mu}\theta(p-p_c) . \tag{2.10}$$

The conductivity exponent μ is one of the dynamic exponents. The value of $\mu \simeq 1.3$ is relatively well established for two dimensions. In the three-dimensional case, the computation is more expensive and reported results are more controversial, $\mu = 1.7-1.9$ (see Table III). The processes of ac conductivity in random resistor networks are described by a set of new exponents studied theoretically by Bergman and Imry (1977) and Hui and Stroud (1985) and experimentally by Yoon and Lee (1990).

Another dynamical property of percolation clusters and other fractals is how they support propagation of classical or quantum waves. A new dynamic exponent a was introduced by Lévy and Souillard (1987; see also Aharony and Harris, 1990) to describe the *superlocalization* of the electron wave function $\psi(\mathbf{x}) \propto \exp(-x^a)$, $x \to \infty$, where ψ is a solution of the Schrödinger equation with a potential $V(\mathbf{x})$ concentrated on a fractal set.

The static critical exponents α, β, γ, δ, and ν characterize the distribution of clusters. For many applications, the structure of an individual cluster is also important. Let us introduce for brevity some terms characterizing the geometry of a percolation cluster. We shall call s (the number of sites belonging to the cluster) the "cluster mass" and a (the maximum linear size of the cluster) the "cluster diameter," or simply the "size." [Notice that some authors refer to the number of sites s an the "size." Sometimes the "mean cluster size" is defined as the ratio of sums on the left-hand side of Eqs. (2.8c) and (2.8b). We shall not follow this notation.] The mass s and the size a of a large cluster are related by $s(a) \propto a^{d_c}$, which is the radius-mass relation (1.10) for a fractal. Of course, the fractal dimension d_c is an invariant. What changes with the probability p, or with the size a, is the scaling range, which is $[\lambda_0, a]$ for a finite cluster and $[\lambda_0, \xi(p)]$ for the infinite one.

The fractal dimension d_c of a percolation cluster can be expressed through other exponents. To establish this relation, let us notice that the density $P_\infty(p)$ of the infinite cluster is its mass-to-volume ratio $M(a)/a^d$ at $a \gg \xi(p)$. Writing this relation at the lower limit of its applicability, $a \simeq \xi(p)$, we find $M[\xi(p)] \simeq \xi^d(p) P_\infty(p)$. On the other hand, we have $M(a) \simeq (a/\lambda_0)^{d_c}$ for $\lambda_0 < a < \xi(p)$. Using this radius-mass relation at the upper limit $a = \xi(p)$ and Eqs. (2.7) and (2.8e), we conclude (Kapitulnik *et al.*, 1984)

$$d_c = d - \frac{\beta}{\nu} . \tag{2.11}$$

[Notice that in the early work by Stanley (1977), who proposed to describe near-critical percolation clusters by an "effective dimension," an incorrect equation for the dimension was given ($d_p = d - 2\beta/\nu$).] Thus the fractal

TABLE IV. Exactly known fractal dimensions of 2D objects and their correspondence to the conformal series.

Object	Fractal dimension $=(100-x^2)/48$	x
Percolation cluster	$91/48$[1]	3
Hull	$7/4$[2]	4
SKW	$7/4$[3]	4
Unscreened perimeter	$4/3$[4,2,5]	6
SAW	$4/3$[6]	6
Red bonds	$3/4$[7]	8

[1]Kapitulnik *et al.* (1984).
[2]Saleur and Duplantier (1987).
[3]Weinrib and Trugman (1985).
[4]Grossman and Aharony (1986, 1987).
[5]Duplantier and Saleur (1987).
[6]Nienhuis (1982).
[7]Coniglio (1981).

dimension d_c of a percolation cluster is always smaller than the dimension d of the ambient space, due to numerous "holes" in the cluster. In two dimensions, $d_c = 91/48 \simeq 1.90$; for $d = 3$, $d_c \simeq 2.5$ (see Table III).

For the problem of the electrical conductivity of a random resistor network and other dynamic properties, another object is relevant—the "backbone" of an infinite percolation cluster. The conductivity problem is more convenient to describe in terms of bond percolation. The backbone is defined as the network of unblocked connected bonds, through which one can go to infinity by at least two nonintersecting paths (Fig. 6). In other words, the backbone is a set of bonds, through which electric current would flow were a voltage applied to the cluster at infinitely remote electrodes. The rest of the cluster is referred to as a collection of "dead" or "dangling ends." A dangling end can be disconnected from the cluster by cutting a single bond.

Similar to the fractal dimension d_c of the whole cluster, one can introduce the backbone fractal dimension d_b. This exponent was determined numerically by Herrmann and Stanley (1984), who found $d_b = 1.62 \pm 0.02$ for $d = 2$ and $d_b = 1.74 \pm 0.04$ for $d = 3$. The inequality $d_b < d_c$ means that almost all of the mass of a large cluster is concentrated in its dangling ends. The closest conformal dimension (2.9) to the 2D d_b value is (at $x = 5$) $25/16 \simeq 1.56$, which lies slightly beyond the reported statistical error. This discrepancy raised questions into the universality of the "magic numbers" (2.9) (Larsson, 1987).

The backbone, in turn, can be divided into multiply-connected paths (Harris, 1983). For example, the singly connected bonds carry all the current flowing through the cluster; hence these bonds are sometimes called "red" (Stanley, 1984; another term for this object is "cutting bonds"). Coniglio (1981) found that the fractal dimension of the set of red bonds is simply related to the correlation length exponent ν: $d_{rb} = 1/\nu$. In two dimensions $d_{rb} = 3/4$, which corresponds to the conformal dimension (2.9) at $x = 8$. The red bonds are present only in the "incipient" infinite cluster—that is, the infinite cluster at $p = p_c$. The backbone of a supercritical infinite cluster ($p > p_c$) has a networklike structure and, as the hole sizes in the network are bounded from above by a finite correlation length $\xi(p)$, the singly connected (generally, finitely connected) bonds do not exist.

From the viewpoint of conduction, a percolation backbone behaves as a multifractal, where the natural measure of fractal inhomogeneity is the Ohmic dissipation density (Paladin and Vulpiani, 1987).

The minimum-distance path connecting two remote points on a near-critical cluster was invoked for the model of "growing clusters" (Alexandrowicz, 1980; Stanley, 1984; Grassberger, 1985). The minimum or chemical path has the fractal dimension $d_{\min} \simeq 1.1$. If this object corresponds to a conformal field, the Larsson (1987) conjecture that $d_{\min} = 17/16$ may be valid; this is the closest conformal dimension (at $x = 7$) to the numerical data (see Table III).

Another geometrical characteristic of a cluster is its outer perimeter, or "hull" L_h, defined as the number of empty sites that (a) are adjacent to the cluster sites and (b) can be related to infinity via a chain of empty sites connected as either nearest or next-to-nearest neighbors. The need to consider next-to-nearest-neighbors empty sites is to guarantee that the hull penetrate between the next-to-nearest-neighbors occupied sites belonging to the cluster. The hull may be represented as a continuous line of the length L_h ($d = 2$) or a surface of the area L_h ($d = 3$), enveloping the cluster from outside (see Fig. 7). Without restriction (b), one would have the full (outer

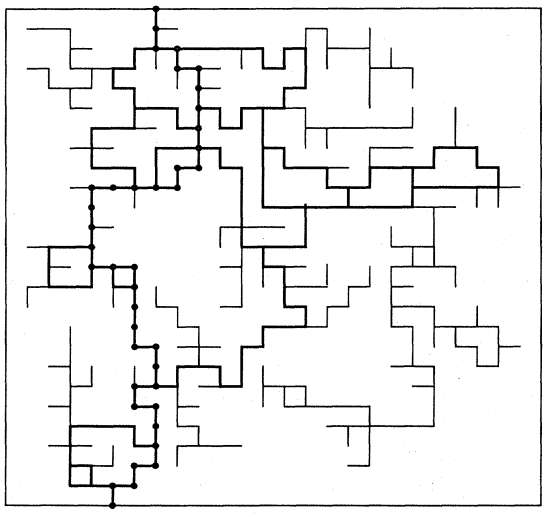

FIG. 6. Schematic of an infinite bond cluster on a 2D square lattice. The backbone is shown in heavy lines, the dangling ends in light lines. Markers denote a minimum path on the backbone.

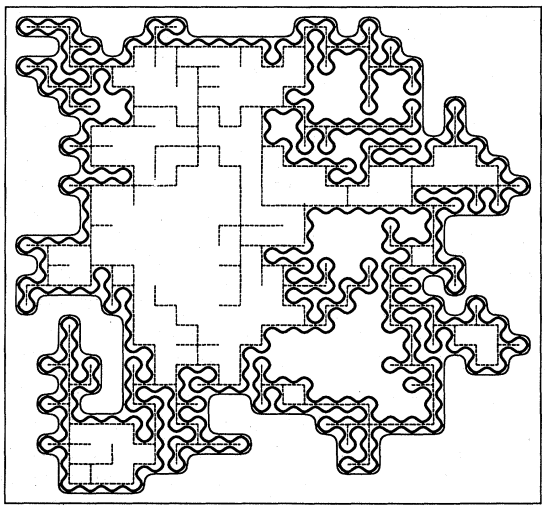

FIG. 7. Finite cluster (dashed lines), its external hull (heavy curve), and the unscreened perimeters (light curve).

and inner) perimeter, which scales directly proportional to the cluster mass s (Reich and Leath, 1978). In two dimensions, the outer and the inner perimeters are topologically disconnected and the external hull mass L_h is much less than the cluster mass s. This leads to the existence of a nontrivial, for $d=2$, hull exponent d_h, which is the fractal dimension of the hull. The hull measure L_h is expressed through its size a as follows:

$$L_h \propto a^{d_h} . \tag{2.12}$$

The hull exponent in two dimensions was computed by Ziff (1986), who found $d_h=1.750\pm0.002$ (see also data in Table III). Sapoval *et al.* (1985) and Bunde and Gouyet (1985) argued on a similarity between diffusion fronts and percolation hulls that led to the heuristic conjecture for the hull exponent

$$d_h=1+1/\nu=7/4, \quad d=2 . \tag{2.13}$$

Later analytical study of Saleur and Duplantier (1987) confirmed result (2.13) from first principles.

The properties of an internal hull, that is, of a line enveloping an internal hole in the cluster, are very similar to those of the external hull. Indeed, an internal hull can be considered to be the external hull of a complementary cluster of vacant sites (probability $1-p$) that fills up a hole in the original cluster.

One can introduce hull critical exponents analogously to those associated with clusters themselves. For example, the beta exponent β_h is defined similarly to Eq. (2.11), $d_h=d-\beta_h/\nu$, $\nu_h\equiv\nu$. The values $\beta_h=1/3$, $\gamma_h=2$ for $d=2$ suggest that percolation hulls are simpler objects than the underlying percolation clusters and are of independent significance. Weinrib and Trugman (1985) showed that percolation hulls are associated with a special kind of random walk called a "smart kinetic walk" (SKW), which can be generated with no regard to clusters (Ziff *et al.*, 1984; Ziff, 1986, 1989). Further importance of percolation hulls lies in their ability to model the fronts of diffusion-limited aggregation (Meakin and Family, 1986) and contour sets of random functions (see Secs. II.E and III.C).

Grossman and Aharony (1986, 1987) found that properties of external perimeters of percolation clusters can be drastically changed by only a slight modification of the perimeter definition. They defined another "unscreened" or "accessible" perimeter as the set of empty sites neighboring the occupied cluster sites and related to infinity through a chain of empty nearest neighbors only (in contrast to the "natural" hull definition that allows also for next-to-nearest neighbors in the chain). The unscreened perimeter can be presented as the "hull of the hull" (see Fig. 7). The numerical result $d_u=1.37\pm0.03$ (Grossman and Aharony, 1986) for the unscreened perimeter of a 2D percolation cluster was quite different from the prediction of Eq. (2.13). A similar result for the modified perimeter, $d_u=1.343\pm0.002$, was reported by Meakin and Family (1986).

Saleur and Duplantier (1987) noticed that a "natural" hull, or a smart kinetic walk with the fractal dimension $d_h=7/4$, is equivalent to a self-avoiding walk (SAW) at the Θ point describing a collapse transition of a polymer chain in a solvent (de Gennes, 1979a), which is an unstable tricritical point (Lawrie and Sarbach, 1984; Duplantier and Saleur, 1987). The Grossman-Aharony modification of the hull definition corresponds, in these terms, to an increase in the repulsive interaction of the polymer chain that drives its fractal dimension to the standard excluded-volume SAW value $d_{\mathrm{SAW}}=4/3$ (Nienhuis, 1984). In Sec. III.C.1 we argue that the natural hull, rather than the unscreened perimeter, represents the scaling properties of the isolines of a random "monoscale" potential $\psi(x,y)$.

For three dimensions, due to the multiconnected topology of the external boundary of a cluster, it was conjectured (Stauffer, 1979; Sokolov, 1986; Gouyet *et al.*, 1988; Strenski *et al.*, 1991) that the external hull comprises a finite fraction of the net cluster perimeter; hence the fractal dimensions of the cluster and of its hull are the same:

$$d_h=d_c=d-\beta/\nu, \quad d=3 . \tag{2.14}$$

B. Scaling and distribution of percolation clusters

Percolation clusters belong to the class of random physical fractals (Gefen *et al.*, 1981; Kapitulnik *et al.*, 1984; Mandelbrot and Given, 1984). Here "random" is an antonym of "deterministic," which describes such regular structures as the Sierpinski carpet (Fig. 1). Unlike deterministic fractals, percolation clusters are not exactly, but only statistically, self-similar. "Physical," meaning an opposite of "mathematical," implies a finite range of this self-similarity. For a single finite cluster, the scaling range is $[\lambda_0,a]$, where λ_0 is the period of the lattice and a is the size of the cluster. For the distribution of all clusters, the range of self-similarity is $[\lambda_0,\xi(p)]$; at $p=p_c$ this range becomes infinite.

Given the "basic" exponents ν, which governs the behavior of the coherence length ξ (2.8e), and the infinite cluster density exponent β, the remaining critical exponents entering Eqs. (2.8) can be obtained phenomenologically using scaling or self-similarity arguments. To do so, we first find the asymptotics of the cluster density $n_s(p)$ for $s\gg1$. Suppose $|p-p_c|\ll1$, so that $\xi(p)\gg\lambda_0$. Let us call clusters of linear size lying between a and $2a$ the "a clusters." Since there is no characteristic scale between λ_0 and $\xi(p)$, the density N_a of a clusters (their number per unit volume) must behave algebraically with a, which is the only kind of dependence without a characteristic scale: $N_a\simeq(\lambda_0/a)^x$, $\lambda_0<a<\xi(p)$. On the other hand, on scales $\lambda>\xi(p)$ the self-similarity is changed by the statistical uniformity in the cluster distribution; that means that the $\xi(p)$ clusters have a density of approximately $\xi^{-d}(p)$. Thus x must equal the space dimension d, and we find

$$N_a=C_1a^{-d}, \quad \lambda_0\ll a\ll\xi(p) , \tag{2.15}$$

where C_1 is a coefficient of the order of unity. The distribution (2.15) implies a dense packing of a clusters in space for each $a \in [\lambda_0, \xi(p)]$. For $a > \xi(p)$, the algebraic dependence (2.15) is changed by an exponential decay (Stauffer, 1985). Notice that formula (2.15) is valid for both under- and supercritical cases. At $p > p_c$, the finite clusters lie in the holes inside the infinite cluster, where the correlation length $\xi(p)$ is the maximum size of the hole. In other words, if the cluster size essentially exceeds the correlation length, this cluster is almost surely infinite.

The density of a clusters (2.15) enables us to calculate the distribution of clusters over masses. For the given size a, a clusters have typically the mass $s(a) \simeq (a/\lambda_0)^{d_c}$; hence

$$N_a \simeq \sum_{s=s(a)}^{2s(a)} n_s \simeq s(a) n_{s(a)} . \tag{2.16}$$

Equations (2.15) and (2.16) lead to the following equation for the density of s clusters:

$$n_s = C_2 \cdot s^{-\tau}, \quad 1 \ll s \ll s(\xi) , \tag{2.17}$$

with the exponent (Stauffer, 1979)

$$\tau = 1 + \frac{d}{d_c} = \frac{2\nu d - \beta}{\nu d - \beta} . \tag{2.18}$$

The equation

$$s(\xi) = \left[\frac{\xi(p)}{\lambda_0} \right]^{d_c} = |p - p_c|^{-1/\sigma} \tag{2.19}$$

is the characteristic mass of the largest finite cluster, where

$$\sigma = \frac{1}{\nu d_c} = \frac{1}{\nu d - \beta} . \tag{2.20}$$

Once the distribution of clusters over masses (2.17) is known, it is easy to calculate the rest of the critical exponents defined in Eqs. (2.8). The result is

$$\alpha = 2 - \nu d, \quad \gamma = \nu d - 2\beta, \quad \delta = \frac{\nu d}{\beta} - 1 . \tag{2.21}$$

If one is interested in the cluster distribution both in the scaling region, $1 < s < s(\xi)$, and in the region of exponential decay, $s > s(\xi)$, a more general formulation of the self-similar distribution may be used. Stauffer (1979) gives the universal scaling in the form

$$n_s(p) = s^{-\tau} f((p - p_c) s^{\sigma}), \quad |p - p_c| \ll 1, \quad s \gg 1 , \tag{2.22}$$

where the universal function $f(z)$ is finite for $z \to 0$ and falls off exponentially for $|z| \to \infty$. Equation (2.22) is a generalization of our simple argument.

C. The universality of critical behavior

A fundamental concept in the physics of phase transitions is the universality of critical exponents. This concept reduces the enormous number of different models to a few universality classes whose sets of critical indices are to be calculated and tabulated. This happy circumstance by no means implies that the calculation of the exponents is easy. In a sense, it is the job for the whole physics of critical phenomena (Domb *et al.*, 1972–1988). In these terms, the percolation problem belongs to one of the simplest universality classes, which is usually called the *universality class of random, or uncorrelated, percolation.* It was established that the critical exponents ν and β, as well as all others, do not depend on the kind of lattice (e.g., square, triangular, etc.) or the kind of percolation problem (site or bond). The only "crude" parameter that affects the value of the exponents is the dimension d of the ambient space. This statement has been confirmed by a vast variety of numerical experiments and is not subject to any serious doubt. (For a partial violation of universality in continuum models, see Sec. II.E.)

There may be seen a certain analogy between the universality of critical behavior in lattice models and the universal behavior of singularities of differentiable mappings studied in the framework of the catastrophe theory (Poston and Stewart, 1978; Arnold, 1983). In both cases the corresponding power exponents are structurally stable; that is, they are unchanged by a small perturbation of the lattice model or the mapping, respectively. A principal difference between critical phenomena and universal catastrophes is that the critical exponents describe *long-range* (in real physical space) correlated behavior, whereas the catastrophe theory deals with the nonanalytical expansion of the inverse mapping (with respect to the original differentiable one) *near* the singular point.

The property of universality complies with the long-range self-similarity of percolation clusters. On spatial scales much longer than the lattice period λ_0, the fine texture of the lattice is "invisible" and thus cannot affect the long-range scaling properties of clusters near the percolation threshold. Formal renormalization-group arguments in favor of the equivalence between the site and the bond percolation were given in Nakanishi and Reynolds (1979) and Shapiro (1979). The universality suggests that one may consider the percolation problem on an irregular lattice, or even without any lattice, and to expect the same critical behavior as in regular-lattice models. This leads to the idea of continuum percolation (Sec. II.E) that exhibits critical properties similar to those of the lattice percolation problem.

One may change not only the lattice but also the rules of the game on it. Kertész *et al.* (1982) studied the percolation model with restricted valence. In this model, the number of occupied nearest neighbors of a site should not exceed the valence v; otherwise, the occupation of the site is prohibited. If v equals the coordination number (i.e., the number of the nearest neighbors of a given site on the lattice), the percolation is unrestricted. It was found that, while the percolation threshold depends on v, the correlation length exponent ν is invariant.

One may also test the patience of universality in other ways. For example, the definition of connectivity can be changed from the nearest-neighbor rule to the next-to-nearest neighbor. In general, one can introduce the range of interaction, or the connectivity range R, such that any two sites separated by a distance less than R are ascribed to the same cluster. Due to the better connectivity of sites, the percolation threshold $p_c(R)$ is decreased for larger R, with the apparent scaling of $p_c(R) \propto R^{-d}$ for R much greater than the lattice constant λ_0. Nevertheless, the exponents of this long-range connected percolation at finite R, studied by Quinn *et al.* (1976), Hoshen *et al.* (1978), and Gouker and Family (1983), did not sow noticeble differences from those of the standard nearest-neighbor ($R=\lambda_0$) percolation. A nontrivial scaling, however, may arise in the limit $R \to \infty$. Aharony and Stauffer (1982) provided a qualitative argument where, for large but finite connectivity radius R, the universal percolation scalings do hold in the immediate vicinity of the critical probability $p_c(R)$; however, as R goes to infinity, the width of this scaling region shrinks as

$$\frac{|p-p_c(R)|}{p_c(R)} \propto R^{-2d/(6-d)}, \quad R \gg \lambda_0 . \tag{2.23}$$

Interestingly, outside the range (2.23), namely, for

$$\left[\frac{R}{\lambda_0}\right]^{-2d/(6-d)} \ll \frac{|p-p_c(R)|}{p_c(R)} \ll 1 , \tag{2.24}$$

another nontrivial scaling takes place corresponding to the so-called classical or effective-medium percolation exponents $\nu=\frac{1}{2}$, $\beta=1$, etc., which are exact in the dimensions $d \geq 6$ (Stauffer, 1979). This conjecture was confirmed by the two-dimensional variable-R computation of Gouker and Family (1983), who convincingly traced both the standard percolation behavior $\nu=4/3$ and the classical limit $\nu=\frac{1}{2}$. This example demonstrates the typical *crossover* behavior from one universality class to another, as the parameters of a system are changed.

Bearing in mind the universality of critical exponents against finite connectivity length, so much more surprising were the numerical results of Meakin and Family (1986) and Grossman and Aharony (1986, 1987), who reported the fractal dimension d_u of the external perimeter of a 2D percolation cluster to be unambiguously less than $d_h=\frac{7}{4}$ under only a slight modification in the definition of the perimeter (see Sec. II.A). This observation led Grossman and Aharony to assume a hierarchy of hull fractal dimensions depending on the definition of the hull. Saleur and Duplantier (1987) ruled out this possibility by arguing that only two perimeter exponents are possible, $d_h=\frac{7}{4}$ (for the "natural hull"—SKW) and $d_u=\frac{4}{3}$ (for the "unscreened perimeter"—SAW). This conjecture appears to recover the concept of universality (although now more sophisticated).

Into the same class of universality may fall problems of quite different natures. Alexandrowicz (1980) proposed a model of a "critically branched self-avoiding walk" (CBSAW), which belongs to the universality class of random percolation, meaning that some of the CBSAW critical characteristics scale similarly to those of percolation clusters. Such an ansatz appeared to be quite useful for the computation of clusters. In a similar sense, we shall refer the contours of certain random potentials to the universality class of random percolation, meaning the same long-range scaling and distribution properties of the contours as those of the corresponding percolation hulls (see Sec. III).

The term "uncorrelated percolation" is not accidental. If one gradually introduces growing long-range correlations between sites or bonds, one will ultimately drive the percolation problem beyond the boundaries of its uncorrelated universality class.

D. Correlated percolation

The standard formulation of the lattice percolation problem assumes independent occupation of sites, characterized by a single parameter—the probability p. This simplified model does not take into account possible correlations that are present in most applications of interest. To allow for correlations, one can characterize the system by an infinite set of random variables θ_i, which are unity at occupied sites (i is the site number) and zero at vacant sites. The average value of θ_i is the occupation probability, $\langle \theta_i \rangle = p$. If the θ_i are independent, then the standard ("random") percolation model is recovered. In general, the site correlations are most simply characterized by the occupation correlation function

$$c_\theta(\mathbf{x}_i - \mathbf{x}_j) = \langle \theta_i \theta_j \rangle - p^2 . \tag{2.25}$$

For the percolation model to be viable, the critical behavior should be insensitive to short-range correlations, when the correlation function (2.25) falls off sufficiently fast (say, exponentially) at large distance $|\mathbf{x}_i - \mathbf{x}_j| \to \infty$. Harris (1974) studied the effect of short correlations on the cluster scaling in the model of a phase transition with randomly fluctuating local critical temperature. He derived the following criterion for the irrelevance of the fluctuations:

$$\nu > 2/d . \tag{2.26}$$

Using Eq. (2.21), the Harris criterion (2.26) can be equivalently written as $\alpha < 0$. The idea of this result is that the behavior of a long-range, near-critical cluster is determined by the occupation probability $p_\xi = \langle \theta_i \rangle_\xi$ averaged over a size of the order of the correlation length $\xi(p)$. The fluctuation of p_ξ can be estimated using the standard "$N^{-1/2}$ rule," where $N \propto \xi^d$ is proportional to the number of sites in a box with the size ξ_p: $\delta p_\xi / p_\xi \propto \xi^{-d/2}$. If we now require that δp_ξ be less than the critical proximity $|p-p_c| \propto \xi^{-1/\nu}$, then we arrive at inequality (2.26). As this criterion is fulfilled in any dimension (see Table III), we conclude that short-range correlations do not drive the percolation problem from

its standard universality class. In a more general context, the Harris criterion (2.26) determines the condition of the irrelevance of short-range "quenched" disorder for critical behavior (Weinrib and Halperin, 1983).

The critical behavior, however, can drastically change for *correlated percolation*, when the occupancy of different sites are long-range correlated. Mathematically, this is expressed by a slow (e.g., algebraic) decay of the correlation function (2.25). One such example is the Ising model, where the probabilities are proportional to the Boltzmann factor $\exp(-E/T)$ with the energy E determined self-consistently from the resulting distribution of sites (Coniglio *et al.*, 1977; Penrose *et al.*, 1978). This analogy is straightforward only in two dimensions, where the critical points of the magnetic and the percolation transition are the same (in 3D they are different).

In another approach to correlated percolation (Weinrib, 1984) the occupation probabilities p_i are considered to be random numbers defined by their average $\langle p_i \rangle = p$ and the correlation function

$$c_p(\mathbf{x}_i - \mathbf{x}_j) = \langle p_i p_j \rangle - p^2 . \tag{2.27}$$

So this formulation involves a two-step process. First, random p_i are drawn for each site; next, the site occupancy is generated according to the probabilities p_i: $\theta_i = \theta(p_i - r)$, where r is a random variable uniformly distributed in [0,1] and $\theta(x)$ is the Heaviside step function. Upon substituting the expression for θ_i into Eq. (2.25), we conclude that the two correlation functions are the same: $c_\theta(\boldsymbol{\rho}) = c_p(\boldsymbol{\rho}) \equiv c(\boldsymbol{\rho})$.

It is believed that, although insufficient for a complete characterization of the distribution of p_i, the two-point correlation function $c(\boldsymbol{\rho})$ contains enough information to determine the critical behavior. For an algebraically decaying correlation, $c(\boldsymbol{\rho}) \propto \rho^{2H}, H < 0$, the criterion of universality can be obtained analogously to the Harris criterion (2.26). Here, the fluctuation of the average occupation probability over the correlation scale ξ can be calculated to be

$$\delta p_\xi = (\langle (p_i - p)^2 \rangle_\xi)^{1/2} \propto \left[\xi^{-d} \int_0^\xi c(\boldsymbol{\rho}) \rho^{d-1} d\boldsymbol{\rho} \right]^{1/2} \propto \xi^H , \tag{2.28}$$

and instead of (2.26) we obtain the following criterion of the irrelevance of correlations:

$$H < -1/\nu . \tag{2.29}$$

For a slower falloff of the correlation function, $-1/\nu < H < 0$, the percolation problem becomes essentially correlated. In this case, the critical behavior becomes different; in particular, the exponent ν is replaced by a new one (Weinrib and Halperin, 1983; Weinrib, 1984),

$$\tilde{\nu}(H) = -1/H > \nu, \quad -1/\nu < H < 0 . \tag{2.30}$$

Here the tilde distinguishes the correlated percolation exponent from that of the uncorrelated percolation. Result (2.30) corresponds to the threshold proximity $|p - p_c|$ balanced by the probability fluctuation (2.28).

Isichenko and Kalda (1991b) have used a heuristic scale-separation method to conjecture that the beta exponent of correlated percolation is the same as in random percolation,

$$\tilde{\beta}(H) \equiv \beta, \quad -1/\nu < H < 0 , \tag{2.31}$$

a result different from the renormalization-group expansion in a series of powers of $(6-d)$ (Weinrieb, 1984; for detailed discussion, see Sec. III.E.5). The same method applied to the 2D hull exponent evaluation leads to the result (see Sec. III.E)

$$\tilde{d}_h(H) = 1 + (1-H)(d_h - 1)\frac{\nu}{\nu+1} = \frac{10-3H}{7} ,$$
$$d = 2, \quad -1/\nu < H < 0 . \tag{2.32}$$

The correlated hull exponent (2.32) is identified with the fractal dimension of a contour line of a random function with a power-law correlator. As a three-dimensional hull has the same fractal dimension as the cluster, we conclude analogously to (2.14) that

$$\tilde{d}_h(H) = \tilde{d}_c(H) = d - \tilde{\beta}(H)/\tilde{\nu}(H) = 3 + \beta H ,$$
$$d = 3, \quad -1/\nu < H < 0 . \tag{2.33}$$

For correlated percolation, the same scaling arguments are valid as those used in the random percolation problem. In particular, one can calculate other correlated exponents, $\tilde{\alpha}, \tilde{\gamma}, \tilde{\delta}$, using relations similar to (2.21). Notice that formula (2.13) for the hull exponent cannot be simply generalized for the correlated percolation problem or for higher dimensions. Relations (2.13) and (2.32) are not consequences of scaling arguments but are rather first-principle results.

When the correlation function exponent H approaches zero from below, the correlation length exponent (2.30) tends to plus infinity, implying the presence of an infinite cluster for an arbitrary probability p—that is, the percolation threshold disappears. This behavior without threshold is extended to the case of *growing* correlations with $0 < H < 1$, whose continuum analog is studied in the framework of the theory of fractional Brownian functions (Sec. III.B). Although the exponent ν has no definite meaning in this case, the hull exponent (2.32) is still sensible, describing the fractal dimension of (individual) fractional Brownian islands (Sec. III.E).

E. Continuum percolation

Although the lattice formulation of the percolation problem is very convenient for both analytical and numerical studies, most natural disordered systems lack perfect lattice structure and require a different approach. The universality of percolation critical exponents well withstands moderate violence such as introducing short-range correlations or changing the type of lattice within

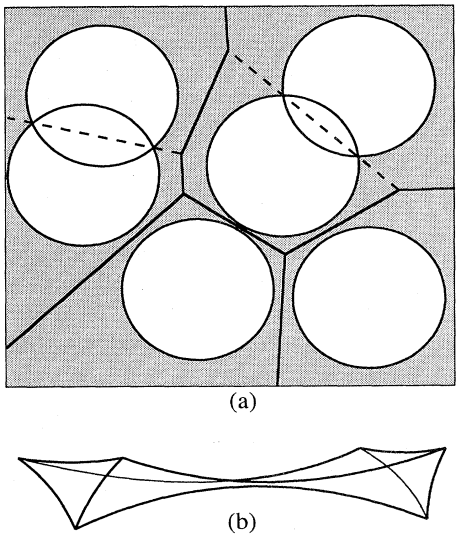

FIG. 8. The "Swiss-cheese" model. (a) The problem of circular voids in a background 2D transport medium. The sites of the equivalent lattice lie in the vertices of the Voronoi polyhedra (the sets of points from which a given void center is the closest one). The edges of the polyhedra represent bonds (solid lines). (b) A "neck" lying between three spherical voids.

the same dimensionality. This invokes the idea that the very existence of a lattice is unnecessary. The *continuum percolation problem* has various formulations, among which the following three are the most popular.

(a) In the *problem of voids*, or "Swiss-cheese" model (Halperin *et al.*, 1985), equally sized (or size-distributed) spherical voids are placed at random in a uniform transport medium (Fig. 8). The spherical holes are allowed to overlap with one another. At a critical value of the hole-volume fraction, the infinite cluster of the underlying medium ceases to exist and the system fails to support any transport or to exhibit a mechanical rigidity. The "Swiss-cheese" model may be appropriate for describing transport and elastic properties of porous media.

(b) In the *problem of spheres*, or "inverted Swiss-cheese" model, also known as the *problem of random sites* (Skal and Shklovskii, 1973; Pike and Seager, 1974), the roles of the two different media are switched: The spheres support the transport and the substrate does not (Fig. 9). One may introduce a "hard core" to model an "excluded volume" repulsive interaction between the spheres (Gawlinski and Redner, 1983; Balberg, 1987a). Such interaction is nothing more than a short-range correlation, which can shift the percolation threshold but leaves the critical exponents intact. At a critical filling factor, $\eta=\frac{4}{3}\pi nr^3$ for $d=3$ and $\eta=\pi nr^2$ for $d=2$ (where n is the density and r the radius of the spheres or discs), the overlapping spheres form an infinite cluster, and the system is able to support a long-range current. It was found that the critical parameter equals $\eta_c\simeq 1.1$ in two dimensions, and $\eta_c\simeq 0.35$ in three dimensions (see Table V). The percolation threshold η_c is only slightly changed by the interaction of spheres (Pike and Seager, 1974; Bug *et al.*, 1985). The fraction ϕ of volume occupied by randomly overlapping objects is less than η (and of course $\phi<1$) and is determined by the simple formula (Shante and Kirkpatrick, 1971)

$$\phi=1-\exp(-\eta)\ , \tag{2.34}$$

which is valid in the limit of a large number of objects. The model of random sites was used to describe hopping conduction in doped semiconductors (Shklovskii and Efros, 1984) and phase transitions in ferromagnetics (Abrikosov, 1980).

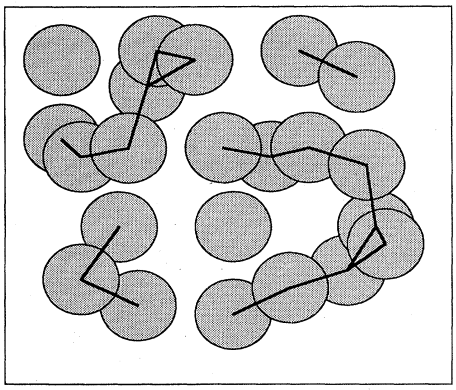

FIG. 9. Problem of random sites (overlapping discs).

(c) In the *potential model*, a smooth random function $\psi(\mathbf{x})$ is considered, and one is interested in the geometry of regions where $\psi(\mathbf{x})\le h=\text{const}$ (see Fig. 10). This model was invoked for the processes of localization of quasiclassical electrons (Ziman, 1969; Zallen and Scher, 1971) where $\psi(\mathbf{x})$ is the potential created by disordered impurities and h is the energy of an electron. The inequality $\psi(\mathbf{x})\le h$ then specifies the classically allowed area for the electron. Above a critical energy level $h=h_c$, a connected subset (cluster) of the allowed region stretches to infinity and electrons can conduct electric current; otherwise, on a macroscopic scale the system behaves like an insulator. The potential model is also relevant for the quantized Hall effect (Trugman, 1983). To describe critical levels of the potential continuum model, Zallen and Scher (1971) used the compelling device of a "flooded landscape," where $\psi(x,y)$ stands for the shape of the Earth relief and h denotes the water level; so the inequality $\psi(x,y)\le h$ describes the flooded area. At sufficiently low h, one clearly has only "ponds" and "lakes" in an infinite land [Fig. 10(a)], whereas at higher levels there will be localized islands in an infinite ocean [Fig. 10(c)]. The specification of two-dimensional geometry implies the impossibility of the simultaneous existence of both land and marine paths to infinity for a generic isotropic landscape. This leads to the existence of a sharp transition, at a certain critical level $h=h_c$, from percolating land to percolating ocean, when the last infinite land path disappears and the first infinite sea path is conceived. Thus at this critical level $h=h_c$ there does

TABLE V. Percolation thresholds in continuum models.

d	Model	η_c		ϕ_c
2	Overlapping disks with the density n and the radius R, $\eta=\pi R^2 n$	1.12 ± 0.06[1(a)]		0.674 ± 0.04[1(a)]
		1.16 ± 0.02[(b)]	$\Longleftarrow$	0.688 ± 0.005[2(a)]
		1.128 ± 0.005[3(a)]	$\Longrightarrow$	0.676 ± 0.002[(b)]
		1.1314[4(a)]	$\Longrightarrow$	0.677[(b)]
		1.175[11(f)]	$\Longrightarrow$	0.691[(b)]
2	Overlapping squares with the density n and the side R, $\eta=nR^2$	1.10[5(a)]	$\Longrightarrow$	0.667[(b)]
		1.11 ± 0.04[6(a)]	$\Longrightarrow$	0.670 ± 0.013[(b)]
		1.10 ± 0.05[1(a)]		0.668[1(a)]
2	Overlapping, random-angle sticks with the density n and the length R, $\eta=nR^2$	5.71 ± 0.12[1(a)]		0
2	Potential model	Not defined		$1/2$[7(c)]
				0.41[8(d)]
				0.387[9(e)]
3	Overlapping spheres with the density n and the radius R, $\eta=\frac{4}{3}\pi nR^3$	0.350 ± 0.008[1(a)]	$\Longrightarrow$	0.295 ± 0.006[(b)]
		0.3480[4(a)]	$\Longrightarrow$	0.294[(b)]
		0.349; 0.355[11(f)]	$\Longrightarrow$	0.294; 0.299[(b)]
3	Overlapping cubes with the density n and the side R, $\eta=nR^3$	0.325[11(f)]	$\Longrightarrow$	0.277[(b)]
3	Potential model	Not defined		0.17 ± 0.01[10(a)]

[1]Pike and Seager (1974).
[2]Vicsek and Kertész (1981).
[3]Gawlinski and Stanley (1977).
[4]Lee (1990).
[5]Domb and Sykes (1960).
[6]Gawlinski and Redner (1983).
[7]Zallen and Scher (1971).
[8]Smith and Lobb (1979).
[9]Weinrib (1982).
[10]Skal *et al.* (1973).
[11]Alon *et al.* (1990).

[(a)]Monte Carlo simulation.
[(b)]Calculated using formula (2.34).
[(c)]Exact for a statistically sign-symmetric potential.
[(d)]Photolithographic film experiment.
[(e)]For the square modulus of a complex Gaussian random field.
[(f)]Direct-connectedness expansion.

exist an infinite coastline—a contour of the potential $\psi(x,y)$ enveloping an incipient infinite cluster [Fig. 10(b)]. For a random function $\psi(\mathbf{x})$, whose statistical properties are equivalent to those of $-\psi(\mathbf{x})$ [without any loss of generality we may put the average $\langle\psi(\mathbf{x})\rangle=0$], the sign symmetry leads to the critical level $h_c=0$ and the area-occupation fraction $\phi_c=\frac{1}{2}$ (Zallen and Scher, 1971). This result is due to the unique value of the percolation level in two dimensions.

In the three-dimensional case, there may exist simultaneous percolation through both 3D "land" and 3D "ocean," as the topology of space admits nonintersecting, statistically isotropic paths to infinity. So one may introduce two percolation levels, $h_{c1}(\equiv h_c)$ and h_{c2}, such that for $h<h_{c1}$ there is percolation only through land $[\psi(\mathbf{x})>h]$, for $h>h_{c2}$ there is percolation only through sea $[\psi(\mathbf{x})<h]$, and in the interval $h_{c1}<h<h_{c2}$ the sea and the land percolate simultaneously. For a sign-symmetric distribution of $\psi(\mathbf{x})$, one has $h_{c1}=-h_{c2}\neq0$ (Shklovskii and Efros, 1984).

Zallen and Scher (1971) proposed to use, instead of the level h, the fraction of "wet" volume,

$$\phi=\phi(h)=\int_{-\infty}^{h}P(h')dh' , \tag{2.35}$$

where $P(h)$ is the distribution function of $h=\psi$ at a point $\mathbf{x}$, and the stationarity of the potential $\psi(\mathbf{x})$—that is, the independence of $P(h)$ of $\mathbf{x}$—is assumed. The critical area fraction, $\phi_c=\frac{1}{2}$, for a 2D sign-symmetric [i.e., $P(h)=P(-h)$] potential is somewhat higher than the critical space occupation probability for lattices (Scher and Zallen, 1970), ϕ_c(2D lattice)$=0.44\pm0.02$. Unlike

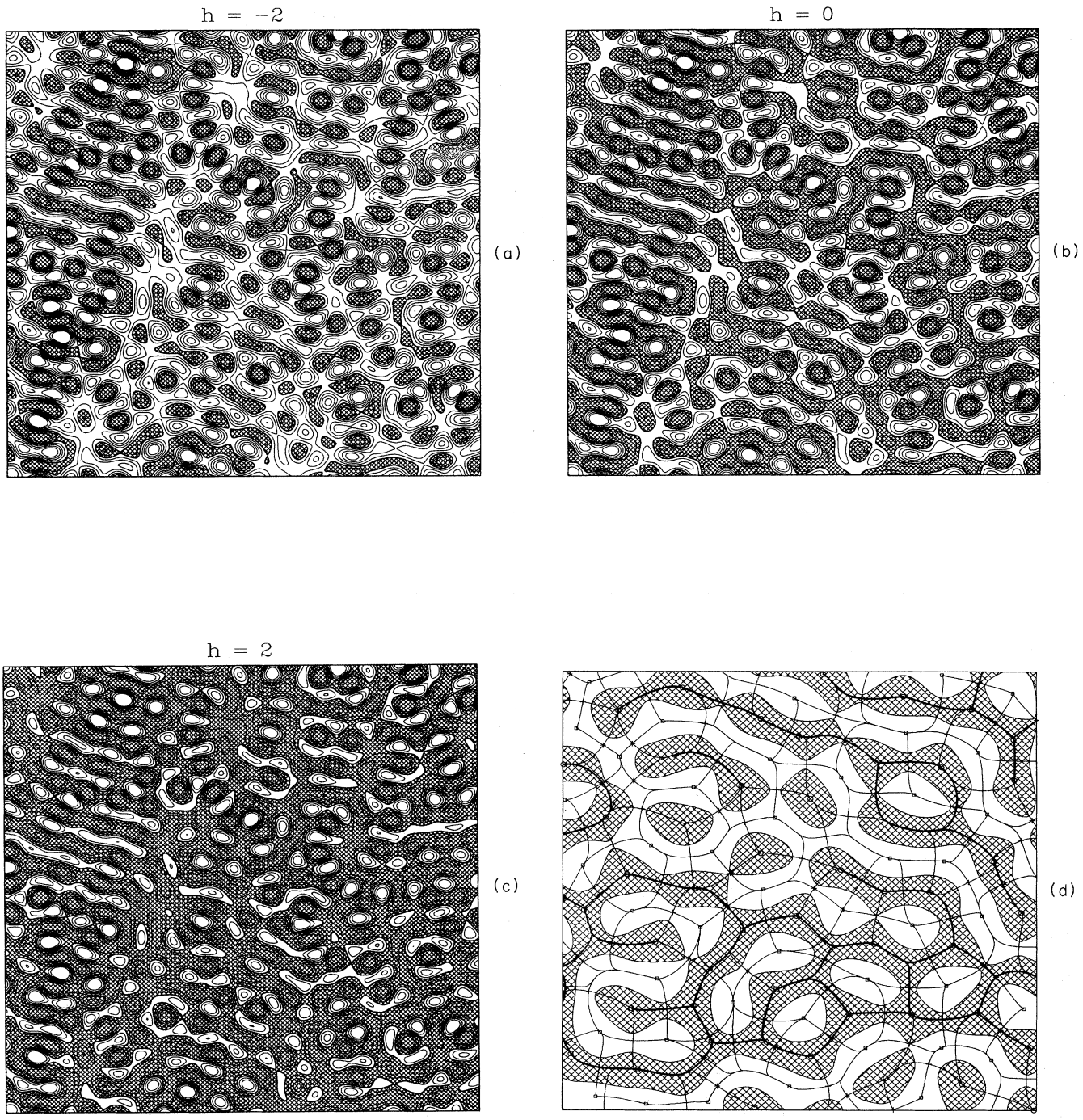

FIG. 10. Potential continuum percolation model in two dimensions: (a) undercritical level $h<h_c$; (b) critical level $h=0=h_c$; (c) overcritical level $h>h_c$; (d) the equivalent lattice of the potential $\psi(x,y)$. Squares and circles denote maxima and minima of ψ, respectively. The steepest descent/ascent paths, connecting the maxima and the minima, cross at the saddle points (shown by +). Bonds on the equivalent lattice connect adjacent minima and are "conducting" (shown heavy) if the corresponding saddle point lies below $h=h_c=0$. To model a random potential, the quasiperiodic function $\psi(\mathbf{x})=\sum_{i=1}^{N}\sin(\mathbf{k}_i\mathbf{x}+\theta_i)$ was taken, where $N=25$, $\mathbf{k}_i=(\cos\alpha_i,\sin\alpha_i)$, and α_i and θ_i are random numbers uniformly distributed in $[0,2\pi]$. The window size is 100×100 (a)–(c) and 45×45 (d). [This stream function satisfies the time-independent 2D Euler equation for an incompressible ideal fluid: $\partial(\psi,\nabla^2\psi)/\partial(x,y)=0$.]

the critical level h_c, the three-dimensional value of $\phi_c \simeq 0.15$ (Zallen and Scher, 1971) is much more universal with respect to particular models of the potential. This quantity turned out to be very close to the corresponding lattice critical volume fraction, ϕ_c(3D lattice)$=0.154\pm0.005$. Skal *et al.* (1973) confirmed this conjecture by calculating ϕ_c for several different Gaussian 3D potentials, which all gave very close results: $\phi_c=0.17\pm0.01$.

The percolation thresholds in the continuum are known mainly from Monte Carlo computation, although some analytical approaches were worked out recently (Alon *et al.*, 1990, 1991). The percolation thresholds of some continuum models are summarized in Table V.[1]

It was established (Pike and Seager, 1974; Geiger and Stanley, 1982; Elan *et al.*, 1984) that the static exponents describing the geometrical properties of continuum clusters near the percolation threshold are in the same universality class as those of lattice models in corresponding dimensions. The dynamic exponents, on the contrary, were found to be not universal, varying from one continuum model to another. (There does exist the universality of the transport exponents within the subclass of lattice models.) Feng *et al.* (1987) explained the universality of static exponents and the nonuniversality of dynamic exponents using mappings of continuum models onto irregular-lattice models.

The Swiss-cheese model is mapped onto bond percolation for a lattice whose bonds are the boundaries of the Voronoi polyhedra constructed around the voids (Elan *et al.*, 1984). A bond is blocked if the corresponding pair of voids are overlapping (Fig. 8). In the inverted Swiss-cheese model, the sites of the equivalent lattice lie in the centers of the spheres (Fig. 9).

The mapping of the potential model onto a lattice was proposed by Ziman (1969) and, more explicitly, by Weinrib (1982). In these constructions, the sites are associated with the local minima of $\psi(\mathbf{x})$, and the bonds come through saddle points connecting two valleys [Fig. 10(d)]. Then the contour lines are the external and internal perimeters of the bond percolation clusters on the equivalent (irregular) lattice. Two neighboring flooded valleys form a connected lake if the water level h exceeds the elevation ψ_s of the mountain pass (saddle) between them. So the inequality $\psi_s < h$ means that the bond coming through the saddle is conducting, whereas at $\psi_s > h$ it is blocked: $\theta_i=\theta[h-\psi_s(\mathbf{x}_i)]$. The bond probability $p(h)=\langle\theta_i\rangle$ is then given by

$$p(h)=\int_{-\infty}^{h} P_s(\psi_s)d\psi_s \ , \tag{2.36}$$

where $P_s(\psi_s)$ is the density of saddle points per unit ψ interval. Similarly, the bonds on the equivalent lattice for the potential $-\psi(\mathbf{x})$ connect maxima of $\psi(\mathbf{x})$ and come through its saddles. In two dimensions, through a nondegenerate saddle point come only two (mutually perpendicular) lines of steepest descent; hence the equivalent lattice of $-\psi(\mathbf{x})$ matches that of $\psi(\mathbf{x})$ [see Fig. 10(d)]. In the case of a statistically sign-symmetric potential $\psi(\mathbf{x})$, where the critical probabilities of these two lattices are the same, we obtain $p_c=\frac{1}{2}$; hence $h_c=0$.

Trugman and Doniach (1982) established the mapping of a potential model, where the potential $\psi(\mathbf{x})$ was defined at random in the sites $\mathbf{x}_i$ of a triangular lattice and linearly interpolated between these sites, to the lattice site percolation problem. For the case of a symmetric distribution of $\psi(\mathbf{x}_i)$, they related the exact critical level $h_c=0$ to the exact critical probability $p_c(T,s)=\frac{1}{2}$ (see Table II). Gruzinov *et al.* (1990) used a similar approach in which one starts from a degenerate, periodic potential $\psi(\mathbf{x})$, then lifts the degeneracy by a small random perturbation (Fig. 11). This procedure maps the potential continuum problem onto the bond percolation problem on a square lattice with $p_c(S,b)=\frac{1}{2}$.

The existence of these mappings clearly explains the universality of static critical exponents in the absence of long correlations in the potential $\psi(\mathbf{x})$. In Sec. III.C we show that the criterion for the universality of critical behavior in the potential continuum model is the sufficiently fast decay of the correlator,

$$C(\boldsymbol{\rho})=\langle\psi(\mathbf{x}+\boldsymbol{\rho})\psi(\mathbf{x})\rangle=O(\rho^{-2/\nu}) \ . \tag{2.37}$$

For the power-law behavior $C(\boldsymbol{\rho})\propto\rho^{2H}$, $-1/\nu<H<0$,

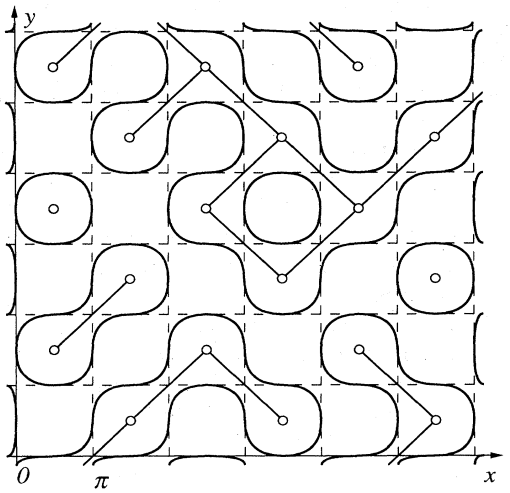

FIG. 11. Level lines $\psi(x,y)=h$ of the potential $\psi(x,y)=\sin x\sin y+\epsilon\psi_1(x,y)$, $\epsilon\ll1$, $|h|\le\epsilon$, where ψ_1 takes on independent random values with zero mean and unit variance in the unperturbed saddle points (where $\sin x\sin y=0$). The contours of this potential represent the external and internal hulls of bond percolation clusters [$p(h)=1/2+h/\epsilon$] on a 2D square lattice with the sites $\{(x,y)$: $\sin x\sin y=-1\}$. At $h=0$ there exists an infinite contour corresponding to the external hull of the critical infinite cluster [$p(0)=\frac{1}{2}=p_c$].

[1]In many references cited in Table V the critical parameter $B_c=2^d\eta_c$ ("the average number of bonds per site") is used. For the sake of uniformity the threshold values are recalculated in terms of the critical filling factor η_c.

the continuum potential model is mapped onto the correlated percolation problem (Sec. II.D).

Regarding the dynamic characteristics, their universality may indeed break, even with universal static exponents, due to broadly varied "strengths of the bonds" resulting from the mapping. Consider, for example, the Swiss-cheese model. Random overlapping of voids leads to randomly varying widths of "necks" (bonds) passing between three neighboring spherical holes [Fig. 8(b)]. The probability distribution of the neck widths remains finite for the width tending to zero; hence the equivalent lattice resistor network has a broad (power-law) distribution of the bond resistances, in contrast to the standard lattice problem where each resistance is either zero or 1. This state of affairs leads to a possible change in transport exponents (Sen *et al.*, 1984; Halperin *et al.*, 1985; Bunde *et al.*, 1986; Lubensky and Tremblay, 1986; Machta *et al.*, 1986; Machta, 1988). Feng *et al.* (1987) analyzed the bond strengths and found that in all three two-dimensional continuum models the conductivity exponent μ is the same as in a standard lattice model, whereas in the 3D Swiss-cheese model μ exceeds its lattice counterpart. The inverted Swiss-cheese model and the potential model preserve the universal (lattice) value of the conductivity exponent μ in three dimensions. A similar analysis was done for the elasticity and permeability exponents. The discussion of experimental data on nonuniversal conductivity in carbon-black-polymer composites was given by Balberg (1987b).

Due to the diversity of various continuum models, of which we discussed only the simplest, the concept of universality of the continuum has a broader sense. Here, the universality means the invariance of critical exponents with respect to gradually changed parameters of the random ensemble (voids, potentials, etc.), provided that these parameters lie within well-defined boundaries of the corresponding universality class. In other words, the critical exponents are piecewise constant functions of the parameters of the model. In these terms, the correlated percolation is not universal, because its critical exponents (2.30)–(2.33) can depend continuously on the parameter H. One may call such a behavior a continuous universality class.

Another approach to the concept of universality can be suggested that does not deal with an ensemble. Instead, a particular realization of, say, potential $\psi(\mathbf{x})$ can be considered and the corresponding critical indices introduced. Then the potential is infinitesimally perturbed by a smooth function whose correlator decays sufficiently fast, and the new critical exponents are determined. If for any such perturbation the exponents remain *exactly the same*, then the initial potential $\psi(\mathbf{x})$ is said to be structurally stable. The concept of structural stability is the central one in the catastrophe theory (Poston and Stewart, 1978; Arnold, 1978, 1983). In various applications, one is usually concerned not with an ensemble of random potentials but rather with a unique but *generic* realization, if there are no special reasons for the potential to be degenerate in one way or another. The intuitive notion of "generic" corresponds to the well-formalized concept of "structurally stable."

For a structurally unstable (degenerate) function, the critical behavior may be different. Trugman and Weinrib (1985) proposed an interesting example of continuous percolation for the potential $W(\mathbf{x})=[\psi(\mathbf{x})-h_0]^2$, where h_0 equals the critical level of $\psi(\mathbf{x})$. Such a system exhibits exotic behavior: its percolation threshold is zero in terms of both the critical level h_c and the critical volume fraction ϕ_c, and the exponents are different from those of the universality class of random percolation. The "$\phi_c=0$" potential $W(\mathbf{x})$ is structurally unstable: any mismatch of h_0 from the critical level of $\psi(\mathbf{x})$ drives the problem to the universality class of standard percolation.

In summary, continuum percolation theory treats the connectivity properties of randomly distributed objects; it has much in common with lattice percolation. Specifically, the contour lines and surfaces of a random potential are associated with the hulls of percolation clusters. In the next section, we discuss the statistics of contours in more detail. For various applications, one may also be interested in the geometry of more complicated objects, such as the regions occupied by level contours with diameters of the given order a, regardless of the level h. These and other issues will be discussed in the framework of a more general *statistical topography*, for which continuum percolation should be regarded as a prerequisite.

III. STATISTICAL TOPOGRAPHY

The term "statistical topography" was introduced by Ziman (1979) for the theory of the shapes of random fields, with a special emphasis on the contour lines and surfaces of a random potential $\psi(\mathbf{x})$. One of the first studies on this subject was undertaken by Rice (1944, 1945), who was basically concerned with random functions of one variable, in respect to the noise effects on telephone transmission. For a Gaussian noise $\psi(t)$, Rice derived the expected frequency of the crossings $\psi(t)=h$ for a given sensitivity threshold h. Longuet-Higgins (1957a, 1957b, 1957c, 1957d) generalized Rice's approach to a two-dimensional random function $\psi(x,y)$ and applied its topographic properties to the specks and twinkles on a random water surface (Longuet-Higgins, 1960a, 1960b, 1960c). The statistics of contour lines were also invoked for studying the information contents of two-dimensional images, for example, in television (Swerling, 1962). A mathematical survey of the statistical topography of Gaussian random fields was given by Adler (1981).

The most compelling example of statistical topography is presented by the diverse and whimsical patterns of natural coastlines and islands. The geographical considerations apparently inspired Mandelbrot (1967) to introduce the concept of fractals. After enjoying a considerable descriptive success, this approach gained predictive force with the introduction of "fractional Brownian functions" (Mandelbrot, 1975b; Berry and Hannay, 1978; Berry and

Lewis, 1980). These functions possess a power Fourier spectrum in a wide range of wavelengths. In turbulent media, such fields are usually described by Kolmogorov-type spectra (Zakharov, 1984). For example, this kind of spectrum for gravity waves results in fractal water surfaces (Stiassnie *et al.*, 1991).

Another approach to the problem of statistical topography has been developed, without any apparent connection to information theory, environmental studies, or turbulence, in the solid-state-physics community (Ziman, 1969; Zallen and Scher, 1971; Skal and Shklovskii, 1973), on the basis of (continuum) percolation theory. Study of the electronic structure of disordered materials inspired the "monoscale" percolation approach, since both the crystalline lattice and the known concentration of impurities suggested a well-defined characteristic scale of the problem. Ziman (1969) was the first to draw attention to the isosurfaces of random potentials that embrace classically accessible regions for the electron motion in a disordered potential. However, as general as the correspondence principle between quantum and classical mechanics might seem, there is no apparent relation between this quasiclassical localization and the intrinsically quantum effect of the Anderson localization of the electron wave function (Anderson, 1958; Thouless, 1974). An exception appears to be a two-dimensional electron gas in a strong magnetic field (Trugman, 1983), experimentally realized with a metal-oxide-semiconductor field-effect transistor (MOSFET; Prange and Girvin, 1990). This system has drawn much attention in the last decade since the discovery of the quantized Hall effect (von Klitzing *et al.*, 1980; von Klitzing, 1986).

More classical effects whose mechanisms depend on random isolines include anomalous diffusion in turbulent plasmas (Kadomtsev and Pogutse, 1979; Isichenko, 1991b; Isichenko and Horton, 1991) and the magnetoresistance of inhomogeneous plasmas and semiconductors (Dreizin and Dykhne, 1972; Kingsep *et al.*, 1990; Isichenko and Kalda, 1991a).

The investigation of transport processes in some random media requires detailed information about the distribution of random contours, whereas the random potential often possesses many length scales. The percolation approach was combined with the multiscale spectral description by Isichenko and Kalda (1991b), who used the heuristic method of the "separation of scales" to develop the statistical topography of random functions with algebraic spectra.

This section is organized as follows. In Sec. III.A the spectral and correlation properties of random functions are described and a discussion is given of the behavior of Gaussian random fields. In Sec. III.B the fractional Brownian approach is presented. In Sec. III.C we briefly return to monoscale reliefs to more generally restate their topographic properties related to the percolation behavior. Section III.D is devoted to the continuum problem of "graded percolation," corresponding to a monoscale potential with a small average gradient. In Sec. III.E the approach of the separation of scales is described in the context of the multiscale statistical topography. In Sec. III.F the statistical properties of the separatrices of random potentials are discussed.

A. Spectral description of random potentials and Gaussianity

When discussing a random potential $\psi(\mathbf{x})$, we should be specific and determine what exactly is random in ψ and what is not. Since we are particularly interested in the spatial geometry of the potential, the first idea is to characterize ψ by a correlation function (covariance),

$$C(\boldsymbol{\rho})=\langle \psi(\mathbf{x})\psi(\mathbf{x}+\boldsymbol{\rho})\rangle \ , \tag{3.1}$$

or by a delta variance,

$$\Delta(\boldsymbol{\rho})\equiv\langle [\psi(\mathbf{x})-\psi(\mathbf{x}+\boldsymbol{\rho})]^2\rangle =2[C(0)-C(\boldsymbol{\rho})] \ . \tag{3.2}$$

Here the angular brackets denote averaging over the statistical ensemble of $\psi(\mathbf{x})$. It is assumed that Eqs. (3.1) and (3.2) do not depend on $\mathbf{x}$—that is, the random potential $\psi(\mathbf{x})$ is *stationary* (or *homogeneous* in the turbulence nomenclature). For stationary random fields, the ensemble average is the same as the space average (over $\mathbf{x}$) for almost any realization of ψ (the ergodicity property). "For almost any" means "with probability 1."

For a general random field, the two-point correlation function (3.1) is insufficient to completely characterize the statistical ensemble. For a comprehensive description of $\psi(\mathbf{x})$, one needs to know the whole set of three-point, four-point, etc., correlation functions. For a Gaussian random potential, on the contrary, all properties of the ensemble can be extracted from only the average $\langle \psi(\mathbf{x})\rangle$ and the correlator $C(\boldsymbol{\rho})$. A standard approach is to take the Fourier expansion to be primary and to consider the Fourier components $\psi_{\mathbf{k}}$ to be independent random variables. Suppose the function $\psi(\mathbf{x})$ is periodic with a sufficiently large period $\mathcal{L}$ along each coordinate axis in a d-dimensional space. Then the Fourier series expansion,

$$\psi(\mathbf{x})=\sum_{\mathbf{k}} \psi_{\mathbf{k}} e^{i\mathbf{k}\cdot\mathbf{x}} \ , \tag{3.3}$$

is taken over the wave vectors $\mathbf{k}$ lying on the nodes of a d-dimensional simple hypercubic lattice with the period $k_{\mathcal{L}}=2\pi/\mathcal{L}$. Assume the following statistical properties of the Fourier harmonics:

$$\langle \psi_{\mathbf{k}}\rangle =0, \quad \langle \psi_{\mathbf{k}}\psi_{\mathbf{k}'}\rangle =P_{\mathbf{k}}\delta_{\mathbf{k}+\mathbf{k}'} \ . \tag{3.4}$$

We shall focus primarily on the case in which the spectral density $P_{\mathbf{k}}$ is an isotropic power function inside a wide wave-number range $[k_m,k_0]$,

$$P_{\mathbf{k}}\equiv\langle |\psi_{\mathbf{k}}|^2\rangle =k_{\mathcal{L}}^d A k^{-\gamma}, \quad k_{\mathcal{L}}\ll k_m<k<k_0 \ , \tag{3.5}$$

and P_k falls off sufficiently fast outside this interval. It is convenient to divide the scaling range $[k_m,k_0]$ into $\log_2(k_0/k_m)$ octaves and to represent the "multiscale" potential $\psi(\mathbf{x})$ as a sum of "monoscale" functions,

$$\psi(\mathbf{x})=\sum_{\lambda_i=2^i\lambda_0}\psi_{\lambda_i}(\mathbf{x})\ , \tag{3.6}$$

where the λ component $\psi_\lambda(\mathbf{x})$ is defined by the partial sum

$$\psi_\lambda(\mathbf{x})=\sum_{1/2<|\mathbf{k}|\lambda<1}\psi_{\mathbf{k}}e^{i\mathbf{k}\cdot\mathbf{x}} \tag{3.7}$$

and represents a function with a single characteristic length λ. Then the Fourier ($\mathbf{k}$) spectrum (3.5) can be translated into the "λ spectrum," defined by the root-mean-square (rms) value of the λ component of ψ:

$$\psi_\lambda\equiv[\psi_\lambda(\mathbf{x})]_{\rm rms}=\left[\sum_{1/2<|\mathbf{k}|\lambda<1}P_{\mathbf{k}}\right]^{1/2}. \tag{3.8}$$

Upon replacing the sum in Eq. (3.8) by an integral according to the usual rule $\sum_{\mathbf{k}}\to k_{\mathcal{L}}^{-d}\int d\mathbf{k}$, we obtain

$$\psi_\lambda=A_1\lambda^H,\quad \lambda_0\ll\lambda\ll\lambda_m\ , \tag{3.9}$$

$$H=\frac{(\gamma-d)}{2}\ , \tag{3.10}$$

$$A_1=\left[AS_d\frac{(2^{2H}-1)}{2H}\right]^{1/2}, \tag{3.11}$$

where $\lambda_0\equiv k_0^{-1}$, $\lambda_m\equiv k_m^{-1}$, and the numerical factor S_d equals 1 (for $d=1$), 2π (for $d=2$), or 4π (for $d=3$).

The representation of the λ spectrum (3.7)–(3.9) is very convenient because the power-law exponent H corresponds to the Hurst (hence the notation) exponent used by Mandelbrot (1983) and by many others in the context of fractional Brownian functions, where $0<H<1$ (Sec. III.B). The Hurst exponent of $\nabla\psi(\mathbf{x})$ is $(H-1)$. Moreover, the potential covariance (3.1) and the delta variance (3.2) are expressed through the Hurst exponent H in a universal way for each dimension d. Using Fourier expansion, Eq. (3.1) can be written as

$$C(\boldsymbol{\rho})=\sum_{\mathbf{k}}P_{\mathbf{k}}e^{i\mathbf{k}\cdot\boldsymbol{\rho}}\ . \tag{3.12}$$

The integral over $\mathbf{k}$ corresponding to the sum in (3.12) converges at both limits (so that we may put $k_m=0$, $k_0=\infty$ without significant change in result) if $-(d+1)/4<H<0$ ($d=1$, 2, or 3). Then we have

$$C(\boldsymbol{\rho})=\zeta_d A\rho^{2H},\quad \lambda_0\ll\rho\ll\lambda_m\ , \tag{3.13}$$

where

$$\zeta_1=2\Gamma(-2H)\cos\pi H,\quad \zeta_2=\frac{\pi\Gamma(-H)}{2^{2H}\Gamma(1+H)}\ ,\quad \zeta_3=-\frac{2\pi^2}{\Gamma(2H+2)\sin\pi H}\ , \tag{3.14}$$

and Γ denotes the Euler gamma function. Similarly, the series for the delta variance,

$$\Delta(\boldsymbol{\rho})=2\sum_k P_{\mathbf{k}}(1-e^{i\mathbf{k}\cdot\boldsymbol{\rho}})\ , \tag{3.15}$$

converges insensitive to k_m and k_0 for $0<H<1$ and equals

$$\Delta(\boldsymbol{\rho})=\eta_d A\rho^{2H},\quad \lambda_0\ll\rho\ll\lambda_m\ , \tag{3.16}$$

with the numeric coefficients

$$\eta_1=\frac{2\pi}{\Gamma(2H+1)\sin\pi H},\quad \eta_2=\frac{\pi\Gamma(1-H)}{2^{2H-1}H\Gamma(1+H)}\ ,\quad \eta_3=\frac{2\pi^2}{(2H+1)\Gamma(2H+1)\sin\pi H}\ . \tag{3.17}$$

Thus the correlation function is a useful spectral characteristic for negative H, whereas for $0<H<1$ the delta variance turns out to be more relevant.

A random potential defined by Fourier series (3.3) with independent random Fourier components $\psi_{\mathbf{k}}$ belongs to the important class of Gaussian random functions. Indeed, according to the Central Limit theorem, the sum of a large number of independent random variables is distributed with the Gaussian probability distribution function

$$P(h)=(2\pi\psi_0^2)^{-1/2}\exp\left[-\frac{(h-\langle\psi\rangle)^2}{2\psi_0^2}\right], \tag{3.18}$$

where h is the value of the potential ψ at a fixed point $\mathbf{x}$. The Gaussian distribution (3.18) is completely defined by two parameters: the expectation $\langle\psi\rangle$ and the variance $\psi_0^2\equiv\langle(\psi-\langle\psi\rangle)^2\rangle$. Gaussian random variables have the nice feature of additivity: A sum of several Gaussian random variables is also Gaussian, with both the expectation and the variance being the sum of the expectations and the variances of the constituents, respectively. Furthermore, the joint probability distribution of several Gaussian random variables ψ_i, $i=1,\ldots,n$, is given by the *multivariate Gaussian distribution* (Adler, 1981)

$$P(\psi_1,\ldots,\psi_n)=(2\pi)^{-n/2}(\det C_{ij})^{-1/2}\exp\left[-\frac{1}{2}\sum_{i,j=1}^{n}(\psi_i-\langle\psi_i\rangle)C_{ij}^{-1}(\psi_j-\langle\psi_j\rangle)\right], \tag{3.19}$$

where

$$C_{ij}=\langle(\psi_i-\langle\psi_i\rangle)(\psi_j-\langle\psi_j\rangle)\rangle \tag{3.20}$$

is the covariance matrix, and C_{ij}^{-1} denotes the element of the inverse matrix. Notice that the multivariate Gaussian distribution (3.19) is completely determined by the first- and second-order moments of the participating variables—that is, by the expectations $\langle\psi_i\rangle$ and the covariance matrix C_{ij}.

A random function $\psi(\mathbf{x})$ is a continuum set of random variables for each value of the parameter $\mathbf{x}$. A Gaussian random function is such that $\psi(\mathbf{x})$ is a Gaussian random variable for any $\mathbf{x}$. A stationary Gaussian random field is completely defined by its average (without loss of generality put $\langle\psi\rangle=0$) and its correlation function (3.1). Given $C(\boldsymbol{\rho})$, one can easily calculate the two-point probability density $P(\psi_1,\psi_2|\mathbf{x}_1,\mathbf{x}_2)$, which is defined so that the probability for the potential value $\psi(\mathbf{x}_1)$ to be within the interval $[\psi_1,\psi_1+d\psi_1]$ simultaneously with $\psi(\mathbf{x}_2)\in[\psi_2,\psi_2+d\psi_2]$ is $P(\psi_1,\psi_2|\mathbf{x}_1,\mathbf{x}_2)d\psi_1 d\psi_2$. Upon substituting $\psi_1=\psi(\mathbf{x}_1)$, $\psi_2=\psi(\mathbf{x}_2)$ into Eqs. (3.19) and (3.20), we find

$$P(\psi_1,\psi_2|\mathbf{x}_1,\mathbf{x}_2)=\frac{1}{2\pi\sqrt{\psi_0^4-C^2(\boldsymbol{\rho})}}\exp\left[-\frac{\psi_0^2(\psi_1^2+\psi_2^2)-2C(\boldsymbol{\rho})\psi_1\psi_2}{2[\psi_0^4-C^2(\boldsymbol{\rho})]}\right], \tag{3.21}$$

where $\boldsymbol{\rho}=\mathbf{x}_1-\mathbf{x}_2$ and the variance $\psi_0^2=C(0)$. In the limiting cases $\rho\to 0$ $[C(\boldsymbol{\rho})\to\psi_0^2]$ and $\rho\to\infty$ $[C(\boldsymbol{\rho})\to 0]$, Eq. (3.21) reduces to

$$P(\psi_1,\psi_2|\mathbf{x}_1,\mathbf{x}_2)=\begin{cases}P(\psi_1)\delta(\psi_1-\psi_2), & \rho\to 0\ , \qquad (3.22a)\\ P(\psi_1)P(\psi_2)\left[1+\dfrac{\psi_1\psi_2}{\psi_0^4}C(\boldsymbol{\rho})+\cdots\right], & \rho\to\infty\ . \qquad (3.22b)\end{cases}$$

Equation (3.22a) corresponds to the identical distribution of ψ_1 and ψ_2 as the points $\mathbf{x}_1$ and $\mathbf{x}_2$ become the same, whereas (3.22b) implies an asymptotically independent distribution of ψ_1 and ψ_2 in the limit of infinitely remote (uncorrelated) points $\mathbf{x}_1$ and $\mathbf{x}_2$. Three-point and higher probability densities can be calculated in quite a similar manner, making the formalism of Gaussian random fields quite workable.

There also exists another, field-theoretic formalism based on the Gaussian probability functional

$$P[\psi]\propto\exp\left[-\frac{1}{2}\int\psi(\mathbf{x}_1)\psi(\mathbf{x}_2)C^{-1}(\mathbf{x}_1-\mathbf{x}_2)d\mathbf{x}_1 d\mathbf{x}_2\right], \tag{3.23}$$

with the procedure of averaging involving functional, or path integration (cf. Abrikosov *et al.*, 1965; Feynman and Hibbs, 1965; Kleinert, 1990). For example, the correlation function (3.1) is calculated as

$$C(\boldsymbol{\rho})=\int\psi(\mathbf{x})\psi(\mathbf{x}+\boldsymbol{\rho})P[\psi]D\psi\ . \tag{3.24}$$

This formalism is not used in this paper.

The integral and the derivative of a Gaussian random function are also Gaussian. Hence one can calculate individual and joint distributions of various random quantities, such as the elevation ψ, the slope $\nabla\psi$, etc. Upon differentiating Eq. (3.1) with respect to $\boldsymbol{\rho}$, we obtain

$$\langle\psi^2(\mathbf{x})\rangle=C(0),\quad \langle\psi(\mathbf{x})\nabla\psi(\mathbf{x})\rangle=\frac{\partial C(0)}{\partial\boldsymbol{\rho}}\ ,$$
$$\langle\nabla_i\psi(\mathbf{x})\nabla_k\psi(\mathbf{x})\rangle=-\frac{\partial^2 C(0)}{\partial\rho_i\partial\rho_k}\ . \tag{3.25}$$

Expressions (3.25) can be used to calculate the expected measure $M_d(h)$ of the isoset $\psi(\mathbf{x})=h$ per unit volume. In d dimensions, the isoset is characterized by a $(d-1)$-dimensional measure: the number of crossings $\psi(x)=h$ or $d=1$, the total length of the contours $\psi(x,y)=h$ for $d=2$, and the total area of the isosurfaces $\psi(x,y,z)=h$ for $d=3$. The quantity $M_d(h)$ equals the modulus of $\nabla\psi(\mathbf{x})$ averaged over the joint distribution of ψ and $\nabla\psi$ at the given level $\psi=h$ (Rice, 1944, 1945; Longuet-Higgins, 1957a; Swerling, 1962):

$$M_d(h)=\langle|\nabla\psi|\rangle_{\psi=h}=\int|\mathbf{g}|P(h,\mathbf{g})d\mathbf{g}\ , \tag{3.26}$$

where $P(h,\mathbf{g})$ is the joint probability distribution function of $h=\psi$ and $\mathbf{g}=\nabla\psi$ at the same point $\mathbf{x}$. Upon using formulas (3.19) and (3.20) for the isotropic case $C(\boldsymbol{\rho})=C(\rho)$, we obtain

$$P(h,\mathbf{g})=\frac{1}{(2\pi)^{(d+1)/2}\psi_0\psi_0'^d}\exp\left[-\frac{h^2}{2\psi_0^2}-\frac{\mathbf{g}^2}{2\psi_0'^2}\right], \tag{3.27}$$

where

$$\psi_0'^2=-(1/d)C''(0) \tag{3.28}$$

is the variance of each component of $\nabla\psi$. Now formula (3.26) can be used to calculate the isoset measure $M_d(h)$. Averaging $|\mathbf{g}|=|\nabla\psi|$ over the distribution (3.27) at a fixed level $\psi=h$, we find the average frequency of the h-level crossings (Rice, 1944, 1945),

$$M_1(h)=\frac{1}{\pi\psi_0}\sqrt{-C''(0)}\exp\left[-\frac{h^2}{2\psi_0^2}\right], \tag{3.29}$$

and the average total length of the isolines $\psi(x,y)=h$ per unit area (Longuet-Higgins, 1957a; Swerling, 1962).

$$M_2(h)=\frac{1}{2\sqrt{2}\psi_0}\sqrt{-C''(0)}\exp\left[-\frac{h^2}{2\psi_0^2}\right]. \tag{3.30}$$

Knowledge of the correlation function $C(\boldsymbol{\rho})$ is sufficient for calculating other average characteristics, such as the number of the saddle points, maxima, and minima of $\psi(\mathbf{x})$. Rice (1944) derived the average number of maxima and minima in one dimension. The distribution of minima of a 3D Gaussian random potential was calculated by Halperin and Lax (1966) in the context of

the low-energy density of states of the Schrödinger equation with a disordered potential. Weinrib and Halperin (1982) investigated the density (per unit ψ interval) of saddles, maxima, and minima of the intensity of a 2D laser speckle field that was modeled by a complex Gaussian random function.

The investigation of the topological characteristics of isosets of Gaussian random fields is a much more difficult task. Swerling (1962) established certain inequalities for the number of connected contours comprising the isoset $\psi(x,y)=h$. Some other characteristics are given by Adler (1981). As discussed in Secs. III.C–III.E, percolation theory presents a powerful, although generally qualitative, tool for studying more subtle topological properties of level lines and surfaces.

Returning to the spectral description of random fields, notice that a decreasing power spectrum (3.9) with $H<0$ implies a finite variance ψ_0^2 of the potential within an arbitrarily large period $\mathcal{L}$, so the above results for Gaussian fields apply. A positive Hurst exponent H, which is the case for the Earth's relief, corresponds to an infinite variance of ψ for $\lambda_m \to \infty$. Nevertheless, this kind of profile may be treated locally using the delta variance $\Delta(\rho)$, which is the subject of the next subsection.

B. Brownian and fractional Brownian reliefs

The Brownian motion of a particle due to the thermal agitation of molecules in an ambient medium is the simplest natural example of a random process. The velocity in the Brownian motion, $d\mathbf{x}(t)/dt=\mathbf{v}_D(t)$, can be approximated on a macroscopic time scale t as a "white noise," that is, as a Gaussian random function with zero mean and with covariance

$$\langle v_{Di}(t)v_{Dj}(t')\rangle = 2D_0\delta_{ij}\delta(t-t') , \tag{3.31}$$

where D_0 is a molecular diffusion coefficient. Then the coordinate of the Brownian particle, $\mathbf{x}(t)=\int_0^t \mathbf{v}_D(t')dt'$, is also Gaussian with average $\langle \mathbf{x}(t)\rangle=0$ and covariance $\langle x_i(t)x_j(t')\rangle = 2D_0\delta_{ij}\min(t,t')$. Notice that $\mathbf{x}(t)$ is not a stationary random process, because its correlator is not a function of $(t-t')$. The delta variance defined by Eq. (3.2), however, is a function of $(t-t')$ and hence can serve as a useful characteristic of this process.

The Brownian motion is a convenient starting point for the generation of various random fields. A Brownian (line-to-line) function $B(x)$ is, by definition, a random function whose increments are Gaussian with zero mean and with variance

$$\langle [B(x_1)-B(x_2)]^2\rangle = b^2|x_1-x_2| . \tag{3.32}$$

The Brownian graph $\{x,B(x)\}$ [see Fig. 12(b)] is a self-affine fractal with the fractal dimension of $D=\frac{3}{2}$ (Taylor, 1955). Indeed, a part of this graph corresponding to the abscissa interval $[x_1,x_2]$ is covered by N_λ boxes with the size λ, where

$$N_\lambda \simeq \frac{x_2-x_1}{\lambda}\frac{[B(x+\lambda)-B(x)]_{\rm rms}}{\lambda} \propto \lambda^{-3/2}, \quad \lambda < b^2 . \tag{3.33}$$

The inequality displayed in Eq. (3.33) requires that the root-mean-square increment $B(x+\lambda)-B(x)$ be larger than λ in order to accommodate many covering squares. At larger scales, $\lambda \gg b^2$, the second factor in (3.33) must be replaced by unity leading to the fractal dimension $D=1$ (see Table I).

One can similarly define a *Brownian surface*, which is the graph of a *Brownian plane-to-line function* $B(x,y)$, namely, a Brownian line-to-line function of each of its arguments [Fig. 13(b)]. In a straightforward analogy to the above calculation, the fractal dimension of the 2D Brownian relief can be shown to be $D=\frac{5}{2}$, which, of course, complies with the cross-section rule (1.15), as a Brownian graph is a vertical (e.g., $y=$const) cross section of a Brownian surface. Another cross section of the Brownian surface can be obtained from a horizontal plane $B(x,y)=h=$const, with the same result for the fractal dimension, $D=\frac{3}{2}$, of the isoset $B(x,y)=h$ [Fig. 14(b)].

As the value $D=\frac{3}{2}$ appreciably overestimated the measured fractal dimensions of natural coastlines, the Brownian surface model of the Earth's relief was rejected and a generalization of the Brownian random function was introduced—a *fractional Brownian function* (Mandelbrot and Van Ness, 1968). The fractional Brownian function $B_H(\mathbf{x})$ of a d-dimensional argument $\mathbf{x}$ is, by definition, a Gaussian random process with the delta variance

$$\langle [B_H(\mathbf{x}_1)-B_H(\mathbf{x}_2)]^2\rangle = b^2|\mathbf{x}_1-\mathbf{x}_2|^{2H} , \tag{3.34}$$

where $H\in[0,1]$ is the Hurst exponent characterizing the spectrum of B_H. According to Eq. (3.16), the fractional Brownian function has a λ spectrum $(B_H)_\lambda \propto \lambda^H$ in an infinite scaling range ($\lambda_0=0$, $\lambda_m=\infty$). The ordinary Brownian function $B(\mathbf{x})$ is a particular case ($H=\frac{1}{2}$) of its fractional generalization: $B(\mathbf{x})=B_{1/2}(\mathbf{x})$. The fractional Brownian graph [$d=1$, $H\neq\frac{1}{2}$; see Fig. 12(a), 12(c)] and the standard Brownian graph [$d=1, H=\frac{1}{2}$; Fig. 12(b)] look qualitatively similar, differing only by the degree of irregularity, which decreases for increasing H. A measure of this irregularity can serve to define the fractal dimension D of the graph. Analogously to calculation (3.33), one finds $D=2-H$ (Orey, 1970) in the scaling range $\lambda < b^{1/(1-H)}$. The same fractal dimension, $D=2-H$, but in an infinite scaling range, refers to the horizontal cross section (isoset) of the fractional Brownian surface $z=B_H(x,y)$, whose own fractal dimension is clearly unity greater, $D=3-H$ ($\lambda < b^{1/(1-H)}$). For a random potential with the delta variance given by Eq. (3.34) with $H=0$ [and for $H<0$ entering the correlator (3.13)], the graph $\{x,B_H(x)\}$ attains the maximum allowed fractal dimension $D=d=2$, meaning the dense filling of the (x,y) plane by the short-scale oscillations of

the potential [Fig. 12(d)]. Still, the fractal dimension of a connected contour piece of such a potential [Fig. 14(d)] may be nontrivial (see Sec. III.E.1).

Another object associated with the function B_H is the trajectory of *fractional Brownian motion*, or the *fractional Brownian trail*, defined by $\mathbf{x}=\mathbf{B}_H(t)$, where each component of $\mathbf{B}_H(t)$ is an independent fractional Brownian function of one-dimensional time. Unlike the self-affine fractional Brownian graph, the fractional Brownian trail is a self-similar fractal. Given the box size λ, the time necessary to pass the distance λ is given by $t_\lambda \propto \lambda^{1/H}$. Then the covering number of a trajectory traversed over the period of time T is $N_\lambda \simeq T/t_\lambda \propto \lambda^{-1/H}$, for $H > 1/d$. Hence the fractal dimension of the fractional Brownian trail, embedded in a d-dimensional space, is given by the formula (Mandelbrot, 1983)

$$D = \min(1/H, d) \ . \tag{3.35}$$

For $H = \frac{1}{2}$ the standard Brownian motion is recovered with $D = 2$ that well explains the finite probability of the return of a random walker to the starting point in two dimensions (Fig. 2) and the zero return probability in three

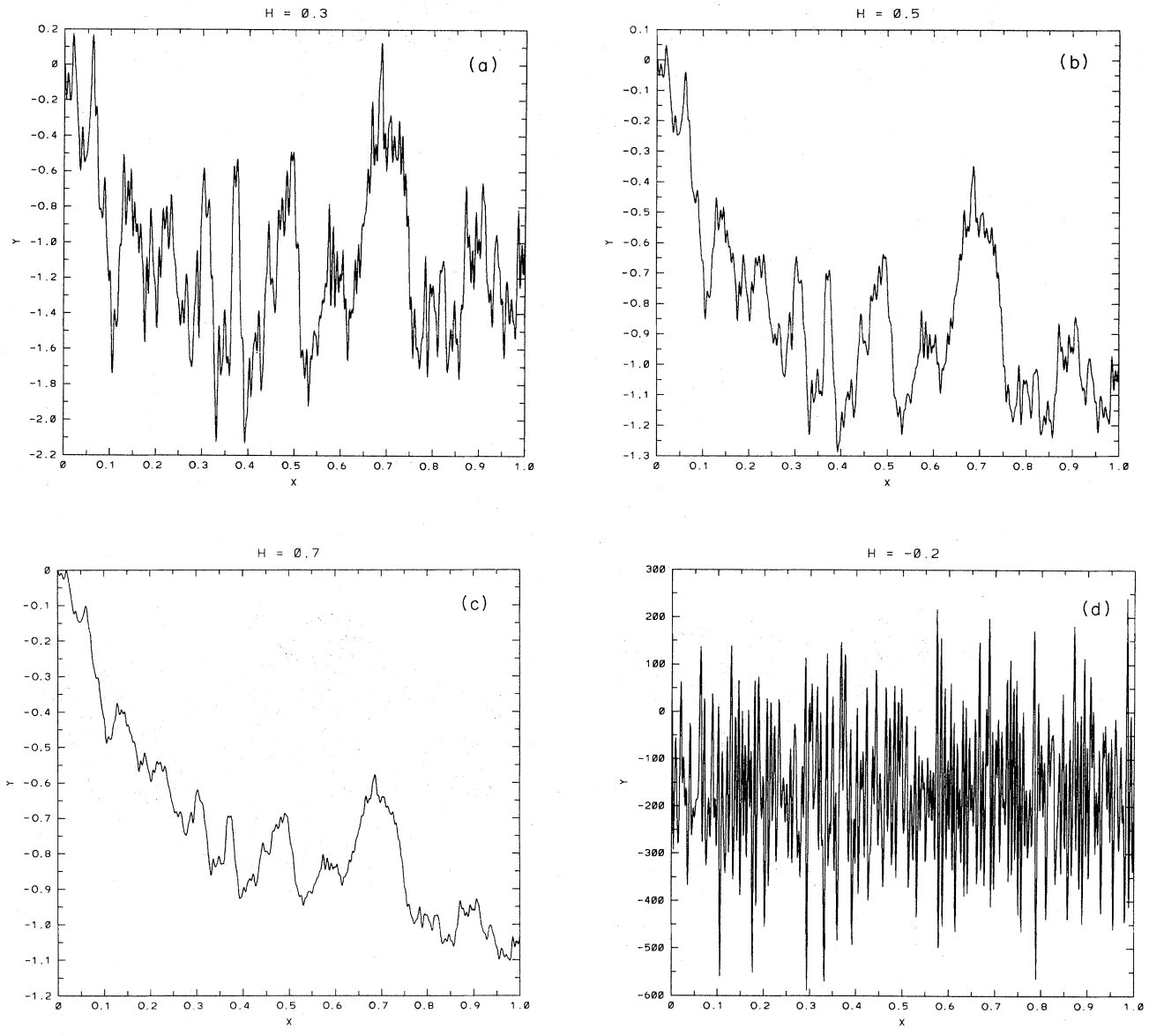

FIG. 12. Graphs of several realizations of line-to-line fractional Brownian functions (a–c): (a) $H = 0.3$ (antipersistent function); (b) $H = 0.5$ (standard Brownian function); (c) $H = 0.7$ (persistent function); (d) graph of a stationary Gaussian random process $y = \psi(x)$, $\psi_\lambda \propto \lambda^H$ with $H = -0.2$. The following model function was used in all four cases: $\psi(x) = \sum_{k=1}^{1000} \psi_k \sin(kx + \theta_k)$, with $\psi_k = k^{-(H+1/2)}$ and the θ_k being random numbers uniformly distributed in $[0, 2\pi]$. The scaling range of these graphs is $[10^{-3}, 1]$.

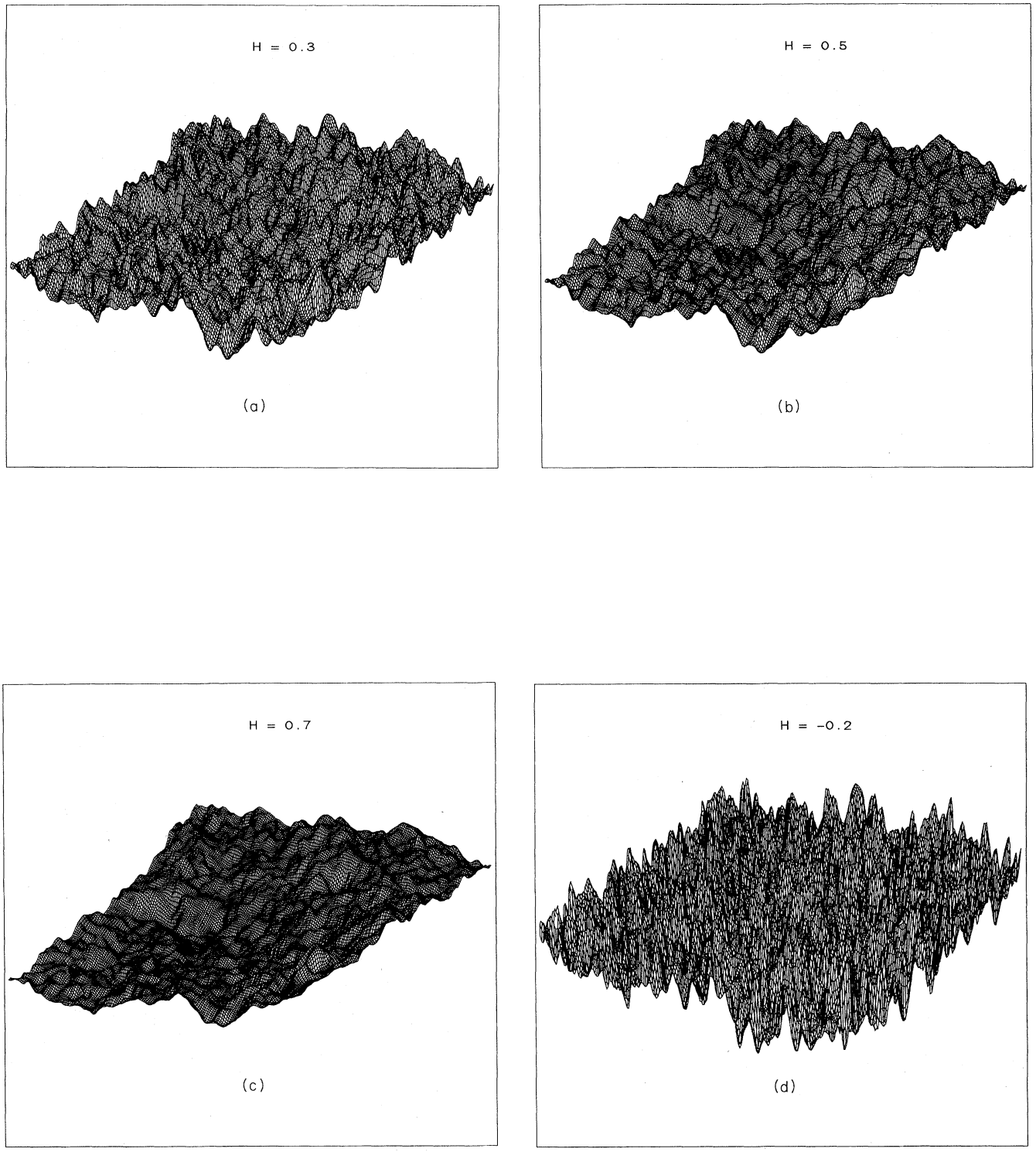

FIG. 13. Several realizations of fractional Brownian surfaces (a–c): (a) $H=0.3$; (b) $H=0.5$; (c) $H=0.7$; (d) graph of a stationary Gaussian random function $y=\psi(x,y)$, $\psi_\lambda \propto \lambda^H$ with $H=-0.2$. The vertical cross sections of these surfaces are similar to the corresponding graphs in Fig. 12. The following model potential was used in all four cases: $\psi(x,y)=\sum_{k_x=1}^{100}\sum_{k_y=1}^{100}\psi_k \sin(k_x x+k_y y+\theta_k)$, with $\psi_k=(k_x^2+k_y^2)^{-(H+1)/2}$ and the θ_k being random numbers uniformly distributed in $[0,2\pi]$. The scaling range is $[10^{-2},1]$.

dimensions (cf. Rammal, 1984).

The fractional Brownian function $B_H(x)$ can be generated by its Fourier spectrum (as shown in Figs. 12–14), or it can be obtained directly from $B(x)$ with the help of fractional differentiation (for the "antipersistent" case $H<\frac{1}{2}$) or fractional integration (for the "persistent" case $H>\frac{1}{2}$): $B_H(x)=\hat{I}^{H-1/2}B(x)$. The Riemann-Liouville fractional integral of the order α is given by the operator (Ross, 1975)

$$\hat{I}^{\alpha}f(x)=\frac{1}{\Gamma(\alpha)}\int_0^{\infty}x'^{\alpha-1}f(x-x')dx' ,$$

$$0<\alpha<1 . \quad (3.36)$$

Substituting f by df/dx in the integrand yields the fractional derivative of order $1-\alpha$.

The model of a fractional Brownian surface $z=B_H(x,y)$ was used to model the Earth's relief (Mandelbrot, 1975b; Berry and Hannay, 1978). The fractal dimension $D=2-H$ of the isoset $B_H(x,y)=h$ predicts the distribution of islands—that is, their number with the size of the order of a—which is essentially the covering number:

$$N_a \propto a^{-D} . \quad (3.37)$$

This distribution fits the empirical number-area rule, or

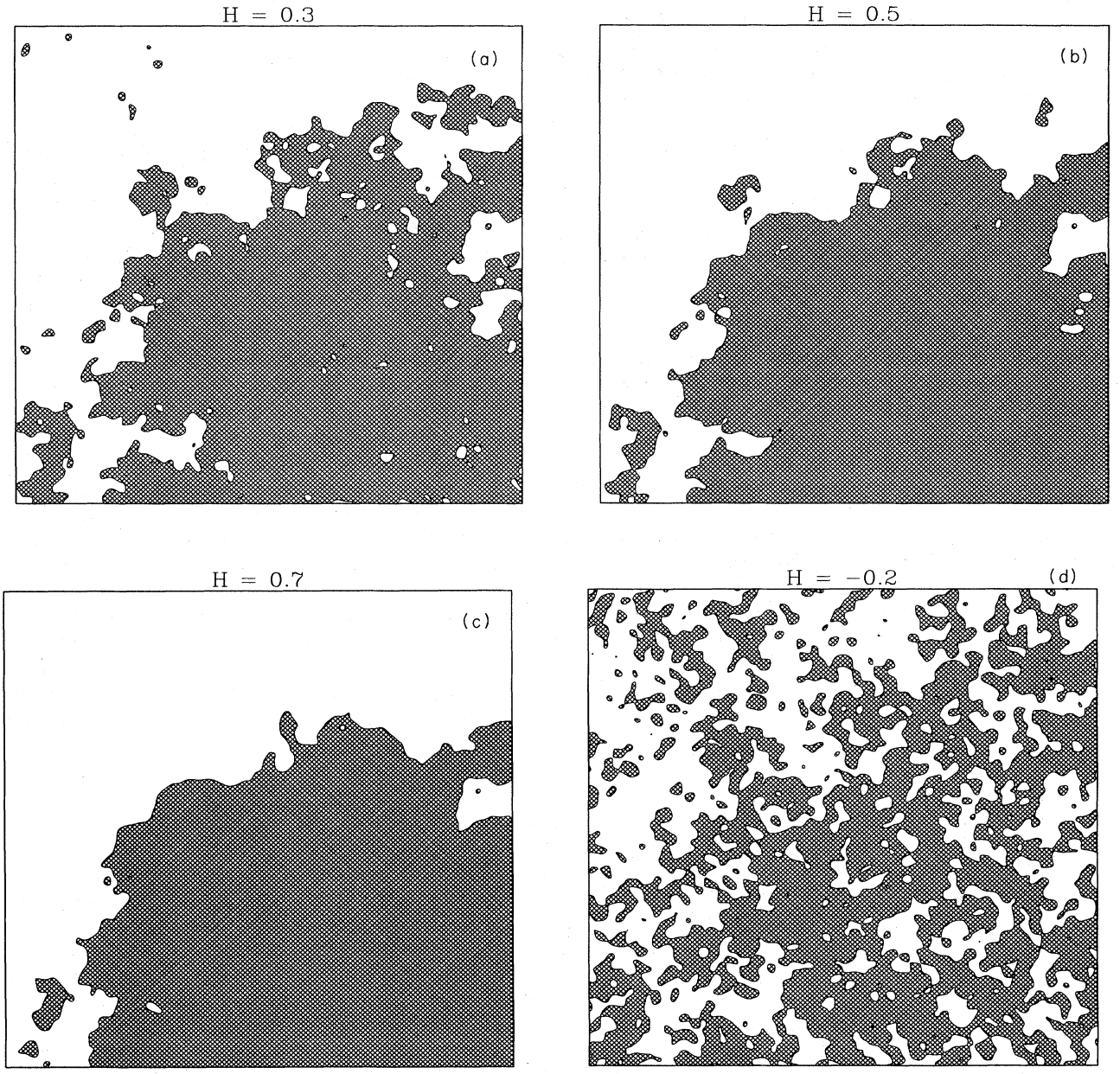

FIG. 14. Zero-level contour lines of the surfaces shown in Fig.13.

the Korčak (1938) law, which states that the numbers of islands with area above A scales as A^{-k}, for $k=2D=2(2-H)$. The Earth average value $k\simeq 0.65$ corresponds to a fractional Brownian relief with $H\simeq 0.7$, although local measurements show significant deviations from the power-law surface spectrum (Isichenko and Kalda, 1991b).

Thus the fractional Brownian approach makes it possible to link the relief spectrum with the fractal dimension of the whole isoset $B_H(x,y)=h$ and with the distribution of islands. However, the fractal dimension of a separate (connected) coastline, a measurable quantity, remains beyond this approach (Mandelbrot, 1983, p. 272). The distribution function of various contours (regardless of the level h) over size remains also unpredicted. These and other issues have to be addressed with the help of a less phenomenological (more "microscopic") approach, and therefore we return to percolation theory.

C. Topography of a monoscale relief

In Sec. II.E we saw that the isoset $\psi(\mathbf{x})=h$ of a random potential behaves like the system of both external and internal perimeters of percolation clusters on a lattice generated by the stationary points (minima, maxima, and saddles) of the potential ψ. As any physically reasonable random function has finite correlations, the corresponding bond probability (2.36) on the equivalent lattice cannot be considered independent from one bond to another, even though the potential $\psi(\mathbf{x})$ has a single characteristic length λ_0. Therefore the percolation network corresponding to the isopotentials $\psi(\mathbf{x})=h$ should be suspected of being long-range correlated, in the sense described in Sec. II.D. We designate by "monoscale uncorrelated," or simply "monoscale," such a potential that generates clusters falling into the universality class of uncorrelated percolation. We wish to establish the criterion for a potential $\psi(\mathbf{x})$ to be monoscale. To do so, we calculate the correlation function (2.27) of the bond probabilities (2.36) using the two-point potential probability distribution function $P(\psi_1,\psi_2|\mathbf{x}_1,\mathbf{x}_2)$. Analogously to Eq. (2.36), we write

$$\langle p_1(h)p_2(h)\rangle=\int_{-\infty}^{h}d\psi_1\int_{-\infty}^{h}d\psi_2 P(\psi_1,\psi_2|\mathbf{x}_1,\mathbf{x}_2)\ . \tag{3.38}$$

Suppose that $\psi(\mathbf{x})$ is Gaussian; so the two-point probability distribution function can be given by Eq. (3.21). In the long-range limit, $\rho\equiv|\mathbf{x}_1-\mathbf{x}_2|\gg\lambda_0$; substituting Eq. (3.22b) into Eq. (3.38) yields the bond probability correlation function,

$$c(\boldsymbol{\rho})\equiv\langle p_1(h)p_2(h)\rangle-p^2(h)=P^2(h)C(\boldsymbol{\rho})\ , \tag{3.39}$$

which scales directly proportional to the potential correlator $C(\boldsymbol{\rho})=\langle\psi(\mathbf{x})\psi(\mathbf{x}+\boldsymbol{\rho})\rangle$. Notice that for this particular result the Gaussianity of $\psi(\mathbf{x})$ is not essential. According to criterion (2.29), the correlations are irrelevant for sufficiently fast decay of the probability correlation function, $c(\rho)=O(\rho^{-2/\nu})$. In terms of the potential correlator $C(\boldsymbol{\rho})$, this criterion reads

$$C(\boldsymbol{\rho})=O(\rho^{-2/\nu}),\quad \rho\gg\lambda_0\ . \tag{3.40}$$

So we infer that the potential $\psi(\mathbf{x})$ with the power-law spectrum $\psi_\lambda\propto\lambda^H$, $\lambda>\lambda_0$, can be considered to be monoscale uncorrelated if $H<-1/\nu$. In two dimensions, this inequality yields $H<-\frac{3}{4}$, whereas for $d=3$ the upper H limit of monoscale behavior is $-1/\nu\simeq-1.1$. The contours of such potentials behave like the hulls of uncorrelated percolation clusters. Accordingly, the topography of a *monoscale correlated* potential—that is, a function with spectrum (3.9) where $-1/\nu<H<0$ and $\lambda_m\to\infty$—is related to the correlated percolation problem. This criterion is valid in any dimension. Other details are dimensionality dependent.

1. Two dimensions

Once the scaling properties of percolation clusters are known, the topography of a monoscale uncorrelated potential can be described in a similar manner by using the scaling properties of percolation perimeters. At this point, however, one must recall the fickle nature of the 2D cluster perimeter, whose fractal dimension is subject to change between the "natural" value $d_h=\frac{7}{4}$ and the "unscreened" value $d_u=\frac{4}{3}$ under a moderate change of the perimeter definition (Grossman and Aharony, 1986). In the "flooding" terms, the perimeters of the first (natural) kind correspond to the coastlines of islands with the gulfs whose widths may be less than λ_0. The second (unscreened) kind of perimeter arises when one dams all narrow straits, i.e., those with width less than a constant of order λ_0 (Fig. 7). Thus we have to choose which cluster perimeter—natural or unscreened—should be used to model the contours of a random function. Since nothing prevents a contour line from coming arbitrarily close to itself (this is indeed the case near a saddle point, when the contour lies close enough to a corresponding separatrix), we conclude that the natural hull (not the unscreened perimeter) is the proper image of a contour line.

Let us formulate the basic topographic properties of a monoscale (λ_0) relief $\psi(x,y)$ with the variance ψ_0^2, using the statistics of 2D percolation clusters (Sec. II) and the idea that the contours $\psi(x,y)=h$ are the external and internal hulls of percolation bond clusters on a lattice with the bond probability $p(h)$ given by formula (2.36).

(i) The level line $\psi(x,y)=h$ coming through a randomly chosen point is closed with probability 1, because the corresponding cluster is almost surely finite.

(ii) Due to the unicity of an infinite percolation cluster, there exists exactly one open isoline (corresponding to the external perimeter of an incipient infinite cluster), which lies at a critical level $h=h_c$. [Note that even among contours $\psi(x,y)=h_c$ the open contour takes zero measure.] Specifically, for a sign-symmetric potential (e.g., Gaussian with $\langle\psi\rangle=0$), the critical level is zero: $h_c=0$.

(iii) The number of connected contours $\psi(x,y)=h$ with diameter in the octave $[a,2a]$ per unit area is given by the number of corresponding clusters (2.15),

$$N_a=\begin{cases}\text{const } a^{-2}, & \lambda_0 \ll a \ll \xi_h \ , \\ \text{exponentially small}, & a \gg \xi_h \ , \end{cases} \tag{3.41}$$

where the correlation length ξ_h is given by formula (2.8e); in terms of the level h we have

$$\xi_h=\lambda_0\left[\frac{|h-h_c|}{\psi_0}\right]^{-\nu} . \tag{3.42}$$

The correlation length exponent $\nu=\frac{4}{3}$ (see Table III and references therein).

(iv) A separate contour piece of ψ with the diameter $a \gg \lambda_0$ is a fractal curve with the scaling range $[\lambda_0,a]$ and the fractal dimension $d_h=\frac{7}{4}$ (hull exponent; see Table III), so the length of the line scales as

$$L(a)\simeq\lambda_0\left[\frac{a}{\lambda_0}\right]^{d_h} . \tag{3.43}$$

(v) Analogously to lattice clusters, a continuum cluster [i.e., a connected region where $\psi(x,y)<h$] of a large linear size a has the fractal dimension (2.11) $d_c=d-\beta/\nu=\frac{91}{48}$ in the scaling range $[\lambda_0,a]$ ($[\lambda_0,\xi_h]$ for an infinite cluster). For $|h-h_c| \ll \psi_0$, the infinite continuum cluster occupies the area fraction given by formula (2.7); that is,

$$P_\infty=\text{const}\left[\frac{h-h_c}{\psi_0}\right]^{\beta}\theta(h-h_c) , \tag{3.44}$$

where $\beta=5/36$.

To complete our discussion of the topography of 2D monoscale random relief, we derive the expression for the distribution function $F(a)$ of all contours of $\psi(x,y)$ over their size a. Let us define $F(a)$ as the fraction of area covered by the contour lines with diameters in the interval $[a,2a]$, whatever be their level h.[2]

First, consider a wider set of contours with diameters $[a,\infty]$. This region may be constructed starting with the contours of the diameter a and adding to them the embracing contours, as shown in Fig. 15. This "dressing procedure," begun with an arbitrary initial contour, will ultimately lead to the infinite isoline, which is unique. Therefore the set of contours bigger than a is a connected weblike region with holes of size a and smaller (Fig. 16). Let us call this region the "a web." According to (iii), the contours with diameter greater than a should have a level sufficiently close to the critical level,

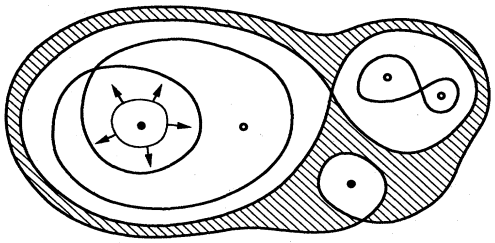

FIG. 15. Procedure of "contour dressing" (schematic). Separatrices (self-intersecting lines) come through saddle points. Extrema (maxima and minima) are shown by empty and solid circles, respectively. The hatched area lying between two neighboring separatrices corresponds to the average area per saddle and is approximately constant ($\simeq\lambda_0^2$) on each step of dressing.

$|h-h_c| \lesssim h(a)=\psi_0(a/\lambda_0)^{-1/\nu}$, because otherwise these contours would be larger than the correlation length (3.42), an exponentially improbable event. Taking into account that the characteristic gradient of $\psi(x,y)$ is ψ_0/λ_0, we conclude that the characteristic width $w(a)$ of the a web is proportional to the level range $h(a)$ and is estimated to be

$$w(a)\simeq\lambda_0\left[\frac{a}{\lambda_0}\right]^{-1/\nu} , \quad a>\lambda_0 . \tag{3.45}$$

The a web is a fractal set in the scaling range of $[\lambda_0,a]$ with the fractal dimension $d_h=7/4$. Indeed, in the limit $a\to\infty$, the web degenerates into the single unclosed isoline of $\psi(x,y)$, whose fractal dimension is d_h and whose scaling range is $[\lambda_0,\infty]$.

The fraction of area occupied by the a web can be calculated to be

$$\Phi(a)\simeq\frac{L(a)w(a)}{a^2}\simeq\left[\frac{\lambda_0}{a}\right]^{2-d_h+1/\nu} , \quad a>\lambda_0 . \tag{3.46}$$

The distribution function $F(a)=\Phi(a)-\Phi(2a)$ is clearly of the same order of magnitude. Using the numerical values of the exponents, we obtain the level-averaged dis-

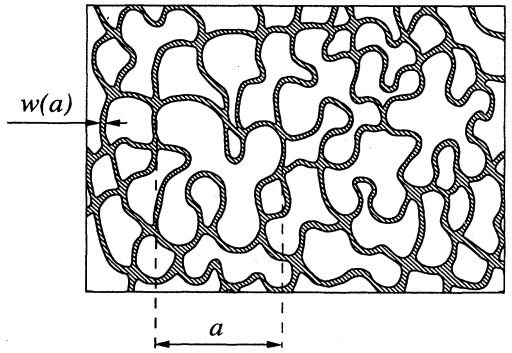

FIG. 16. Schematic of the set of contours with linear size larger than a: the a web.

[2]The dimensionless distribution function $F(a)$, which relates the area fraction to the octave of scales, is here more convenient than a standard distribution function $f(a)\simeq F(a)/a$ yielding the infinitesimal probability $f(a)da$ to find a contour of a linear size in the interval $[a,a+da]$.

tribution of contour sizes (Gruzinov *et al.*, 1990)

$$F(a)\simeq\frac{\lambda_0}{a},\quad a>\lambda_0\ . \tag{3.47}$$

To imagine what the set of contours of diameters $[a,2a]$ looks like, subtract the $2a$ web from the a web. The result will be a disconnected set consisting of connected "a cells" with both the cells' width and the gaps between the cells given by the characteristic quantity $w(a)$ (see Fig. 17).

2. Three dimensions

The monoscale topography of a three-dimensional potential differs from the 2D case in that there exist two different critical levels, h_{c1} and h_{c2}, whose difference is of the order of the potential amplitude, $h_{c2}-h_{c1}\simeq\psi_0$ (see Sec. II.E). If the level h satisfies $h<h_{c1}$ or $h>h_{c2}$, the isosurfaces of $\psi(x,y,z)$ are all closed but may be multiconnected (that is, have "handles"). The isoset $\psi(x,y,z)=h$ at $h_{c1}<h<h_{c2}$ consists of many closed parts and only one open surface (because of the unicity of an infinite cluster for given h). According to Eq. (2.15), the number of isosurfaces with linear size between a and $2a$ per unit volume scales as $N_a\simeq a^{-3}$ for $\lambda_0<a<\xi_h$ and is exponentially small for finite $a>\xi_h$. The correlation length is given by

$$\xi_h=\lambda_0\max\left[\left|\frac{h-h_{c1}}{\psi_0}\right|^{-\nu},\left|\frac{h-h_{c2}}{\psi_0}\right|^{-\nu}\right], \tag{3.48}$$

where $\nu\simeq0.9$ (see Table III). If h is close to one of the critical levels, the correlation length is large, $\xi_h\gg\lambda_0$,

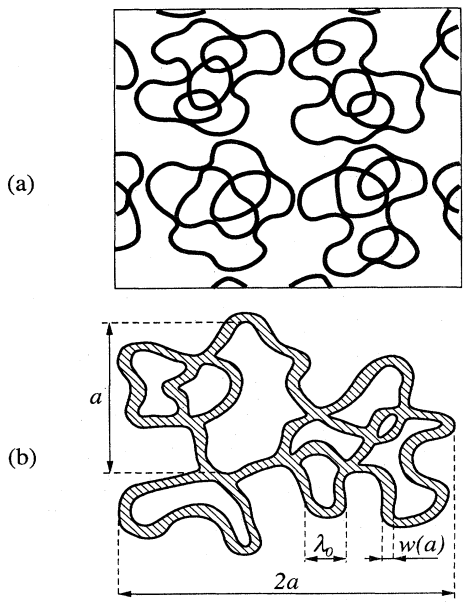

FIG. 17. Selecting contours by size. (a) The set of contours with linear size between a and $2a$, consisting of a cells; (b) schematic of a typical a cell.

and there arises a scaling range of self-similarity. The fractal dimension d_h of an isosurface is equal to the cluster fractal dimension, $d_h=d_c=3-\beta/\nu\simeq2.50$, whose scaling range is $[\lambda_0,a]$ for a closed isosurface and $[\lambda_0,\xi_h]$ for an open one. Specifically, the isosurface area $S(a)$ scales, for diameter a lying in the scaling range, as

$$S(a)\simeq\lambda_0^2(a/\lambda_0)^{d_h}\ . \tag{3.49}$$

Regarding the distribution function $F(a)$ of isosurfaces over size, it can be concluded that a finite fraction of space is covered by open surfaces (one for each $h\in[h_{c1},h_{c2}]$). This fraction of volume can be accounted for by $F(\infty)$, which is (roughly) of order one-half. The distribution of finite-size isosurfaces can be found similarly to Eq. (3.46),

$$F(a)\simeq\frac{S(a)w(a)}{a^3}\simeq\left[\frac{\lambda_0}{a}\right]^{3-d_h+1/\nu}=\left[\frac{\lambda_0}{a}\right]^{(\beta+1)/\nu},\qquad \lambda_0<a<\infty\ . \tag{3.50}$$

Upon substituting the numerical value of the exponents, $\nu\simeq0.9$, $\beta\simeq0.4$, we find that $F(a)$ scales approximately as $a^{-1.6}$.

Topographic properties of monoscale potentials also apply to monoscale correlated potentials ($-1/\nu<H<0$ and $\lambda_m=\infty$) if the exponents ν,d_h,β, etc., are replaced by the corresponding H-dependent exponents (2.30)–(2.33) of the correlated percolation problem. This issue is addressed in more detail in Sec. III.E.

D. Monoscale relief on a gentle slope

In the previous subsection, we discussed the level lines and surfaces of random potentials with finite variance. One may also be interested in the topography of a "tilted relief"—that is to say, of a random function with an average gradient that is too small to destroy local hills and valleys but clearly dominates the long-range topographic behavior.

This problem can be relevant, for example, for the quantized Hall effect characterized by extremely low dissipative components of the conductivity tensor (Trugman, 1983). In a two-dimensional electron gas embedded in the magnetic field $\mathbf{B}$ parallel to the z axis, the electrons are localized near the lines of constant electric potential $\phi(x,y)$, or, in other words, drift in crossed electric and magnetic fields with the velocity $\mathbf{v}=c\mathbf{E}\times\mathbf{B}/B^2$ (Laughlin, 1981). The radius of electron localization near the isopotentials is $l=(\hbar c/eB)^{1/2}$, which is the electron gyroradius corresponding to the energy $\hbar\omega_B/2$ of the lowest Landau level, $\omega_B=eB/mc$ being the gyrofrequency. If the background electric field $\mathbf{E}_0(\mathbf{x})=-\nabla\phi_0(x,y)$ is created by a statistically uniform impurity distribution, the isopotentials of ϕ_0 are (almost) all closed: an average electric current is absent. When the system is embedded in an external uniform electric field $\mathbf{E}_1$, $E_1\ll E_0$, an average (Hall) electric current emerges that is carried

along the open isolines of the perturbed potential $\phi(x,y)=\phi_0(x,y)-\mathbf{E}_1\cdot\mathbf{x}$. This highly simplified model assumes essentially individual motion of noninteracting electrons. A similar topographic problem of a tilted relief arises in the essentially collective classical Hall effect in high-temperature pulsed plasmas (Chukbar and Yankov, 1988; Kingsep *et al.*, 1990), where the electric current must flow along the level lines of a two-dimensional plasma density.

In this section, we discuss the topography of a monoscale uncorrelated relief on a gentle slope in some detail, both for its own sake and also because this problem serves as an auxiliary one in the approach of "separated scales" (Sec. III.E).

Following the model of $\mathbf{E}\times\mathbf{B}$ electron drifts along random equipotentials, it is convenient to represent the isolines of a potential $\psi(x,y)$ as the streamlines of a two-dimensional incompressible flow,

$$\mathbf{v}(x,y)=\nabla\psi(x,y)\times\hat{\mathbf{z}}\ , \tag{3.51}$$

where $\hat{\mathbf{z}}$ denotes a unit vector in the z direction. In this representation, $\psi(x,y)=-c\phi(x,y)/B$ is the stream function of the flow.

Let $\mathbf{v}(x,y)$ be the sum of a monoscale (λ_0) flow $\mathbf{v}_0(x,y)=\nabla\psi_0(x,y)\times\hat{\mathbf{z}}$ and a small uniform component, $\mathbf{v}_1=v_1\hat{\mathbf{x}}$:

$$\mathbf{v}(x,y)=\mathbf{v}_0(x,y)+\mathbf{v}_1\ . \tag{3.52}$$

This corresponds to the stream function with a small average gradient,

$$\psi(x,y)=\psi_0(x,y)+v_1 y\ . \tag{3.53}$$

As the potential $\psi_0(x,y)$ is bounded, $\mathbf{v}_0(x,y)$ has zero mean: (almost) any streamline is closed and there is no long-range fluid flux. When a uniform component $\mathbf{v}_1$ is imposed, an average flux arises in the x direction. Therefore some fraction of streamlines must open to produce channels carrying this flux [Fig. 18(a)]. For very small $\varepsilon=v_1/v_0\ll 1$, $v_0\equiv[v_0(x,y)]_{\rm rms}$, the perturbation clearly cannot affect the absolute value of the velocity in the channels. Hence the smallness of $\mathbf{v}_1$ is manifested only in that the channels are narrow (the width $\delta_\varepsilon\ll\lambda_0$) and well separated (the characteristic distance between them $\Delta_\varepsilon\gg\lambda_0$) (Trugman, 1983; Zeldovich, 1983). Given the characteristic velocity v_0 in the channels, the average flux $\mathbf{v}_1$ can be estimated to be $v_0\delta_\varepsilon/\Delta$; hence

$$\frac{\delta_\varepsilon}{\Delta_\varepsilon}=\varepsilon\ . \tag{3.54}$$

The transverse (with respect to $\mathbf{v}_1$) walk Δ_ε of an open streamline lying in the channels can be found from the argument of "graded percolation" (Trugman, 1983; Bunde and Gouyet, 1985; Sapoval *et al.*, 1985). The idea behind this argument is that the local behavior of clusters $\psi(x,y)<h$ is the same as for the unperturbed potential $\psi_0(x,y)$; however, the local critical level h_c becomes slowly dependent on y together with the average value of the potential:

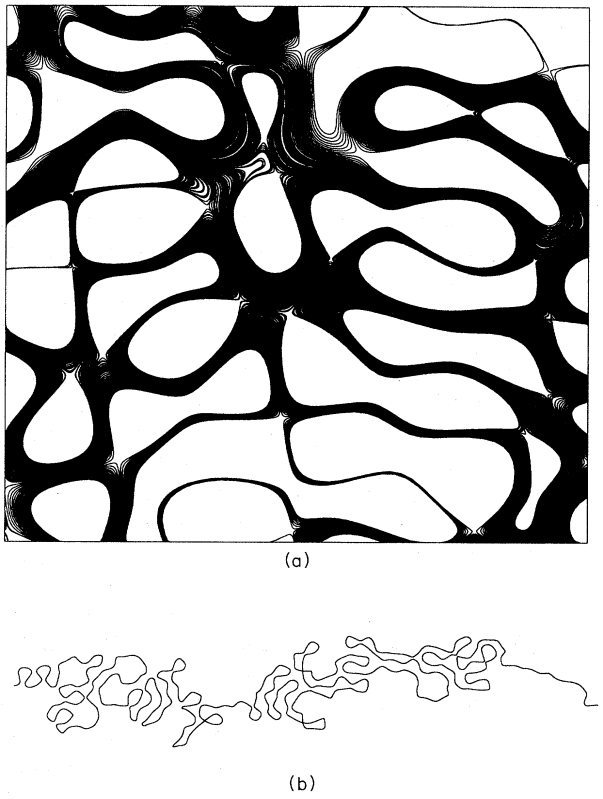

FIG. 18. Topography of a tilted relief. (a) The set of open contour lines of potential (3.53) forms a network of channels. For the simulation, $\psi_0(x,y)$ was taken the same as in Fig. 10 and $\mathbf{v}_1=0.5\hat{\mathbf{x}}$, so that $\varepsilon=v_1/(\nabla\psi_0)_{\rm rms}=(10\sqrt{2})^{-1}\simeq 0.07$. The window size is 30×30. As a criterion of the contour openness the requirement was used that the contour extend at least twice the window size in the x direction. (b) Unclosed contour line of the horizontal size 200.

$$h_c(y)=h_c(0)+v_1 y\ . \tag{3.55}$$

Let us consider an open level line of potential (3.53) and put the origin on this line. On relatively small scales, namely, for $|y|\ll\Delta_\varepsilon$, the line does not "feel" the average gradient of $\psi(x,y)$ and behaves like an open isoline of the unperturbed function $\psi_0(x,y)$. According to properties (ii) and (iii) of monoscale level contours (Sec III.C.1), the level h of the considered isoline is close to the local critical level: $h\simeq h_c(0)$. Walking in this unperturbed manner, the isoline explores different regions where the critical level (3.55) becomes different from h. According to (iii), this makes the line try to close, or, in other words, to return to the region $y\simeq 0$. So the unclosed level line of the tilted relief (3.53) is constrained to walk in a strip parallel to the x axis [Fig. 18(b)]. The characteristic width of such wandering Δ_ε is determined to be the self-consistent correlation length ξ_h (3.42):

$$\Delta_\varepsilon=\lambda_0\left[\frac{|h_c(0)-h_c(\Delta_\varepsilon)|}{\psi_0}\right]^{-\nu}. \tag{3.56}$$

Substituting Eq. (3.55) into Eq. (3.56), we find the slope-generated correlation scale

$$\Delta_\varepsilon=\lambda_0\varepsilon^{-\nu/(\nu+1)}=\lambda_0\varepsilon^{-4/7},\quad d=2\ . \tag{3.57}$$

This scale determines the maximum diameter of closed contours on the tilted relief. The width of the channels is then found from Eq. (3.54):

$$\delta_\varepsilon=\lambda_0\varepsilon^{1/(\nu+1)}=\lambda_0\varepsilon^{3/7}\ . \tag{3.58}$$

Thus we conclude that the contours of a monoscale uncorrelated relief on a gentle slope behave in a nonperturbed manner on scales below Δ_ε. In other words, the contours of $\psi_0(x,y)$ with diameter $a<\Delta_\varepsilon$ are relatively "robust" with respect to the perturbation, whereas the "fragile" contours with $a>\Delta_\varepsilon$ open to form a network of percolating channels. So this network is topologically similar to the Δ_ε web shown in Fig. 17. (Unless an individual percolating line is plotted, it is hard to tell the direction of the mean flow from the appearance of the channel network.) As expected, the channel width (3.58) is consistent with the Δ_ε-web width (3.45): $\delta_\varepsilon=w(\Delta_\varepsilon)$.

Results (3.57) and (3.58) can be extended to level lines of a 2D monoscale correlated relief ($-1/\nu<H<0$, $\lambda_m=\infty$) on a gentle slope. To do so, we replace the uncorrelated percolation exponent $\nu=\frac{4}{3}$ by its correlated counterpart $\tilde{\nu}(H)=-1/H$, and for $-3/4<H<0$ we find

$$\Delta_\varepsilon=\lambda_0\varepsilon^{-1/(1-H)}\ , \tag{3.59}$$

$$\delta_\varepsilon=\lambda_0\varepsilon^{-H/(1-H)}\ . \tag{3.60}$$

It can be shown that formulas (3.59) and (3.60) for the extent of allowed isoline walk and for the width of the channels of open isolines, respectively, are also valid for a fractional Brownian relief with $0<H<1$ (see Sec. III.B) on a gentle slope.

The experimental consequences of the above results are concerned with the nonlinear broadening of steps in the quantized Hall conductivity (Trugman, 1983). The width of the steps in the Hall conductivity as a function of electron density is proportional to the number of current-carrying extended states. The latter is in turn proportional to the fraction of area $F(\Delta_\varepsilon)$ occupied by the web comprised of open isopotential channels, a quantity which is nonlinear in the small applied electric field. For the case of a monoscale impurity potential $\phi_0(x,y)$, we find, upon using formulas (3.47) and (3.57),

$$F(\Delta_\varepsilon)\simeq\lambda_0/\Delta_\varepsilon=\varepsilon^{\nu/(\nu+1)}=\varepsilon^{4/7}\ . \tag{3.61}$$

The experimental aspects of the nonlinear broadening of the steps in the quantized Hall conductivity and the possible observability of this effect were discussed by Trugman (1983), who used in his analysis an incorrect hull exponent. (At the time the correct exponent was not known.)

Now we consider the three-dimensional case. Due to the openness of a finite fraction of the isosurfaces $\psi_0(x,y,z)=h$, which takes place at $h_{c1}<h<h_{c2}$ ($h_{c2}-h_{c1}\simeq\psi_0$), the effect of a small average slope is not as pronounced as in two dimensions. The topology of open surfaces is, nevertheless, changed. Consider a surface $\psi_0(x,y,z)+v_1z=h$, $\varepsilon\equiv v_1\lambda_0/\psi_0\ll1$. This surface can span only a layer parallel to the (x,y) plane with width

$$\Delta_\varepsilon=\lambda_0/\varepsilon,\quad d=3\ , \tag{3.62}$$

where the local level $h_0(z)=h-v_1z$ of $\psi_0(x,y,z)$ lies between the critical levels h_{c1} and h_{c2}.

E. Multiscale statistical topography

The standard percolation theory seems to be inapplicable for describing the statistical topography of "scaleless" random fields, such as those characterized by a power spectrum $\psi_\lambda\propto\lambda^H$. The applicability of percolation theory is nevertheless recovered by the observation that "scaleless" is virtually the same as "multiscale." The idea of the *separation of scales* (Isichenko and Kalda, 1991b) is to decompose a multiscale field into a series of monoscale fields. Namely, we consider the potential

$$\psi(\mathbf{x})=\sum_{\lambda_i}\psi_{\lambda_i}(\mathbf{x})\ , \tag{3.63}$$

where $\psi_{\lambda_i}(\mathbf{x})$ are monoscale (λ_i) functions with the amplitudes

$$\psi_\lambda\equiv[\psi_\lambda(\mathbf{x})]_{\rm rms}=\psi_0\left[\frac{\lambda}{\lambda_0}\right]^H \tag{3.64}$$

and the sum in Eq. (3.63) is taken over a geometrical progression of scales

$$\lambda_i=\lambda_0,\ \mu\lambda_0,\ \mu^2\lambda_0,\ \ldots,\lambda_m;\quad \mu\gg1\ . \tag{3.65}$$

To be more exact, the components in series (3.63) must be written as

$$\psi_\lambda(\mathbf{x})=\left[\frac{\lambda}{\lambda_0}\right]^H\psi_0\left[\frac{\lambda_0}{\lambda}\mathbf{x}\right]\ , \tag{3.66}$$

where $\psi_0(\mathbf{x})$ is a monoscale (λ_0) random potential with ψ_0^2 variance and new realizations are taken for each λ in formula (3.66). In the Gaussian case with independent Fourier harmonics, $\psi_\lambda(\mathbf{x})$ is given by Eq. (3.7).

The statistical topography of potential (3.63)–(3.65) with strongly separated scales is analytically tractable in terms of a recursive percolation analysis, where each subsequent term in series (3.63) is considered locally to be a "gentle slope" imposed on the previous term. The final results for the "correct" potential (3.6) (that is, with $\mu=2$) is obtained by extrapolating the results for the "incorrect" potential with $\mu\gg1$ to the marginally applicable limit $\mu=2$. This method shares a common spirit with the renormalization-group technique (Wilson, 1975) but is technically different. It must be emphasized that

the method of separated scales is poorly based, especially regarding the limit $\mu \to 2$ (for discussion of the difficulties, see Sec. III.E.5). A partial excuse is given by the fact that all predictions of the theory of fractional Brownian functions are recovered by the method of separated scales, which also yields new results inaccessible through the fractional Brownian approach. These new results may have to be checked numerically and/or experimentally.

1. Two dimensions

For a two-dimensional potential $\psi(x,y)$, we introduce an incompressible flow $\mathbf{v}=\nabla\psi(x,y)\times\hat{\mathbf{z}}$, whose multiscale features can be described similarly to Eq. (3.63):

$$\mathbf{v}(\mathbf{x})=\sum_{\lambda_i}\mathbf{v}_{\lambda_i}(\mathbf{x}) . \tag{3.67}$$

Then the stream function spectrum (3.64) corresponds to the velocity spectrum

$$v_\lambda = v_0\left[\frac{\lambda}{\lambda_0}\right]^{H-1} . \tag{3.68}$$

For $H>1$, the long-scale components of the flow are more intensive than the short scales; therefore the streamline behavior is dominated by the largest scale λ_m. Thus the topography of the power-spectrum random function with $H>1$ is essentially the same as for the monoscale uncorrelated λ_m potential $\psi_{\lambda_m}(x,y)$. This clearly remains true in the limit $\mu=2$.

The case $H<1$ is more interesting. Here, the flow component $\mathbf{v}_{\lambda_0}(\mathbf{x})$ dominates the absolute value of the velocity field and $\mathbf{v}_{\lambda_1}(\mathbf{x})$ may be considered a weak [because $\varepsilon = v_{\lambda_1}/v_{\lambda_0}=(\lambda_0/\lambda_1)^{1-H}\ll 1$] and quasihomogeneous (because $\lambda_1 \gg \lambda_0$) perturbation to $\mathbf{v}_{\lambda_0}(\mathbf{x})$. According to the results of Sec. III.D, this perturbation leaves most streamlines of $\mathbf{v}_{\lambda_0}(\mathbf{x})$ nearly intact but "quasiopens" some of them; that is, it makes them walk around the direction of $\mathbf{v}_{\lambda_1}(\mathbf{x})$ in the strips of width (3.57):

$$\Delta_{01}=\lambda_0\left[\frac{\lambda_1}{\lambda_0}\right]^{(1-H)\nu/(\nu+1)} . \tag{3.69}$$

For $H<-1/\nu$, the equation for Δ_{01} becomes formally larger than $\lambda_1=\mu\lambda_0$. This means that the assumption of the local homogeneity of the perturbation $\mathbf{v}_{\lambda_1}(\mathbf{x})$ breaks down; in other words, the perturbation turns out to be too small to appreciably affect the pattern of the streamlines. Thus in this case the topography of the relief $\psi(x,y)$ is essentially the same as for the monoscale potential $\psi_{\lambda_0}(\mathbf{x})$. Notice that the same inequality (2.26) [see also Eq. (3.40)] is the criterion for the irrelevance of correlations and hence for the membership of the potential $\psi(\mathbf{x})$ in the universality class of random percolation.

In this way, we arrive at the essentially multiscale case

$$-\frac{1}{\nu}<H<1 , \tag{3.70}$$

where a nontrivial *interaction of scales* must take place, implying an essential dependence of the topographic properties on all scales, that is, on the form of the potential spectrum.

In terms of separated scales, inequality (3.70) implies $\lambda_0 \ll \Delta_{01} \ll \lambda_1$, justifying the assumptions of both the weakness and the quasihomogeneity of the perturbation $\mathbf{v}_{\lambda_1}(\mathbf{x})$. In this limit, the fraction of area covered by the streamlines with diameter of order λ_1 is given by Eq. (3.46) with $a=\Delta_{01}$:

$$F(\lambda_1)\simeq\left[\frac{\lambda_0}{\Delta_{01}}\right]^{2-d_h+1/\nu} = \left[\frac{\lambda_1}{\lambda_0}\right]^{-(1-H)[1+\nu(2-d_h)]/(\nu+1)} . \tag{3.71}$$

Indeed, once a streamline has reached the displacement Δ_{01}, it becomes quasiopen, that is, it walks in the Δ_{01} strip whose axis follows a streamline of $\mathbf{v}_{\lambda_1}(\mathbf{x})$. The latter is typically closed with the diameter of order λ_1.

The fractal properties of an open isoline depend on the length scale. In the inertial range $[\lambda_0,\Delta_{01}]$, the effect of the slope is unessential and the fractal dimension of the curve is $d_h=\frac{7}{4}$. On scales between Δ_{01} and λ_1, the strip is almost straight, meaning a fractal dimension of unity in the corresponding scaling range. So the length of the streamline within the displacement λ_1 is given by

$$L(\lambda_1)\simeq\lambda_0\left[\frac{\Delta_{01}}{\lambda_0}\right]^{d_h}\frac{\lambda_1}{\Delta_{01}} \simeq\lambda_0\left[\frac{\lambda_1}{\lambda_0}\right]^{1+(1-H)(d_h-1)\nu/(\nu+1)} . \tag{3.72}$$

Now, we consider the next-order perturbation, $\mathbf{v}_{\lambda_2}(\mathbf{x})$, to the velocity field. It has the same effect on the streamlines of $\mathbf{v}_{\lambda_1}(\mathbf{x})$ as that of the λ_1 component of the flow on the lines of $\mathbf{v}_{\lambda_0}(\mathbf{x})$. So we find that the lines of $\mathbf{v}_{\lambda_1}(\mathbf{x})$, which are already the guidelines for the Δ_{01} strips, become, in turn, constrained into the Δ_{12} strips following the streamlines of $\mathbf{v}_{\lambda_2}(\mathbf{x})$ (see Fig. 19). The expressions for Δ_{12}, $F(\lambda_2)$, and $L(\lambda_2)$ differ from those in Eqs. (3.69), (3.71), and (3.72) by only the replacement of λ_1 by λ_2. This argument can be repeated for longer scales, up to λ_m. Generally, we obtain the following equations for the distribution function of the multiscale level lines over the diameter λ,

$$F(\lambda)\simeq\left[\frac{\lambda}{\lambda_0}\right]^{-(1-H)[1+\nu(2-d_h)]/(\nu+1)} = \left[\frac{\lambda}{\lambda_0}\right]^{-4(1-H)/7} , \quad \lambda_0<\lambda<\lambda_m , \tag{3.73}$$

and for the length of a contour exercising the displacement λ,

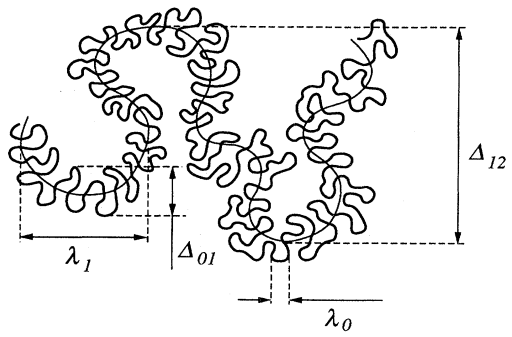

FIG. 19. Interaction of scales in terms of the behavior of a percolating isoline of the separated-scale potential (3.63).

$$L(\lambda)\simeq\lambda_0\left[\frac{\lambda}{\lambda_0}\right]^{D_h},\quad \lambda_0<\lambda<\lambda_m\ , \tag{3.74}$$

where the fractal dimension of a connected contour line is

$$D_h(H)=1+(1-H)(d_h-1)\frac{\nu}{\nu+1}=\frac{10-3H}{7}\ . \tag{3.75}$$

The transition to a smooth spectrum limit ($\mu=2$) implies simply the omission of subscripts of λ in Eqs. (3.73) and (3.74) and treatment of λ as a continuum variable. Notice that, in the region of its applicability determined by condition (3.70), the fractal dimension (3.75) of a multiscale isoline satisfies the inequality

$$1<D_h<d_h=\tfrac{7}{4}\ , \tag{3.76}$$

where the maximum value is attained in the monoscale uncorrelated limit $H=-1/\nu=-\frac{3}{4}$.

For longer scales, $\lambda>\lambda_m$, the topography is again governed by the monoscale features of the λ_m component of the potential $\psi(\mathbf{x})$ [see Eq. (3.47)]; hence the distribution function falls off somewhat more rapidly than (3.73):

$$F(\lambda)\simeq\left[\frac{\lambda_0}{\lambda_m}\right]^{4(1-H)/7}\frac{\lambda_m}{\lambda},\quad \lambda>\lambda_m\ . \tag{3.77}$$

A contour with the diameter $a\gg\lambda_m$ has fractal dimension (3.75) in the scaling range $[\lambda_0,\lambda_m]$ and the fractal dimension $d_m=\frac{7}{4}$ in the range $[\lambda_m,a]$. It follows that the length of such a contour is determined by

$$L(a)\simeq\lambda_0\left[\frac{\lambda_m}{\lambda_0}\right]^{D_h}\left[\frac{a}{\lambda_m}\right]^{d_h},\quad a>\lambda_m\ . \tag{3.78}$$

Analogously to Eq. (3.46), the distribution function $F(\lambda)$ may be represented in the general form

$$F(\lambda)=\frac{L(\lambda)w(\lambda)}{\lambda^2}\ , \tag{3.79}$$

where $w(\lambda)$ is the characteristic width of the connected set of contours with diameters λ to 2λ (the λ cell). Upon using Eqs. (3.73), (3.74), (3.75), and (3.78), we obtain the width of the cell,

$$w(\lambda)=\frac{\lambda^2F(\lambda)}{L(\lambda)}\simeq\begin{cases}\lambda_0\left[\dfrac{\lambda}{\lambda_0}\right]^H, & \lambda_0<\lambda<\lambda_m\ , \\ \lambda_0\left[\dfrac{\lambda_m}{\lambda_0}\right]^H\left[\dfrac{\lambda}{\lambda_m}\right]^{-1/\nu}, & \lambda>\lambda_m\ .\end{cases} \tag{3.80a}$$

(3.80b)

The behaviors of the isoline fractal dimension (3.75) and the contour distribution function (3.77) do not depend qualitatively on the sign of the spectral exponent H, provided that inequality (3.70) holds. However, the appearance of the vertical (Fig. 12) and the horizontal (Fig. 14) cross sections of multiscale surfaces suggests a qualitative difference in the topography of the reliefs with $H>0$ and $H<0$. This difference lies in the fractal dimension D of the whole isoset $\psi(x,y)=h$ (Fig. 14). According to Eq. (3.16), for $0<H<1$ the random function $\psi(x,y)$ in the scaling range $[\lambda_0,\lambda_m]$ may be considered a fractional Brownian plane-to-line function; hence

$$D=2-H,\quad 0<H<1\ . \tag{3.81}$$

The same result can be obtained with the method of separated scales (Isichenko and Kalda, 1991b). For $H=0$, the isoset $\psi(x,y)=h$ becomes dense in the plane (x,y): $D=2$. For $H<0$, D cannot exceed the ambient space dimension $d=2$; hence

$$D=2,\quad H<0\ . \tag{3.82}$$

Result (3.82) agrees with the finite measure (3.30) of the isoset of a Gaussian random function with finite variance. For $H>0$, this measure would tend to zero at $\lambda_m\to\infty$ because $D<2$.

Thus there is a qualitative difference between the case of a fractional Brownian relief ($0<H<1$) and the case of correlated percolation ($-1/\nu<H<0$). However, Eq. (3.75) for the fractal dimension D_h holds in both limits. On the one hand, D_h is the fractal dimension of a connected contour piece on a fractional Brownian relief, where $1<D_h<10/7$. On the other hand, $D_h=\tilde{d}_h$ is identified with the hull exponent of a 2D correlated percolation cluster, where $\frac{10}{7}<D_h<\frac{7}{4}$.

It is interesting to note that the appearance of formula (3.75) implies a corollary for the correlated percolation exponent $\tilde{\nu}(H)$. The arguments used in deriving (3.75) can be repeated for the case in which one starts with the correlated percolation problem corresponding to an exponent H' such that $-1/\nu<H'<H<0$ and adds stronger correlations (H) using the procedure of the separation of scales. In this way we arrive at result (3.75), where d_h and ν are replaced by the correlated exponents $\tilde{d}_h(H')\equiv D_h(H')$ and $\tilde{\nu}(H')$, respectively:

$$D_h(H)=1+(1-H)[D_h(H')-1]\frac{\tilde{\nu}(H')}{\tilde{\nu}(H')+1}\ ,$$
$$-1/\nu<H'<H<0\ . \tag{3.83}$$

Putting in Eq. (3.83) $H'=H$, we recover the formula $\tilde{\nu}(H)=-1/H$ as a necessary consistency condition.

2. Three dimensions

Now we wish to repeat the scale separation argument for a three-dimensional random potential $\psi(x,y,z)$. For this purpose we use Eq. (3.62) for the "walk" width of an isosurface subject to a small average potential gradient. Then instead of Eq. (3.69) we have

$$\Delta_{01}=\lambda_0\left[\frac{\lambda_1}{\lambda_0}\right]^{1-H}, \tag{3.84}$$

where $\lambda_0 \ll \lambda_1$. For the method of separated scales to work, we must have $\lambda_0 \ll \Delta_{01} \ll \lambda_1$, which is the case only for $0<H<1$. In this case we can calculate the area $S(\lambda_1)$ of the isosurface contained in a λ_1-sized box similarly to Eq. (3.72). The difference, however, is that in the scaling range $[\lambda_0,\Delta_{01}]$ the isosurface fractal dimension is $D=3$, because its level is far from the critical levels of $\psi_{\lambda_0}(x,y,z)$. In the scaling range $[\Delta_{01},\lambda_1]$ we have $D=2$, as the isosurface of $\psi_{\lambda_0}(\mathbf{x})+\psi_{\lambda_1}(\mathbf{x})$ follows a smooth isosurface of $\psi_{\lambda_1}(\mathbf{x})$. Hence we have

$$S(\lambda_1)\simeq\lambda_0^2\left[\frac{\Delta_{01}}{\lambda_0}\right]^3\left[\frac{\lambda_1}{\Delta_{01}}\right]^2\simeq\lambda_0\left[\frac{\lambda_1}{\lambda_0}\right]^{3-H}. \tag{3.85}$$

Thus the fractal dimension of a connected three-dimensional contour piece,

$$D_h(H)=3-H, \tag{3.86}$$

turns out to be the same as that of the whole fractional Brownian isoset $\psi(x,y,z)=h$. [The isoset of a two-dimensional fractional Brownian function with the fractal dimension (3.81) is a plane cross section of a three-dimensional isoset.] This means a fairly good connectedness of 3D contour surfaces: a connected contour piece of the size λ comprises a finite fraction of the whole isoset (with the same level h) in the λ-sized box, for each $\lambda\in[\lambda_0,\lambda_m]$.

3. Correlated cluster density exponent

The case $-1/\nu<H<0$, corresponding to the long-range correlated percolation, requires a different approach. To obtain the cluster scaling, one has to know the correlated percolation exponents $\tilde{\nu}(H)$ and $\tilde{\beta}(H)$. The first one is given by Eq. (2.30). Here we show that the method of separated scales predicts the infinite cluster density exponent β to be insensitive to correlations and is the same as in the uncorrelated percolation problem (Isichenko and Kalda, 1991b). The following argument refers to any dimensionality d.

Consider the infinite continuum cluster $\psi(\mathbf{x})<h=h_c+\delta$, where $h_c\equiv h_{c1}$ is the lower critical level of $\psi(\mathbf{x})$ and the positive δ satisfies $\psi_{\lambda_m}\ll\delta\ll\psi_{\lambda_0}$. Let us separate scales as in Eq. (3.63). Denote by λ_δ the solution of the equation $\psi_{\lambda_\delta}=\delta$ and, for brevity, let $\lambda_{\delta-1},\lambda_{\delta-2},\ldots,\lambda_0$ be the shorter, separated scales. Since the monoscale potentials $\psi_\lambda(\mathbf{x})$ differ only by rescaling, their own critical levels are given by the same formula,

$$h_c^{(\lambda)}=K\psi_\lambda, \tag{3.87}$$

with a numerical coefficient K depending on the properties of the ensemble. For example, $K=0$ for a 2D sign-symmetric potential, but $K<0$ for $d=3$. First, consider the infinite connected region (let us call it the "λ_δ cluster") where

$$\psi_{\lambda_\delta}(\mathbf{x})<K\psi_{\lambda_\delta}+\delta. \tag{3.88}$$

This cluster is fairly supercritical; hence it occupies the volume fraction of order unity:

$$P_\infty^{(\lambda_\delta)}\simeq 1. \tag{3.89}$$

Now consider the $\lambda_{\delta-1}$ cluster defined by the inequality

$$\psi_{\lambda_{\delta-1}}(\mathbf{x})<K\psi_{\delta-1}+[K\psi_{\lambda_\delta}+\delta-\psi_{\lambda_\delta}(\mathbf{x})]. \tag{3.90}$$

The second term on the right-hand side of Eq. (3.90) is a slowly varying function which is positive in the λ_δ cluster. As the local correlation length of the $\lambda_{\delta-1}$ cluster,

$$\xi^{(\lambda_{\delta-1})}\simeq\lambda_{\delta-1}\left[\frac{\psi_{\lambda_\delta}}{\psi_{\lambda_{\delta-1}}}\right]^{-\nu}=\lambda_{\delta-1}\left[\frac{\lambda_\delta}{\lambda_{\delta-1}}\right]^{-\nu H}, \tag{3.91}$$

is much less than λ_δ (because $-1/\nu<H<0$), the infinite $\lambda_{\delta-1}$ cluster lies entirely in the λ_δ cluster and occupies the volume fraction

$$P_\infty^{(\lambda_{\delta-2})}\simeq P_\infty^{(\lambda_\delta)}\left[\frac{\psi_{\lambda_\delta}}{\psi_{\lambda_{\delta-1}}}\right]^{\beta}, \tag{3.92}$$

where β is the infinite cluster density exponent of uncorrelated percolation. Analogously, we can consider the $\lambda_{\delta-2}$ cluster where

$$\psi_{\lambda_{\delta-1}}(\mathbf{x})<K\psi_{\delta-2}+[K\psi_{\lambda_{\delta-1}}+K\psi_{\lambda_\delta}+\delta-\psi_{\lambda_{\delta-1}}(\mathbf{x})-\psi_{\lambda_\delta}(\mathbf{x})],$$

and so on down to the scale λ_0. This procedure corresponds to the successive increase in resolution as we view the cluster of $\psi(\mathbf{x})<h=h_c+\delta$, with $h_c=K(\psi_{\lambda_0}+\cdots+\psi_{\lambda_\delta})\simeq K\psi_0$. Finally, we obtain the expression for the density of the correlated infinite cluster,

$$P_\infty(h)\equiv P_\infty^{(\lambda_0)}\simeq P_\infty^{(\lambda_\delta)}\left[\frac{\psi_{\lambda_\delta}}{\psi_{\lambda_0}}\right]^{\beta}\simeq\left[\frac{\delta}{\psi_0}\right]^{\beta},\qquad 0<\delta\equiv h-h_c\ll\psi_0. \tag{3.93}$$

Equation (3.93) means the universality of the exponent β for both random and correlated percolation, for a given dimension d:

$$\tilde{\beta}(H,d)\equiv\beta(d)\ . \tag{3.94}$$

Notice that the above construction automatically implies $\tilde{\nu}(H)=-1/H$, because the scale $\lambda_\delta=\lambda_0(\delta/\psi_0)^{1/H}$ is nothing but the correlation length ξ_h.

Once the correlated percolation exponents are known, the fractal dimension $D_h(H)$ of a connected isosurface $\psi(x,y,z)$ can be calculated as the correlated hull dimension, which is the same as that of a correlated percolation cluster,

$$D_h\equiv\tilde{d}_h(H)=\tilde{d}_c(H)=d-\tilde{\beta}(H)/\tilde{\nu}(H)=3+\beta H\ , \qquad d=3,\quad -1/\nu<H<0\ . \tag{3.95}$$

Analogously to the uncorrelated monoscale case, the distribution function of isosurfaces over size a includes a finite $F(\infty)$, with a finite-size component given by the formula similar to (3.50):

$$F(a)\simeq\frac{S(a)w(a)}{a^3}\simeq\left[\frac{\lambda_0}{a}\right]^{(\tilde{\beta}+1)/\tilde{\nu}}=\left[\frac{\lambda_0}{a}\right]^{-(\beta+1)H}\ , \qquad \lambda_0<a<\lambda_m,\quad -1/\nu<H<0\ . \tag{3.96}$$

4. An example: Potential created by disordered charged impurities

To demonstrate an application of the multiscale topography, let us recall the example of random isopotentials in the quantized Hall conductance or elsewhere. Consider the electrostatic field created by charged impurities randomly distributed in the (x,y) plane ($d=2$) or in space ($d=3$). It might seem that, due to the well-defined scale of the separation of disordered impurities, $\lambda_0=n_i^{-1/d}$ (where n_i is the average density of impurities), the monoscale continuum percolation model is appropriate (Trugman, 1983). This, however, depends on the impurity distribution and the Debye screening length.

The variation ρ_λ of the impurity charge density $\rho(\mathbf{x})$ over scale $\lambda>\lambda_0$ can be estimated by using the $\sqrt{N}$ rule, where $N=n_i\lambda^d$ is the expected number of impurities in the volume λ^d:

$$\lambda^d\rho_\lambda\propto(n_i\lambda^d)^{1/2}\ . \tag{3.97}$$

Hence the charge-density λ spectrum is

$$\rho_\lambda\propto\lambda^{-d/2},\quad \lambda\gg\lambda_0\ . \tag{3.98}$$

Taking into account the possible effect of Debye screening, we describe the electric potential $\Phi(\mathbf{x})$ by the generalized Poisson equation

$$\nabla^2\Phi(x,y,z)-\lambda_D^2\Phi(x,y,z)=\begin{cases}-4\pi\delta(z)\rho(x,y), & d=2\ ,\\ -4\pi\rho(x,y,z), & d=3\ ,\end{cases} \tag{3.99}$$

where $\lambda_D\gg\lambda_0$ is the Debye length. In the case of a solitary charge, $\rho(\mathbf{x})=e\delta(\mathbf{x})$, the solution of Eq. (3.99) would yield the standard screened Coulomb potential $\Phi=(e/r)\exp(-r/\lambda_D)$, $r\equiv|\mathbf{x}|$. For impurities distributed in the plane $z=0$, the solution of (3.99) can be found using Fourier transformation in (x,y),

$$\Phi_{\mathbf{k}}(z)=\frac{2\pi k}{k^2+\lambda_D^{-2}}\rho_{\mathbf{k}}\exp(-k|z|)\ . \tag{3.100}$$

So the electric potential in the plane, $\phi(x,y)=\Phi(x,y,0)$, has the λ spectrum

$$\phi_\lambda\propto\frac{\lambda}{\lambda^2+\lambda_D^2}\rho_\lambda\propto\begin{cases}\text{const}, & \lambda_0\ll\lambda\ll\lambda_D\ ,\\ \lambda^{-3}, & \lambda\gg\lambda_D\ .\end{cases} \tag{3.101}$$

The $\phi(x,y)$ spectrum exponent $H=0$ (for the scaling range $[\lambda_0,\lambda_D]$) falls into the multiscale regime (3.70). Specifically, the fractal dimension (3.75) of an isopotential line is $D_h=\frac{10}{7}$. When a small uniform electric field $\mathbf{E}_1$ is applied, percolating current channels are formed whose characteristic transverse walk Δ_ε and width δ_ε are given by formulas (3.59) and (3.60) in the limit $H\to0$:

$$\Delta_\varepsilon=\lambda_0/\varepsilon,\quad \delta_\varepsilon=\lambda_0,\quad \varepsilon\equiv E_1/E_0\ll1\ . \tag{3.102}$$

In the scaling range above the Debye length, the isopotentials behave in a monoscale manner ($H=-3<-1/\nu=-\frac{3}{4}$).

In the case of statistically uniform three-dimensional impurities, we similarly obtain

$$\Phi_\lambda\propto\frac{\lambda^2}{\lambda^2+\lambda_D^2}\rho_\lambda\propto\begin{cases}\lambda^{1/2}, & \lambda_0\ll\lambda\ll\lambda_D\ ,\\ \lambda^{-3/2}, & \lambda\gg\lambda_D\ .\end{cases} \tag{3.103}$$

The unscreened behavior of $\Phi(\mathbf{x})$ with $H=\frac{1}{2}$ corresponds to a Brownian function, whose 3D isopotentials have the fractal dimension of $\frac{5}{2}$, whereas the connected pieces of their planar cross section have $D_h=(10-3H)/7=\frac{17}{14}$ and produce wide channels with parameters given by Eqs. (3.59) and (3.60), when a small constant electric field is applied.

This example demonstrates the possible complexity of topographic behaviors in the potential created by a fairly simple disorder, although in real systems the situation is far more complicated (Prange, 1990). The complex character of electron motion in three-dimensional potentials is discussed in Sec. IV.C.

5. Difficulties of the method of separated scales

The method of the separation of scales is a surrogate for an exact solution which is unknown, so one should be cautious in applying this technique. The calculation of multiscale topographic exponents, such as $D_h(H)$ and $\tilde{\beta}(H)$, involved the estimation of a product of a large number, up to $m=m(\mu)\simeq\log\Lambda/\log\mu$ ($\Lambda=\lambda_m/\lambda_0\gg1$, $\mu=\lambda_{i+1}/\lambda_i$), of terms known only by the order of magnitude. To be more exact, Eq. (3.74) at $\lambda=\lambda_m$ should read

$$L(\lambda_m)=\lambda_0\prod_{i=1}^{m(\mu)}E_i(\mu)\left[\frac{\lambda_i}{\lambda_{i-1}}\right]^{D_h^{(\infty)}}, \tag{3.104}$$

where all $E_i(\mu)\simeq 1$, and $D_h^{(\infty)}$ is given by formula (3.75). If there is a systematic error in the evaluation of the factors in Eq. (3.104), characterized by the geometric mean $E(\mu)\neq 1$ of $E_i(\mu)$, then Eq. (3.104) can be written as

$$L(\lambda_m)=\lambda_0\left[\frac{\lambda_m}{\lambda_0}\right]^{D_h^{(\mu)}}, \tag{3.105}$$

where

$$D_h^{(\mu)}(H)=D_h^{(\infty)}(H)+\frac{\log E(\mu)}{\log\mu}. \tag{3.106}$$

While giving a correct value for the fractal dimension of an isoline of a separated-scale potential ($\mu\gg 1$), the equation $D_h^{(\infty)}=(10-3H)/7$ may be wrong in the limit $\mu=2$ if $E(2)\neq 1$.

On the other hand, when applied to the evaluation of the fractal dimension of the fractional Brownian isoset $\psi(\mathbf{x})=h$, $0<H<1$, the method of separated scales predicts a correct result, $D=d-H$, confirmed by direct box-counting calculation and the cross-section rule (Sec. III.B). The correlation length exponent of the correlated percolation problem given in the framework of the method of separated scales, $\tilde{\nu}(H)=-1/H$, also agrees with an independent calculation (Weinrib, 1984).

A specific cause for concern is the discrepancy between the correlated percolation beta exponent predicted by the method of separated scales (3.94) and the one predicted by the renormalization-group (RG) theory. Weinrib (1984) has developed the RG expansion of the exponent $\tilde{\eta}(d,H)=2-d+2\tilde{\beta}(d,H)/\tilde{\nu}(d,H)$ in a series in $(6-d)>0$ and $(H+2)>0$ up to linear terms. The η exponent describes the behavior of a cluster correlation function (Shklovskii and Efros, 1984). At $d=6$ and higher, the uncorrelated percolation exponents take on their effective-medium values $\nu=\frac{1}{2}$, $\beta=1$, $\eta=0$ (Stauffer, 1979); hence the correlated behavior for $d=6$ takes place at $H<-1/\nu=-2$. The Weinrib result, $\tilde{\eta}(d,H)=\frac{2}{11}(H+2)-\frac{1}{11}(6-d)+\cdots$, corresponds, in terms of the beta exponent, to $\tilde{\beta}(6,H)=1+\frac{6}{11}(H+2)+\cdots$, whereas the scale-separation prediction is $\tilde{\beta}(6,H)\equiv 1$. Still, the RG expansion method is far from a rigorous calculation, just as is the method of separation of scales.

In summary, for the evaluation of the exponents of multiscale statistical topography/correlated percolation, an independent approach, or, at least, a specially designed numerical code, is strongly desired.

F. Statistics of separatrices

To show the existence of arbitrarily large contours, we have used two types of argument: "flood in the hills" and the correspondence of the contour problem to a lattice percolation problem. Another approach to generating large-scale contour lines and surfaces is based on the topological device of "dressing."

Consider a closed level line of $\psi(x,y)$ or a level surface of $\psi(x,y,z)$. Move outwards from it and explore neighboring level sets that enclose the initial one. The topology of the nested contours will not change until we encounter a separatrix coming through a saddle point of ψ (Fig. 15). For a nondegenerate potential $\psi(\mathbf{x})$, every saddle (hyperbolic) point lies on a different level; therefore every separatrix looks like a figure eight (self-enclosed, perhaps), in two dimensions, or a dumbbell, in three dimensions. After encountering the separatrix, we go on and construct a nested set of separatrices similar to Russian *Matreshkas*. Nothing in this construction prevents one from inflating the contours up to infinity.

For a power-spectrum random function with $H<1$, the density of stationary points [i.e., points where $\nabla\psi(\mathbf{x})=0$] per unit volume is governed by the λ_0 component of the potential, because this component dominates the potential gradient. It follows, in particular, that the average density of saddle points per unit volume is of the order of λ_0^{-d}. As on each step of the dressing procedure, the saddle point closest to the given separatrix is caught; the gap $s(a)$ between two nearest-neighbor separatrices of size a is determined from the requirement that the volume between the separatrices be approximately constant (λ_0^d). Thus $s(a)$ decreases with growing size a inversely proportional to the separatrix measure (length or area):

$$s(a)\propto a^{-D_h}. \tag{3.107}$$

Although telling nothing about critical levels, the topological argument can be used to develop the statistics of separatrices (Gruzinov *et al.*, 1990). Each nondegenerate closed separatrix divides the space into three parts: two bounded and one unbounded (Fig. 15). Each bounded part contains at least one extremum of ψ. Introduce the index (i,j) of a saddle point as the numbers of extrema in the two bounded parts of its separatrix. (We can distinguish the order of i and j, assuming, for example, that the first index corresponds to the part located lower.) Let $P(i,j)$ be the number, per unit volume, of saddle points with the corresponding index. These numbers are related by certain topological constraints. Indeed, each closed separatrix with the index (i,j) is necessarily surrounded by a nearest separatrix with the index $(i+j,k)$ or $(k,i+j)$, so that

$$\sum_{i=1}^{l-1}P(i,l-i)=\sum_{k=1}^{\infty}[P(l,k)+P(k,l)]+P(l,\infty)+P(\infty,l). \tag{3.108}$$

In Eq. (3.108), the possibility is taken into account of the presence of a finite number of open separatrices (corresponding to the infinite indices), which is the case in three dimensions. In two dimensions, there exists only one unclosed level line; hence $P(l,\infty)=P(\infty,l)=P(\infty,\infty)=0$.

A corollary of Eq. (3.108) is the well-known *sum rule* for a two-dimensional potential $\psi(x,y)$ (Longuet-Higgins, 1960b),

$$N_{\text{saddle}}=N_{\max}+N_{\min},\quad d=2\ , \tag{3.109}$$

for the number of saddles, maxima, and minima of $\psi(x,y)$. Indeed, there are exactly as many extrema (minima plus maxima) as the number of saddles, one of whose indices is unity (that is, whose separatrix is the one closest to the given extremum). Relating the number of stationary points to the unit volume, we write in the general case

$$N_{\text{extr}}\equiv N_{\max}+N_{\min} =\sum_{i=1}^{\infty}[P(1,i)+P(i,1)]+P(1,\infty)+P(\infty,1)\ . \tag{3.110}$$

On the other hand, the total number of saddles is

$$N_{\text{saddle}}=\sum_{i=1}^{\infty}\sum_{j=1}^{\infty}P(i,j)+\sum_{i=1}^{\infty}[P(i,\infty)+P(\infty,i)] +P(\infty,\infty)\ . \tag{3.111}$$

Upon summing Eq. (3.108) over l and using expressions (3.110) and (3.111), we finally infer

$$N_{\text{saddle}}=N_{\text{extr}}+P(\infty,\infty)\ . \tag{3.112}$$

In two dimensions, Eq. (3.112) reduces to the sum rule (3.109); however, it yields an inequality in the three-dimensional case:

$$N_{\text{saddle}}\geq N_{\max}+N_{\min},\quad d=3\ . \tag{3.113}$$

The usual proof of the formula (3.109) (Longuet-Higgins, 1960b) uses the correspondence of the saddles, minima, and maxima of a function defined on a torus to the edges, vertices, and faces, respectively, of a polyhedron, and the Euler theorem (Coxeter, 1973) $N_{\text{edge}}=N_{\text{vertex}}+N_{\text{face}}$.

We continue discussing the two-dimensional case. The topological constraint (3.108) can be rewritten in terms of a generating function

$$G(x,y)=(1/N_{\text{saddle}})\sum_{i=1}^{\infty}\sum_{j=1}^{\infty}P(i,j)x^iy^j\ . \tag{3.114}$$

Upon multiplying Eq.(3.108) by x^l and summing over l, we obtain the functional equation

$$G(x,x)=2G(x,1)-x\ , \tag{3.115}$$

where the normalization condition $G(1,1)=1$ was taken into account.

Sure enough, being exact for any nondegenerate potential, relation (3.115) is insufficient for determining $G(x,y)$ and thereby $P(i,j)$. If we assume, heuristically referring to randomness, that the two closed parts of each separatrix are independent, that is, $P(i,j)=P(i)P(j)$, then G is also factorized: $G(x,y)=G(x)G(y)$. Under this assumption, Eq. (3.115) immediately yields

$$G(x)=1-(1-x)^{1/2}=\sum_{i=1}^{\infty}\frac{(2i-3)!!}{(2i)!!}x^i\ ; \tag{3.116}$$

hence

$$P(i,j)=\frac{(2i-3)!!(2j-3)!!}{(2i)!!(2j)!!} \simeq\frac{1}{4\pi}i^{-3/2}j^{-3/2},\quad i,j\gg 1\ . \tag{3.117}$$

It was established (Gruzinov *et al.*, 1990) that such a distribution of separatrices is consistent with the long-range behavior of a monoscale uncorrelated potential $\psi(x,y)$. In all other cases, the two parts of a separatrix are not independent.

IV. TRANSPORT IN RANDOM MEDIA

In this section, three wide classes of transport phenomena are discussed: the advection diffusion of a tracer (impurity, temperature, etc.) in an incompressible flow (Sec. IV.A), the conductivity of a medium with spatially fluctuating properties (Sec. IV.B), and the random walk of charged particles in fluctuating electromagnetic fields (Secs. IV.A.5 and IV.C). Physically, the most interesting are the cases involving large parameters such as Péclet number (the ratio of convective term to molecular diffusion term) or the strength of the fluctuations in microscopic characteristics of the medium. We shall try to demonstrate that, in many cases, percolation theory and/or statistical topography provide helpful tools in theoretical studies of such transport processes.

In Sec. IV.A the advective-diffusive transport of a passive tracer is reviewed. In two dimensions, incompressible streamlines are represented by the contour lines of a stream function; hence the geometry of a random flow is described in terms of the statistical topography. For a bounded stream function, the passive transport is asymptotically diffusive and is characterized by a finite effective (turbulent) diffusion coefficient D^* (Avellaneda and Majda, 1991; Tatarinova *et al.*, 1991). When the stream function (velocity vector potential in 3D) is not bounded, or when it is characterized by many scales of length, the passive transport may be *superdiffusive,* meaning that the average square displacement grows faster than linear with time. For special initial conditions and on limited time scales, a more exotic *subdiffusive* tracer behavior is also possible.

In Sec. IV.B selected problems of transport in randomly inhomogeneous media are discussed. The simplest example of such a system is a random mixture of conducting and insulating phases (random resistor network) was described in the framework of standard percolation problem (Sec. II). Two-dimensional systems *at* the percolation threshold have a remarkable symmetry (Keller, 1964; Dykhne, 1970a), which allows one to calculate exactly the effective conductivity for arbitrary conductivi-

ties of the two phases. Other examples include plasma heat conduction in a stochastic magnetic field and the electrical conductivity of randomly inhomogeneous media with the Hall effect.

In Sec. IV.C the multifaceted aspects of electron motion in disordered potentials are discussed in the examples of a few models. Special attention is given to the long-range correlation effects that the magnetic field introduces into the processes of electron scattering by disordered potentials.

A. Advective-diffusive transport

Everyone will acknowledge the striking effect the stirring of a teaspoon exerts on the sugar dissolution in a cup of coffee. A vast variety of processes, ranging from everyday propagation of smell to heat transport in fusion plasma, can be cast into the simplest form of the advection-diffusion equation

$$\frac{\partial n}{\partial t}+\nabla\cdot[n\mathbf{v}(\mathbf{x},t)]=D_0\nabla^2 n \ , \tag{4.1}$$

where n is the density of a passively advected agent (concentration of an impurity, temperature, etc.), $\mathbf{v}$ is a velocity field, and D_0 is the molecular diffusion coefficient or thermal conductivity. In most practically applicable cases, velocity $\mathbf{v}(\mathbf{x},t)$ can be considered to be incompressible: $\nabla\cdot\mathbf{v}=0$, or $\mathbf{v}=\nabla\times\boldsymbol{\psi}(\mathbf{x},t)$, where $\boldsymbol{\psi}$ is a vector potential. Along with Eq. (4.1), the problem can be equivalently formulated in terms of a random trajectory of tracer particle described by the Langevin equation (Chandrasekhar, 1943)

$$\frac{d\mathbf{x}}{dt}=\mathbf{v}(\mathbf{x},t)+\mathbf{v}_D(t) \ , \tag{4.2}$$

where $\mathbf{v}_D(t)$ is a Gaussian random noise corresponding to the molecular diffusion, so that

$$\langle\mathbf{v}_D(t)\rangle=0, \quad \langle v_{Di}(t)v_{Dj}(t')\rangle=2D_0\delta(t-t')\delta_{ij} \ . \tag{4.3}$$

Then the probability distribution function $n(\mathbf{x},t)$ of the particle position $\mathbf{x}$ evolves according to the Fokker-Planck equation (4.1).

In 1921, G. Taylor put forward the hypothesis of "diffusion by continuous movements." According to this hypothesis, the solution of Eq. (4.2) for a turbulent, zero mean velocity field $\mathbf{v}(\mathbf{x},t)$ behaves diffusively in the long-time limit, so that

$$\lim_{t\to\infty}\frac{\langle(\mathbf{x}_i(t)-\mathbf{x}_i(0))(\mathbf{x}_j(t)-\mathbf{x}_j(0))\rangle}{2t}=D_{ij}^* \ , \tag{4.4}$$

where D_{ij}^* is the effective, or turbulent, diffusivity tensor. Taylor (1921) related the effective diffusivity to the Lagrangian velocity correlator

$$V_{ij}(t)=\langle v_i(\mathbf{x}(t),t)v_j(\mathbf{x}(0),0)\rangle$$

as follows:

$$D_{ij}^*=\int_0^\infty V_{ij}(t)dt \ . \tag{4.5}$$

This well-known result, however, is almost a tautology, because in order to obtain $V_{ij}(t)$ one has first to solve the equation of motion (4.2). The Taylor hypothesis of the turbulent diffusion behavior corresponds to a decay of Lagrangian correlations sufficiently fast so that integral (4.5) converges.

Richardson (1926) analyzed then-available experimental data on diffusion in air. Those data varied by 12 orders of magnitude, indicating that there is something wrong with the Taylor hypothesis. Richardson phenomenologically conjectured that the diffusion coefficient D_λ in turbulent air depended on the scale length λ of the measurement. The Richardson law,

$$D_\lambda\propto\lambda^{4/3} \ , \tag{4.6}$$

was related to the Kolmogorov-Obukhov turbulence spectrum, $v_\lambda\propto\lambda^{1/3}$, by Batchelor (1952). So the effective diffusion limit (4.4) does not necessarily exist. It must be emphasized that the Richardson law (4.6) describes the *relative diffusivity* of suspended particles, that is, the rate of growth of the mean-square distance between two fluid elements in the turbulent medium. The *absolute diffusion* in Kolmogorov turbulence is not universal because the boundary-condition-dependent long-scale velocity pulsations govern the absolute motion of a fluid element and may make the integral (4.5) diverge (Moffatt, 1981).

There exists, however, an important class of incompressible flows that do lead to a finite absolute turbulent diffusion coefficient (4.4), namely, the flows with a bounded velocity vector potential $\boldsymbol{\psi}(\mathbf{x},t)$. In Sec. IV.A.1 recent rigorous results are reviewed concerning such flows. In Sec. IV.A.2 certain regular flows are listed for which the effective diffusivity D^* is known exactly or can be easily estimated in order of magnitude. Section IV.A.3 is devoted to the problem of turbulent diffusion in random, steady 2D flows, which are described using percolation/statistical topography theory. In Sec. IV.A.4 chaotic mixing properties of unsteady random flows are studied and characterized by Kolmogorov entropy. Effective diffusion in such flows is discussed in Sec. IV.A.5. The applications of the theory of transport by time-dependent random flows are primarily concerned with and exemplified by the anomalous transport in turbulent plasmas.

Even when the effective diffusivity D^* governs the asymptotic tracer behavior in an advection-diffusion system, this behavior has finite set-in (mixing) time and length scales. On time and space scales below the mixing time τ_m and the mixing scale ξ_m, passive scalar transport can be anomalous, meaning that the propagation rate is described by

$$\langle[\mathbf{x}(t)-\mathbf{x}(0)]^2\rangle^{1/2}\propto t^\zeta \ , \tag{4.7}$$

with $\zeta\neq\frac{1}{2}$ instead of the behavior of Eq. (4.4). For flows with unbounded vector potential $\boldsymbol{\psi}(\mathbf{x})$ the mixing time

τ_m may be infinite, with the anomalous diffusion (4.7) featuring the long-time behavior. The mechanisms of anomalous diffusion, including both *superdiffusion* ($\zeta > \frac{1}{2}$) and *subdiffusion* ($\zeta < \frac{1}{2}$), are discussed in Sec. IV.6.A.

1. When is the effective transport diffusive, and what are the bounds on effective diffusivity?

This question has been posed frequently, first by Zeldovich (1937), who showed that the lower bound for the effective diffusivity D^* is simply the molecular diffusivity D_0. To be more exact, his result was that arbitrary incompressible convection in a fluid necessarily increases (with respect to the absence of convection) the average impurity flux J between two surfaces where the two constant impurity densities, n_1 and n_2, are maintained. The idea of the proof is based on a simple variational principle: Integrate the quantity $(n\mathbf{v}-D_0\nabla n)\cdot\nabla n$ over the volume outside the two closed surfaces. Then the result is

$$J(n_1-n_2)=D_0\int(\nabla n)^2 d\mathbf{x} \ . \tag{4.8}$$

The right-hand side of Eq. (4.8) is minimized by a harmonic function, $\nabla^2 n=0$, which corresponds to the zero velocity field in the time-independent (or time-averaged) Eq. (4.1).

Effective transport in a convection-diffusion system is governed by the dimensionless parameter

$$P=\frac{\psi_0}{D_0} \ , \tag{4.9}$$

known as the *Péclet number,* where ψ_0 is some characteristic (for example, root-mean-square) value of the vector potential $\boldsymbol{\psi}(\mathbf{x},t)$. According to the Zeldovich variational principle, effective diffusivity, if it exists, must expand in a series of even powers of the Péclet number:

$$D^*=D_0(1+a_2P^2+a_4P^4+\cdots), \quad P\ll 1 \ , \tag{4.10}$$

where $a_2>0$. In the limit of a large Péclet number, it is natural to expect that the effective diffusivity greatly exceeds the molecular one:

$$D^*\simeq D_0P^\alpha, \quad P\gg 1 \ , \tag{4.11}$$

where the non-negative exponent α depends on the topology of the flow.

A more difficult question concerns the very realizability of the effective diffusion regime and the upper bounds for effective diffusivity. Strictly speaking, condition (4.4) does not yet imply the effective diffusion of a tracer. A stronger requirement is that the local-average tracer density $\langle n\rangle$ evolve according to the effective diffusion equation

$$\frac{\partial\langle n\rangle}{\partial t}=\frac{\partial}{\partial x_i}D_{ij}^*\frac{\partial\langle n\rangle}{\partial x_j} \ . \tag{4.12}$$

The local average of the density n is taken near the point $(\mathbf{x},t)$ over such length scales ξ and time scales τ that satisfy

$$\xi_m\ll\xi\ll l^*, \quad \tau_m\ll\tau\ll t^* \ , \tag{4.13}$$

where ξ_m and τ_m are the flow-dependent *mixing length* and *mixing time*, respectively, and l^* and t^* are the characteristic length and time scales of $\langle n\rangle$. As inequalities (4.13) show, the set-in of effective diffusion takes finite mixing time τ_m; hence Eq. (4.12) becomes valid only asymptotically.

Another approach to the effective diffusion problem is to consider the velocity field $\mathbf{v}(\mathbf{x},t)$ as a stationary random field and to average the tracer density n over the statistical ensemble of $\mathbf{v}$. Pioneered by Taylor (1921), this approach remains the most popular (Kraichnan, 1970; McLaughlin *et al.*, 1985; Avellaneda and Majda, 1989, 1991). Kraichnan (1970) undertook the explicit computation of the mean-square particle displacement in 2D and 3D Gaussian velocity fields, averaging over 2000 realizations for each ensemble. There was no molecular diffusion in this simulation, and both time-dependent and "frozen" velocity fields were tested. In each case, except for the case of two-dimensional time-independent flows, Kraichnan observed a well-established turbulent diffusivity (4.4).

Another computational approach, proposed by Isichenko *et al.* (1989), used a prescribed quasiperiodic stream function $\psi(x,y)$ (such as the one shown in Fig. 10) as a model of random flow. Although not random, the flow has no apparent degeneracies, such as periodicity, and looks quite generic. However, one still can visually identify a "trace of periodicity," especially for a small number N of harmonics, because the flow pattern is a two-dimensional projection of an N-dimensional periodic structure. (In Fig. 10, the case of $N=25$ is shown.) In addition, the space-averaged correlator $C(\boldsymbol{\rho})=\langle\psi(\mathbf{x})\psi(\mathbf{x}+\boldsymbol{\rho})\rangle_{\mathbf{x}}$ does not vanish at large scales, showing long correlations that are characteristic for quasicrystals (Levine and Steinhardt, 1984; Kalugin *et al.*, 1985; Steinhardt and Ostlund, 1987; Arnold, 1988). These correlations were not found to affect appreciably the advective-diffusive transport in steady flows for $N>3$ (Isichenko *et al.*, 1989). Yet, the quasicrystallic correlations appear to be much more pronounced for diffusion in time-dependent 2D flows (see Sec. IV.A.5).

Analytical results regarding the criterion of the transition to effective diffusion were obtained by McLaughlin *et al.* (1985), who proved the following *homogenization property* of time-independent, incompressible, zero mean, stationary random flow $\mathbf{v}(\mathbf{x})$. If the Fourier transform $V_{ij}(\mathbf{k})$ of the velocity correlator $V_{ij}(\boldsymbol{\rho})=\langle v_i(\mathbf{x})v_j(\mathbf{x}+\boldsymbol{\rho})\rangle$ is continuous at the origin $\mathbf{k}=0$, then the ensemble-averaged solution of Eq. (4.1), $\langle n\rangle=N_\varepsilon(\mathbf{x},t)$, corresponding to the initial condition $n(\mathbf{x},0)=n_0(\varepsilon\mathbf{x})$, becomes very close, as $\varepsilon\to 0$, to $N(\mathbf{x}/\varepsilon,t/\varepsilon^2)$, where $N(\mathbf{x},t)$ is the solution of the initial-value problem

$$\frac{\partial N}{\partial t}=\frac{\partial}{\partial x_i}D_{ij}^{*}\frac{\partial N}{\partial x_j}\ ,$$
$$N(\mathbf{x},0)=n_0(\mathbf{x})\ , \tag{4.14}$$

and effective diffusivity in any direction $\mathbf{n}$ exceeds molecular diffusivity:

$$D^{*}(\mathbf{n})\equiv|\mathbf{n}|^{-2}D_{ij}^{*}n_in_j\geq D_0\ . \tag{4.15}$$

Battacharya *et al.* (1989) obtained a similar result for arbitrary periodic incompressible flow, without ensemble averaging. Kalugin *et al.* (1990) proved a homogenization theorem for periodic flows using the analytical continuation of $D_{ij}^{*}(P)$, considered as a function of the Péclet number $P=\psi_{\rm rms}/D_0$, to the complex plane of P. Such an approach led to an efficient algorithm for the computation of D_{ij}^{*} for any periodic flow using continuous fractions.

Avellaneda and Majda (1989, 1991) generalized the McLaughlin *et al.* (1985) result and showed that the finiteness of the Péclet number (4.9) (with ψ_0 understood as the ensemble root-mean-square vector potential) is a necessary and sufficient condition to guarantee the homogenization property for time-independent random flows $\mathbf{v}(\mathbf{x})=\nabla\times\boldsymbol{\psi}(\mathbf{x})$. They also developed a theory of Padé approximants using a Stieltjes measure representation formula for effective diffusivity. This theory led to a sequence of rigorous bounds on D^{*}, of which the simplest one is

$$D_0\leq D^{*}\leq D_0\left[1+\frac{1}{d}P^2\right]\ , \tag{4.16}$$

where d is the dimension of the problem. Generally, the first two terms in the low-P expansion (4.10) turn out to be an upper bound for D^{*} at any P.

Independently, Tatarinova *et al.* (1991) considered the most general case of an arbitrary incompressible 3D time-dependent flow. They gave an elegant proof of the following theorem: If the vector potential $\boldsymbol{\psi}(\mathbf{x},t)$ of a given flow is bounded, $|\boldsymbol{\psi}(\mathbf{x},t)|\leq\psi_{\max}$, then the solution of the initial-value problem (4.1) with $n(\mathbf{x},0)=\delta(\mathbf{x}-\mathbf{x}_0)$ behaves as follows. The mean-square displacement,

$$R^2(t,\mathbf{x}_0)\equiv\int(\mathbf{x}-\mathbf{x}_0)^2n(\mathbf{x},t)d\mathbf{x}\ , \tag{4.17}$$

grows with progressing time not slower and not faster than linearly in the sense that

$$D_0\leq\frac{\langle R^2(t,\mathbf{x}_0)\rangle_{\mathbf{x}_0}}{2td}\leq D_0+\frac{\psi_{\max}^2}{D_0}\ . \tag{4.18}$$

Most likely, the averaging of R^2 over the initial position $\mathbf{x}_0$ is not essential for this result. The comparison of the Tatarinova *et al.* theorem with the Avellaneda-Majda theorem suggests that the boundedness of the vector potential $\boldsymbol{\psi}(\mathbf{x},t)$ is also sufficient for the global transport homogenization, that is, for the asymptotic transition from Eq. (4.1) to Eq. (4.12). In such a general form, however, the homogenization theorem has not yet been proved.

Thus one may conclude that, in the presence of finite molecular diffusivity D_0, the finite vector potential is a sufficient and "almost necessary" condition for effective diffusion to be established, with effective diffusivity satisfying the inequality

$$D_0\leq D^{*}\leq D_0+\frac{\psi_{\max}^2}{D_0}\ . \tag{4.19}$$

In terms of the scaling exponent α entering Eq. (4.11), this implies $0\leq\alpha\leq2$.

For the case of anisotropic molecular diffusivity tensor $\hat{D}_0$ and a possible anisotropy of the flow, following the lines of Tatarinova *et al.* (1991), inequality (4.19) can be generalized to

$$D_{0\mathbf{n}}\leq D_{\mathbf{n}}^{*}\leq D_{0\mathbf{n}}+\max_{\mathbf{x},t}\max_{\mathbf{m}}\frac{[\mathbf{m}\times\mathbf{n}\cdot\boldsymbol{\psi}(\mathbf{x},t)]^2}{|\mathbf{m}|^2|\mathbf{n}|^2D_{0\mathbf{m}}}\ , \tag{4.20}$$

where $D_{\mathbf{n}}\equiv D_{ij}n_in_j/|\mathbf{n}|^2$ denotes the diffusivity in the $\mathbf{n}$ direction. It is clear that inequality (4.19) is a consequence of (4.20). Result (4.20) will be used in Sec. IV.B.3 to establish bounds on the effective conductivity of heterogeneous media. Without restricting the class of the vector potential $\boldsymbol{\psi}$, inequalities (4.19) and (4.20) cannot be further improved in the sense that both the lower and the upper bounds on the effective diffusivity can be realized in particular cases.

2. Effective diffusivity: Simple scalings

There exist several classes of flows, whose transport properties can be calculated exactly. As we shall see, the rigorous bounds on the effective diffusivity (4.19) are attainable.

The simplest example of a shear flow in a tube was considered by Taylor (1953, 1954), who noticed that the axial dispersion of a solute advected by the Poiseuille flow $v(r)=v_0(1-r^2/a^2)$ [where $v(r)$ is the axial velocity in a tube of the radius a] is described, in a mean velocity frame of reference, by a diffusive law. For $av_0\gg D_0$, Taylor found the following equation for the "virtual coefficient of the diffusivity": $D^{*}=a^2v_0^2/(192D_0)$. He proposed to use this result for the investigation of the propagation of salts in bloodstreams. Aris (1956) has generalized Taylor's result to the case of arbitrary Péclet number $P=av_0/D_0$ and different tube cross sections, where all possibilities are covered by one exact formula,

$$D^{*}=D_0+K\frac{a^2v_0^2}{D_0}\ , \tag{4.21}$$

with different values of the numerical constant K. Further generalizations are reviewed by Young and Jones (1991).

Zeldovich (1982) considered the periodic time-dependent flow in the (x,y) plane,

$$\mathbf{v}=v_0\hat{\mathbf{x}}\cos ky\cos\omega t\ , \tag{4.22}$$

and found the effective diffusivity in the x direction:

$$D_{xx}^{*}=D_0\left[1+\frac{1}{2}\frac{k^2v_0^2}{\omega^2+k^4D_0^2}\right] . \tag{4.23}$$

In the case of a general time-independent shear flow $\mathbf{v}=\hat{\mathbf{x}}\,d\psi(y)/dy$, $\langle\psi(y)\rangle_y=0$, one has (Avellaneda and Majda, 1990; Isichenko and Kalda, 1991a) $D_{yy}^{*}=D_0$,

$$D_{xx}^{*}=D_0+\frac{\langle\psi^2(y)\rangle_y}{D_0} . \tag{4.24}$$

The above results are obtained by separating the tracer density n into an oscillating and a smoothed component, a method similar to the technique of multiple-scale expansion (cf. Bender and Orszag, 1978). The physical meaning of result (4.24) is quite simple: Due to the molecular diffusion in the y direction, a tracer particle resides in a channel with the same direction of velocity for a characteristic correlation time $\tau_m=\lambda_0^2/D_0$, where λ_0 is the characteristic scale of the flow. The advective displacement experienced by the particle during this time is $\xi_m=v_0\tau_m$. The effective diffusivity in the x direction is then estimated as $D^{*}\simeq\xi_m^2/\tau_m=\lambda_0^2v_0^2/D_0$, in accordance with (4.24). Quantities ξ_m and τ_m represent the mixing length in the x direction and the mixing time, respectively.

In terms of the scaling exponent α [see Eq. (4.11)], the result (4.24) corresponds to the maximum possible value $\alpha=2$. This is quite sensible because open (e.g., straight) streamlines promote the best imaginable mixing along their direction, the exact straightness of streamlines being not necessary for the $\alpha=2$ scaling to hold (Childress and Soward, 1989; Crisanti *et al.*, 1990). By the way, the exact maximum of D_{xx}^{*}, given by Eq. (4.19), is also attained by a shear flow with a steplike stream function

$$\psi(y)=\psi_0\mathrm{sgn}f(y),\quad \langle\psi(y)\rangle_y=0 , \tag{4.25}$$

corresponding to vanishingly narrow velocity jets located at the zero lines of $f(y)$. According to formula (4.24), we have $D_{xx}^{*}=D_0+\psi_0^2/D_0=D_0+\psi_{\max}^2/D_0$.

The second class of flow with a simple effective diffusion scaling is a periodic array of convection rolls, such as those modeled by the stream function

$$\psi(x,y)=\psi_0\sin k_x x\,\sin k_y y \tag{4.26}$$

(see Fig. 20). For this, topologically similar flows, and its simplest generalizations, it was noticed (Dykhne, 1981; Moffatt, 1983) that the large-Péclet-number asymptotics of D^{*} correspond to the exponent $\alpha=\frac{1}{2}$:

$$D^{*}=C\sqrt{D_0\psi_0},\quad P\equiv\psi_0/D_0\gg1 . \tag{4.27}$$

It was later in 1987 that flow (4.22) drew much attention (Osipenko *et al.*, 1987; Perkins and Zweibel, 1987; Rosenbluth *et al.*, 1987; Shraiman, 1987; Soward, 1987). Using an asymptotic expansion for periodic fields (Bensoussan *et al.*, 1978; Brenner, 1980) or methods similar in spirit, the problem was reduced to the effectively one-dimensional cross-stream diffusion within one convection cell, making it possible to calculate the numerical constant C in Eq. (4.27). Formula (4.27) was confirmed in a specially designed experiment (Solomon and Gollub, 1988), where passive tracer transport was studied in a periodic system of controlled Rayleigh-Bénard convection rolls.

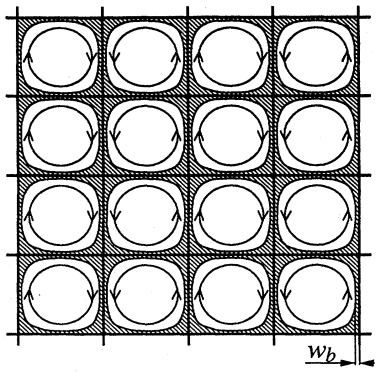

FIG. 20. Periodic system of convection rolls described by the stream function (4.26). The hatched region denotes diffusive boundary layers near the separatrices, where the tracer density gradients are localized in the high-Péclet-number limit.

The $\sqrt{D_0}$ scaling is due to the formation, in the large-Péclet-number limit, of diffusive boundary layers near the separatrices (Fig. 20), where the tracer density gradients turn out to be concentrated. Being of major significance for effective transport, the boundary layer width w_b is determined as the characteristic diffusive displacement a tracer particle undergoes in the course of the advective rotation period:

$$w_b=\sqrt{D_0\lambda_0/v_0} , \tag{4.28}$$

where λ_0 is the cell size and $v_0=\psi_0/\lambda_0$ is the characteristic velocity. Then the effective diffusivity is estimated in terms of the usual random-walk expression $\lambda_0^2/(\lambda_0/v_0)$ multiplied by the fraction of "active" particles w_b/λ_0 lying in the boundary layer. This leads to the result

$$D^{*}\simeq v_0w_b , \tag{4.29}$$

revealing scaling (4.27).

It is interesting to note that, while the periodic flow (4.26) was generally invoked to model steady Rayleigh-Bénard convection (Chandrasekhar, 1961; Haken, 1977; Busse, 1978), the effective diffusivity in the Rayleigh-Bénard system may behave quite differently from the prediction of formula (4.27) (Dykhne, 1981). There are two principle patterns of steady convection in a fluid heated from below, namely, rolls [Fig. 21(a)] and hexagons [Fig. 21(b); Busse, 1978]. The transport properties of rolls are properly modeled by flow (4.26) for the case of "free-slip" boundaries at the bottom of the vessel. In the case of "no-slip" boundary condition, the effective diffusivity D^{*} scales proportional to $D_0^{2/3}$ (Rosenbluth *et al.*, 1987). Unlike the roll convection pattern, the separatrices of Rayleigh-Bénard hexagons include not only the interfaces between the cells but also the cells' axes [Fig. 21(b)].

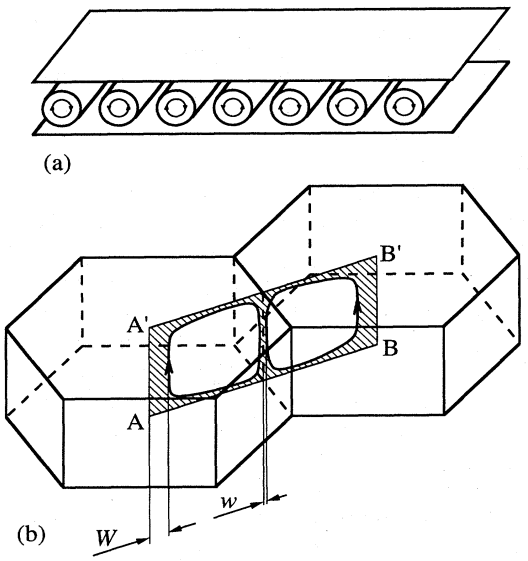

FIG. 21. Two types of steady Rayleigh-Bénard convection patterns: rolls (a) and hexagons (b). Axes AA' and BB' of the hexagons act on the streamlines as "free-slip" rigid boundaries. The hatched region shows the cross section of a diffusive boundary layer by the plane $AA'BB'$. To leave the trap of these two hexagons, a tracer particle has to diffuse (radially or azimuthally) all the way across the wider (near-axis) boundary layer (W).

Due to the incompressibility of the flow, a near-axis boundary layer is much wider ($W \gg w$) than a corresponding near-interface boundary layer (w). Assuming the same order of magnitude in velocity, the fluid flux conservation yields $v_0 \lambda_0 w = v_0 W^2$; hence

$$W(w) = \sqrt{\lambda_0 w} \ , \tag{4.30}$$

where λ_0 is the horizontal size of the hexagonal cells. For the effective diffusion to be established, the tracer particle has to diffuse all the way through the near-axis layer: until then it will just walk between two neighboring cells [Fig. 21(b)]. The widths of the diffusive boundary layers are estimated from $W^2(w_b)/D_0 = \lambda_0/v_0$; hence

$$w_b = \frac{D_0}{v_0}, \quad W_b = \sqrt{D_0 \lambda_0 / v_0} \ . \tag{4.31}$$

The simplest evaluation (4.29) would then give $D^* = D_0$, which is, however, somewhat of an underestimate. In fact, one must sum the contributions of approximately $\log(\lambda_0/w_b)$ different layers, $w = w_b, 2w_b, 4w_b, \ldots, \lambda_0$, each contribution being $D^*(w) \simeq (w/\lambda_0)\lambda_0^2/[W^2(w)/D_0] = D_0$. As a result, for the steady Rayleigh-Bénard convection pattern, the effective diffusivity scales as (Dykhne, 1981)

$$D^* \simeq D_0 \log P, \quad P = \frac{\lambda_0 v_0}{D_0} \gg 1 \ , \tag{4.32}$$

showing an anomalously weak transport enhancement.

A yet smaller enhancement, down to the lower bound in Eq. (4.19), is realized for flows with localized, nonoverlapped domains of nonvanishing velocity, for sufficiently small fraction of volume occupied by these domains. This becomes quite obvious if one replaces the advective domains by infinite-diffusivity domains. Well below the percolation threshold, this will not significantly increase the transport properties of the medium relative to the background diffusivity D_0. By approaching the percolation threshold for the advective domains, one can in principle construct flows with an arbitrary transport scaling exponent $\alpha \in [0,2]$. One such example, with $\alpha = \frac{1}{2}$, was given by Avellaneda and Majda (1991).

The next exactly solvable example is the 2D isotropic system of narrow velocity jets:

$$\psi(x,y) = \psi_0 \mathrm{sgn} f(x,y), \quad \langle \psi(x,y) \rangle = 0 \ , \tag{4.33}$$

where the isotropy of the effective diffusivity D^* is *assumed*. The function $f(x,y)$ may be a checkerboard pattern, $f = \sin kx \sin ky$, or a realization of a random field such as the one shown in Fig. 10. Using the correspondence between the advection-diffusion problem and the effective conductivity of an inhomogeneous medium with the Hall effect (Dreizin and Dykhne, 1972; see Sec. IV.B.3.b) and the solution of the conductivity problem for a 2D, two-phase system (Dykhne, 1970b; see Sec. IV.B.3.a), D^* can be calculated exactly. The result is the "Pythagorean formula" (Dykhne, 1981; Tatarinova, 1990)

$$D^* = \sqrt{D_0^2 + \psi_0^2} \ , \tag{4.34}$$

corresponding to the scaling exponent $\alpha = 1$. Result (4.34) is valid for arbitrary Péclet number. The mixing length and time are less universal and depend on the details of $\psi(x,y)$.

Regarding time-dependent advecting flows, it is generally believed that, while being of importance for smoothing the small-scale tracer density structure (Moffatt, 1981; Vulpiani, 1989), weak molecular diffusion does not significantly affect the long-range passive transport. In the limit of vanishing molecular diffusivity D_0, the effective diffusivity remains finite, $D^* \simeq \psi$ (Kraichnan, 1970; Pettini *et al.*, 1988; Horton, 1989), that is, $\alpha = 1$. The Zeldovich (1982) result (4.22) and (4.23) is exceptional in this respect due to the special kind of flow time dependence that preserves the topology of the streamlines. Another special case of preserved topology is the system of localized traveling vortices, which can arise in the course of the evolution of two-dimensional turbulence in atmosphere, ocean, or plasmas (Larichev and Reznik, 1976; Hasegawa *et al.*, 1979; Flierl *et al.*, 1980; Kraichnan and Montgomery, 1980; Petviashvili and Yankov, 1989). The dominant feature of a localized traveling vortex is the presence of a separatrix, inside which the fluid is carried by the vortex (Fig. 22) moving at a constant speed **u**. This feature makes vortices efficient mixing agents, so that the scaling exponent α in Eq. (4.11) attains its maximum value, $\alpha = 2$, for a flow represented as a vortex gas—that is, an ensemble of a

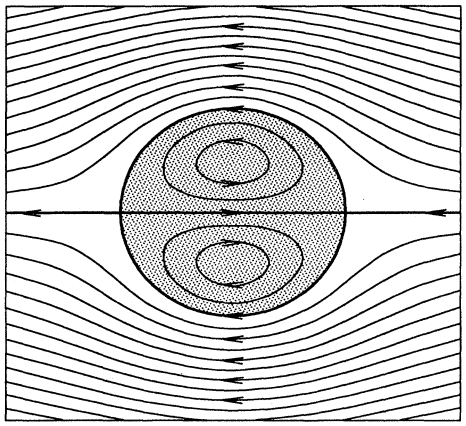

FIG. 22. Typical pattern of streamlines in a traveling dipole vortex, shown in the frame of reference moving together with the vortex. The hatched region surrounded by a separatrix (heavy line) represents the trapped fluid transported by the vortex.

large number of traveling vortices—whose interactions are unessential. The effective diffusivity of the vortex gas for the large-Péclet-number limit was calculated by Isichenko *et al.* (1989):

$$D_{ij}^{*}=\eta\langle s\tau_m u_i u_j\rangle+D_0\delta_{ij}\ , \tag{4.35}$$

where η is the number of vortices per unit area, $s\simeq\lambda_0^2$ is the area enclosed by the separatrix of a vortex, $\tau_m\simeq\lambda_0^2/D_0$ is a diffusion time inside the vortex, and the averaging in (4.35) is taken over the vortices. The estimate of the exact result (4.35) can be obtained as follows. A tracer particle is trapped and carried by a vortex for the diffusion time $\tau_m=\lambda_0^2/D_0$ and then released the distance $\xi_m=u\tau_m$ away from the point of trapping. The effective diffusivity is then obtained as ξ_m^2/τ_m multiplied by the fraction of area, $\eta\lambda_0^2$, where the trapping processes take place. The resulting expression, $D^{*}\simeq\eta\lambda_0^4u^2/D_0$, agrees with formula (4.35) for sufficiently high Péclet number, $P=\lambda_0u/D_0\gg(\eta\lambda_0^2)^{-1/2}\gg1$. The effects of vortex collisions (Horton, 1989) and of the inhomogeneity of the vortex-supporting medium (Zabusky and McWilliams, 1982; Nycander and Isichenko, 1990) lead to various regimes of effective diffusion, including those for which the molecular diffusivity D_0 is unessential. Advective transport by time-dependent random flows is discussed in Sec. IV.A.5.

3. Diffusion in two-dimensional random, steady flows

As we have seen, the behavior of effective diffusivity in the large-Péclet-number limit depends on the topology of flow streamlines. The best mixing properties are exhibited by flows with extended streamlines, such as shear flows, where the mixing length ξ_m tends to infinity as $D_0\to0$. The geometry of 2D random flows assumes the presence of arbitrarily large streamlines, although their share falls with the increasing size. To estimate the effective diffusivity in such a flow, statistical topography must be used for the description of the streamlines (Isichenko *et al.*, 1989; Gruzinov *et al.*, 1990; Isichenko and Kalda, 1991c).

It is difficult to imagine a time-independent or a slowly time-dependent 2D random flow in such traditional 2D hydrodynamic objects as atmosphere and ocean where the characteristic frequency ω is typically of the order of the inverse eddy rotation time, $\omega\simeq v_0/\lambda_0$. The practical implications of "frozen," or "quenched" 2D random flows involve primarily condensed-matter objects, such as quantum diffusion (Kravtsov *et al.*, 1986), the quantum Hall effect (Prange and Girvin, 1990), or inhomogeneously doped semiconductors (Dreizin and Dykhne, 1972; Isichenko and Kalda, 1991a).

The first percolation theory analysis of effective diffusion in a 2D, random, incompressible, steady flow (Isichenko *et al.*, 1989) was motivated by the observation that the periodic flow pattern (4.26) is structurally unstable: A vanishingly small perturbation of the stream function will destroy the regular system of elementary convective cells, gather them into various conglomerates, and thereby produce arbitrary length scales in the isolines of $\psi(x,y)$ (see Fig. 11). Although there is no doubt about the existence of a well-defined effective diffusivity D^{*} for a bounded random stream function $\psi(x,y)$, there has been developed no formal theory leading to the rigorous calculation of D^{*} for a large Péclet number. The small-Péclet-number expansion for random flows was developed by Derrida and Luck (1983), Fisher (1984), Kravtsov *et al.* (1986), and Bouchaud *et al.* (1987) using path integrals and the renormalization-group theory.

For a monoscale stream function $\psi(x,y)$ (Fig. 10) heuristic arguments were used (Isichenko *et al.*, 1989) to derive the $\alpha=\frac{10}{13}$ scaling

$$D^{*}\simeq D_0\left[\frac{\psi_0}{D_0}\right]^{10/13},\quad \psi_0\equiv\psi_{\rm rms}\gg D_0\ , \tag{4.36}$$

where the exponent was expressed through the 2D percolation indices $\nu=\frac{4}{3}$ and $d_h=\frac{7}{4}$:

$$\alpha=\frac{\nu d_h+1}{\nu d_h+2}=\frac{10}{13}\ . \tag{4.37}$$

Due to the role of extended streamlines of a random flow, the effective diffusivity (4.36) greatly exceeds Eq. (4.27), valid for finite-size convection cells, at the same large Péclet number.

The derivation of result (4.36) employs a hypothesis of broken coherence. This hypothesis assumes that the particle displacements governed by Eq. (4.2) may be considered to be uncorrelated if the streamlines on which these displacements are experienced differ twice or more in size. In this way, one comes naturally to the concept of convection cells being the conglomerates of stream-

lines with diameter between a and $2a$ ("a cells"; see Fig. 17). The mixing length ξ_m is then determined as the size of convection cells producing the most efficient coherent contribution to transport. The calculation is quite similar to that based on the boundary-layer argument for a periodic array of vortices (Fig. 20). The difference, however, is that the convection cells of a random flow are diverse, and their size a, width $w(a)$, and perimeter $L(a)$ are coupled in a fashion determined by the statistics of the random field $\psi(x,y)$. For example, for a monoscale (λ_0) flow, the relations given by Eqs. (3.43) and (3.45) should be used. Using the standard boundary-layer argument, we find the mixing length ξ_m to be the cell size where the convection time equals the transverse diffusion time,

$$\frac{L(\xi_m)}{v_0}=\frac{w^2(\xi_m)}{D_0}\ , \tag{4.38}$$

where $v_0=\psi_0/\lambda_0$ is the characteristic velocity. Substituting Eqs. (3.43) and (3.45) for the length $L(a)$ and the width $w(a)$ of the convection cell, we find

$$\xi_m=\lambda_0 P^{\nu/(\nu d_h+2)},\quad P\equiv\frac{\psi_0}{D_0}\gg 1\ . \tag{4.39}$$

The effective diffusivity is then estimated to be

$$D^*\simeq F(\xi_m)\frac{\xi_m^2}{w^2(\xi_m)/D_0}=v_0 w(\xi_m)\ , \tag{4.40}$$

where $F(a)=L(a)w(a)/a^2$ is the distribution function (area fraction) of the convection cells over their size. Upon substituting Eq. (4.39) into (4.40), we arrive at the result (4.36). The mixing time in a monoscale λ_0 flow is given by the formula

$$\tau_m=\frac{\lambda_0^2}{D_0}\ , \tag{4.41}$$

corresponding to the time of diffusive sampling of all "undermixing" (that is, with $a<\xi_m$) convection cells.

Equation (4.40) describes the effective diffusion contribution of mixing (ξ_m) convection cells only. Nevertheless, this contribution constitutes of order one-half the effective diffusivity, thereby yielding a correct estimate of D^*. The contribution of more numerous undermixing cells with $\lambda<\xi_m$ can be written similarly to (4.40):

$$D_\lambda\simeq F(\lambda)\frac{\lambda^2}{w^2(\lambda)/D_0}=D_0\frac{L(\lambda)}{w(\lambda)},\quad \lambda_0<\lambda<\xi_m\ . \tag{4.42}$$

The hypothesis of broken coherence implies that effective diffusivity can be estimated as the sum of *partial diffusivities* D_λ, for $\lambda=\lambda_0,2\lambda_0,4\lambda_0,\ldots,\xi_m$, that is,[3]

$$D^*\simeq\int_{\lambda_0}^{\xi_m} D_\lambda\frac{d\lambda}{\lambda}\ . \tag{4.43}$$

The partial diffusivity $D_\lambda\propto\lambda^{d_h+1/\nu}$ increases with increasing scale λ, making expression (4.43) peak near the upper integration limit.

The percolation scaling of effective diffusivity involving the exponent $\alpha=\frac{10}{13}$ appears to be as universal as the static exponents of continuum percolation (see Sec. II.E). This implies that the randomness (in the sense of the ensemble averaging) of the velocity field is not really necessary for the result (4.36) to be valid; the *genericity* (i.e., the absence of exceptional features like periodicity, etc.) of the flow will suffice. The computation of effective diffusion for quasiperiodic flows having extended streamlines showed a fair agreement with the $\frac{10}{13}$ scaling (Isichenko *et al.*, 1989).

A similar approach was used to calculate the effective diffusivity in a multiscale random flow with the stream function spectrum $\psi_\lambda\propto\lambda^H$, $\lambda_0<\lambda<\lambda_m$ (Isichenko and Kalda, 1991c). Due to a more sophisticated dependence of $L(a)$ and $w(a)$ [see Eqs. (3.74), (3.78), and (3.80)], there are several regimes of effective diffusion in this flow. The regimes are depicted in Fig. 23, where the parameter space $(H,\log_{\psi_0/D_0}(\lambda_m/\lambda_0))$ is shown. One of these regimes, corresponding to the monoscale correlated

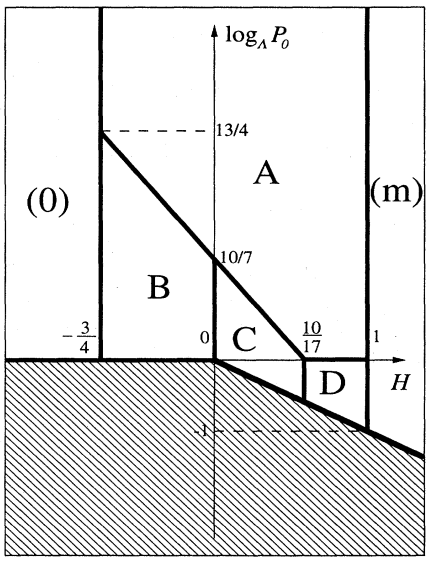

FIG. 23. Regimes of effective diffusion in a multiscale, steady, random 2D flow (Isichenko and Kalda, 1991c) shown in the parameter space $(H,\log P_0/\log\Lambda)$, where $P_0=\psi_{\lambda_0}/D_0$ is the short-scale Péclet number and $\Lambda=\lambda_m/\lambda_0$ is the width of the flow spectrum. Expression $D^*\simeq\psi_0 P_0^\alpha\Lambda^\gamma$ for effective diffusivity includes the following exponents in regimes (A–D): (A) $\alpha=-1/(\nu d_h+2)$, $\gamma=(\nu H d_h+D_h)/(\nu d_h+2)$; (B) $\alpha=H/(D_h-2H)$, $\gamma=0$; (C) $\alpha=0$, $\gamma=H$; (D) $\alpha=(2-D_h/H)/(\nu d_h+2)$, $\gamma=(\nu H d_h+D_h)/(\nu d_h+2)$. Regimes (0) and ($m$) correspond to diffusion in the monoscale flows $\psi_{\lambda_0}(\mathbf{x})$ and $\psi_{\lambda_m}(\mathbf{x})$, respectively. In the hatched region, D^* is of the order of D_0.

[3]The contribution of "overmixing" convection cells with diameter $\lambda\gg\xi_m$ is negligible due to both the scarcity of such cells and the diffusive decorrelation that occurs well before particles sample their extent.

stream function (regime B in Fig. 23), is recovered by simple replacement of the random percolation exponents by their correlated counterparts (see Sec. II.D),

$$\nu \to -\frac{1}{H}, \quad d_h \to D_h, \quad -\frac{1}{\nu} < H < 0 . \tag{4.44}$$

In this case we have from Eq. (4.37)

$$\alpha = \frac{-D_h/H+1}{-D_h/H+2} = \frac{10(1-H)}{10-17H}, \quad -\frac{3}{4} < H < 0 . \tag{4.45}$$

For H tending to zero, α tends to unity and the effective diffusivity D^* becomes independent of D_0. Such independence extends to regime C. Regime A, which is characterized by the monoscalelike scaling $D^* \propto D_0^{3/13}$, is obtained by substituting the partial diffusivity D_{λ_m} (4.42) into the monoscale flow $\psi_{\lambda_m}(x,y)$ and using formula (4.36). In this representation, D_{λ_m} is the renormalized molecular diffusivity, which accounts for the transport effect of the flow spectral components with $\lambda < \lambda_m$.

4. Lagrangian chaos and Kolmogorov entropy

Thus far we have been concerned with "frozen" flows, or systems with "unessential" time dependence that preserves the topology of streamlines, that is, where the tracer orbits would be regular in the absence of the microdiffusivity. In the case of an "essential" time dependence in two dimensions, where the topology is changed, or in three dimensions even without time dependence, the orbits are generally chaotic, leading to a diffusionlike random walk.

The general reason for the decay of orbit correlations in (4.5), and hence for the transition to the effective diffusion or other kinds of random walk, is found in Hamiltonian chaos (Chirikov, 1979; Lichtenberg and Lieberman, 1983; Sagdeev *et al.*, 1988). Consider a two-dimensional flow with $D_0 = 0$. Then the equations of motion of a fluid element,

$$\frac{dx}{dt} = \frac{\partial \psi(x,y,t)}{\partial y}, \quad \frac{dy}{dt} = -\frac{\partial \psi(x,y,t)}{\partial x} , \tag{4.46}$$

correspond to the Hamiltonian ψ defined in the phase space (x,y). The Liouville theorem is equivalent to the incompressibility of the flow $\mathbf{v} = \nabla\psi \times \hat{\mathbf{z}}$. The one-degree-of-freedom time-dependent Hamiltonian $\psi(x,y,t)$ is equivalent to a two-degree-of-freedom autonomous Hamiltonian in a four-dimensional phase space (Lichtenberg and Lieberman, 1983). Subtracting one dimension for the conservation of the autonomous Hamiltonian, we get an essentially three-dimensional isoenergetic manifold, which is the lowest critical dimension for stochastic phase-space orbits. Indeed, a self-avoiding smooth Hamiltonian orbit can behave chaotically in a 3D space, a situation that is impossible in two dimensions. In fact, stochastic behavior is a structurally stable property of Hamiltonian systems that are far from (degenerate) integrable; that is, chaos is not eliminated by a small change in the Hamiltonian (Arnold, 1978). Note that the obverse is also true: A small perturbation to an integrable Hamiltonian leaves most of the finite motion regular; the measure of arising chaotic regions is small for a small perturbation (KAM theorem: Kolmogorov, 1954a, 1954b; Arnold, 1963a, 1963b; Moser, 1962, 1967). Note, however, that the extended phase space of a 2D unsteady flow is $(x,y,z=t)$, with the (steady) phase-space flow given by

$$\frac{\partial x}{\partial t} = \partial\psi(x,y,z)/\partial y , \quad \frac{\partial y}{\partial t} = -\partial\psi(x,y,z)/\partial x , \quad \frac{\partial z}{\partial t} = 1 . \tag{4.47}$$

If $\mathbf{v}(\mathbf{x},t)$ is not time periodic, then no would-be cylinder can be identified with a torus, the motion is infinite, and the KAM theory does not apply. Even though the flow $\mathbf{v}(\mathbf{x},t)$ changes in time very slowly and the system is formally very close to integrable, multiple crossings of multiple separatrices eventually lead to large changes in the adiabatic invariants (Tennyson *et al.*, 1986a, 1986b; Neishtadt, 1986, 1991), apparently smearing out any trace of integrability in generic nonlocalized flows. Thus it is quite plausible that in general there is no partition of the phase space by (x,y)-localized invariant surfaces, and the diffusion of particles to infinity takes place at arbitrary amplitude in the velocity field.

In cases of special symmetry, such as time-periodic flows, there will in general be regions of both integrable and stochastic particle motion. The stochastic region consists of domains bounded by embracing KAM tori and, possibly, unbounded domains that admit percolation to infinity, resulting in long-range particle diffusion. Depending on the kind of Hamiltonian, the percolation of stochastic regions can occur either above a certain threshold perturbation amplitude (as in situations reducible to the standard map; cf. Lichtenberg and Lieberman, 1983) or without any threshold whatsoever (stochastic webs: cf. Zaslavsky, 1991).

The principal manifestation of stochasticity is the extreme sensitivity of phase orbits to the initial conditions. Two infinitesimally close trajectories starting in a chaotic region diverge in time exponentially fast, so that even a tiny uncertainty in the initial data grows soon to an extent where a statistical description becomes not just a matter of convenience. The quantitative measure of the stochastic exponentiation is the *Kolmogorov entropy*,

$$K = \lim_{t\to\infty} \lim_{|\delta\mathbf{x}(0)|\to 0} \frac{1}{t} \log \frac{\langle |\delta\mathbf{x}(t)| \rangle}{|\delta\mathbf{x}(0)|} , \tag{4.48}$$

where $\delta\mathbf{x}(t)$ designates the distance between two neighboring orbits, and an average over the initial conditions in a given region is taken. In the absence of this average, formula (4.48) would define the maximum Lyapunov ex-

ponent $\Lambda_1(\mathbf{x})$, which is a function of the initial point, for almost any direction of $\delta\mathbf{x}(0)$ (Oseledec, 1968). For the purpose of advective transport, the case of positive K is usually referred to as *chaotic advection* (Aref, 1984) or *Lagrangian chaos* (Dombre *et al.*, 1986; Zaslavsky *et al.*, 1988; Ottino, 1989; Crisanti *et al.*, 1991).

The Kolmogorov entropy in a rapidly oscillating isotropic 2D random flow was first calculated by Kadomtsev and Pogutse (1979) using a variational principle,

$$K \simeq \frac{v_0^2}{\lambda_0^2 \omega}, \quad \omega \gg \frac{v_0}{\lambda_0}, \tag{4.49}$$

where v_0, λ_0, and ω are the characteristic amplitude, scale, and frequency of the velocity field, respectively. The quasilinear result (4.49) can also be obtained using a Fokker-Planck–equation approach (Rechester *et al.*, 1979) or by averaging the second-order moments of linearized Eq. (4.46) (Krommes *et al.*, 1983; Isichenko, 1991a).

All these methods fail in the low-frequency limit $\omega \ll v_0/\lambda_0$, calling for new approaches such as those based on geometrical considerations. Berry *et al.* (1979) proposed the study of mappings of curves rather than points. They described two principal types of convolution of a "liquid curve": "whorls" and "tendrils" (Fig. 24). The advantage of the liquid-curve representation lies in the fact that, at any time, the curve consists of close points; hence the rate of elongation of the curve provides a natural measure of the average stochastic exponentiation of neighboring orbits. Moreover, the Kolmogorov entropy as defined by Eq. (4.48) can be shown to be the exact growth rate of an average liquid-curve length. Indeed, consider a square region $a \times a$ and introduce the array of $N^2 = (a/\Delta)^2$ initial points $\mathbf{x}_{ij}(0)$ with the spacing $\Delta \ll a$ (Fig. 25). Using the fact that the asymptotic growth rate of an infinitesimal vector does not depend on its orientation for almost all orientations, we may take all the initial vectors $\delta\mathbf{x}_{ij}(0)$ parallel to the x direction and with the same length $|\delta\mathbf{x}(0)|$. Then the average $\langle |\delta\mathbf{x}(t)| \rangle$ in formula (4.48) can be represented as

$$\begin{aligned} \langle |\delta\mathbf{x}(t)| \rangle &= \lim_{N\to\infty} \frac{1}{N^2} \sum_{i,j=1}^{N} |\delta\mathbf{x}_{ij}(t)| \\ &= \lim_{N\to\infty} \frac{1}{N^2} \sum_{j=1}^{N} \mathcal{L}_j(t) \frac{|\delta\mathbf{x}(0)|}{\Delta} \\ &= |\delta\mathbf{x}(0)| \frac{\langle \mathcal{L}(t) \rangle}{a}, \end{aligned} \tag{4.50}$$

where $\langle \mathcal{L}(t) \rangle$ is the average length of liquid curves with the initial length a and the horizontal orientation in the considered region. Formula (4.50) is valid only in the limit $|\delta\mathbf{x}(0)| \to 0$, *following* the limit $\Delta \to 0 (N \to \infty)$ but *preceding* the limit $t \to \infty$ when the sum of a horizontal chain of $|\delta\mathbf{x}_{ij}(t)|$ is simply the $(|\delta\mathbf{x}(0)|/\Delta)$-folded length $\mathcal{L}_j(t)$ (in Fig. 25, the case with the ratio $|\delta\mathbf{x}(0)|/\Delta = 2$ is shown). Upon substituting (4.50) into (4.48), we obtain

$$K = \lim_{t\to\infty} \frac{1}{t} \log \frac{\langle \mathcal{L}(t) \rangle}{a}; \tag{4.51}$$

that is, the average, or a "typical," liquid-curve length

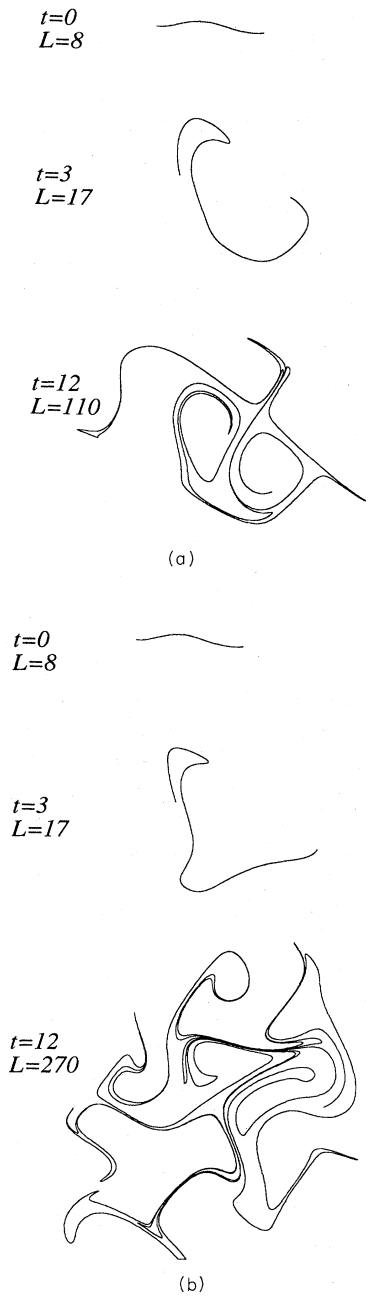

FIG. 24. Principal morphology of an incompressible map. The liquid-curve convolution is of two types: whorls (a) and tendrils (b) (Berry *et al.*, 1979). Whorls are generated by velocity fields of unchanged topology and lead to elongation of a passively advected curve that is asymptotically linear with time. Tendrils are created by essentially time-dependent flows and lead to an exponential elongation of a liquid curve. For the simulation, a stream function was chosen of the kind shown in Fig 10, with $N = 5$ frozen (a) or traveling (b) waves.

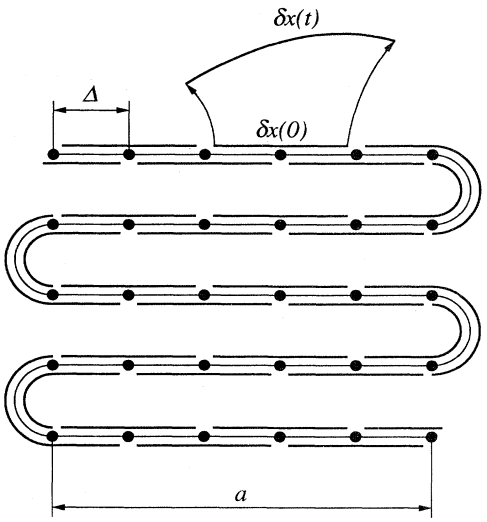

FIG. 25. Relation between the Kolmogorov entropy and the elongation of a liquid curve.

grows at large time as

$$\langle \mathcal{L}(t) \rangle = a \exp(Kt) \ . \tag{4.52}$$

A useful example of such a dependence is given by the observation that a liquid curve is draped over saddle points of the velocity field (Fig. 26) and stretched in the interseparatrix channels. For a steady flow, this leads to only a linear growth of the liquid curve via the whorls. When the flow topology is changed, the curve produces exponentiating tendrils via repeated stretching and folding. Consider a flow with a shear structure whose direction is periodically changed. If these changes are slow enough, $\omega \ll v_0/\lambda_0$, then during the first half of a period the curve length is stretched approximately $v_0/\lambda_0\omega$ times, leading to a "fish-bone" structure [Fig. 27(a)]. During the second half-period, when the topology of the channels is changed, each piece of the primary fish bone

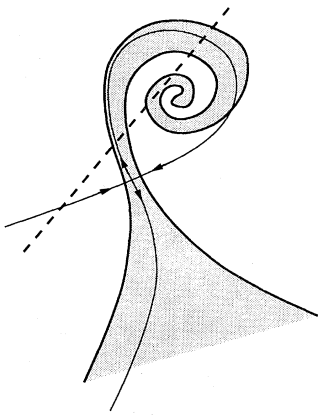

FIG. 26. Interaction of a liquid curve with a saddle point of a velocity field. Featured is the hooking of the curve over the saddle. The dashed line denotes the initial position of the curve, the heavy solid line is its final state, and the light lines with arrows show the velocity field.

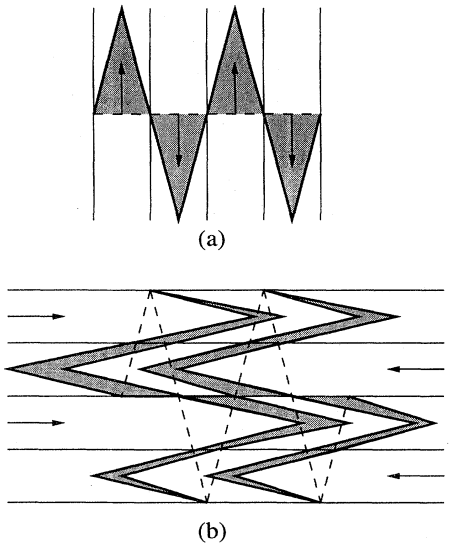

FIG. 27. Exponentiation of a liquid curve (the dashed line is the initial position and the solid heavy line is its final position) in a periodically changing shear flow during the first half-period (a) and during the second half-period (b).

is stretched into a secondary fish bone, so that the liquid-curve pattern becomes quite intricate [Fig. 27(b)]. The process will continue, thereby leading to an exponential growth in the curve length,

$$\mathcal{L}(t) \simeq a \left[\frac{v_0}{\lambda_0 \omega} \right]^{\omega t} , \tag{4.53}$$

that is,

$$K \simeq \omega \log \left[\frac{v_0}{\lambda_0 \omega} \right] . \tag{4.54}$$

The logarithmic dependence of the Kolmogorov entropy on the velocity amplitude was numerically observed by Kleva and Drake (1984) in the flow $\psi = \psi_0[\cos x \cos y - \varepsilon \sin x \cos(y - t)]$ for $\psi_0 \gg 1$. The spatial structure of the extended streamlines of this flow is similar to that shown in Fig. 27, although cells of closed streamlines with the corresponding whorls are also present.

In nonperiodic flows, one expects a stronger exponentiation rate, because a continuous distribution of saddle points over the level of ψ and the abundance of separatrices imply a much faster rate of separatrix reconnection. Gruzinov *et al.* (1990) studied the stretching and folding of a curve advected in a monoscale 2D random flow, a process stemming from the elementary reconnections of the separatrices [Fig. 28(a)]. In terms of the liquid-curve behavior, this results in the multiple draping of the curve over saddles and its stretching in the channels between the separatrices [Fig. 28(b)]. The most efficient contribution to the elongation of the liquid curve is made by the channels where the convective revolution period is balanced by the reconnection time of the two

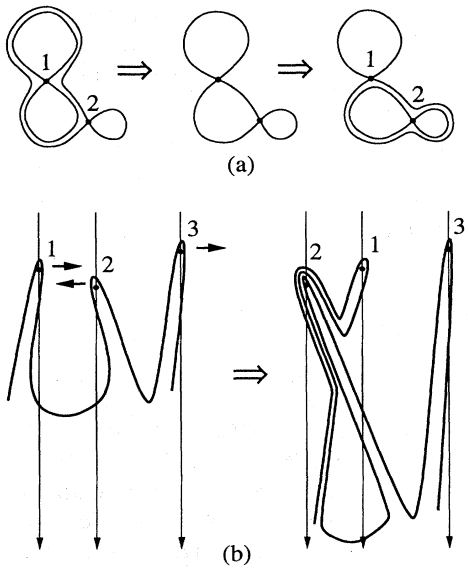

FIG. 28. Reconnection of two separatrices in a random flow. Reconnection takes place when two saddles, 1 and 2, cross the same level of the stream function (a). This is accompanied by the folding and stretching of a liquid curve (b). The light lines denote the separatrices, which are shown for simplicity to be straight and open (imagine a periodic boundary condition along the vertical direction). The curve drapes over the slowly moving saddle points 1, 2, and 3 and is rapidly stretched into the channels between the separatrices, The exponential behavior results from the intersection of separatrices, causing multiple foldings of the curve.

neighboring separatrices. Consider a monoscale random flow changing at the characteristic frequency $\omega \ll v_0/\lambda_0$. As the distance $s(a)$ between two neighboring separatrices is inversely proportional to the length $L(a)$ of a streamline [see Eq. (3.107)], the reconnection occurs in the characteristic time $\tau_s(a)=\omega^{-1}s(a)/\lambda_0=\omega^{-1}\lambda_0/L(a)$, corresponding to the level difference $\psi_0 s(a)/\lambda_0$ passed by a saddle at the velocity $\psi_0\omega$. The rate of exponentiation is dominated by those streamlines (diameter a_K) that reconnect in the advective revolution time: $\tau_s(a_K)=L(a_K)/v_0$. Hence we find $L(a_K)=(\lambda_0 v_0/\omega)^{1/2}$, and the Kolmogorov entropy is estimated to be $K \propto v_0/L(a_K)$. The multiplicity of separatrices inside one a_K cell leads to a logarithmic correction to K, so that

$$K \simeq \left[\frac{\omega v_0}{\lambda_0}\right]^{1/2} \log\frac{v_0}{\lambda_0\omega}, \quad \omega \ll \frac{v_0}{\lambda_0} . \tag{4.55}$$

The square-root scaling (4.55) of the Kolmogorov entropy appears to be fairly universal for nonperiodic flows having arbitrarily extended streamlines.

In terms of the behavior of a passive tracer, the Lagrangian chaos in the absence of molecular diffusion leads to exponentially growing tracer density gradients (Moffatt, 1981; Ott and Antonsen, 1989; Crisanti *et al.*, 1991). This is well understood by bearing in mind the stretching of liquid curves. Consider a narrow annulus formed by two adjacent contour lines of the initial tracer density $n(\mathbf{x},0)$ in an incompressible flow. The annulus is advected and exponentially stretched by the flow, with the density values on the contours, n_1 and n_2, and the area between the contours being conserved. This leads to an exponential decrease in the width of the annulus, which is inversely proportional to the annulus perimeter. The average tracer gradient, that is, the ratio of the density difference $|n_1-n_2|$ to the width of the annulus, is then increased according to

$$\langle |\nabla n(\mathbf{x},t)| \rangle \propto \exp(Kt), \quad t \to \infty . \tag{4.56}$$

Because of the exponential behavior (4.56) even a tiny amount of molecular diffusion soon comes into play to calm down the raging gradients.

Another effect associated with the exponentiation is the highly nonuniform gradient buildup due to the possible inhomogeneity of the Lyapunov exponent $\Lambda_1(\mathbf{x})$. Upon being normalized to the average gradient (4.56), local gradients tend to be asymptotically concentrated in a region of zero measure typically having a fractal geometry, and the distribution of passive gradients is then a multifractal (Ott and Antonsen, 1988, 1989; Városi *et al.*, 1991). A small microdiffusivity results in a finite lower limit of the scaling range of such structures.

5. Diffusion in time-dependent random flows

Although important for the small-scale structure of chaotically advected passive fields, small molecular diffusivity is usually irrelevant for the long-range transport described by effective, or turbulent, diffusion. The effective diffusivity, however, can scale nontrivially with the velocity amplitude and other parameters. For the case of zero molecular diffusion, no homogenization theorem has been proved. That is, unlike the case of $D_0 \neq 0$ (Sec. IV.A.1), it is not generally known what the exact criterion for effective diffusion behavior in chaotic advection must be, although many specific flows have been shown to exhibit effective diffusion numerically (Kleva and Drake, 1984; Horton, 1985; Pettini *et al.*, 1988; Ottaviani, 1992) or analytically (Chernikov *et al.*, 1991).

For a generic 2D fluid motion characterized by the velocity amplitude v_0 and length scale λ_0, the velocity field evolves at the characteristic frequency $\omega = v_0/\lambda_0$. In this case the turbulent diffusivity and the Kolmogorov entropy can be estimated from the simplest dimensional consideration, $D^* \simeq \lambda_0 v_0$, $K \simeq v_0/\lambda_0$, because there are no other independent parameters. In the case of plasma turbulence, however, ω can be independent of λ_0 and v_0. For example, the drift-wave frequency ω_* is determined from a linear dispersion relation, whereas the drift turbulence amplitude is governed by various nonlinear effects (Horton, 1990). The guiding-center motion of a charged particle in crossed electric $[\mathbf{E}=-\nabla\phi(\mathbf{x},t)]$ and magnetic $(\mathbf{B}=B_0\hat{\mathbf{z}})$ fields is described by

$$\frac{d\mathbf{x}}{dt}=v_{\parallel}\hat{\mathbf{z}}+c\frac{\mathbf{E}\times\mathbf{B}}{B^2}\ , \tag{4.57}$$

which corresponds to an incompressible motion across the magnetic field with the stream function

$$\psi(x,y,t)=-\frac{c}{B_0}\phi\left[x,y,z_0+\int_0^t v_{\parallel}(t')dt',t\right]\ . \tag{4.58}$$

The characteristic frequency, $\omega=\max(\omega_*,k_{\parallel}v_{\parallel})$ (where $k_{\parallel}\simeq|\partial\log\phi/\partial z|$), is thus decoupled from the amplitude of ψ. This may lead to the possibility of both the high-frequency regime ($\omega\gg v_0/\lambda_0$, also known as the *quasilinear* limit) and the low-frequency ($\omega\ll v_0/\lambda_0$), or *percolation*, regime of turbulent diffusion (Isichenko and Horton, 1991).

Another example is plasma heat conduction in a magnetic field with a small random component, $\mathbf{B}=B_0\hat{\mathbf{z}}+\delta\mathbf{B}_{\perp}(\mathbf{x})$, $\delta\mathbf{B}_{\perp}=\nabla A_{\parallel}(\mathbf{x})\times\hat{\mathbf{z}}$. The equation of a magnetic-field line in the form

$$\frac{d\mathbf{x}_{\perp}}{dz}=\frac{\delta\mathbf{B}_{\perp}}{B_0} \tag{4.59}$$

is equivalent to Eq. (4.46) with the stream function $\psi(\mathbf{x}_{\perp},z)=A_{\parallel}(\mathbf{x}_{\perp},z)/B_0$ and the coordinate z standing for time. The turbulent diffusivity stemming from Eq. (4.59) is known as the magnetic-field-line diffusivity D_m (Rosenbluth *et al.*, 1966). This quantity has the dimensionality of length. In a collisionless plasma, the diffusive walk of magnetic lines causes an enhanced electron thermal conductivity across the background magnetic field (Krommes, 1978; Rechester and Rosenbluth, 1978; Kadomtsev and Pogutse, 1979)

$$\chi_{\perp}^{*}\simeq D_m v_e\ , \tag{4.60}$$

where v_e is the thermal velocity of electrons. Particle transport coefficients are also proportional to D_m (Finn *et al.*, 1992). The processes of heat conduction in a collisional plasma are more complicated, the expression for χ^* involving both the magnetic-line diffusivity D_m and the Kolmogorov entropy K (see Sec. IV.B.2).

The above examples inspired studies of turbulent diffusion in two dimensions, with the characteristic flow frequency ω considered to be a free parameter. In the high-frequency (low amplitude) limit, $\omega\gg v_0/\lambda_0$, the effective diffusivity is insensitive to the topology of streamlines because the flow is changed in the correlation time ω^{-1}—that is, well before a tracer particle is displaced by a distance λ_0. This corresponds to the so-called *quasilinear approximation*, which consists, roughly, in the following. Represent the tracer density $n(\mathbf{x},t)$ as the sum of a smoothed component N, evolving slowly in both space and time, and a fluctuating component $\tilde{n}$ due to the driving velocity field, and then substitute the sum into Eq. (4.1). Upon separating oscillatory and averaged parts, we have

$$\partial\tilde{n}(\mathbf{x},t)/\partial t=-\mathbf{v}(\mathbf{x},t)\nabla N(\mathbf{x},t)\ , \tag{4.61}$$

$$\partial N(\mathbf{x},t)/\partial t=-\langle\mathbf{v}(\mathbf{x},t)\nabla\tilde{n}(\mathbf{x},t)\rangle\ , \tag{4.62}$$

where the averaging is taken over "small scales" and "fast time" or, alternatively, over an ensemble of flows. Upon integrating Eq. (4.61) over fast time and substituting $\tilde{n}$ into (4.62), we obtain

$$\partial N/\partial t=\nabla_i\int_0^t dt'\langle v_i(\mathbf{x},t)v_k(\mathbf{x},t')\rangle\nabla_k N\ ; \tag{4.63}$$

that is, the turbulent diffusivity is given by the time integral of the *Eulerian* velocity correlation function, which corresponds to the estimate

$$D^*\simeq\frac{v_0^2}{\omega},\quad \omega\gg\frac{v_0}{\lambda_0}\ . \tag{4.64}$$

In the above derivation, the limits of the applicability of the quasilinear approximation are swept under the rug. The comparison with the Taylor formula (4.5), involving the *Lagrangian* velocity correlator, reveals the inequality displayed in Eq. (4.64) specifying the small difference, on time scales of interest, between the Eulerian velocity $\mathbf{v}(\mathbf{x}(0),t)$ and the Lagrangian velocity $\mathbf{v}(\mathbf{x}(t),t)$. Mnemonically, one can view the *quasilinear* approximation as the neglect of the $\mathbf{v}(\mathbf{x},t)$ dependence on $\mathbf{x}$ making the particle orbit equation (4.2) *linear*.

In the opposite, low-frequency limit $\omega\ll v_0/\lambda_0$, a tracer particle can move along an almost steady streamline to a large distance before the flow pattern has changed appreciably. Consider a monoscale, random, slowly varying two-dimensional flow. The mixing length ξ_m is defined as the maximum coherent particle displacement that occurs in the lifetime $\tau(\xi_m)$ of the convection cell:

$$L(\xi_m)=v_0\tau(\xi_m) \tag{4.65}$$

[compare with (4.38)]. The lifetime $\tau(a)$ of an a cell is the time of unrecognizable change (for example, doubling the diameter) in the contour $\psi(x,y,t)=h$ with the initial diameter a. Such a change is undergone through the contour reconnection process [Fig. 28(a)]. The reconnection takes place when the saddles corresponding to neighboring separatrices come through the same level. An essential change in the shape of the convection cell occurs when the saddles pass the level difference $\delta\psi=\psi_0 w(a)/\lambda_0$ corresponding to the width of the cell $w(a)$ given by Eq. (3.45). As the level of a saddle point changes at the characteristic rate $\psi_0\omega$, the lifetime of the convection cell is estimated to be

$$\tau(a)=\frac{\delta\psi}{\psi_0\omega}=\frac{w(a)}{\lambda_0\omega}\ . \tag{4.66}$$

Upon substituting Eq. (4.66) into (4.65), we find the mixing scale

$$\xi_m=\lambda_0\left[\frac{v_0}{\lambda_0\omega}\right]^{\nu/(\nu d_h+1)}\ . \tag{4.67}$$

The turbulent diffusivity is then estimated similarly to (4.40),

$$D^*\simeq F(\xi_m)\frac{\xi_m^2}{\tau(\xi_m)}=v_0 w(\xi_m)\ . \tag{4.68}$$

Thus the percolation scaling of the turbulent diffusion coefficient is given by (Gruzinov *et al.*, 1990)

$$D^*=\psi_0\left[\frac{\omega\lambda_0}{v_0}\right]^{1/(vd_h+1)}=\psi_0\left[\frac{\omega\lambda_0}{v_0}\right]^{3/10},\quad \omega\ll\frac{v_0}{\lambda_0}\ . \tag{4.69}$$

Ottaviani (1992) studied the effective diffusion in a time-dependent 2D flow numerically. He used a quasiperiodic stream function with $N=64$ standing waves modulated by random Gaussian amplitudes with a variable correlation time ω^{-1}. In the high-frequency limit the quasilinear diffusivity (4.64) scaling was demonstrated. In the low-frequency limit, the observed scaling of the turbulent diffusivity, $D^*\propto\psi_0^{0.8\pm0.04}$, was close to, but still distinct from, the dependence $D^*\propto\psi_0^{7/10}$ predicted by the formula (4.69) (see Fig. 29). The finite number of waves is likely to be responsible for the discrepancy, because a quasiperiodic potential has a nondecaying (quasiperiodic) correlator and certainly does not belong to the universality class of uncorrelated percolation. It is not clear to what extent the N-wave quasiperiodic potentials can serve a good model of monoscale random potentials, although it is plausible that in the limit $N\to\infty$ the model must be good.

The low-frequency/large-Péclet-number turbulent diffusion theory, which employs statistical topography analysis, was extended in several directions. Kalda (1992) studied the general case of multiscale, time-dependent, incompressible 2D flow, including the effect of molecular diffusion, where numerous effective diffusion regimes have been identified.

Gruzinov (1991) considered the effective diffusion in a weakly compressible random flow

$$\mathbf{v}=\nabla\psi(x,y,t)\times\hat{\mathbf{z}}+\varepsilon\nabla\psi(x,y,t)\ . \tag{4.70}$$

The last term in (4.70), which models a non-Hamiltonian friction experienced by a drifting guiding center, makes particles move at a small angle $\varepsilon\ll1$ with respect to the contours of ψ. Random walk in fields with finite divergence was also discussed in the context of the vortex motion in inhomogeneous superconducting films (Trugman and Doniach, 1982) or random-hopping models in disordered solids (Derrida and Luck, 1983; Fisher, 1984; Kravtsov *et al.*, 1986). The compressibility of advecting flow results in the occurrence of limit cycles and stable foci, which attract and trap tracer particles (Fig. 30) until they are released due to molecular diffusion or flow time dependence destroying the traps. So the diffusion process results from the particle flights from one trap to another. In the low-frequency limit, these flights are approximately along the contours of $\psi(x,y,t)$ and may be quite long (Lévy flights; cf. Shlesinger *et al.*, 1987). For the monoscale compressible flow (4.70), the effective diffusivity scales as

$$D^*\simeq\lambda_0^2\omega\varepsilon^{-vd_h/(vd_h+1)},\quad \frac{\lambda_0\omega}{v_0}\ll\varepsilon\ll1\ . \tag{4.71}$$

For smaller ε, the effect of compressibility is unimportant and D^* is given by formula (4.69). In the case of time-independent compressible flow with finite molecular diffusivity D_0, the effect of traps can result in an exponentially small effective diffusivity D^*.

Yushmanov (1992) studied the neoclassical diffusion in a turbulent plasma. Mathematically, this problem was reduced to chaotic advection in a random 2D flow with a temporally varying average component. The average velocity component in an equation similar to (4.57) results

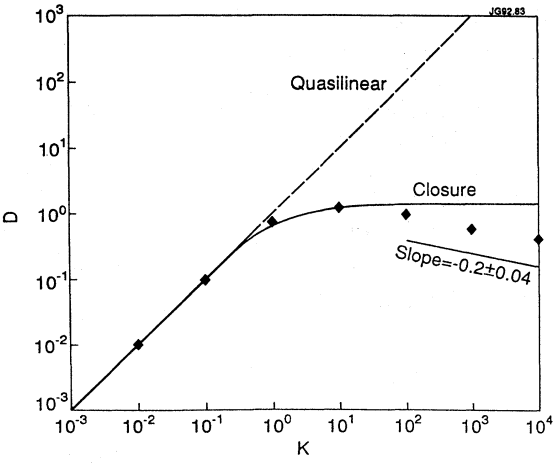

FIG. 29. Dependence of the turbulent diffusivity on the "Kubo number" $K=v_0/(\lambda_0\omega)$ at $\lambda_0=v_0=1$ (Ottaviani, 1992). The dashed line $D\propto K$ represents the diffusion behavior in the high-frequency limit $K<1$ and corresponds to the quasilinear scaling (4.64). The low-frequency behavior shows a systematic decline from the prediction of a Markovian closure theory (solid line; for a recent discussion see Fradkin, 1991).

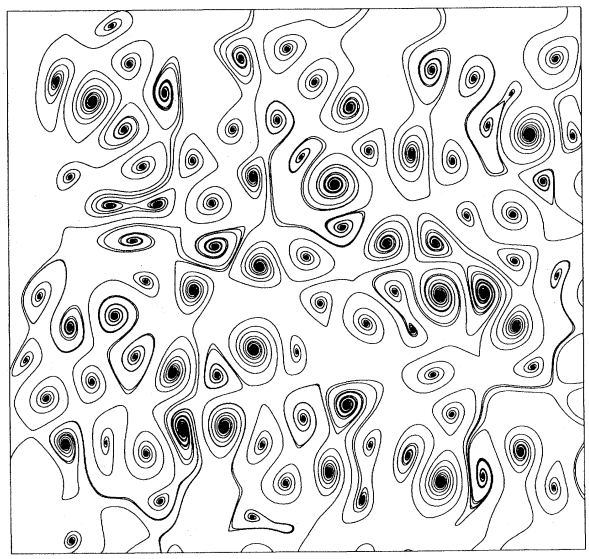

FIG. 30. Streamlines of weakly compressible flow (4.70) with $\varepsilon=0.1$ and $\psi(x,y)$ the same as in Fig. 10.

from bounce oscillations of particle guiding centers due to the toroidal geometry of a tokamak. Causing alternating opening and closing of random streamlines, such an effect leads to the onset of effective diffusion at zero collisional diffusivity.

6. Anomalous diffusion

Effective diffusion in an advection-diffusion system results from asymptotically decaying correlations in the particle trajectory. This "loss of memory," which is due to molecular diffusion, Lagrangian chaos, or both, occurs in a finite mixing time τ_m. On a time scale $t<\tau_m$ the advection-diffusion transport can exhibit more sophisticated, "anomalous" behavior (Bouchaud and Georges, 1990). In particular, the root-mean-square particle displacement can scale differently from the standard square root of time,

$$\lambda(t)=\langle[\mathbf{x}(t)-\mathbf{x}(0)]^2\rangle^{1/2}\propto t^{\zeta}\ , \tag{4.72}$$

where $\zeta\neq\frac{1}{2}$ is the exponent of *anomalous diffusion*. We use the notation ζ for the anomalous diffusion exponent in place of the more standard notation ν, which is already used for the correlation length exponent in percolation theory.

Similarly to the scalings for effective diffusivity D^* in incompressible flows, the exponent ζ also forms certain classes of universality, including continuous classes (that is, depending on the flow specrum). In a compressible flow ($\nabla\cdot\mathbf{v}\neq0$), however, the universality may break down, because the presence of "traps" such as stable foci of the flow (Fig. 30) results in qualitatively new transport effects. This can lead to the intriguing continuous dependence of the exponent ζ on the degree of compressibility (Bouchaud and Georges, 1990).

Anomalous diffusion can also take place in nonintegrable Hamiltonian systems where the velocity field is the phase-space flux (Afanasiev *et al.*, 1991; Swägerl and Krug, 1991). In some cases the onset of anomalous diffusion is similar to a percolation threshold (Chaikovsky and Zaslavsky, 1991).

One might suppose that the coordinates $\mathbf{x}(t)$ of a particle undergoing an anomalous diffusion (4.72) can be modeled by a fractional Brownian function $\mathbf{B}_{\zeta}(t)$. In the general case, however, this is not true, as the increments of $\mathbf{x}(t)$ may not be Gaussian (Ball *et al.*, 1987; Bouchaud *et al.*, 1990). The probability distribution function $n(\mathbf{x},t)$ of $\mathbf{x}$, for $n(\mathbf{x},0)=\delta(\mathbf{x})$, is given by the solution of the complete advection-diffusion equation. In the long-time limit, one can expect a self-similar behavior in the form

$$n(\mathbf{x},t)=Ct^{-\zeta d}f(|\mathbf{x}|/t^{\zeta})\ , \tag{4.73}$$

where an isotropic transport is assumed. The apparently typical behavior is described by the Fisher (1966) model of a random self-avoiding walk,

$$f(u)\propto\exp(-u^{1/(1-\zeta)})\ , \tag{4.74}$$

which becomes Gaussian only in the case of a standard Brownian motion ($\zeta=\frac{1}{2}$). Still, for a sufficiently rapidly decreasing $f(u)$ the distribution (4.73) is qualitatively similar to the Gaussian probability distribution function, so that a fractional Brownian motion can serve as a reasonable model for anomalous diffusion. Specifically, the fractal dimension D of the particle trail is given by formula (3.35), whose derivation is not hinged on the Gaussianity of $\mathbf{x}(t)$:

$$D=\min(1/\zeta,d)\ , \tag{4.75}$$

where d is the corresponding space dimension.

Two physically different regimes of anomalous diffusion should be distinguished between: superdiffusion ($\zeta>\frac{1}{2}$) and subdiffusion ($\zeta<\frac{1}{2}$). Bouchaud and Georges (1990) (see also Zaslavsky, 1991) identify the statistical mechanisms of anomalous diffusion in the example of generalized random walks, where a random walker undertakes a random step of length $l_i=\mathbf{x}_{i+1}-\mathbf{x}_i$, upon a random waiting period $\tau_i=t_i-t_{i-1}$. For independent and narrow distributions of l_i and τ_i, the standard diffusion is recovered. Superdiffusion can result from a wide distribution of l_i (meaning sufficiently slowly decaying probability of large steps) or from persisting correlations between successive steps, whereas subdiffusion results from a wide distribution of waiting times. In what follows, we attempt to exemplify these mechanisms on the grounds of passive advection.

a. Superdiffusion

One can imagine flows with long-range velocity correlations resulting in a "persistent" particle orbit, whose at least partial memory of the previous history lasts forever: $\tau_m=\infty$. According to the Tatarinova *et al.* (1991) and the Avellaneda and Majda (1991) theorems, in the presence of finite molecular diffusivity such flows should have an unbounded vector potential $\psi(\mathbf{x},t)$. The simplest example of superdiffusion was described by Dreizin and Dykhne (1972). Consider a shear flow with the velocity taking at random two constant values, $v=v_x(y)=\pm v_0$, in strips of width λ_0 (Fig. 31). The average velocity for almost every realization of this flow is zero, while the

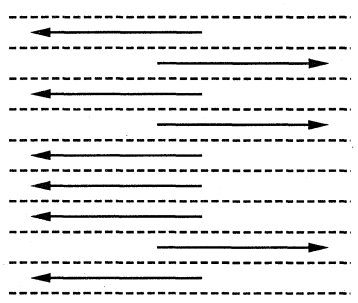

FIG. 31. Randomly directed shear flow with zero mean velocity but with a Brownian-type stream function.

stream function $\psi(y)=\int_0^y v_x(y')dy'$ is unbounded at $y\to\infty$. By time t, a tracer particle gets quasiuniformly dispersed in the y direction over the distance $\lambda_y=(D_0t)^{1/2}$, covering approximately $N=\lambda_y/\lambda_0$ flow strips. Given the random distribution of velocity directions, one can expect approximately $N^{1/2}$, say, left-directed strips in excess of right-directed ones. The fraction of time the particle spends in these excessive (left-directed) strips is of order $N^{1/2}/N=N^{-1/2}$. Hence the expected (rms) particle displacement in the x direction is given by

$$\lambda_x\simeq v_0tN^{-1/2}=v_0(\lambda_0^2/D_0)^{1/4}t^{3/4}\ , \tag{4.76}$$

a superdiffusive behavior ($\zeta=\frac{3}{4}>1/2$).

A continuum generalization of this steplike flow is a one-dimensional random stream function $\psi=\psi(y)$, with the spectrum $\psi_\lambda=\psi_0(\lambda/\lambda_0)^H$, $\lambda>\lambda_0$, $0<H<1$. [The example of Dreizin and Dykhne (1972) corresponds to $H=\frac{1}{2}$.] The velocity spectrum of such a flow, $v_\lambda=v_0(\lambda/\lambda_0)^{H-1}$, also implies zero mean velocity: $\langle v\rangle=v_{\lambda=\infty}=0$. The superdiffusion law is similarly obtained as

$$\begin{aligned}&\lambda_y(t)=\sqrt{D_0t}\ ,\\ &\lambda_x(t)=v_{\lambda_y(t)}t=v_0(\lambda_0^2/D_0)^{(1-H)/2}t^{(1+H)/2}\ ,\\ &\qquad\qquad t>\lambda_0^2/D_0\ .\end{aligned} \tag{4.77}$$

The averaged transport equation describing superdiffusion (4.77) cannot be cast into a local form; however, the average tracer density $\langle n\rangle$ may be represented asymptotically as the ensemble average of the solutions of the simple equation

$$\partial n/\partial t=\mathcal{R}t^H\partial^2 n/\partial x^2\ , \tag{4.78}$$

where $\mathcal{R}$ is a random coefficient with known distribution (Avellaneda and Majda, 1990).

Bouchaud *et al.* (1990; see also Redner, 1989 and Gaveau and Schulman, 1992) considered an isotropic 2D generalization of the random-directional shear flow—the "Manhattan system"

$$\psi(x,y)=\psi_1(x)+\psi_2(y) \tag{4.79}$$

(see Fig. 32). Suppose each component of the stream function (4.79) has a power spectrum with the exponent $H>0$: $\psi_\lambda\propto\lambda^H$. Anomalous diffusion in such a flow can be obtained similarly to Eq. (4.77). Due to the statistical isotropy of the system, the rms displacement $\lambda(t)$ is self-consistently coupled to the result:

$$\lambda(t)=v_{\lambda(t)}t\ . \tag{4.80}$$

It follows that

$$\lambda(t)=\lambda_0\left[\frac{v_0t}{\lambda_0}\right]^{1/(2-H)},\quad t>\frac{\lambda_0^2}{D_0}\ . \tag{4.81}$$

At $H=\frac{1}{2}$ one has the superdiffusion exponent $\zeta=1/(2-H)=\frac{2}{3}$ (Bouchaud *et al.*, 1990).

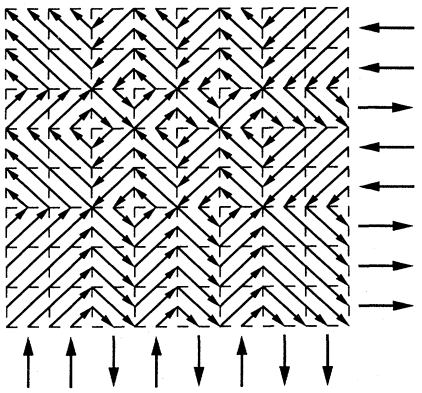

FIG. 32. Isotropic random flow of the "Manhattan-grid" type shown by the superposition of two mutually perpendicular random shear flows.

Given the way result (4.81) has been derived, one can expect its wider generality. In fact, the superdiffusive law (4.81) is valid not only for a Manhattan flow, but also for an arbitrary random stream function with the isotropic power spectrum $\psi_\lambda\propto\lambda^H$ (Isichenko and Kalda, 1991c). The validity of (4.81) for a two-dimensional random flow, however, is restricted by the inequality $0<H<\frac{10}{17}$ (region C in Fig. 23). Formula (4.81) also extends to the three-dimensional case. Koch and Brady (1989; see also Brady, 1990) considered random, steady 3D flows with the algebraically decaying velocity correlator $\langle v_i(\mathbf{x})v_j(\mathbf{x}+\boldsymbol{\rho})\rangle\propto\delta_{ij}|\boldsymbol{\rho}|^{-\gamma}$ and found the superdiffusive tracer dispersion (4.72) with the exponent

$$\zeta=\frac{2}{\gamma+2},\quad 0<\gamma<2\ . \tag{4.82}$$

The velocity covariance $\propto|\boldsymbol{\rho}|^{-\gamma}$ corresponds to the spectrum $v_\lambda\propto\lambda^{-\gamma/2}$ [see Eqs. (3.9)–(3.13)] and hence to the vector potential $\boldsymbol{\psi}(\mathbf{x})$ λ-spectrum exponent $H=1-\gamma/2$. Then Eq. (4.82) is equivalent to $\zeta=1/(2-H)$, in accordance with Eq. (4.81).

The marginal case $H=0$ requires special analysis because the delta variance of the stream function, $\Delta(\boldsymbol{\rho})=\langle[\psi(\mathbf{x}+\boldsymbol{\rho})-\psi(\mathbf{x})]^2\rangle$, behaves as $\log\rho$ for $\lambda_0<\rho<\lambda_m$. For $\lambda(t)<\lambda_m$ the stream function, as sampled by tracer particles, is logarithmically unbounded. This leads to a new regime of logarithmical superdiffusion (Kravtsov *et al.*, 1986; Bouchaud *et al.*, 1987),

$$\lambda(t)\simeq\sqrt{\Delta^{1/2}(\lambda(t))t}\simeq\sqrt{\psi_0t}\,\log^{1/4}(\psi_0t/\lambda_0^2),\quad H=0\ . \tag{4.83}$$

The superdiffusive laws (4.81) and (4.83) do not exhaust all anomalous regimes in 2D random, steady power-spectrum flows. Another superdiffusive regime in a multiscale flow corresponds to the random walk with the self-consistently determined partial diffusivity (4.42)

$$\lambda^2(t)=D_{\lambda(t)}t\ . \tag{4.84}$$

Substituting formulas (3.74) and (3.80a) into $D_\lambda = D_0 L(\lambda)/w(\lambda)$, we obtain $D_\lambda \propto \lambda^{D_h - H}$; hence (Isichenko and Kalda, 1991c)

$$\lambda(t) = \lambda_0 \left[\frac{D_0 t}{\lambda_0^2} \right]^{1/(2+H-D_h)}, \quad \lambda_0 < \lambda(t) < \min(\xi, \lambda_m) , \tag{4.85}$$

where ξ is the solution of Eq. (4.38). For $H < 1$ we have

$$\zeta = \frac{1}{2+H-D_h} = \frac{7}{10H+4} > \frac{1}{2} . \tag{4.86}$$

This superdiffusive regime is possible for $H > -\frac{2}{5}$ in the region C in Fig. 23. It is interesting to note that, for $-\frac{2}{5} < H < \frac{3}{10}$, Eq. (4.69) predicts the root-mean-square particle displacement to grow faster than linear with time ($\zeta > 1$), that is, with an acceleration ("superballistic" regime).

It must be emphasized that, by definition, regime (4.86) corresponds to a "typical" initial position of a tracer particle in a given flow, that is, on a streamline with the size of order λ_0; hence it cannot be obtained by averaging over the initial position or the ensemble of flows. Such an averaging would lead to something different due to the significant transport role played by scarce long streamlines. These lines will eventually dominate the transport after effective diffusion sets in, but one should not necessarily perform the ensemble average when studying transient anomalous behavior for a specified initial condition. To exemplify this remark, consider a monoscale (λ_0) 2D steady flow in the absence of molecular diffusion ($D_0 = 0$). Then for almost any initial position the particle displacement is forever bounded by the diameter a of the corresponding streamline; typically, $a \simeq \lambda_0$. Denote by $x(a,t)$ the particle displacement averaged over a time interval $[t, 2t]$. This displacement clearly behaves as

$$x(a,t) \simeq \begin{cases} \lambda_0 (v_0 t/\lambda_0)^{1/d_h}, & v_0 t < L(a) = \lambda_0 (a/\lambda_0)^{d_h} , \\ a, & v_0 t > L(a) , \end{cases} \tag{4.87}$$

where $d_h = \frac{7}{4}$ is the fractal dimension of the monoscale streamline. For a single particle released on a long enough streamline, the first equation (4.87) predicts a superdiffusive displacement ($\zeta = 1/d_h = 4/7$). However, the average square displacement over the ensemble of flows or, equivalently, over the initial conditions, corresponds to a subdiffusive behavior. Upon averaging the square expression (4.87) with the help of the distribution function (3.47) of the streamlines, we obtain

$$\langle \lambda^2(t) \rangle = \int_{\lambda_0}^{\infty} x^2(a,t) F(a) \frac{da}{a} \simeq \lambda_0^2 \left[\frac{v_0 t}{\lambda_0} \right]^{1/d_h} , \tag{4.88}$$

a subdiffusive behavior [$\zeta - 1/(2d_h) = 2/7$] with an unbounded displacement. A subdiffusive behavior was numerically observed by Kraichnan (1970) for the case of an ensemble of 2D incompressible steady flows. This subdiffusion clearly has little to do with the generic behavior of a passively advected particle in a particular realization of the flow. Still, for the corresponding conductivity problem (for the correspondence, see Sec. IV.B.3.b), the ensemble-averaged anomalous diffusion in the advection-diffusion system may be relevant, upon being translated into a size effect—that is, the dependence of the specific conductance of a sample on its size (Dreizin and Dykhne, 1972; Isichenko *et al.*, 1989; Isichenko and Kalda, 1991a). Here the interesting problem of the relation between the ensemble-averaged transport, on the one hand, and the typical behavior for a given realization of a disordered system, on the other hand, is only posed without being duly addressed.

Perhaps the most important implications of anomalous diffusion concern real turbulent (time-dependent) flows. The Richardson law (4.6) means, by definition of D_λ, that the root-mean-square *relative* displacement of advected particles behaves as $\lambda(t) = (D_{\lambda(t)} t)^{1/2}$; hence

$$\lambda(t) \propto t^{3/2} . \tag{4.89}$$

The Richardson superdiffusion (4.89) is naturally obtained from the Kolmogorov-Obukhov spectrum[4] (Kolmogorov, 1941; Monin and Yaglom, 1971, 1975; Rose and Sulem, 1978; Batchelor, 1982) $v_\lambda \propto \lambda^{1/3}$ upon using the relation $\lambda(t) = v_{\lambda(t)} t$. Indeed, v_λ is the characteristic velocity difference between two points that are a distance λ apart from each other. The superdiffusion law (4.89) was derived by Obukhov (1941) from a dimensional analysis similar to the one that led Kolmogorov (1941) to the $\lambda^{1/3}$ ($H = \frac{1}{3}$) velocity spectrum. The detailed discussion of the relation between the Kolmogorov spectrum and the Richardson superdiffusion was given by Batchelor (1952).

In the case of a decreasing velocity spectrum, $v_\lambda \propto \lambda^{H-1}$, $H < 1$, a nontrivial *absolute* superdiffusion is also possible. Time dependence can be introduced in the form of the characteristic frequency ω_λ at which the λ component $v_\lambda(\mathbf{x},t)$ of the velocity field is evolved:

$$\omega_\lambda = \omega_0 \left[\frac{\lambda}{\lambda_0} \right]^{-G}, \quad \lambda_0 < \lambda < \lambda_m . \tag{4.90}$$

In a pure fluid turbulence, one would have $\omega_\lambda = v_\lambda/\lambda$, that is, $G = 2 - H$. For the turbulence of Rossby waves in a rotating fluid, drift waves in plasmas (Hasegawa and Mima, 1978; Hasegawa *et al.*, 1979), or other systems having a characteristic velocity V such as the phase velocity of linear waves, regimes with $\omega_\lambda = V/\lambda$ are possi-

[4]The standard form for this spectrum is usually given in terms of the energy spectral density, $E(k) \propto k^{-5/3}$. The relation between $E(k)$ and $E_\lambda \propto v_\lambda^2$ is given by $E_\lambda = \int_{1/(2\lambda)}^{1/\lambda} E(k)\,dk \propto \lambda^{2/3}$.

ble, that is, $G=1$. The superdiffusive law for arbitrary $G>0$ and $H<1$ can be obtained as follows. The displacement of a tracer particle, released in the flow at $t=0$, is governed at time t by the flow component with $\lambda=\lambda^*(t)$ determined from the equation $\omega_{\lambda^*(t)}t=1$. Indeed, at $H<1$ longer scales $[\lambda\gg\lambda^*(t)]$ have smaller velocity, whereas shorter scales $[\lambda\ll\lambda^*(t)]$ have fast-oscillation velocity components: $\omega_\lambda t\gg 1$. In the absence of other scales, these oscillations would lead to the turbulent diffusivity given by formula (4.64): $D_\lambda=v_\lambda^2/\omega_\lambda\propto\lambda^{G+2H-2}$. If D_λ increases with growing λ—that is, $G>2-2H$—then the $\lambda^*(t)$ velocity scale dominates the tracer motion. In this case, we can write the root-mean-square displacement $\lambda(t)$ in two equivalent forms, $\lambda(t)=v_{\lambda^*(t)}t=(D_{\lambda^*(t)}t)^{1/2}$. Thus we obtain

$$\lambda(t)=\frac{v_0}{\omega_0}(\omega_0 t)^{(G+H-1)/G},\quad G>2-2H>0\ . \tag{4.91}$$

In the opposite case, $G<2-2H$, the small-scale velocity pulsations dominate the particle motion, leading to the turbulent diffusivity $D^*\simeq v_0^2/\omega_0$. The validity of result (4.91) in two dimensions is further restricted by the inequality $G\le 2-H$ to ensure the absence of an additional integral of motion—the adiabatic invariant of the stream function $\psi[x(t),y(t),t]$—which is approximately conserved at $\omega_\lambda\ll v_\lambda/\lambda$. The low-frequency transport in a two-dimensional multiscale time-dependent flow is more complicated and requires the statistical topography analysis of particle orbits (Kalda, 1992).

Osborne and Caponio (1990) studied numerically passive transport in a 2D time-dependent random flow with spectral exponents $G=1$, $\frac{1}{2}<H<3$. They found the superdiffusion exponent ζ to behave as $\zeta=H$, for $\frac{1}{2}<H<1$, in accordance with Eq. (4.91).

Notice that in the case of a turbulence with the eddy-revolution characteristic frequency $\omega_\lambda=v_\lambda/\lambda$, that is, $G=2-H$, Eq. (4.91) leads to the superdiffusive exponent $\zeta=1/(2-H)$, the same as in Eq. (4.81) describing the superdiffusion in steady flows.

Avellaneda and Majda (1990) considered anomalous diffusion in random, unsteady shear flows, $v=v_x(y,t)$. They identified several regimes of the tracer behavior and established the equations describing the average density $\langle n\rangle$.

The anomalous diffusion scalings, such as in Eqs. (4.81), (4.85), and (4.91), can be used to recover turbulent spectra from the observed tracer motion, such as satellite-tracked buoys deployed in the ocean (Osborne *et al.*, 1986; Brown and Smith, 1991). To do so, one can use either complete time-coordinate records $\{t_i,x_i,y_i\}$ or only the trail $\{x_i,y_i\}$, whose fractal dimension D is related to the anomalous diffusion exponent ζ by formula (4.75). However, for deciphering turbulence spectra $\psi_\lambda\propto\lambda^H$ with $H>1$, the information stored in the relative particle dispersion has to be used.

Another manifestation of a self-similar (power-spectrum) turbulence is the fractal structure of the isoscalar surfaces, that is, the surfaces where the density of a passive scalar takes a constant value. Constantin *et al.* (1991) give theoretical expressions for the fractal dimension of isoscalar surfaces, $D_{\rm in}=2+H/2$, in the internal region of a turbulent spot, and $D_{\rm ex}=1+H$, near the boundary of a turbulent jet, where $v_\lambda\propto\lambda^{H-1}$ is the velocity spectrum. These predictions agree with experimental data (Sreenivasan and Prasad, 1989; Sreenivasan *et al.*, 1989; Constantin *et al.*, 1991). Recent experiments on turbulent diffusion, superdiffusion, and fractal behavior also include those conducted by Swinney and Tam (1987), Ramshankar *et al.* (1990), and Ramshankar and Gollub (1991). Some other fractal and multifractal properties of passive scalars are discussed by Mandelbrot (1975b), Hentschel and Procaccia (1983a), Ott and Antonsen (1988), Voss (1989), Vulpiani (1989), Fung and Vassilicos (1991), and Városi *et al.* (1991).

b. Subdiffusion

The superdiffusive (persistent) random walk does not exhaust the variety of anomalous diffusion regimes in incompressible flows. The subdiffusive (antipersistent) tracer motion with $\zeta<\frac{1}{2}$ is also possible (Pomeau *et al.*, 1988; Young, 1988; Young *et al.*, 1989). In a time-independent flow, such behavior arises from the tracer particles resting in closed pockets of recirculation. Once in a region of such closed streamlines, the particle resides there for a time before proceeding with its propagation. This waiting time is governed by molecular diffusion and hence is a random quantity with a wide distribution. The resulting retarded ($\zeta<\frac{1}{2}$) dispersion (Montroll and Scher, 1973) is quite similar to the diffusion on comblike structures (Fig. 33; Havlin and Ben-Avraham, 1987). The system of regular convection rolls (Fig. 20) is equivalent to a comb whose base represents the diffusive boundary layers and whose teeth correspond to the inner area of the convection cells. To complete this analogy, one should position the teeth, λ_0 long, the distance $w_b=\lambda_0 P^{-1/2}$ ($P\equiv\psi_0/D_0\gg 1$) apart from each other and should ascribe a diffusion coefficient of the order of the molecular diffusivity D_0 to the whole structure. Such a representation of the transport properties of flow (4.22) is valid on the time scale $t\gg\lambda_0/v_0$, when (a) the boundary-layer structure of transport has set in and (b) the tracer dispersion inside the convection rolls can be described by the

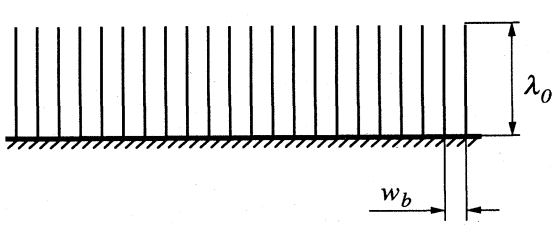

FIG. 33. Diffusion comb corresponding to a periodic array of convection rolls.

averaged one-dimensional cross-stream diffusion equation

$$\frac{\partial n(J,t)}{\partial t}=\frac{\partial}{\partial J}D(J)\frac{\partial n(J,t)}{\partial J} \tag{4.92}$$

instead of the full 2D advection-diffusion equation (4.1). In Eq. (4.92), $n(J,t)$ designates the tracer density averaged over a streamline $\psi(x,y)=$const with the area J inside it. The idea of such averaging stems from the perturbation theory of nearly integrable Hamiltonian systems (Arnold, 1978), where one switches from the phase-space variables (x,y) to the action-angle variables (J,ϕ) of the unperturbed (integrable) motion. The action-diffusion coefficient $D(J)$ is given by

$$D(J)=D_0\oint|\nabla\psi|dl\oint|\nabla\psi|^{-1}dl\ , \tag{4.93}$$

where the integrals are taken around the streamline (Isichenko *et al.*, 1989; Young *et al.*, 1989).

Suppose a small spot of dye (passive tracer) is deposited at $t=0$ close to the separatrix mesh of a periodic array of vortices (Fig. 20) corresponding to the base of the comb (Fig. 33). Consider time scales $\lambda_0/v_0\ll t\ll\lambda_0^2/D_0$. Then the dye invades a distance $(D_0t)^{1/2}$ along the teeth. The fraction $F(t)$ of "active" particles—that is, those residing on the base and determining the long-range tracer dispersion—decreases with time as

$$F(t)=\frac{w_b}{(D_0t)^{1/2}}\ . \tag{4.94}$$

In terms of the random walk of a single particle, Eq. (4.94) yields the fraction of time spent on the comb base. Then the propagation rate along the base coordinate b is given by

$$b^2(t)=F(t)D_0t=w_b(D_0t)^{1/2}\ . \tag{4.95}$$

This corresponds to the root-mean-square displacement in real space (Havlin and Ben-Avraham, 1987; Pomeau *et al.*, 1988; Young *et al.*, 1989)

$$\lambda(t)=b(t)\frac{\lambda_0}{w_b}=(\lambda_0^2D_0t)^{1/4}\ , \tag{4.96}$$

a subdiffusive law ($\zeta=\frac{1}{4}$) sometimes referred to as "double diffusion" (Krommes *et al.*, 1983). Such tracer behavior is valid for nonvanishing velocity on the separatrix mesh (free-slip boundary condition). For no-slip (rigid) boundary, where the velocity falls linearly to zero, one has $\zeta=\frac{1}{3}$ (Pomeau *et al.*, 1988; Young *et al.*, 1989), a behavior that was confirmed experimentally (Cardoso and Tabeling, 1988).

Not only the rms displacement scaling but also the governing equation for the tracer envelope can be established for periodic flows. The general form of this equation was derived by Young *et al.* (1989):

$$\frac{\partial}{\partial t}\int_0^tK(t-\tau)f(\mathbf{x},\tau)d\tau=D^*\nabla^2f(\mathbf{x},t)\ , \tag{4.97}$$

where f is the tracer density on a separatrix considered as a function of "slow" coordinate $\mathbf{x}$, D^* is the effective diffusivity, and $K(\tau)$ is an integral kernel satisfying the normalization condition

$$\int_0^\infty K(\tau)d\tau=1\ . \tag{4.98}$$

The sense of Eq. (4.97) is that the tracer flux is determined solely by the density f in the diffusive boundary layers and the effective diffusivity D^* (right-hand side), while the left-hand side specifies the change in the average tracer density $\langle n\rangle=\int_0^tK(t-\tau)f(\mathbf{x},\tau)d\tau$. The latter is obtained from f via a linear integral operator describing the tracer invasion into a convection cell. In the limiting case $t\gg\tau_m$, where the mixing time $\tau_m\simeq\lambda_0^2/D_0$ is the characteristic time of the convergence of integral (4.98), the kernel K can be replaced by a delta function; hence $\langle n\rangle=f$ and the effective diffusion equation is recovered from (4.97). In the opposite case, $\lambda_0/v_0\ll t\ll\tau_m$, the kernel behaves as a power, $K(\tau)=(\tau_m\tau)^{-1/2}$, and the operator on the left-hand side of Eq. (4.97) becomes the operator of fractional differentiation [see Eq. (3.36)]:

$$\left[\frac{\pi}{\tau_m}\frac{\partial}{\partial t}\right]^{1/2}f=D^*\nabla^2f\ . \tag{4.99}$$

Zaslavsky (1992) phenomenologically suggested using a generalization of Eq. (4.99),

$$\left[\frac{\partial}{\partial t}\right]^{\beta}f(x,t)=\left[\frac{\partial}{\partial x}\right]^{\alpha}[\mathcal{D}(x)f(x,t)]\ , \tag{4.100}$$

to describe an arbitrary anomalous diffusion with $\zeta=\beta/\alpha$.

As the nonlocal time operator $\sqrt{\partial/\partial t}$ commutes with the space operator ∇^2, one can write the consequence of Eq. (4.99) in a local differential form,

$$\frac{\partial f}{\partial t}=\frac{\tau_mD^{*2}}{\pi}\nabla^4f\ , \tag{4.101}$$

which emphasizes the term "double diffusion." The simplicity of (4.101) is, nevertheless, deceptive. While including all solutions of the nonlocal equation (4.99), the local double-diffusion equation (4.101) has many extraneous solutions[5] that well manifest themselves in a strongly unstable behavior of Eq. (4.101): A monochromatic solution $f\propto\exp(-i\omega t+i\mathbf{k}\cdot\mathbf{x})$ grows with time exponentially, $\omega=ik^4\tau_mD^{*2}/\pi$, whereas our intuitive conception of (sub)diffusion suggests a behavior of f that smoothes out initial inhomogeneities.

Subdiffusive behavior is also possible in random velocity fields (Isichenko and Kalda, 1991c). As in regular convection cells, this behavior is transient ($t<\tau_m$) and takes place for special initial conditions, namely, for the initial tracer spot deposited in a mixing convection cell. (Remember that the mixing convection cells of the size ξ_m play the role of boundary layers.) The difference be-

[5]Those of Eq. (4.99) with D^* substituted by $-D^*$.

tween random flows and regular flows lies in the appearance of their equivalent loopless structures. Due to the presence of numerous separatrices in a random flow, the tracer fills up the holes in a ξ_m cell topologically nontrivially, as on each separatrix the converging diffusion front breaks into two (in a nondegenerate case; see Fig. 34). Hence the equivalent "diffusion comb" of a random flow has branching teeth and looks like a thicket (Fig. 35). The rate of filling up the branches of these trees can be found using the topographic properties of random flows.

Introduce the "action distance" x_J across the streamlines according to $dJ=\pm L(x_J)dx_J$, where $L(x_J)$ is the length of a closed streamline and J is the area inside this line. The action-diffusion coefficient (4.93) being estimated as $D(J)\simeq D_0 L^2(x_J)$, one can rewrite Eq. (4.92) in terms of the action distance x_J:

$$\frac{\partial n}{\partial t}=\frac{1}{L(x_J)}\frac{\partial}{\partial x_J}\left[D_0 L(x_J)\frac{\partial n}{\partial x_J}\right] . \tag{4.102}$$

Hence the segments of the "diffusion tree" (Fig. 34) can be measured in the action-distance units, with the diffusivity along the branches of order D_0.

Consider a monoscale uncorrelated, random, steady flow with the characteristic scale λ_0. The action distance between the external boundary of an a cell and the innermost point of a hole in the cell can be calculated as the sum of the widths (3.45) of the nested cells of diameter $\lambda_0, 2\lambda_0, \ldots, a$. For any $a \gg \lambda_0$, this sum is estimated to be λ_0. It follows, in particular, that the action distance between two arbitrary points on the (x,y) plane is bounded by a constant of the order of λ_0. Hence the mixing time in the monoscale flow equals

$$\tau_m=\frac{\lambda_0^2}{D_0} . \tag{4.103}$$

Consider time scales $w^2(\xi_m)/D_0 \ll t \ll \tau_m$. Then the diffusion front invades the action distance $x_J(t)=\sqrt{D_0 t}$ along each branch of the diffusion tree. To calculate the total area $S(x_J)$ (in physical space) covered by the invaded region inside one ξ_m cell, introduce a new topographic exponent δ, which can be called "dimension of the diffusion tree": $S(x_J)\propto x_J^{\delta}$. Using the matching conditions $S[w(\xi_m)]=L(\xi_m)w(\xi_m)$ [where $L(\xi_m)$ is the perimeter (3.43) of the ξ_m cell] and $S(\lambda_0)=\xi_m^2$ (all the holes are filled up by $t=\tau_m$, when $x_J=\lambda_0$), we find

$$\delta=1+\nu(2-d_h)=\tfrac{4}{3} . \tag{4.104}$$

The fractional value of the tree dimension δ between 1 and 2 indicates that, while the complete 2D description (4.1) is redundant, purely one-dimensional action diffusion oversimplifies the transport in topologically complex flows.

The rest of the calculation essentially repeats that for the simplest nonbranching diffusion comb, whose dimension δ is unity. The fraction of active particles lying on the base of the comb is

$$F(t)=\frac{S[w(\xi_m)]}{S(\sqrt{D_0 t})}\propto t^{-\delta/2} . \tag{4.105}$$

The tracer propagation along the comb base is given by $b^2(t)=F(t)D_0 t$, and, as the distance $w(\xi_m)$ between the treelike teeth of the comb corresponds to the physical distance ξ_m, we obtain

$$\lambda(t)=b(t)\frac{\xi_m}{w(\xi_m)}=\xi_m\left[\frac{D_0 t}{w^2(\xi_m)}\right]^{\zeta}, \qquad \frac{w^2(\xi_m)}{D_0}<t<\tau_m , \tag{4.106}$$

where the subdiffusion exponent for 2D monoscale random flow equals

$$\zeta=\frac{1}{2}-\frac{\delta}{4}=\frac{1}{6} . \tag{4.107}$$

The "triple diffusion," Eqs. (4.106) and (4.107), can also be described by a nonlocal integro-differential equation involving the operator $(\partial/\partial t)^{1/3}$.

The generalization of the above result to the case of multiscale flows is easily done for the monoscale correlated spectrum with the exponent $-1/\nu<H<0$. In this case one simply substitutes the percolation exponents ν and d_h in Eq. (4.104) by their correlated percolation

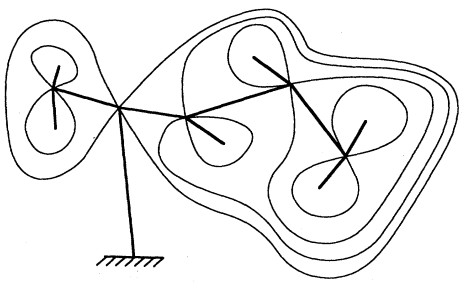

FIG. 34. Diffusion tree (branches shown in heavy lines) corresponding to passive transport in a topologically complex flow. For a nondegenerate flow each separatrix divides the plane into two inner regions and one outer region; hence all branching points on the tree are Y points.

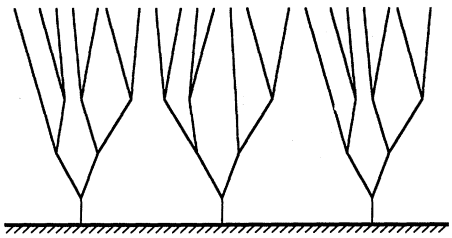

FIG. 35. Diffusion comb of a random flow, which looks like a thicket. The subdiffusive propagation along the "ground" (network of mixing convection cells) stems from the delay caused by random walk in the "bushes."

counterparts (4.44). As a result, we have the dimension of the diffusion tree

$$\delta=\frac{H+D_h-2}{H}, \quad -1/\nu<H<0 , \tag{4.108}$$

and the subdiffusion exponent

$$\zeta=\frac{1}{2}-\frac{\delta}{4}=\frac{2+H-D_h}{4H}=\frac{5H+2}{14H} . \tag{4.109}$$

The subdiffusion law (4.106)–(4.109) is valid for $-\frac{3}{4}\le H<-\frac{2}{5}$, where $0<\zeta\le\frac{1}{6}$.

B. Conductivity of inhomogeneous media

The problem of the average characteristics of spatially fluctuating dielectrics and conductors is as old as electrodynamics itself (Maxwell, 1873). The review of early work by Clausius, Mossotti, Lorentz, and others on polarizability of heterogeneous media was given by Landauer (1978). Up to now, there has been no general solution of this classical problem, which is mathematically formulated as follows. Denote by $\mathbf{e}(\mathbf{x})$ the microscopic electric field and by $\mathbf{j}(\mathbf{x})$ the microscopic current density in a medium with a nonuniform conductivity tensor $\hat{\sigma}(\mathbf{x})$:

$$\mathbf{j}(\mathbf{x})=\hat{\sigma}(\mathbf{x})\mathbf{e}(\mathbf{x}) . \tag{4.110}$$

To satisfy the time-independent Maxwell's equations, the electric field should be irrotational and the current density solenoidal:

$$\nabla\times\mathbf{e}=0, \quad \nabla\cdot\mathbf{j}=0 . \tag{4.111}$$

Given a deterministic (or statistical) description of the fluctuating conductivity $\hat{\sigma}(\mathbf{x})$, what is the space- (or ensemble-) average conductivity $\hat{\sigma}^*$? By definition, the effective conductivity is the proportionality coefficient (tensor, in general) between the average electric field $\mathbf{E}=\langle\mathbf{e}(\mathbf{x})\rangle$ and the average current density $\mathbf{J}=\langle\mathbf{j}(\mathbf{x})\rangle$:

$$\mathbf{J}=\hat{\sigma}^*\mathbf{E} . \tag{4.112}$$

Analogously to the advection-diffusion problem, one can introduce the mixing length ξ_m characterizing the minimum scale of the effective conduction behavior (4.112).

Electrical conductivity is not the only problem described by Eqs. (4.110)–(4.112). Mathematically equivalent are the problems of averaging the dielectric constant $\hat{\varepsilon}$ (where $\mathbf{j}$ is replaced by the electric induction $\mathbf{D}$), diffusivity $\hat{D}$ (where $\mathbf{E}$ is replaced by minus the density gradient of a diffusing substance and $\mathbf{j}$ is its flux), and thermal conduction tensor $\hat{\chi}$ (with $\mathbf{E}$ standing for the temperature gradient and $\mathbf{j}$ for the thermal flux). Among various transport processes occurring in heterogeneous media, we discuss primarily those involving a large parameter, such as the strength of the fluctuations of $\hat{\sigma}(\mathbf{x})$ or the strength of its anisotropy. It is believed that a qualitative analysis of scaling relations for the effective conductivity σ^* is most important for the physical understanding of the problem. Nevertheless, the few available examples of nontrivial exact solutions will also be reviewed.

The extreme case of a binary mixture of an ideal insulator with a conducting phase was discussed in Sec. II in the framework of the percolation theory. The behavior of such a mixture involves a sharp transition from an insulator to a conductor. However, due to the reasons discussed in Sec. II.E, the behavior of the three-dimensional effective conductivity σ^* near the continuum percolation threshold may not be quite universal. In Sec. IV.B.1 we discuss the special case of a two-dimensional, two-phase system, which is *exactly at the percolation threshold.* For an arbitrary ratio of the phase conductivities, it is possible to calculate effective conductivity using a reciprocity relation discovered by Keller (1964) and Dykhne (1970a). This method is also applicable to polycrystals and to heat conduction in anisotropic plasmas (Sec. IV.B.2). In Sec. IV.B.3 the anomalous magnetoresistance taking place in inhomogeneous conductors with the Hall effect is discussed.

1. Keller-Dykhne reciprocity relations

One of the very few exact results on the conductivity of composite materials was obtained for a two-dimensional binary mixture. Once again we notice the remarkable (and exceptional) feature of two dimensions favoring successful analytical advance. In the long run, the availability of exact percolation exponents, as well as of the results discussed below, stems from the highly nontrivial fact of the existence of complex numbers and the resulting conformal maps. (Indeed, it is not easy to expect that a vector algebra can be introduced, including the operation of division, similar to the algebra of real numbers. And such an algebra cannot be naturally introduced in three dimensions.)

Originally, Keller (1964; see also 1987) considered a composite medium consisting of a rectangular lattice of identical parallel cylinders of any cross section, having electrical conductivity σ_2 and embedded in a medium of conductivity σ_1. Using the theory of harmonic functions, Keller proved the following relation for the principal values of the effective conductivity tensor $\hat{\sigma}^*(\sigma_1,\sigma_2)$:

$$\sigma^*_{xx}(\sigma_1,\sigma_2)\sigma^*_{yy}(\sigma_2,\sigma_1)=\sigma_1\sigma_2 , \tag{4.113}$$

where the x and y axes lie along the axes of the lattice. The second factor on the left-hand side of Eq. (4.113) refers to the conductivity of a *reciprocal medium*—that is, a medium of the same geometry but with interchanged phases σ_1 and σ_2.

Independently, Dykhne (1970a) derived formula (4.113) under more general assumptions using an elegant reciprocity transformation. Following his work, we consider new vector fields

$$\mathbf{j}'(\mathbf{x})=\sigma_*\hat{\mathbf{R}}\mathbf{e}(\mathbf{x}),\quad \mathbf{e}'(\mathbf{x})=\frac{1}{\sigma_*}\hat{\mathbf{R}}\mathbf{j}(\mathbf{x})\ , \tag{4.114}$$

where σ_* is a constant and $\hat{\mathbf{R}}=\hat{\mathbf{z}}\times\cdots$ is the operator of rotation in the plane (x,y) through the angle of 90°. The choice of $\mathbf{j}'$ and $\mathbf{e}'$ is designed to satisfy the relations

$$\nabla\cdot\mathbf{j}'=0,\quad \nabla\times\mathbf{e}'=0 \tag{4.115}$$

that follow from (4.111). Upon comparing Ohm's law (4.110) with Eqs. (4.114), one easily finds the relation between the "primed" vector fields:

$$\mathbf{j}'(x)=\hat{\sigma}'(\mathbf{x})\mathbf{e}'(\mathbf{x}),\quad \hat{\sigma}'(\mathbf{x})=\sigma_*^2\hat{\mathbf{R}}\hat{\sigma}^{-1}(\mathbf{x})\hat{\mathbf{R}}^{-1}\ . \tag{4.116}$$

For the case of an isotropic tensor $\sigma_{ij}(\mathbf{x})=\sigma(\mathbf{x})\delta_{ij}$, with $\sigma(\mathbf{x})$ taking on only the two values σ_1 and σ_2 in the regions I and II, respectively, it is convenient to choose $\sigma_*^2=\det\hat{\sigma}=\sigma_1\sigma_2$, so that $\sigma'_{ij}=\sigma'(\mathbf{x})\delta_{ij}$ and

$$\sigma'(\mathbf{x})=\frac{\sigma_1\sigma_2}{\sigma(\mathbf{x})}=\begin{cases}\sigma_2, & \text{in } I\ ,\\ \sigma_1, & \text{in } II\ .\end{cases} \tag{4.117}$$

Thus the system of Eqs. (4.115) and (4.116) becomes quite similar to (4.110) and (4.111) and describes the current flow in a new two-dimensional system differing from the old one by the interchange of the conductivities σ_1 and σ_2. If we assume that from (4.110) and (4.111) follows relation (4.112) for the average current and electric field, with the effective conductivity $\hat{\sigma}^*(\sigma_1,\sigma_2)$ being a definite function of σ_1 and σ_2, then we conclude that the effective conductivity, $\hat{\sigma}^{*\prime}$, of the primed system exists:

$$\mathbf{J}'=\hat{\sigma}^{*\prime}\mathbf{E}'\ , \tag{4.118}$$

where

$$\sigma^{*\prime}=\hat{\sigma}^*(\sigma_2,\sigma_1)\ . \tag{4.119}$$

In Eq. (4.118), $\mathbf{J}'$ and $\mathbf{E}'$ denote the average values of $\mathbf{j}'(\mathbf{x})$ and $\mathbf{e}'(\mathbf{x})$, respectively. According to (4.114), we have

$$\mathbf{J}'=(\sigma_1\sigma_2)^{1/2}\hat{\mathbf{R}}\mathbf{E},\quad \mathbf{E}'=(\sigma_1\sigma_2)^{-1/2}\hat{\mathbf{R}}\mathbf{J}\ . \tag{4.120}$$

The final result comes from the comparison of Eq. (4.112) with Eq. (4.118). With the constraint (4.120), they are compatible for any $\mathbf{E}$ if and only if the tensor operator $(\sigma_1\sigma_2)^{-1}\hat{\mathbf{R}}^{-1}\hat{\sigma}^{*\prime}\hat{\mathbf{R}}\hat{\sigma}^*$ is the identity. In terms of the principal values $\sigma^*_{xx}(\sigma_1,\sigma_2)$ and $\sigma^*_{yy}(\sigma_1,\sigma_2)$ of the effective conductivity $\hat{\sigma}^*(\sigma_1,\sigma_2)$, this results in the reciprocity relation (4.113).

Now consider a composite medium that is macroscopically isotropic: $\sigma^*_{xx}(\sigma_1,\sigma_2)=\sigma^*_{yy}(\sigma_1,\sigma_2)=\sigma^*(\sigma_1,\sigma_2)$. Then Eq. (4.113) reads

$$\sigma^*(\sigma_1,\sigma_2)\sigma^*(\sigma_2,\sigma_1)=\sigma_1\sigma_2\ . \tag{4.121}$$

In the case of statistically equivalent distributions of the two phases, which implies a split 50/50 area occupation, the function $\sigma^*(\sigma_1,\sigma_2)$ becomes a symmetric function of σ_1 and σ_2. Then it follows (Dykhne, 1970a) that

$$\sigma^*=(\sigma_1\sigma_2)^{1/2}\ . \tag{4.122}$$

This exact result is valid for arbitrary values of σ_1 and σ_2. Specifically, if σ_1 tends to infinity and σ_2 to zero, the effective conductivity σ^* *may* still remain finite. Such a behavior is possible only *exactly at the percolation threshold.* (Here we mean the continuum percolation through the high-conducting phase σ_1.) Indeed, below the threshold σ^* *should* tend to zero at $\sigma_2\to 0$, whatever be σ_1, while above the threshold σ^* *should* tend to infinity even at $\sigma_2=0$. Thus, for isotropic random mixtures in two dimensions, the critical fraction of volume (percolation threshold) equals $\frac{1}{2}$, the same value as in the potential continuum percolation with a sign-symmetric potential (see Sec. II.E).

It is noteworthy that for any σ_1 and σ_2 the symmetry leading to Eq. (4.122) extends to the equipartition of Ohmic dissipation in phases I and II (Dykhne, 1970a):

$$\frac{1}{\sigma_1}\langle\mathbf{j}^2(\mathbf{x})\rangle_{\mathrm{I}}=\frac{1}{\sigma_2}\langle\mathbf{j}^2(\mathbf{x})\rangle_{\mathrm{II}}=\frac{\mathbf{J}^2}{\sigma^*}\ . \tag{4.123}$$

The method of reciprocal media can be also used for the calculation of the impedance of a uniform, symmetrical, finite-size conducting sample in a magnetic field, taking into account boundary effects, where the reciprocal sample has a different geometry of electrodes (Isichenko and Kalda, 1992).

There exists no universal formula for the effective conductivity of a material with an unequal amount of randomly distributed phases or with more than two phases, because the information about the volume fractions and the conductivities of the phases is not enough to determine the effective conductivity. The result will also depend on the spatial distribution of phases. Specifically, the conductivity behavior near the percolation threshold may depend crucially on the presence of long-range correlations in the distribution. In addition, the percolation conductivity exponent μ [see Eq. (2.10)] is not exactly known even for the uncorrelated lattice model. Schulgasser (1976) showed the nonexistence of a Keller-Dykhne–type theorem in three dimensions. Instead, using the classical variational principle (cf. Dykhne, 1967) that the electric current distribution minimizes the integral Ohmic heat under appropriate constraints, Schulgasser established the inequality

$$\sigma^*_{xx}(\sigma_1,\sigma_2)\sigma^*_{yy}(\sigma_2,\sigma_1)\geq\sigma_1\sigma_2\ , \tag{4.124}$$

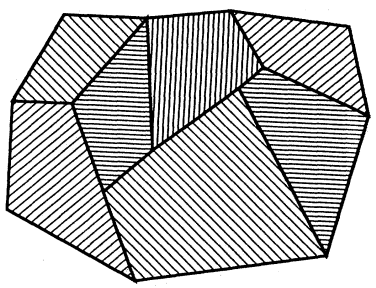

FIG. 36. Schematic of a polycrystal. The hatches indicate the principal axes of the crystallites' conductivity tensors.

which is valid for arbitrary 3D two-phase composites and becomes an equality only in two dimensions. Some other inequalities were obtained by Bergman (1978), Milton (1982), and Golden and Papanicolaou (1983), where the analytical continuation of $\hat{\sigma}^*/\sigma_1$, considered as a function of σ_1/σ_2, was used.

2. Systems with inhomogeneous anisotropy

a. Polycrystals

Another classical example of a heterogeneous medium is a polycrystal consisting of multiple grains (crystallites) of an identical anisotropic material with random orientations (Fig. 36). The importance of the problem of electrical and heat conduction in such media is emphasized by the fact that all metals are typically polycrystals.

In two dimensions, effective conductivity of a macroscopically isotropic polycrystal is also amenable to the Keller-Dykhne approach. Let σ_1 and σ_2 be the principal values of the microscopic conductivity tensor

$$\hat{\sigma}(\mathbf{x})=\hat{\theta}(\mathbf{x})\begin{bmatrix}\sigma_1 & 0\\ 0 & \sigma_2\end{bmatrix}\hat{\theta}^{-1}(\mathbf{x}) , \tag{4.125}$$

where $\hat{\theta}(\mathbf{x})$ is the rotation matrix through the angle $\theta(\mathbf{x})$, which varies from one crystallite to another. Again introducing the primed fields (4.114), we obtain the reciprocal Ohm's law with a new conductivity, as shown in Eq. (4.116). Upon using formula (4.125) and taking into account the commutivity of the rotation matrices $\hat{\mathbf{R}}$ and $\hat{\theta}$, we find

$$\hat{\sigma}'(\mathbf{x})=\frac{1}{\sigma_*^2}\hat{\theta}(\mathbf{x})\begin{bmatrix}\sigma_2 & 0\\ 0 & \sigma_1\end{bmatrix}\hat{\theta}^{-1}(\mathbf{x}) . \tag{4.126}$$

Under the choice of $\sigma_*^2=\sigma_1\sigma_2$, $\hat{\sigma}'(\mathbf{x})$ becomes identically equal to $\hat{\sigma}(\mathbf{x})$. Hence, for the effective conductivity $\hat{\sigma}^*(\sigma_1,\sigma_2)$ of the considered system, instead of Eq. (4.113) the reciprocity relation reads

$$\sigma_{xx}^*(\sigma_1,\sigma_2)\sigma_{yy}^*(\sigma_1,\sigma_2)=\sigma_1\sigma_2 , \tag{4.127}$$

where x and y are the principal axes of $\hat{\sigma}^*$. Thus, for a macroscopically isotropic 2D polycrystal, formula (4.122) yields an exact result (Dykhne, 1970a). Unlike the case of a two-phase system, the polycrystal result does not require the equipartition of phases (which is quite a strong limitation on the two-phase result), since both principal axes, σ_1 and σ_2, are naturally equally represented in each crystallite. A similar method applies to two-dimensional ferrimagnets (Bouchaud and Zerah, 1989).

To understand the meaning of the Dykhne formula (4.122), it is instructive to consider extreme anisotropy, $\sigma_1 \gg \sigma_2$ (Dreizin and Dykhne, 1983). The current in a resistive medium is known to be distributed so as to minimize the Ohmic dissipation. Hence, to first approximation, the current flows along the local direction of high conductivity σ_1. Hence we are led to study the typical pattern of "lines of force" in a general compressible field. This question has been addressed in the qualitative theory of ordinary differential equations, which was developed in order to understand the nature of turbulence (Ruelle and Takens, 1971; Lanford, 1981). In two dimensions, the geometry of *generic* compressible fields is quite simple, with the inventory of invariant sets being reduced to merely fixed points (stable and unstable foci and saddles) and limit cycles. Each line of force (the line of electrical current in our case) runs several characteristic scales (the crystalline size λ_0) and terminates in a trap formed by a focus [Fig. 37(a)] or a limit cycle [Fig. 37(b)]. Hence in the limit $\sigma_2=0$ there is no macroscopic conductivity in the system. To escape the traps, the current is forced to flow across the well-conducting lines, engaging the finite conductivity σ_2. To make the dissipation smaller, this is done close enough to the trap. Denote by l_1 the characteristic length and by l_2 the characteristic width of the bundle of high-conductivity lines near a focus where the main resistance r occurs. Then r can be estimated as the sum of the resistances of the high-conductivity path (along the bundle) and of the low-conductivity path (across the bundle):

$$r=\frac{1}{\sigma_1}\frac{l_1}{l_2}+\frac{1}{\sigma_2}\frac{l_2}{l_1} . \tag{4.128}$$

Equation (4.128) is minimized at $l_1/l_2\simeq(\sigma_1/\sigma_2)^{1/2}$, where it takes on the value $r_{\min}\simeq(\sigma_1\sigma_2)^{-1/2}$. Thus the conducting properties of the polycrystal can be represented by an equivalent network of resistors with the characteristic resistivity $r_{\min}$ connected by well-conducting (σ_1) wires. This network is similar to the field shown in Fig. 30. Such a network has the macro-

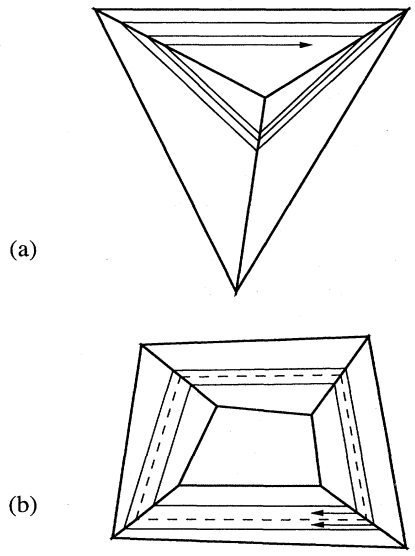

FIG. 37. Electric current streamlines in a strongly anisotropic polycrystal. These streamlines terminate in two types of traps: a focus (a) and a limit cycle (b).

scopic conductivity of order $(\sigma_1\sigma_2)^{1/2}$, in accordance with the exact result (4.122). The above argument also shows that the main Ohmic dissipation occurs in the traps occupying a small fraction of area, of order $(\sigma_2/\sigma_1)^{1/2} \ll 1$.

For three-dimensional polycrystals, no exact results are known. A set of rigorous inequalities on the effective conductivity $\hat{\sigma}^*$ were obtained by Hashin and Shtrikman (1963), Schulgasser (1982), and Avellaneda *et al.* (1988). The scaling behavior of σ^* for the case of a strong anisotropy can be predicted by a qualitative theory (Dreizin and Dykhne, 1983; Dykhne *et al.*, 1991).

Let $\sigma_1 \gg \sigma_2 \gg \sigma_3$ be the principal values of the microscopic conductivity tensor. Then the high-conductivity (σ_1) lines terminate in several types of traps. In addition to (1) foci[6] and (2) limit cycles, a generic 3D compressible vector field possesses (3) doubly periodic orbits (invariant tori) and (4) chaotic, or "strange," attractors (Lanford, 1981; Ruelle, 1989). Such a name is given to fractal attracting sets of low-dimensional non-Hamiltonian dynamical systems that exhibit exponentiation of close orbits and are characterized by finite size but zero volume in the configuration space. Along with foci, limit cycles, and irrationally wound tori, strange attractors represent a typical attracting set of a 3D vector field. The fractal dimension of an attractor, as given by formula (1.18), is not universal as the Lyapunov exponents Λ_1 and Λ_3 change from one attractor to another, being everywhere of order λ_0^{-1} (reciprocal crystallite size) and thereby introducing a peculiar "multifractality" of the problem.

It is easy to see that the conductance of all regular attractors is proportional to $(\sigma_1\sigma_2)^{1/2}$, similarly to the two-dimensional case. Due to the presence of both shrinking ($\Lambda_1 > 0$) and stretching ($\Lambda_3 < 0$) directions, the conductance of a "strange trap" turns out to be much larger (Fig. 38). Using the usual rule for series and parallel connections, the resistance of a strange attractor can be estimated similarly to Eq. (4.128), that is, by minimizing the equation

$$r(l)=\frac{1}{\sigma_1}\int_0^l \frac{dl'}{l_1(l')l_3(l')}+\left[\sigma_2\int_0^l \frac{l_1(l')dl'}{l_3(l')}\right]^{-1}, \tag{4.129}$$

where l is the distance along the high-conductivity (σ_1) axes, the subscripts of $l_i(l)\simeq\lambda_0\exp(\Lambda_i l)$ correspond to the ordering of the Lyapunov exponents

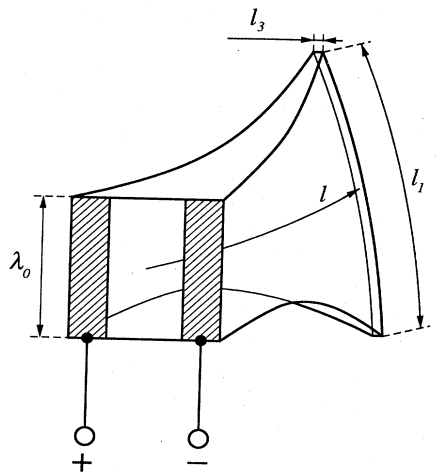

FIG. 38. A bundle of high-conductivity lines in a polycrystal, which looks like an axe, due to the exponential divergence in one direction (l_1) and the exponential compression in the other (l_3). For simplicity the axe is shown smooth. As the distance l is increased, the Dykhne's axe swings into a fractal set (strange attractor). The conductance of the attractor is defined as the conductance between the two hatched plates on the butt.

($\Lambda_1 > \Lambda_2 = 0 > \Lambda_3$), and the fact is used that, generically, the projection of the σ_2 conductivity axis onto the shrinking direction (l_3) is not zero. Equation (4.129) is minimized by $l = l^* \simeq (1/|2\Lambda_3|)\log(\sigma_1/\sigma_2)$, which results in the conductivity of the attractor scaling as

$$\sigma_D^* \equiv [\lambda_0 r(l^*)]^{-1} \simeq \sigma_1 \left[\frac{\sigma_2}{\sigma_1}\right]^{(\Lambda_1+\Lambda_3)/\Lambda_3}. \tag{4.130}$$

Upon using formula (1.18) for the fractal dimension D of the attractor, (4.130) can be rewritten as (Dykhne, 1986)

$$\sigma_D^* \simeq \sigma_1^{(D-1)/2}\sigma_2^{(3-D)/2}. \tag{4.131}$$

For the limiting case of a regular attractor, such as an invariant torus ($D = 2$), (4.131) is reduced to the geometric mean of σ_1 and σ_2.

So the equivalent network of a 3D polycrystal includes a countable number of resistors-attractors of several kinds with a broad distribution of resistances. Due to the inequality $2 < D < 3$, the conductivity of a strange attractor (4.131) is much larger than that of a focus, a limit cycle, or a torus ($\simeq \sigma_1^{1/2}\sigma_2^{1/2}$). Thus whether or not the equivalent network of a generic polycrystalline configuration admits percolation through higher-conductivity (strange attractor) traps depends on the value of a pure number. Preliminary numerical results (Dykhne *et al.*, 1991) indicate that the concentration of such traps is well below the percolation threshold, so that foci and other regular attractors are likely to be responsible for the asymptotics of the effective conductivity, which thus scales similarly to the two-dimensional case, $\sigma^* \simeq (\sigma_1\sigma_2)^{1/2}$. In both two and three dimensions, the mixing length ξ_m is of order the crystallite size λ_0.

[6]Discontinuities of the vector field of high-conductivity directions in a polycrystal (on the faces between crystallites) introduce certain peculiarities to the appearance of attracting sets that apparently do not change the conclusions of this qualitative theory. For example, the foci in a continuous system may become attracting segments (lying on the edges between crystallites) in a discontinuous system.

b. Plasma heat conduction in a stochastic magnetic field

While being somewhat artificial, the problem of conductance in a strongly anisotropic polycrystal invokes the geometry of generic (random, in particular) compressible fields in a rather instructive manner. The approximation of highly anisotropic transport, however, is quite natural for the heat conduction in a magnetized high-temperature plasma, where the longitudinal [with respect to the magnetic field $\mathbf{B}(\mathbf{x})$] heat conductivity $\chi_\parallel$ can exceed the transverse conductivity $\chi_\perp$ by many orders of magnitude (cf. White, 1989).

The idea of magnetic confinement fusion is to organize the geometry of the magnetic field (e.g., nested toroidal magnetic surfaces) in such a way that $\chi_\perp$ controls the heat losses from plasma. In reality, however, there may arise irregularities of $\mathbf{B}(\mathbf{x})$, which, due to the triggering of the large longitudinal conductivity $\chi_\parallel$, can significantly increase the effective heat conductivity $\chi_\perp^*$ across the unperturbed magnetic field (Rosenbluth *et al.*, 1966; Krommes, 1978; Rechester and Rosenbluth, 1978; Kadomtsev and Pogutse, 1979). In the approximation of frequent collisions, the problem of the effective heat conductivity belongs to the same category as polycrystals, with $\sigma_1=\chi_\parallel$, $\sigma_2=\sigma_3=\chi_\perp$. The difference is that the high-conduction lines in a magnetized plasma are the magnetic-field lines, which are incompressible [$\nabla\cdot\mathbf{B}(\mathbf{x})=0$] and hence cannot terminate in traps.

In a two-dimensional magnetic field, $\mathbf{B}(\mathbf{x})=\nabla\psi(x,y)\times\hat{\mathbf{z}}$, the reciprocity theorem (4.127) is still valid, since in its proof nothing was assumed about the type of the local anisotropy field $\mathbf{B}(\mathbf{x})$. Hence in the macroscopically isotropic case the effective heat conductivity is given by (Kadomtsev and Pogutse, 1979).

$$\chi^*=(\chi_\parallel\chi_\perp)^{1/2} . \tag{4.132}$$

Although having the same scaling as the conductivity of a 2D polycrystal, Eq. (4.132) originates from quite a different heat conduction pattern (Isichenko, 1991b). Consider the case of a random 2D magnetic field with the monoscale (λ_0) flux potential $\psi(x,y)$. Since the magnetic lines [contours of $\psi(x,y)$] are not trapped, one can expect a significant role to be played by extended magnetic lines, so that the mixing length ξ_m is much greater than the characteristic scale λ_0. To establish the transition to the effective heat conduction, it is more convenient to argue in terms of the diffusion of "caloric" (the heat substance), whose particles diffuse with the diffusivity $\chi_\parallel$ along the magnetic lines and with the diffusivity $\chi_\perp$ across them. The mixing length ξ_m can be estimated as the size of a cell formed by magnetic lines, such that a caloric particle is decorrelated from it in the time of the longitudinal diffusion:

$$\tau_m=\frac{w^2(\xi_m)}{\chi_\perp}=\frac{L^2(\xi_m)}{\chi_\parallel} , \tag{4.133}$$

where $w(\xi_m)$ and $L(\xi_m)$ denote the width and the length of the bundle of magnetic lines with diameters of the order of ξ_m. Using formulas (3.43) and (3.45), we find from (4.133)

$$\xi_m=\lambda_0\left[\frac{\chi_\parallel}{\chi_\perp}\right]^{1/2(d_h+1/\nu)}=\lambda_0\left[\frac{\chi_\parallel}{\chi_\perp}\right]^{1/5}\gg\lambda_0 . \tag{4.134}$$

The effective heat conductivity can be estimated in a "diffusive manner" as follows:

$$\chi^*\simeq F(\xi_m)\frac{\xi_m^2}{\tau_m} , \tag{4.135}$$

where $F(\xi_m)=L(\xi_m)w(\xi_m)\xi_m^{-2}$ is the fraction of area covered by the ξ_m cells where most of the transport takes place. Upon taking into account Eq. (4.133), one reduces formula (4.135) to Eq. (4.132) without regard to the specific topography of the magnetic field.

For the case in which a strong background magnetic field $\mathbf{B}_0=B_0\hat{\mathbf{z}}$ is present, the result (4.132) is modified by the substitution $\chi_\parallel\to\chi_\parallel(\delta B/B_0)^2$, which is simply a projection of the longitudinal conductivity onto the (x,y) plane, where $\delta\mathbf{B}=\nabla\psi(x,y)\times\hat{\mathbf{z}}$ is a 2D magnetic fluctuation (Kadomtsev and Pogutse, 1979):

$$\chi_\perp^*\simeq\frac{\delta B}{B_0}(\chi_\perp\chi_\parallel)^{1/2} ,\qquad \chi_\parallel\left[\frac{\delta B}{B_0}\right]^2>\chi_\perp . \tag{4.136}$$

In a more realistic model of a general three-dimensional magnetic perturbation, $\mathbf{B}(\mathbf{x})=B_0\hat{\mathbf{z}}+\delta\mathbf{B}(x,y,z)$, the magnetic lines undergo stochastic exponentiation. Indeed, the equation of a magnetic line,

$$\frac{d\mathbf{x}_\perp}{dz}=\frac{\delta\mathbf{B}_\perp(\mathbf{x}_\perp,z)}{B_0} , \tag{4.137}$$

is similar to that of a particle orbit in a nearly incompressible, 2D, time-dependent flow if the coordinate z is treated as time. Note that, in the absence of appreciable longitudinal perturbation $\delta B_\parallel$, the considered magnetic field is nothing but the extended phase space of a 2D flow, as represented by Eq. (4.47). In the quasilinear limit, corresponding to the high-frequency limit of passive advection, the Kolmogorov exponentiation length $l_K\equiv K^{-1}$ is given by formula (4.49). In terms of the magnetic field, this results in

$$l_K\simeq\lambda_\parallel\cdot R^{-2},\quad R\equiv\frac{\delta B}{B_0}\frac{\lambda_\parallel}{\lambda_\perp}\ll 1 , \tag{4.138}$$

where $\lambda_\parallel$ and $\lambda_\perp$ denote the characteristic scales of $\delta\mathbf{B}(\mathbf{x}_\perp,z)$ along and across the background magnetic field, respectively. The exponentiation of magnetic lines leads to a convoluted geometry of magnetic-flux tubes (Fig. 39).

To estimate the effective heat conductivity in a stochastic magnetic field, we again argue in terms of diffusion. A "caloric" particle can be believed to have

decorrelated from a given magnetic line when the particle leaves a magnetic-flux tube encompassing this line, with the initial radius $\lambda_\perp$. At sufficiently small transverse diffusivity $\chi_\perp$, this is easier to do by first longitudinally diffusing to a distance z of several exponentiation lengths l_K, where the magnetic tube becomes strongly convoluted, then undertaking a short transverse diffusion to a distance

$$w(z)\simeq\lambda_\perp\exp\left[-\frac{|z|}{l_K}\right], \tag{4.139}$$

which is the characteristic width of the flux tube wall (Fig. 39). The optimum value of $z=l_m$ (the longitudinal mixing length) is obtained from the comparison of longitudinal and transverse diffusion times:

$$\tau_m=\frac{l_m^2}{\chi_\parallel}=\frac{w^2(l_m)}{\chi_\perp}. \tag{4.140}$$

Upon substituting Eq. (4.139) into (4.140), we find

$$l_m\simeq l_K\log\left[\frac{\chi_\parallel}{\chi_\perp}\frac{\lambda_\perp^2}{l_K^2}\right]. \tag{4.141}$$

This result is valid if the expression under logarithm is large.

During the decorrelation time τ_m, the transverse particle displacement ξ_m is given by the diffusion of magnetic lines, $\xi_m\simeq(D_m l_m)^{1/2}$, where

$$D_m\simeq\lambda_\parallel\left[\frac{\delta B}{B_0}\right]^2 \tag{4.142}$$

is the quasilinear diffusivity of magnetic lines [compare with Eq. (4.64)]. Finally, the effective cross-field heat conductivity is given by the formula (Rechester and Rosenbluth, 1978; Kadomtsev and Pogutse, 1979)

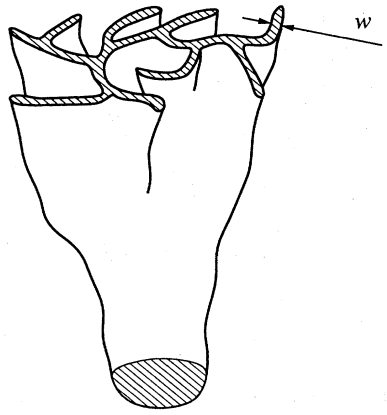

FIG. 39. Magnetic-flux tube in a magnetic field with a 3D random component. The tube is convoluted due to the exponentiation of neighboring magnetic lines. Because of the magnetic-flux conservation within the tube, the exponentiation of the lines leads to exponentially decreasing thickness w of the flux tube wall.

$$\chi^*\simeq\frac{\xi_m^2}{\tau_m}=\chi_\parallel\frac{D_m}{l_m}=\chi_\parallel\frac{D_m}{l_K}\log^{-1}\left[\frac{\chi_\parallel}{\chi_\perp}\frac{\lambda_\perp^2}{l_K^2}\right]. \tag{4.143}$$

In the case of stronger magnetic perturbations,

$$R\equiv\frac{\delta B}{B_0}\frac{\lambda_\parallel}{\lambda_\perp}\gg 1,$$

the magnetic line diffusivity is given by the percolation scaling (4.69),

$$D_m\simeq\lambda_\perp\frac{\delta B}{B_0}R^{-1/(vd_h+1)}\propto\left[\frac{\delta B}{B_0}\right]^{7/10}, \tag{4.144}$$

and there are several regimes of the effective heat conductivity (Isichenko, 1991b), one of which reduces to the Kadomtsev-Pogutse regime (4.136) in the 2D limit $R\to\infty$.

3. Magnetoresistance of inhomogeneous media with the Hall effect

Thus far we have been concerned with conductance in media that were either microscopically isotropic (Sec. IV.B.1) or anisotropic with a symmetric conductivity tensor (Sec. IV.B.2). Here we consider inhomogeneous anisotropic media with fixed direction of anisotropy (given, for example, by an external magnetic field), but with a conductivity tensor having an essential antisymmetric part $\hat{\sigma}^a$ associated with the Hall effect (called the Righi-Leduc effect in the case of thermal conduction):

$$\sigma_{ij}(\mathbf{x})=\sigma_{ij}^s(\mathbf{x})+\sigma_{ij}^a(\mathbf{x}), \tag{4.145}$$

where $\sigma_{ij}^s=\sigma_{ji}^s$ and $\sigma_{ji}^a=-\sigma_{ji}^a$. The simplest form of Ohm's law in such media can be written as

$$\mathbf{j}+\mathbf{j}\times\boldsymbol{\beta}(\mathbf{x})=\sigma_0(\mathbf{x})\mathbf{e}, \tag{4.146}$$

where $\boldsymbol{\beta}(\mathbf{x})=\beta(\mathbf{x})\hat{\mathbf{z}}$ is the Hall parameter proportional to the external magnetic field $\mathbf{B}$. The conductivity tensor corresponding to (4.146) is

$$\hat{\sigma}(\mathbf{x})=\frac{\sigma_0(\mathbf{x})}{1+\beta^2(\mathbf{x})}\begin{bmatrix}1 & -\beta(\mathbf{x}) & 0\\ \beta(\mathbf{x}) & 1 & 0\\ 0 & 0 & 1+\beta^2(\mathbf{x})\end{bmatrix}. \tag{4.147}$$

This tensor is a good model of conductance in noncompensated metals and semiconductors (Lifshitz and Pitaevskii, 1981) and in pulsed plasmas (Kingsep *et al.*, 1990). Heat conduction in a magnetic field is described by a law mathematically equivalent to (4.146), with $\mathbf{j}$ understood as the heat flux and $\mathbf{E}$ as the minus temperature gradient $-\nabla T$ (Braginskii, 1965). In both cases of electrical and heat conductivity, the Hall (or Righi-Leduc) parameter is given by $\beta=\omega_B\tau$, where ω_B is the electron gyrofrequency and τ the collision time.

In this section we discuss two different methods of calculating the effective electrical or heat conductivity on the example of Ohm's law (4.146).

a. The method of reciprocal media

This approach, which is restricted to a two-dimensional, two-phase system, is based on generalized Keller-Dykhne reciprocity relations (Dykhne, 1970b; Balagurov, 1978, 1986; Bozhokin and Bykov, 1990).

Let the parameters $\sigma_0(\mathbf{x})$ and $\beta(\mathbf{x})$ in the conductivity tensor (4.147) fluctuate, each taking on only two values, σ_1 and σ_2 [for $\sigma_0(\mathbf{x})$] and β_1 and β_2 [for $\beta(\mathbf{x})$], in phases I and II, respectively. The idea of the approach (Dykhne, 1970b) is to use linear transformations from $\mathbf{j}$ and $\mathbf{e}$ to new fields $\mathbf{j}'$ and $\mathbf{e}'$ such that the macroscopic properties of the new system are equivalent to those of the original system. In the presence of the Hall effect, one such transformation is not sufficient for calculating the effective conductivity tensor. However, there exist two independent linear transformations satisfying the desired conditions. Of course, the result can be achieved only for a statistically equivalent and isotropic distribution of phases I and II. Dykhne (1970b) considered the case in which only $\sigma_0(\mathbf{x})$ fluctuates ($\sigma_1 \neq \sigma_2$, $\beta_1 = \beta_2$). Balagurov (1978) generalized the result for the more general case $\beta_1 \neq \beta_2$. The effective conductivity tensor $\hat{\sigma}^*$ can be written similarly to Eq. (4.147) with the substitution $\sigma_0(\mathbf{x}) \to \sigma_0^*$, $\beta(\mathbf{x}) \to \beta^*$, where

$$\sigma_0^* = \left[\frac{\sigma_1 \sigma_2}{1 + (\sigma_1 \beta_2 - \sigma_2 \beta_1)^2 / (\sigma_1 + \sigma_2)^2} \right]^{1/2} , \tag{4.148}$$

$$\beta^* = \sigma_0^* \frac{\beta_1 + \beta_2}{\sigma_1 + \sigma_2} . \tag{4.149}$$

In the absence of a magnetic field ($\beta_1 = \beta_2 = 0$), formula (4.148) reproduces result (4.122).

In the limit of a strong magnetic field ($\beta \equiv (|\beta_1| + |\beta_2|)/2 \gg 1$) and strong fluctuations of the Hall conductance [$\beta\Delta \equiv |\sigma_1 \beta_2 - \sigma_2 \beta_1| / (\sigma_1 + \sigma_2) \gg 1$], the effective conductivity (4.148) becomes anomalously low:

$$\sigma_0^* \simeq \sigma_0 (\beta\Delta)^{-1} . \tag{4.150}$$

This anomalous resistance is caused by the strongly nonuniform flow of electric current in the presence of the fluctuations. The linear dependence of the transverse magnetoresistance $\rho^*(B) \equiv 1/\sigma_0^*(B) \propto B$ on the external magnetic field $\mathbf{B}$ ($\beta \propto B$) is not an exceptional property of the exact solution (4.148). Such behavior extends to generic 3D *sharp* inhomogeneities of the medium, such as voids or cracks (Herring, 1960; Pippard, 1989). A similar magnetoresistance behavior can also result from the effect of the sample boundaries (Rendell and Girvin, 1981; Chukbar and Yankov, 1988). It is interesting that in the first measurements of the magnetoresistance in metals in strong magnetic field (Kapitza, 1928, 1929) a linear dependence $\rho^*(B) \propto B$ was observed even for monocrystalline samples. Such a pronounced effect was not reproduced in later experiments (for a review, see Pippard, 1989). The polycrystalline structure of metals would lead either to the saturation of the transverse magnetoresistance $\rho^*(B)$ or to its growth as $B^{2/3}$, $B^{4/3}$, or B^2, depending on the topology of the metal Fermi surface (Dreizin and Dykhne, 1972; Stachowiak, 1978). The explanation (Isichenko and Kalda, 1992) of the linear Kapitza law $\rho^*(B) \propto B$ is that in Kapitza's experiments (unlike later ones) no separate potential leads were used and both the potential and power leads were (improperly) brought from the same electrodes, thus introducing the boundary effect of a sharp interface. A similar linear magnetoresistance is well known in the quantum Hall effect (Rendell and Girvin, 1981) and in the electron magnetohydrodynamics of pulsed plasmas, where Kingsep, Chukbar, and Yankov (1990) call it the "electron MHD resistance."

As shown in the next section, in the case of smooth inhomogeneities the behavior of the magnetoresistance is different.

b. Determination of effective conductivity using an advection-diffusion analogy

A noticeable feature of conducting media with the Hall effect is that the conductivity processes are related to the advection-diffusion transport in an incompressible steady flow, which is amenable to a more or less clear qualitative analysis. The correspondence between the two problems (Dreizin and Dykhne, 1972; Dykhne, 1984) follows from the microscopic Ohm's law, $\mathbf{j}(x) = \hat{\sigma}(\mathbf{x})\mathbf{e}(\mathbf{x})$, $\mathbf{e}(\mathbf{x}) = -\nabla\phi(\mathbf{x})$, and the requirement that the current density $\mathbf{j}(\mathbf{x})$ be divergence-free:

$$\frac{\partial}{\partial x_i} \sigma_{ij}(\mathbf{x}) \frac{\partial \phi}{\partial x_j} = 0 . \tag{4.151}$$

Upon substituting Eq. (4.145) into (4.151), we obtain

$$\mathbf{v}\nabla\phi = \nabla(\hat{\sigma}^s \nabla\phi) , \tag{4.152}$$

where

$$v_i(\mathbf{x}) = \frac{\partial \sigma_{ij}^a(\mathbf{x})}{\partial x_j} \tag{4.153}$$

is an incompressible ($\nabla \cdot \mathbf{v} = \nabla_i \nabla_j \sigma_{ij}^a = 0$) field. Equation (4.152) can be thought of as describing the steady distribution of a tracer, with the density ϕ advected by the velocity field $\mathbf{v}(\mathbf{x})$ and subject to the molecular diffusion $\hat{\sigma}^s(\mathbf{x})$ (anisotropic, perhaps). Notice that the vector potential $\boldsymbol{\psi}(\mathbf{x})$ of the incompressible flow $\mathbf{v}(\mathbf{x})$ is given by

$$\psi_i = \tfrac{1}{2} \varepsilon_{ijk} \sigma_{jk}^a , \quad \sigma_{ij}^a = \varepsilon_{ijk} \psi_k , \tag{4.154}$$

where ε_{ijk} is the Levi-Cività tensor. For bounded perturbations in the antisymmetric conductivity $\hat{\sigma}^a(\mathbf{x})$ the vector potential $\boldsymbol{\psi}(\mathbf{x})$ is also bounded, leading to the existence of a finite effective diffusivity $\hat{D}^*$ (see Sec. IV.A.1). In terms of a steady tracer distribution, this means that the average flux is proportional to the average density gradient:

$$\langle \mathbf{v}\phi - \hat{\sigma}^s \nabla\phi \rangle = -\hat{D}^* \langle \nabla\phi \rangle , \tag{4.155}$$

where the angular brackets denote a spatial average over scales much larger than a certain mixing scale ξ_m. Upon integrating the left-hand side of Eq. (4.155) by parts, one finds

$$\langle \hat{\sigma} \nabla \phi \rangle = \hat{D}^* \langle \nabla \phi \rangle + \langle \psi \rangle \times \langle \nabla \phi \rangle \ . \tag{4.156}$$

Since the left-hand side of Eq. (4.156) is the average current density, we recover the average Ohm's law with the effective conductivity tensor (Dreizin and Dykhne, 1972)

$$\hat{\sigma}^* = \hat{D}^* + \langle \hat{\sigma}^a(\mathbf{x}) \rangle \ . \tag{4.157}$$

Thus, if one is able to determine the effective diffusivity $\hat{D}^*$ in the flow (4.153) with the molecular diffusivity $\hat{\sigma}^s$, formula (4.157) yields the result for the effective conductivity of the inhomogeneous medium with the Hall effect.

Let us first identify the implications of the exact results (4.148) and (4.149) for a two-phase system in terms of the advection-diffusion analogy (4.152)–(4.157). To do so, put $\sigma_1 = \sigma_2 = \sigma_0$ and $\beta_1 = -\beta_2 = \beta_0$. Then the symmetric part of tensor (4.147) becomes homogeneous, corresponding to the "molecular diffusivity" in the (x,y) plane

$$D_0 = \frac{\sigma_0}{1+\beta_0^2} \ , \tag{4.158}$$

and the flow (4.153) becomes two-dimensional with the stream function

$$\psi(x,y) = \begin{cases} -\psi_0, & \text{in I} \ , \\ \psi_0, & \text{in II} \ , \end{cases} \tag{4.159}$$

where

$$\psi_0 = \frac{\sigma_0 \beta_0}{1+\beta_0^2} \ . \tag{4.160}$$

According to Eq. (4.148), the effective conductivity, or the diffusivity in the flow (4.158), is equal to

$$\sigma^* = D^* = \sigma_0 (1+\beta_0^2)^{-1/2} = (D_0^2 + \psi_0^2)^{1/2} \ . \tag{4.161}$$

Thus one concludes (Dykhne, 1981; Tatarinova, 1990) that the "Pythagorean formula" (4.161) exactly describes effective diffusivity in the isotropic system (4.33) of narrow jets separating statistically equivalent regions I and II. For results (4.148), (4.149), and (4.161) to be valid, the width w of the jets (in the advection-diffusion system) or of the transition layer between phases I and II must be small not only in comparison with the characteristic inhomogeneity scale λ_0, but also in comparison with the width of a diffusive boundary layer: $w \ll (D_0 \lambda_0 / v_0)^{1/2}$, where $v_0 = \psi_0 / w$ is the characteristic velocity in the jets. Hence we obtain $w \ll \lambda_0 / P_0$, where $P_0 = \psi_0 / D_0 = \beta\Delta \gg 1$ is the Péclet number.

More naturally, the advection-diffusion analogy serves in the opposite direction, namely, as a means of calculating the effective conductivity of a Hall medium using the presumably known effective diffusivity in a corresponding velocity field (Dreizin and Dykhne, 1972; Isichenko and Kalda, 1991a). In the case of monoscale isotropic 3D fluctuations of the off-diagonal conductivity $\sigma_{xy}(x,y,z)$ with the correlation length λ_0, one has the velocity field (4.153),

$$\mathbf{v}(\mathbf{x}) = -\nabla \sigma_{xy}(x,y,z) \times \hat{\mathbf{z}} \ , \tag{4.162}$$

representing a two-dimensional incompressible random flow in each plane $z = \text{const}$, with the stream function $\psi(x,y,z) = -\sigma_{xy}$ varying smoothly with z. The characteristic velocity in the flow is $v_0 \Delta / (\beta \lambda_0)$, where σ_0 and $\beta \gg 1$ are the average values of $\sigma_0(\mathbf{x})$ and $\beta(\mathbf{x})$, respectively, and Δ is the relative fluctuation amplitude of $\sigma_{xy} = \sigma_0(\mathbf{x}) / \beta(\mathbf{x})$. The "molecular diffusivity" $\hat{\sigma}^s$ in this flow is anisotropic. At $\beta \gg 1$, the diffusivity in the (x,y) plane ($\sigma_{xx} = \sigma_{yy} = \sigma_0 \beta^{-2}$) is much smaller than that in the z direction ($\sigma_{zz} = \sigma_0$). If the fluctuations of σ_{xx} and σ_{zz} are not too large, they may be neglected in comparison with the effect of the fluctuations in the Hall conductivity σ_{xy}. In the considered case the long-range topography of the stream function $\psi(x,y,z)$ in a plane $z = \text{const}$ is irrelevant because the tracer particle diffuses over the correlation length λ_0 in the z direction long before the flow shows an inhomogeneity in the (x,y) plane: $v_0 \lambda_0^2 / \sigma_0 = \lambda_0 \Delta / \beta \ll \lambda_0$. This means that on the time scale[7] $t \gtrsim \lambda_0^2 / \sigma_0$, the velocity field can be replaced by a 3D shear flow $\mathbf{v} = \mathbf{v}_\perp(z)$ with randomly changed (on the correlation scale λ_0) direction of $\mathbf{v}_\perp$. For this situation, formula (4.76) predicts a superdiffusive particle displacement in the (x,y) plane,

$$x_\perp(t) \simeq v_0 \left[\frac{\lambda_0^2}{\sigma_0} \right]^{1/4} t^{3/4} \ , \tag{4.163}$$

while the effect of the transverse molecular diffusivity $\sigma_0 \beta^{-2}$ may be neglected. The superdiffusion (4.163) takes place until the transverse displacement $x_\perp(t)$ attains the correlation length λ_0; beyond this point, a crossover to effective diffusion occurs. Denote by t_c the crossover, or correlation time: $x_\perp(t_c) = \lambda_0$. Then the effective transverse diffusivity, and thereby the effective transverse conductivity, is estimated as

$$D_\perp^* = \sigma_\perp^* \equiv \frac{\sigma_0^*}{\beta^{*2}} \simeq \frac{x_\perp^2(t_c)}{t_c} \simeq \sigma_0 \left[\frac{\Delta}{\beta} \right]^{4/3} \ . \tag{4.164}$$

The effective Hall parameter β^* is then calculated by using formula (4.157): $\sigma_{xy}^* \equiv -\sigma_0^* / \beta^* = \langle \sigma_{xy}(\mathbf{x}) \rangle \simeq -\sigma_0 / \beta$; hence we have (Dreizin and Dykhne, 1972)

$$\sigma_0^* \simeq \sigma_0 (\beta \Delta^2)^{-2/3} \ , \tag{4.165}$$

$$\beta^* \simeq \beta^{1/3} \Delta^{-4/3} \ . \tag{4.166}$$

[7] In the employed advection-diffusion analogy the dimensionalities of v_0 and σ_0 are different from those of a velocity and a diffusivity. Only the final results expressed in terms of the effective conductivity will be dimensionally correct.

Formula (4.165) describes an anomalous resistance $\rho^*(B) \propto B^{2/3}$ growing with B slower than in the linear law (4.150). The difference between the two mechanisms of anomalous resistance lies in the geometry of the current streamlines in media with smooth and sharp inhomogeneities. In the case of sharp interfaces the main Ohmic dissipation occurs in the narrow boundary layers near the discontinuities of $\bar{\sigma}(\mathbf{x})$. For isotropic, smooth inhomogeneities, the anomalous resistance results from a long $[\xi_z = (\sigma_0 t_c)^{1/2} = \lambda_0 (\beta/\Delta)^{2/3} \gg \lambda_0]$ walk of current streamlines in the direction of the magnetic field (Fig. 40). In the general case of anisotropic fluctuations in the microscopic conductivity $\hat{\sigma}(\mathbf{x})$, both mechanisms of anomalous resistance (contraction in boundary layers and tangled walk of current streamlines) can coexist, leading to the fractal geometry of both individual current streamlines and the dissipation-containing region (Isichenko and Kalda, 1991a).

The extreme situation of a very strong anisotropy of fluctuations, corresponding to a two-dimensional geometry ($\partial/\partial z = 0$), can be realized in a magnetized plasma. Here, flow (4.162) becomes purely two dimensional, with the microdiffusivity $D_0 = \sigma_0 \beta^{-2}$. The Péclet number in this flow is estimated to be

$$P = \frac{\lambda_0 v_0}{D_0} = \beta\Delta \ . \tag{4.167}$$

For monoscale fluctuations of $\sigma_0(\mathbf{x})/\beta(\mathbf{x})$ with a sufficiently large amplitude, $\beta\Delta \gg 1$, the effective diffusivity, and thereby the conductivity, across the magnetic field is given by formula (4.36),

$$\sigma_\perp^* \equiv \frac{\sigma_0^*}{\beta^{*2}} \simeq D_0 P^{10/13} = \frac{\sigma_0}{\beta^2} (\beta\Delta)^{10/13} \ , \tag{4.168}$$

which corresponds to (Isichenko *et al.*, 1989)

$$\sigma_0^* \simeq \sigma_0 (\beta\Delta)^{-10/13} \ , \tag{4.169}$$

$$\beta^* \simeq \beta^{3/13} \Delta^{-10/13} \ . \tag{4.170}$$

The behavior of the conductivity (4.169) is intermediate between the case of sharp boundaries (4.150) and isotropic 3D fluctuations (4.165).

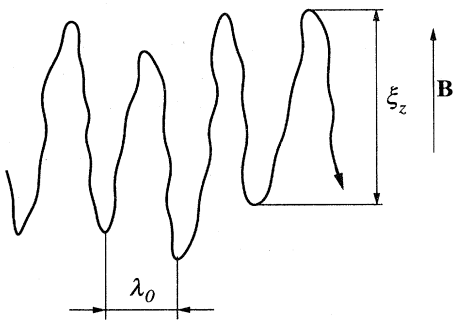

FIG. 40. Schematic of a current streamline corresponding to a steady flow of electric current across the magnetic field **B** in a conducting medium with three-dimensional fluctuations.

The inequality (4.20), specifying the allowed range of effective diffusivity in an advection-diffusion system, can be translated into bounds on the effective conductivity of an inhomogeneous medium with the Hall effect. Using the above notation, this results in the following inequalities:

$$C_1 \sigma_0 / (1 + \beta^2 \Delta^2) \le \sigma_0^* \le C_2 \sigma_0 \ , \tag{4.171}$$

$$C_3 \beta / (1 + \beta^2 \Delta^2) \le \beta^* \le C_4 \beta \ , \tag{4.172}$$

where the parameters C_i, accounting for moderate variation of the symmetric part of $\hat{\sigma}(\mathbf{x})$, are of the order of unity. For $\hat{\sigma}^s(\mathbf{x}) \equiv \text{const}$, all $C_i = 1$ and the bounds in (4.171) and (4.172) become exact. The limiting case of the anomalous resistance described by the left-hand side of inequality (4.171) is attained in the direction across layer-shaped inhomogeneities, $\sigma_{xy}(\mathbf{x}) = \sigma_{xy}(x)$ (Chukbar and Yankov, 1988).

C. Classical electrons in disordered potentials

In Sec. IV.B we were concerned with the transport properties of media with a characteristic inhomogeneity scale λ_0 much greater than the electron (or other transport carrier) mean free path l, that is, media where Ohm's law $\mathbf{j} = \hat{\sigma}(\mathbf{x})\mathbf{E}$ applies locally. In this subsection we briefly discuss the opposite limit where $\lambda_0 \ll l$, where the detailed electron kinetics must be dealt with. In this discussion we avoid the issue of the quantum behavior of electrons in disordered systems, a problem started by Anderson (1958) and having a tremendous literature by now.

A classical analog of the Anderson localization was pointed out by Ziman (1969, 1979), who presented a qualitative discussion of the electron motion in a classical potential $V(\mathbf{x}) = -e\phi(\mathbf{x})$. The equation of the motion

$$m \frac{d^2 \mathbf{x}}{dt^2} = -\nabla V(\mathbf{x}) \tag{4.173}$$

conserves the total energy $E(\mathbf{x}, \dot{\mathbf{x}}) = m\dot{\mathbf{x}}^2/2 + V(\mathbf{x})$. Here m denotes the (effective) mass of the electron. Due to the positiveness of the kinetic energy $m\dot{\mathbf{x}}^2/2$, the electron has to reside in a connected domain (cluster) determined by the inequality

$$V(\mathbf{x}) \le E \ . \tag{4.174}$$

The three-degrees-of-freedom motion (4.173) implies the six-dimensional phase space $(\mathbf{x}, \dot{\mathbf{x}})$ projected onto the five-dimensional isoenergetic manifold $E(\mathbf{x}, \dot{\mathbf{x}}) = \text{const}$. The generic five-dimensional Hamiltonian motion features chaotic behavior with Arnold diffusion (Chirikov, 1979; Lichtenberg and Lieberman, 1983). The latter arises because of the failure of possible 3D-invariant KAM tori to divide the 5D manifold into isolated chaotic regions, just as 1D curves do not divide the 3D space. Thus it is plausible that in a generic case the real-space domain (4.174) is not partitioned, other than by the natural condition of connectivity. Hence all of the cluster is visited by the electron quasiergodically.

The geometry of the cluster (4.174) depends on the appearance of the potential $V(\mathbf{x})$ and assumes a critical behavior at the continuum percolation threshold $E=E_c$ (Sec. II.E). Above this energy threshold, the electron can participate in macroscopic conductance. Without the application of an external electric field, the stochastic electron motion in the infinite cluster can be both superdiffusive (Bouchaud and Le Doussal, 1985) and normally diffusive (Bunimovich and Sinai, 1980, 1981), as suggested by the Sinai (1970) billiard example—that is, the Arnold diffusion in a wider sense may include nondiffusive random walks.

In the case of a time-dependent potential $V(\mathbf{x},t)$, the energy E is not conserved and no percolation threshold is present. For a Gaussian random potential $V(\mathbf{x},t)$ of $(d+1)$ arguments with exponentially decaying correlations, Golubović, Feng, and Zeng (1991) used the Martin, Siggia, and Rose (1974) formalism to derive the superdiffusive behavior

$$\langle \mathbf{x}^2(t)\rangle^{1/2} \propto \begin{cases} t^{6/5}, & d=1 , \\ t^{9/8}, & d>1 . \end{cases} \tag{4.175}$$

This author does not know how to "simply" explain the result (4.175).

In the presence of a strong magnetic field $\mathbf{B}=B\hat{\mathbf{z}}$—such that the Larmor radius $r_B=v_\perp/\omega_B$ (where $\omega_B=eB/mc$ is the electron cyclotron frequency) is much smaller than the potential correlation length λ_0—the electron motion becomes nearly one-dimensional along the magnetic-field lines. To next order in the expansion in the small parameter of $r_B/\lambda_0 \ll 1$, the drift motion of the electron guiding center is recovered. The $\mathbf{E}\times\mathbf{B}$ drift velocity is given by (Sivukhin, 1965)

$$\mathbf{v}_d \equiv \frac{d\mathbf{x}_\perp}{dt} = \frac{c}{eB}\nabla V(x,y,z)\times\hat{\mathbf{z}} , \tag{4.176}$$

which is also valid in the quantum case (Laughlin, 1981). Conservation of the transverse adiabatic invariant $\mu_\perp=v_\perp^2/B$ in a uniform magnetic field results in the invariance of the kinetic energy of the electron gyration, $E_\perp=mv_\perp^2/2$, and hence the conservation of the longitudinal energy $E_\parallel=mv_\parallel^2/2+V(x,y,z)$. The equation of longitudinal motion,

$$dz/dt=v_\parallel=\pm\sqrt{(2/m)[E_\parallel-V(x,y,z)]} , \tag{4.177}$$

can result either in passing motion (when $E_\parallel>\max V$) or in trapped oscillations between two turning points $z_{1,2}(x,y,E_\parallel)$, where $z_{1,2}$ are the solutions of the equation $V(x,y,z)=E_\parallel$.

The passing electron motion, which is typical in high-temperature plasmas, is reducible (see Sec. IV.A.5) to two-dimensional unsteady advection with a time-dependent stream function $\psi(x,y,t)=(c/Be)V(x,y,z(t))$, where $z(t)$ is the (monotonic) solution of Eq. (4.177). Thus for sufficiently large B the electron diffusivity always scales quasilinearly [Eq. (4.64)], $D^*\propto B^{-2}$. However, for the intermediate strengths of the magnetic field, the percolation scaling (4.69) is also possible (Isichenko and Horton, 1991):

$$D^*\simeq\psi_0\left[\frac{\omega\lambda_0^2}{\psi_0}\right]^{3/10}\propto B^{-7/10} , \tag{4.178}$$

where $\psi_0=[\psi(x,y,t)-\langle\psi(x,y,t)\rangle]_{\rm rms}$ and ω is the characteristic frequency of the variation of $\psi(x,y,t)$.

The trapped electron motion is typical for metals and semiconductors at low (helium) temperatures (Azbel, 1985; Azbel and Entin-Wohlman, 1985; Mehr and Aharony, 1988). The oscillatory behavior of $z(t)$ results in a qualitatively different behavior due to the conservation of the second, longitudinal adiabatic invariant (action)

$$\mu_\parallel(x,y,E_\parallel)=\sqrt{2m}\int_{z_1(x,y,E_\parallel)}^{z_2(x,y,E_\parallel)}\sqrt{E_\parallel-V(x,y,z)}\,dz . \tag{4.179}$$

The conservation of $\mu_\parallel$ can also be seen upon the averaging of the drift velocity (4.176) over a period of the longitudinal oscillations (Kadomtsev, 1958):

$$\langle\mathbf{v}_d\rangle=\frac{\int_{z_1}^{z_2}(\mathbf{v}_d/v_\parallel)dz}{\int_{z_1}^{z_2}(1/v_\parallel)dz}=\frac{1}{2m\omega_B}\frac{\nabla\mu_\parallel(x,y,E_\parallel)\times\hat{\mathbf{z}}}{\partial\mu_\parallel(x,y,E_\parallel)/\partial E_\parallel} . \tag{4.180}$$

Thus electron motion is characterized by three strongly different frequencies: the fastest motion ($\omega_1=\omega_B\propto B$) is the Larmor gyration, the intermediate one ($\omega_2\simeq\lambda_0/v_\parallel\propto B^0$) is the bouncing between the reflecting potential walls, and the slowest motion ($\omega_3\simeq v_d/\lambda_0\propto B^{-1}$) is the guiding-center drift.

The existence of the additional integral of motion $\mu_\parallel$ makes the averaged electron motion regular, that is, electrons are constrained to move on the cylinders of constant $\mu_\parallel(x,y,E_\parallel)$ propping up the isosurfaces of the potential $V(x,y,z)$ like pillars (Fig. 41). Thus the effective number of degrees of freedom is the same as in the two-dimensional case (Trugman, 1983). This observation led Azbel (1985) to suggest a new mechanism for magnetic localization of electrons in the bulk of an impure metal sample. The sample may be an insulator or a conductor, show the quantized Hall effect, or demonstrate edge conductivity, depending on $\mu_\perp$, $\mu_\parallel$, and $E_\parallel$ that correspond to the Fermi energy.

It is not an easy task to figure out the statistical properties of the integral (4.179), given those of $V(x,y,z)$ e.g., as discussed in Sec. III.E.4). Numerical experiments of Mehr and Aharony (1988) show the presence of extended isolines of $\mu_\parallel(x,y,E_\parallel)$ (i.e., the electron orbit projections on the plane perpendicular to the magnetic field) with the fractal dimension $d_h=1.5\pm0.3$, which is not inconsistent with $d_h=\frac{7}{4}$ for the monoscale uncorrelated potential $\mu_\parallel$ (Sec. III.C.1). However, an important point appears to be missing from this simple model, namely, the discontinuous change of the longitudinal adiabatic invariant $\mu_\parallel$

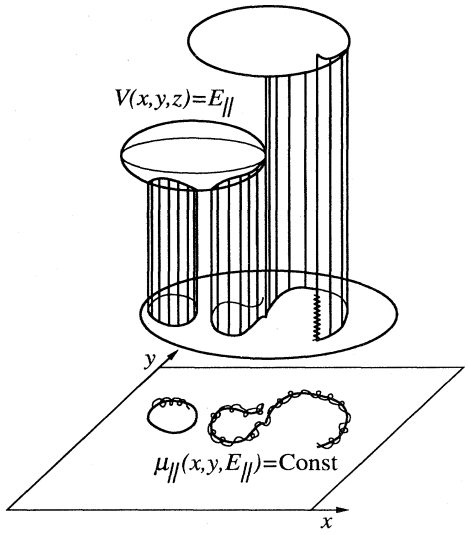

FIG. 41. Bounce motion of a magnetized electron, constrained to a cylinder of constant longitudinal invariant $\mu_{\|}$. The projection of the electron motion represents the averaged $\mathbf{E}\times\mathbf{B}$ drift with a precession due to the dependence of this drift on z.

due to the possibility that a discontinuous change in one of the turning points can occur. This leads to a jump in the cylinder length that props up disconnected or folded surface with the same $E_{\|}$ (Fig. 41). This happens near the "equator" of the isopotential surface $V(x,y,z)=E_{\|}$, defined by the equation $\partial V(x,y,z)/\partial z=0$, where the cylinder of the electron locus is tangential to the surface. This is accompanied by a discontinuous change in $\mu_{\|}$ and a change in the shape of the trajectory projection.[8] Upon encompassing a new cylinder, the electron may return to a cylinder between the two original reflecting isosurfaces of $V(x,y,z)$, but with a different value of $\mu_{\|}$. There is also the possibility for trapping in another gap (e.g., switching the reflecting wall from the "Southern" to the "Northern hemisphere"). As there are many solutions for the turning points $z_{1,2}$ at given x, y, and $E_{\|}$, there is not just one but an infinite (countable) number of "maps" with the corresponding contours of $\mu_{\|}(x,y,E_{\|})$. Electrons can undergo transitions between the maps by way of the equator crossing.

The discontinuities introduced by the interplay of a smooth 3D potential and a strong magnetic field violate the adiabaticity near the equators, which can result in an extremely complex (chaotic) classical motion (Trugman, 1989) having nontrivial quantum implications (Nicopoulos and Trugman, 1990; see also Trugman and Nicopoulos, 1992). The Hamiltonian chaos stemming from the nonconservation of $\mu_{\|}$ results in a probabilistic nature of the equator crossing; hence the electron propagation in the considered system is in fact a percolation-like process. In terms of the drift approximation involved, the randomness results from the high-frequency electron precession around its averaged trajectory projection $\mu_{\|}(x,y,E_{\|})=$const (Fig. 41). [An illuminating discussion of how probability arises in dynamical systems involving both fast and slow motion was given by Neishtadt (1991).] Although a finite volume must correspond to the isolines of $\mu_{\|}$ that never cross the equator projections, a finite volume must correspond to the crossing behavior and the possible electron transitions between the maps. The dynamically accessible region may (or may not) percolate to infinity (perhaps one should distinguish between the longitudinal and the transverse percolation). Since all the above nontrivially depends on the value of the longitudinal energy $E_{\|}$, the challenging task of determining the corresponding electron kinetics remains. A similar kind of particle motion takes place in tokamak plasmas where the effective potential V is due to the inhomogeneities of the magnetic field (Yushmanov, 1990a).

Polyakov (1986) considered the analogous problem of the magnetized electron kinetics in a screened potential of dilute charged impurities. This kind of potential represents localized minima (for positively charged impurities) and maxima (for negative impurities) of $V(x,y,z)$, with the size of localization of order the Debye length. The trapping of electrons is possible only in the presence of negative impurities. The corresponding maxima of V can be passed around due to the electric drift (4.180). If one assumes that there are no long-range correlations between consecutive equator crossings, both the longitudinal and the transverse electron diffusion coefficients scale as

$$D^{*}\simeq\lambda_0 v_d\propto B^{-1} \tag{4.181}$$

for large B.

If, in addition to the deterministic motion in the potential, electrons experience random (say, electron-electron) collisions, the corresponding transport problem becomes similar to the advection-diffusion problem (Sec. IV.A). The case of passing electrons that freely diffuse with the diffusivity D_0 along the magnetic-field lines is mathematically equivalent to the problem discussed in Sec. IV.B.3.b. Specifically, we deal with the longitudinal diffusion accompanied by the transverse incompressible advection analogous to Eq. (4.162), where $\sigma_{xy}(x,y,z)$ must be replaced by $\psi(x,y,z)=cV(x,y,z)/(eB)$. If the longitudinal diffusion is strong enough, $D_0>\psi_0$ [where ψ_0 is the characteristic amplitude of the variation of $\psi(x,y,z)$], then the result (4.164) is translated into the transverse electron diffusion scaling as

$$D_{\perp}^{*}\simeq D_0\left[\frac{\psi_0}{D_0}\right]^{4/3}\propto B^{-4/3},\quad \psi_0\ll D_0 \tag{4.182}$$

(see also Murzin, 1984). Polyakov (1986) argued that the transverse diffusion (4.182)—contrary to the classical B^{-2} scaling (Braginskii, 1965)—can take place even in

[8] In addition to the discontinuity in value, the quantity $\mu_{\|}$ has a logarithmic singularity in gradient near the projection of the "equator."

equilibrium gaseous plasmas for a sufficiently wide range of B, this range being bounded from above by the effect of the motion of ions.

For smaller longitudinal diffusion, $D_0 < \psi_0$, quite a different regime occurs. Isichenko and Kalda (1991a) argued that in this limit the effect of the longitudinal diffusion can be taken into account by introducing the transverse diffusivity $D_\perp = D_0(\lambda_\perp/\lambda_\parallel)^2$, where $\lambda_\perp$ and $\lambda_\parallel$ are the correlation lengths of the potential $\psi(\mathbf{x})$ across and along the magnetic field, respectively, and by treating the stream function as independent of z. Then, applying formula (4.36) for a monoscale random potential with $\lambda_\perp = \lambda_\parallel = \lambda_0$, we obtain another intermediate asymptotic regime,

$$D_\perp^* \simeq D_0 \left[\frac{\psi_0}{D_0} \right]^{10/13} \propto B^{-10/13}, \quad \psi_0 \gg D_0 . \quad (4.183)$$

The general reason for the "anomalous" diffusion scalings (4.178) and (4.181)—(4.183) (contrary to the "classical" scaling B^{-2}) lies in the long-range correlations that the strong magnetic field introduces in the process of electron scattering by a disordered potential. The correlations are due to the effectively one-dimensional motion of the electrons (to first approximation), which causes the multiple returns of electrons to the same scattering centers, for both the trapped regular oscillations and the diffusive random walk.

V. CONCLUDING REMARKS

Throughout this paper, a general idea was pursued about the usefulness of the geometrical images of physical phenomena. Geometry unifies and interconnects very different physical problems, enriching methods for their solution. For phenomena involving many length scales (usually associated with the presence of a large parameter), fractal geometry provides sensible guidelines for qualitative analysis.

The quantitative description of random media in terms of the scaling behavior of effective transport coefficients involves a set of power exponents, to which the large parameters of the problem are to be raised. We tried to demonstrate that in many cases these exponents form certain universality classes—that is, they depend on the system parameters in a piecewise constant manner. The universality class of random percolation covers a variety of lattice and continuum models, including the contour lines and surfaces of a monoscale random potential. The latter problem is particularly relevant for two-dimensional incompressible flows, which describe the advection-diffusion transport of a tracer, the guiding-center drift in a turbulent plasma, the currents in a quantized two-dimensional electron gas, or the geometry of stochastic magnetic-field lines. Some other problems, including the averaging of randomly inhomogeneous conductance, can be related to the percolation model in more or less direct ways.

In addition to the discrete universality classes, there exists a continuum universality, whose characteristic exponents depend continuously on a spectral parameter H. There are various standard ways to define self-similar (power-law) spectra of a physical quantity $\psi(\mathbf{x})$, such as the Fourier component $\psi_\mathbf{k} \propto k^{\alpha_1}$, the power spectra $|\psi_\mathbf{k}|^2 \propto k^{\alpha_2}$ and $|\psi_\mathbf{k}|^2 k^{d-1} \propto k^{\alpha_3}$, etc. It appears that the most convenient characterization is given by the Hurst-Mandelbrot exponent H entering the "λ spectrum" $\psi_\lambda \propto \lambda^H$. This representation makes various formulas, such as the expressions for the fractal dimensions (see Table I), more unified, recognizable, and often independent of the dimensionality d. For example, the diffusive Brownian motion $x(t)$ is an $H = \frac{1}{2}$ random process, whereas the $1/f$ noise (cf. Dutta and Horn, 1981) is an $H = 0$ signal. An example of a continuous universality class is the long-range correlated percolation, with $H < 0$ being an exponent of the algebraic decay of lattice correlations. An extension of this problem to the continuum is the statistical topography of potentials with algebraic spectra. I hope that this classical geometrical problem will see further development and new areas of application.

ACKNOWLEDGMENTS

It is a pleasure to acknowledge the many discussions and exchanges of ideas held with Jaan Kalda. I am grateful to A. Aharony, M. Avellaneda, I. Balberg, J.-P. Bouchaud, A. M. Dykhne, M. Ottaviani, E. B. Tatarinova, S. A. Trugman, A. Vulpiani, and G. M. Zaslavsky for communicating their work, including unpublished results, and to A. D. Beklemishev for helping with computer simulations. I have benefited from discussions with M. V. Berry, J.-P. Bouchaud, P. Le Doussal, A. M. Dykhne, E. Ott, E. B. Tatarinova, S. A. Trugman, and P. N. Yushmanov, who provided answers to some of my questions. I am indebted to J. A. Krommes for editing the manuscript and for making many useful suggestions and to P. J. Morrison for also helping with the editing. Special thanks to Tanya Isichenko, who generated pictures on the computer and provided necessary support. This work was supported by the U.S. Department of Energy under Contract No. DE-FG05-80ET53088.

REFERENCES

Abrikosov, A. A., 1980, "Spin glasses with short range interaction," Adv. Phys. **29**, 869.

Abrikosov, A. A., L. P. Gorkov, and I. Ye. Dzyaloshinskii, 1965, *Quantum Field Theoretical Methods in Statistical Physics* (Pergamon, New York).

Adler, R. J., 1981, *The Geometry of Random Fields* (Wiley, New York).

Adler, J., Y. Meir, A. Aharony, and A. B. Harris, 1990, "Series study of percolation moments in general dimension," Phys. Rev. B **41**, 9183.

Afanasiev, V. V., R. Z. Sagdeev, and G. M. Zaslavsky, 1991, "Chaotic jets with multifractal space-time random walk," Chaos **1**, 143.

Aharony, A., 1984, "Percolation, fractals, and anomalous diffusion," J. Stat. Phys. **34**, 931.

Aharony, A., and A. B. Harris, 1990, "Superlocalization, correlations and random walks on fractals," Physica A **163**, 38.

Aharony, A., and A. B. Harris, 1992, "Multifractals, in *Growth Patterns in Physical Sciences and Biology,* edited by E. Louis *et al.* (Plenum, New York).

Aharony, A., and D. Stauffer, 1982, "On the width of the critical region in dilute magnets with long range percolation," Z. Phys. B **47**, 175.

Alexandrowicz, Z., 1980, "Critically branched chains and percolation clusters," Phys. Lett. A **80**, 284.

Alon, U., I. Balberg, and A. Drory, 1991, "New, heuristic, percolation criterion for continuum systems," Phys. Rev. Lett. **66**, 2879.

Alon, U., A. Drory, and I. Balberg, 1990, "Systematic derivation of percolation thresholds in continuum systems," Phys. Rev. A **42**, 4634.

Anderson, P. W., 1958, "Absence of diffusion in certain random lattices," Phys. Rev. **109**, 1492.

Aref, H., 1984, "Stirring by chaotic advection," J. Fluid Mech. **143**, 1.

Aris, R., 1956, "On the dispersion of a solute in a fluid flowing through a tube," Proc. R. Soc. London, Ser. A **235**, 67.

Arnold, V. I., 1963a, "Proof of a theorem of A. N. Kolmogorov on the invariance of quasi-periodic motions under small perturbations of the Hamiltonian," Russ. Math. Surv. **18**, 9.

Arnold, V. I., 1963b, "Small denominators and problems of stability of motions in classical and celestial mechanics," Russ. Math. Surv. **18**, 85.

Arnold, V. I., 1978, *Mathematical Methods in Classical Mechanics* (Springer, Heidelberg).

Arnold, V. I., 1983, "Singularities, bifurcations and catastrophes," Usp. Fiz. Nauk (SSSR) **141**, 569 [Sov. Phys. Usp. **26**, 1025 (1983)].

Arnold, V. I., 1988, "Remarks on quasicrystallic symmetries," Physica D **33**, 21.

Avellaneda, M., A. V. Cherkaev, K. A. Lurie, and G. M. Milton, 1988, "On the effective conductivity of polycrystals and three-dimensional phase-interchange inequality," J. Appl. Phys. **63**, 4989.

Avellaneda, M., and A. J. Majda, 1989, "Stieltjes integral representation and effective diffusivity bounds for turbulent transport," Phys. Rev. Lett. **62**, 753.

Avellaneda, M., and A. J. Majda, 1990, "Mathematical models with exact renormalization for turbulent transport," Commun. Math. Phys. **131**, 381.

Avellaneda, M., and A. J. Majda, 1991, "An integral representation and bounds on the effective diffusivity in passive advection by laminar and turbulent flows," Commun. Math. Phys. **138**, 339.

Azbel, M. Ya., 1985, "New type of conductivity?" Solid State Commun. **54**, 127.

Azbel, M. Ya., and O. Entin-Wohlman, 1985, "Electron orbits in an impure metal in the presence of a strong magnetic field," Phys. Rev. B **32**, 562.

Baker, G., and P. Graves-Monris, 1981, *Padé approximants* (Addison-Wesley, New York).

Balagurov, B. Ya., 1978, "Galvanomagnetic properties of thin inhomogeneous films," Fiz. Tverd. Tela **20**, 3332 [Sov. Phys. Solid State **20**, 1922 (1978)].

Balagurov, B. Ya., 1986, "Thermogalvanomagnetic properties of two-dimensional two-component systems," Fiz. Tverd. Tela **28**, 2068 [Sov. Phys. Solid State **28**, 1156 (1986)].

Balberg, I., 1987a, "Recent developments in continuum percolation," Philos. Mag. B **56**, 991.

Balberg, I., 1987b, "Tunneling and nonuniversal conductivity in composite materials," Phys. Rev. Lett. **59**, 1305.

Balberg, I., B. Berkowitz, and G. E. Drachsler, 1991, "Application of a percolation model to flow in fractured hard rocks," J. Geophys. Res. B **96**, 10015.

Ball, R. C., S. Havlin, and G. H. Weiss, 1987, "Non-Gaussian random walks," J. Phys. A **20**, 4055.

Batchelor, G. K., 1952, "Diffusion in a field of homogeneous turbulence II. The relative motion of particles," Proc. Cambridge Philos. Soc. **48**, 345.

Batchelor, G. K., 1982, *The Theory of Homogeneous Turbulence* (Cambridge University, Cambridge).

Battacharya, R., V. Gupta, and H. F. Walker, 1989, "Asymptotics of solute dispersion in periodic porous media," SIAM J. Appl. Math. **49**, 86.

Baxter, R. J., 1982, *Exactly Solved Models in Statistical Mechanics* (Academic, London).

Belavin, A. A., A. M. Polyakov, and A. B. Zamolodchikov, 1984, "Infinite conformal symmetry of critical fluctuations in two dimensions," J. Stat. Phys. **34**, 763.

Bender, C. M., and S. A. Orszag, 1978, *Advanced Mathematical Methods for Scientists and Engineers* (McGraw-Hill, New York).

Bensoussan, A., J. L. Lions, and G. Papanicolaou, 1978, *Asymptotic Analysis for Periodic Structures* (North-Holland, Amsterdam).

Benzi, R., L. Biferale, G. Paladin, A. Vulpiani, and M. Vergassola, 1991, "Multifractality in the statistics of the velocity gradients in turbulence," Phys. Rev. Lett. **67**, 2299.

Bergman, D. J., 1978, "The dielectric constant of a composite material—a problem in classical physics," Phys. Rep. **43**, 377.

Bergman, D. J., and Y. Imry, 1977, "Critical behavior of the complex dielectric constant near the percolation threshold of a heterogeneous material," Phys. Rev. Lett. **39**, 1222.

Berry, M. V., N. L. Balazs, M. Tabor, and A. Voros, 1979, "Quantum maps," Ann. Phys. (N.Y.) **122**, 26.

Berry, M. V., and J. H. Hannay, 1978, "Topography of random surfaces," Nature **273**, 573.

Berry, M. V., and Z. V. Lewis, 1980, "On the Weierstrass-Mandelbrot fractal function," Proc. R. Soc. London, Ser. A **370**, 459.

Besicovitch, A. S., 1929, "On linear sets of points of fractional dimensions," Math. Ann. **101**, 161.

Besicovitch, A. S., 1935a, "On the sum of digits of real numbers represented in the diadic system. (On linear sets of points of fractional dimensions II)," Math. Ann. **110**, 321.

Besicovitch, A. S., 1935b, "Sets of points of non-differentiability of absolutely continuous functions and of divergence of Fejér sums. (On linear sets of points of fractional dimensions III)" Math. Ann. **110**, 331.

Bouchaud, J.-P., A. Comete, A. Georges, and P. Le Doussal, 1987, "Anomalous diffusion in random media at any dimensionality," J. Phys. (Paris) **48**, 1455.

Bouchaud, J.-P., and A. Georges, 1990, "Anomalous diffusion in disordered media: Statistical mechanics, models and physical applications," Phys. Rep. **195**, 127.

Bouchaud, J.-P., A. Georges, J. Koplik, A. Provata, and S. Redner, 1990, "Superdiffusion in random velocity fields," Phys. Rev. Lett. **64**, 2503.

Bouchaud, J.-P., and P. Le Doussal, 1985, "Numerical study of a D-dimensional periodic Lorentz gas with universal properties," J. Stat. Phys. **41**, 225.

Bouchaud, J.-P., and P. G. Zérah, 1989, "Spontaneous resonances and universal behavior in ferrimagnets: Effective-medium theory," Phys. Rev. Lett. **63**, 1000.

Bozhokin, S. V., and A. M. Bykov, 1990, "Transport processes in a randomly inhomogeneous plasma in a magnetic field," Fiz. Plazmy **16**, 717 [Sov. J. Plasma Phys. **16**, 415 (1990)].

Brady, J. F., 1990, "Dispersion in heterogeneous media," in *Hydrodynamics of Dispersed Media,* edited by J. P. Hulin, A. M. Cazabat, E. Guyon, and F. Carmona (Elsevier, Amsterdam), p. 271.

Braginskii, S. I., 1965, "Transport processes in a plasma," in *Reviews of Plasma Physics,* edited by M. A. Leontovich (Consultants Bureau, New York), Vol. 1, p. 205.

Brenner, H., 1980, "Dispersion resulting from flow through spatially periodic porous media," Philos. Trans. R. Soc. London, Ser. A **297**, 81.

Broadbent, S. R., and J. M. Hammersley, 1957, "Percolation processes, I. Crystals and mazes," Proc. Cambridge Philos. Soc. **53**, 629.

Brown, M. G., and K. B. Smith, 1991, "Ocean stirring and chaotic low-order dynamics," Phys. Fluids A **3**, 1186.

Bug, A. L. R., S. A. Safran, G. S. Grest, and I. Webman, 1985, "Do interactions raise or lower a percolation threshold?" Phys. Rev. Lett. **55**, 1896.

Bunde, A., and J. F. Gouyet, 1985, "On scaling relations in growth models for percolation clusters and diffusion fronts," J. Phys. A **18**, L285.

Bunde, A., H. Harder, and S. Havlin, 1986, "Nonuniversality of diffusion exponents in percolation systems," Phys. Rev. B **34**, 3540.

Bunde, A., and S. Havlin, 1991, Eds., *Fractals in Disordered Systems* (Springer, New York).

Bunimovich, L. A., and Ya. G. Sinai, 1980, "Markov partitions for dispersed billiards," Commun. Math. Phys. **78**, 247.

Bunimovich, L. A., and Ya. G. Sinai, 1981, "Statistical properties of Lorentz gas with periodic configuration of scatterers," Commun. Math. Phys. **78**, 479.

Burrough, P. A., 1981, "Fractal dimensions of landscapes and other environmental data," Nature **234**, 240.

Busse, F. H., 1978, "Non-linear properties of thermal convection," Rep. Prog. Phys. **41**, 1929.

Cardoso, O., and P. Tabeling, 1988, "Anomalous diffusion in a linear array of vortices," Europhys. Lett. **7**, 225.

Chandresekhar, S., 1943, "Stochastic problems in physics and astronomy," Rev. Mod. Phys. **15**, 1.

Chandrasekhar, S., 1961, *Hydrodynamic and Hydromagnetic Stability* (Dover, New York).

Chernikov, A. A., A. I. Neishtadt, A. V. Rogalsky, and V. Z. Yakhnin, 1991, "Lagrangian chaos in time-dependent convection," Chaos **1**, 206.

Childress, S., and A. M. Soward, 1989, "Scalar transport and alpha-effect for a family of cat's-eye flows," J. Fluid Mech. **205**, 99.

Chirikov, B. V., 1979, "A universal instability of many-dimensional oscillator systems," Phys. Rep. **52**, 263.

Chukbar, K. V., and V. V. Yankov, 1988, "Evolution of the magnetic field in plasma opening switches," Zh. Tekh. Fiz. **58**, 2130 [Sov. Phys. Tech. Phys. **33**, 1293 (1988)].

Clerc, J. P., G. Giraud, S. Alexander, and E. Guyon, 1980, "Conductivity of a mixture of conducting and insulating grains: Dimensionalty effects," Phys. Rev. B **22**, 2489.

Coniglio, A., 1981, "Thermal phase transition of the dilute s-state Potts and n-vector models at the percolation threshold," Phys. Rev. Lett. **46**, 250.

Coniglio, A., C. R. Nappi, F. Peruggi, and L. Russo, 1977, "Percolation points and critical point of the Ising model," J. Phys. A **10**, 205.

Constantin, P., I. Procaccia, and K. R. Sreenivasan, 1991, "Fractal geometry of isoscalar surfaces in turbulence: Theory and experiments," Phys. Rev. Lett. **67**, 1739.

Coxeter, H. S. M., 1973, *Regular Polytopes* (Dover, New York).

Crisanti, A., M. Falcioni, G. Paladin, and A. Vulpiani, 1990, "Anisotropic diffusion in fluids with steady periodic velocity fields," J. Phys. A **23**, 3307.

Crisanti, A., M. Falcioni, G. Paladin, and A. Vulpiani, 1991, "Lagrangian chaos: Transport, mixing, and diffusion in fluids," Riv. Nuovo Cimento **14**, 1.

Dean, P., and N. F. Bird, 1967, "Monte Carlo estimates of critical percolation probabilities," Proc. Cambridge Philos. Soc. **63**, 477.

de Gennes, P. G., 1979a, *Scaling Concepts in Polymer Physics* (Cornell University, Ithaca).

de Gennes, P. G., 1979b, "Incoherent scattering near a sol gel transition," J. Phys. (Paris) Lett. **40**, L198.

de Gennes, P. G., P. Lafore, and J. Millot, 1959, "Amas accidentals dan les solutions solides désordonnées," J. Phys. Chem. Solids **11**, 105.

den Nijs, M. P. M., 1979, "A relation between the temperature exponents of the eight-vertex and q-state Potts model," J. Phys. A **12**, 1857.

Derrida, B., and J. M. Luck, 1983, "Diffusion on a random lattice: Weak-disorder expansion in arbitrary dimension," Phys. Rev. B **28**, 7183.

Derrida, B., and J. Vannimenus, 1982, "A transfer-matrix approach to random resistor network," J. Phys. A **15**, L557.

Deutscher, G., R. Zallen, and J. Adler, 1983, Eds., *Percolation Structures and Processes* (Hilger, Bristol).

Domb, C., M. S. Green, and J. L. Lebowitz, 1972–1988, Eds., *Phase Transitions and Critical Phenomena,* Vols. 1 through 12 (Academic, London).

Domb, C., and M. F. Sykes, 1960, "Cluster size in random mixtures and percolation processes," Phys. Rev. **122**, 77.

Dombre, T., U. Frisch, J. M. Greene, M. Hénon, A. Mehr, and A. M. Soward, 1986, "Chaotic streamlines in the ABC flows," J. Fluid Mech. **167**, 353.

Dotsenko, Vl. S., and V. A. Fateev, 1984, "Conformal algebra and multipoint correlation functions in 2D statistical models," Nucl. Phys. B **240**, [FS12], 312.

Dreizin, Yu. A., and A. M. Dykhne, 1972, "Anomalous conductivity of inhomogeneous media in a strong magnetic field," Zh. Eksp. Teor. Fiz. **63**, 242 [Sov. Phys. JETP **36**, 127 (1973)].

Dreizin, Yu. A., and A. M. Dykhne, 1983, "A qualitative theory of the effective conductivity of polycrystals," Zh. Eksp. Teor. Fiz. **84**, 1756 [Sov. Phys. JETP **57**, 1024 (1983)].

Dunn, A. G., J. W. Essam, and D. S. Ritchie, 1975, "Series expansion study of the pair connectedness in bond percolation models," J. Phys. C **8**, 4219.

Duplantier, B., and H. Saleur, 1987, "Exact tricritical exponents for polymers at the Θ point in two dimensions," Phys. Rev. Lett. **58**, 539.

Dutta, P., and P. M. Horn, 1981, "Low-frequency fluctuations in solids: $1/f$ noise," Rev. Mod. Phys. **53**, 497.

Dykhne, A. M., 1967, "Calculation of the kinetic coefficients of media with random inhomogeneities," Zh. Eksp. Teor. Fiz. **52**, 264 [Sov. Phys. JETP **25**, 170 (1967)].

Dykhne, A. M., 1970a, "Conductivity of a two-dimensional two-phase system," Zh. Eksp. Teor. Fiz. **59**, 110 [Sov. Phys. JETP **32**, 63 (1971)].

Dykhne, A. M., 1970b, "Anomalous plasma resistance in a strong magnetic field," Zh. Eksp. Teor. Fiz. **59**, 641 [Sov. Phys. JETP **32**, 348 (1971)].

Dykhne, A. M., 1981, unpublished.

Dykhne, A. M., 1984, "Physical models reducible to the problem of random walks in randomly inhomogeneous media," in *Nonlinear and Turbulent Processes in Physics,* edited by R. Z. Sagdeev (Harwood, Academic, New York), Vol. 3, p. 1323.

Dykhne, A. M., 1986, unpublished.

Dykhne, A. M., S. Kurchatov, and S. Marianer, 1991, private communication.

Eckmann, J.-P., and D. Ruelle, 1985, "Ergodic theory of chaos and strange attractors," Rev. Mod. Phys. **57**, 617.

Edwards, B. F., and A. R. Kerstein, 1985, "Is there a lower critical dimension for chemical distance?" J. Phys. A **18**, L1081.

Elan, W. T., A. R. Kerstein, and J. J. Rehr, 1984, "Critical exponents of the void percolation problem for spheres," Phys. Rev. Lett. **52**, 1516.

Essam, J. W., 1972, "Percolation and cluster size," in *Phase Transitions and Critical Phenomena,* edited by C. Domb, M. S. Greene, and J. L. Lebowtiz (Academic, London), Vol. 2, p. 197.

Essam, J. W., 1980, "Percolation theory," Rep. Prog. Phys. **43**, 833.

Falconer, K. J., 1985, *The Geometry of Fractal Sets* (Cambridge University, New York).

Falconer, K. J., 1990, *Fractal Geometry: Mathematical Foundations and Applications* (Wiley, New York).

Family, F., 1984, "Polymer statistics and universality: Principles and Applications of cluster renormalization," in *Random Walks and Their Applications in the Physical and Biological Sciences,* edited by M. F. Shlesinger and B. J. West, AIP Conf. Proc. No. 109 (AIP, New York), p. 3.

Family, F., and A. Coniglio, 1985, "Flory theory for conductivity of random resistor network," J. Phys. (Paris) Lett. **46**, L-9.

Farmer, J. D., E. Ott, and J. A. Yorke, 1983, "The dimension of chaotic attractors," Physica D **7**, 153.

Feder, J., 1988, *Fractals* (Plenum, New York).

Feng, S., B. I. Halperin, and P. N. Sen, 1987, "Transport properties of continuum systems near the percolation threshold," Phys. Rev. B **35**, 197.

Feynman, R. P., and A. R. Hibbs, 1965, *Quantum Mechanics and Path Integrals* (McGraw-Hill, New York).

Finn, J. M., P. N. Guzdar, and A. A. Chernikov, 1992, "Particle transport and rotation damping due to stochastic magnetic field lines," Phys. Fluids B **4**, 1152.

Fisher, D. S., 1984, "Random walks in random environments," Phys. Rev. A **30**, 960.

Fisher, M. E., 1966, "Shape of a self-avoiding walk or polymer chain," J. Chem. Phys. **44**, 616.

Flierl, G. R., V. D. Larichev, J. C. McWilliams, and G. M. Reznik, 1980, "The dynamics of baroclinic and barotropic solitary eddies," Dyn. Atmos. Oceans **5**, 1.

Flory, P. J., 1969, *Statistical Mechanics of Chain Molecules* (Interscience, New York).

Fogelholm, R., 1980, "The conductivity of large percolation network samples," J. Phys. C **13**, L571.

Fortuin, C. M., and P. W. Kasteleyn, 1972, "On the random cluster model I. Introduction and relation to other models," Physica (Utrecht) **57**, 536.

Fradkin, L., 1991, "Comparison of Lagrangian and Eulerian approaches to turbulent diffusion," Plasma Phys. Controlled Fusion **33**, 685.

Frisch, U., and G. Parisi, 1985, "On the singularity structure of fully developed turbulence," in *Turbulence and Predictability in Geophysical Fluid Dynamics and Climate Dynamics,* edited by M. Ghil, R. Benzi, and G. Parisi (North-Holland, New York), p. 84.

Fung, J. C. H., and J. C. Vassilicos, 1991, "Fractal dimension of lines in chaotic advection," Phys. Fluids A **3**, 2725.

Garland, J. C., and D. B. Tanner, 1978, Eds., *Electrical Transport and Optical Properties of Inhomogeneous Media* (AIP, New York).

Gaunt, D. S., and M. F. Sykes, 1983, "Series study of random percolation in three dimensions," J. Phys. A **16**, 783.

Gaveau, B., and L. S. Schulman, 1992, "Anomalous diffusion in a random velocity field," J. Stat. Phys. **66**, 375.

Gawlinski, E. T., and S. Redner, 1983, "Monte Carlo renormalization group for continuum percolation with excluded-volume interaction," J. Phys. A **16**, 1063.

Gawlinski, E. T., and H. E. Stanely, 1977, "Continuum percolation in two dimensions: Monte Carlo tests of scaling and universality for non-interacting discs," J. Phys. A **10**, 205.

Gefen, Y., A. Aharony, B. B. Mandelbrot, and S. Kirkpatrick, 1981, "Solvable fractal family, and its possible relation to the backbone of percolation," Phys. Rev. Lett. **47**, 1771.

Gefen, Y., B. B. Mandelbrot, and A. Aharony, 1980, "Critical phenomena on fractal lattices," Phys. Rev. Lett. **45**, 855.

Geiger, A., and H. E. Stanely, 1982, "Test of universality of percolation exponents for a three-dimensional continuum system for interacting water-like particles," Phys. Rev. Lett. **49**, 1895.

Golden, K., and G. C. Papanicolaou, 1983, "Bounds for effective parameters of heterogeneous media by analytic continuation," J. Math. Phys. **90**, 473.

Golubović, L., S. Feng, and F.-A. Zeng, 1991, "Classical and quantum superdiffusion in a time-dependent random potential," Phys. Rev. Lett. **67**, 2115.

Good, I. J., 1941, "The fractional dimensional theory of continuous fractions," Proc. Cambridge Philos. Soc. **37**, 199.

Gouker, M., and F. Family, 1983, "Evidence for the classical critical behavior in long-range site percolation," Phys. Rev. B **28**, 1449.

Gouyet, J.-F., M. Rosso, and B. Sapoval, 1988, "Fractal structure of diffusion and invasion fronts in three-dimensional lattices through the gradient percolation approach," Phys. Rev. B **37**, 1832.

Grassberger, P., 1983a, "On the critical behavior of the general epidemic processes and dynamical percolation," Math. Biosci. **62**, 157.

Grassberger, P., 1983b, "Generalized dimensions of strange attractors," Phys. Lett. A **97**, 227.

Grassberger, P., 1985, "On the spreading of two-dimensional percolation," J. Phys. A **18**, L215.

Grassberger, P., 1986a, "Spreading of percolation in three and four dimensions," J. Phys. A **19**, 1681.

Grassberger, P., 1986b, "On the hull of two-dimensional percolation clusters," J. Phys. A **19**, 2675.

Grassberger, P., and I. Procaccia, 1983, "Measuring the strangeness of strange attractors," Physica D **9**, 189.

Grimmett, G. R., 1989, *Percolation* (Springer, New York).

Grossman, T., and A. Aharony, 1986, "Structure and perimeters of percolation clusters," J. Phys. A **19**, L745.

Grossman, T., and A. Aharony, 1987, "Accessible external perimeters of percolation clusters," J. Phys. A **20**, L1193.

Gruzinov, A. V., 1991, "Percolation diffusion of a Larmor ra-

dius," Kurchatov Institute of Atomic Energy Report No. IAE-5331/6, Moscow.
Gruzinov, A. V., M. B. Isichenko, and J. Kalda, 1990, "Two-dimensional turbulent diffusion," Zh. Eksp. Teor. Fiz. **97**, 476 [Sov. Phys. JETP **70**, 263 (1990)].
Gurevich, M. I., E. Z. Meilikhov, O. V. Telkovskaya, and V. V. Yankov, 1988, "A computation of the voltage-current characteristics of three-dimensional Josephson contact networks with random parameters," Sverkhprovodimost: Fizika, Khimiya, Tekhnika (Superconductivity: Physics, Chemistry, Engineering) **4**, 80 (in Russian).
Haken, H., 1975, "Cooperative phenomena in systems far from thermal equilibrium and in nonphysical systems," Rev. Mod. Phys. **47**, 67.
Halperin, B. I., S. Feng, and P. N. Sen, 1985, "Difference between lattice and continuum percolation transport exponents," Phys. Rev. Lett. **54**, 2391.
Halperin, B. I., and M. Lax, 1966, "Impurity-band tails in the high-density limit. I. Minimum counting methods," Phys. Rev. **148**, 722.
Halsey, T. C., M. H. Jensen, L. P. Kadanoff, I. Procaccia, and B. I. Shraiman, 1986, "Fractal measures and their singularities: The characterization of strange sets," Phys. Rev. A **33**, 1141.
Hans, J. W., and K. W. Kehr, 1987, "Diffusion in regular and disordered lattices," Phys. Rep. **150**, 263.
Harris, A. B., 1974, "Effect of random defects on the critical behavior of Ising models," J. Phys. C **7**, 1671.
Harris, A. B., 1983, "Field-theoretic approach to biconnectedness in percolating systems," Phys. Rev. B **28**, 2614.
Harris, A. B., 1987, "Resistance correlations in random structures," Philos. Mag. B **56**, 833.
Harris, A. B., Y. Meir, and A. Aharony, 1987, "Diffusion on percolation clusters," Phys. Rev. B **36**, 8752.
Hasegawa, A., C. G. Maclennan, and Y. Kodama, 1979, "Nonlinear behavior and turbulence spectra of drift waves and Rossby waves," Phys. Fluids **22**, 2122.
Hasegawa, A., and K. Mima, 1978, "Pseudo-three-dimensional turbulence in magnetized nonuniform plasma" Phys. Fluids **21**, 87.
Hashin, Z., and S. Shtrikman, 1963, "Conductivity of polycrystals," Phys. Rev. **130**, 129.
Hausdorff, F., 1918, "Dimension und äusseres Mass," Math. Ann. **79**, 157.
Havlin, S., and D. Ben-Avraham, 1987, "Diffusion in disordered media," Adv. Phys. **36**, 695.
Heermann, D. W., and D. Stauffer, 1981, "Phase diagram for three-dimensional correlated site-bond percolation," Z. Phys. B **44**, 339.
Hentschel, H. G. E., and I. Procaccia, 1983a, "Fractal nature of turbulence as manifested in turbulent diffusion," Phys. Rev. A **27**, 1266.
Hentschel, H. G. E., and I. Procaccia, 1983b, "The infinite number of generalized dimensions of fractals and strange attractors," Physica D **8**, 435.
Herring, C., 1960, "Effect of random inhomogeneities on electrical and galvanomagnetic measurements," J. Appl. Phys. **31**, 1939.
Herrmann, J. J., D. C. Hong, and H. E. Stanley, 1984, "Backbone and elastic backbone of percolation clusters obtained by the new method of 'burning,'" J. Phys. A **17**, L261.
Herrmann, H. J., and H. E. Stanley, 1984, "Building blocks of percolation," Phys. Rev. Lett. **53**, 1121.
Horton, W., 1985, "Onset of stochasticity and the diffusion approximation in drift waves," Plasma Phys. **27**, 937.
Horton, W., 1989, "Drift wave vortices and anomalous transport," Phys. Fluids B **1**, 524.
Horton, W., 1990, "Nonlinear drift waves and transport in magnetized plasmas," Phys. Rep. **192**, 1.
Hoshen, J., R. Kopelman, and E. M. Monberg, 1978, "Percolation and critical distribution II. Layers, variable range interactions, and exciton cluster model," J. Stat. Phys. **19**, 219.
Hui, P. M., and D. Stroud, 1985, "Anomalous frequency-dependent transport in composites," Phys. Rev. B **32**, 7728.
Isichenko, M. B., 1991a, "Effective plasma heat conductivity in a 'braided' magnetic field—I. Quasi-linear limit," Plasma Phys. Controlled Fusion **33**, 795.
Isichenko, M. B., 1991b, "Effective plasma heat conductivity in a 'braided' magnetic field—II. Percolation limit," Plasma Phys. Controlled Fusion **33**, 809.
Isichenko, M. B., and W. Horton, 1991, "Scaling laws of stochastic $\mathbf{E}\times\mathbf{B}$ plasma transport," Comments Plasma Phys. Controlled Fusion **14**, 249.
Isichenko, M. B., and J. Kalda, 1991a, "Anomalous resistance of randomly inhomogeneous Hall media," Zh. Eksp. Teor. Fiz. **91**, 224 [Sov. Phys. JETP **72**, 126 (1991)].
Isichenko, M. B., and J. Kalda, 1991b, "Statistical topography. I. Fractal dimension of coastlines and number-area rule for islands," J. Nonlinear Sci. **1**, 255.
Isichenko, M. B., and J. Kalda, 1991c, "Statistical topography. II. 2D transport of a passive scalar," J. Nonlinear Sci. **1**, 375.
Isichenko, M. B., and J. Kalda, 1992, "Shape effects of magnetoresistance," J. Moscow Phys. Soc. **2**, 55.
Isichenko, M. B., J. Kalda, E. B. Tatarinova, O. V. Telkovskaya, and V. V. Yankov, 1989, "Diffusion in a medium with vortex flow," Zh. Eksp. Teor. Fiz. **96**, 913 [Sov. Phys. JETP **69**, 517 (1989)].
Ising, E., 1925, "Beitrag zur Theorie des Ferromagnetismus," Z. Phys. **31**, 252.
Jensen, M. H., L. P. Kadanoff, A. Libchaber, I. Procaccia, and J. Stavans, 1985, "Global universality at the onset of chaos: results of a forced Rayleigh-Bénard experiment," Phys. Rev. Lett. **55**, 2798.
Jensen, M. H., G. Paladin, and A. Vulpiani, 1991, "Multiscaling in multifractals," Phys. Rev. Lett. **67**, 208.
Kac, V. G., 1979, "Contravariant form for infinite-dimensional Lie algebras and superalgebras," Lecture Notes in Physics Vol. 94, edited by W. Beiglböck, A. Böhm, and E. Takasugi (Springer-Verlag, Berlin), p. 441.
Kadanoff, L. P., 1978, "Lattice Coulomb gas representation of two-dimensional problems," J. Phys. A **11**, 1399.
Kadomtsev, B. B., 1959, "Magnetic traps with a 'corrugated' field," in *Plasma Physics and the Problem of Controlled Thermonuclear Reactions*, edited by M. A. Leontovich (Pergamon, New York), Vol. III, p. 340.
Kadomtsev, B. B., and O. P. Pogutse, 1979, "Electron heat conductivity of the plasma across a 'braided' magnetic field," in *Plasma Physics and Controlled Nuclear Fusion Research*, Proceedings of the 7th International Conference, Innsbruck, 1978 (IAEA, Vienna), Vol. I, p. 649.
Kalda, J., 1992, "On transport of a passive scalar in 2D turbulent flow," unpublished.
Kalugin, P. A., A. Yu, Kitaev, and L. S. Levitov, 1985, "$Al_{0.86}Mn_{0.14}$: A six-dimensional crystal," Pis'ma Zh. Eksp. Teor. Fiz. **41**, 119 [JETP Lett. **41**, 148 (1985)].
Kalugin, P. A., A. V. Sokol, and E. B. Tatarinova, 1990, "Analytical properties of the effective-diffusion coefficient in periodic flows," Europhys. Lett. **13**, 417.

Kapitulnik, A., A. Aharony, G. Deutscher, and D. Stauffer, 1984, "Self-similarity and correlations in percolation," J. Phys. A **16**, L269.

Kapitza, P. L., 1928, "The study of the specific resistance of bismuth crystals and its change in strong magnetic fields and some allied problems," Proc. R. Soc. London, Ser. A **119**, 358.

Kapitza, P. L., 1929, "The change of electrical conductivity in strong magnetic fields. Part I—Experimental results," Proc. R. Soc. London, Ser. A **123**, 292.

Kaplan, J. L., and J. A. Yorke, 1979, "Chaotic behavior of multidimensional difference equations," Lecture Notes in Mathematics Vol. 730, edited by H.-O. Peitgen and H.-O. Walther (Springer, New York), p. 204.

Keller, J., 1964, "A theorem on the conductivity of a composite material," J. Math. Phys. **5**, 548.

Keller, J., 1987, "Effective conductivity of reciprocal media, in *Random Media*, edited by G. Papanicolaou (Springer, New York), p. 183.

Kertész, J., 1986, "Extrapolation of transfer matrix data for percolation and lattice animals by the Romberg-Beleznay algorithm," J. Phys. A **19**, 599.

Kertész, J., B. K. Chakrabarti, and J. A. M. S. Duarte, 1982, "Threshold and scaling in percolation with restricted valence," J. Phys. A **15**, L13.

Kesten, H., 1982, *Percolation Theory for Mathematicians* (Birkhauser, Boston).

Kikuchi, R., 1970, "Concept of the long-range order in the percolation problem," J. Chem. Phys. **53**, 2713.

Kingsep, A. S., K. V. Chukbar, and V. V. Yankov, 1990, "Electron magnetohydrodynamics," in *Reviews of Plasma Physics*, edited by B. B. Kadomtsev (Consultants Bureau, New York), Vol. 16, p. 243.

Kirkpatrick, S., 1973, "Percolation and conduction," Rev. Mod. Phys. **45**, 574.

Kleinert, H., 1990, *Path Integrals in Quantum Mechanics, Statistics, and Polymer Physics* (World Scientific, Singapore).

Kleva, R. G., and J. F. Drake, 1984, "Stochastic $\mathbf{E}\times\mathbf{B}$ particle transport," Phys. Fluids **27**, 1686.

von Klitzing, K., 1986, "The quantized Hall effect," Rev. Mod. Phys. **58**, 519.

von Klitzing, K., G. Dorda, and M. Pepper, 1980, "New method for high-accuracy determination of the fine-structure constant based on quantized Hall resistance," Phys. Rev. Lett. **45**, 494.

Koch, D. L., and J. F. Brady, 1989, "Anomalous diffusion due to long-range velocity fluctuations in the absence of a mean flow," Phys. Fluids A **1**, 47.

Kolmogorov, A. N., 1941, "Local structure of turbulence in an incompressible viscous fluid at very high Reynolds numbers," Dokl. Akad. Nauk SSSR **30**, 299 (in Russian). Reprinted in Usp. Fiz. Nauk **93**, 476 (1967)] [Sov. Phys. Usp. **10**, 734 (1968)] and in Proc. R. Soc. London, Ser. A **434**, 9 (1991).

Kolmogorov, A. N., 1954a, "On the conservation of quasi-periodic motion for a small change in the Hamiltonian function," Dokl. Akad. Nauk SSSR **98**, 527 (in Russian).

Kolmogorov, A. N., 1954b, "The general theory of dynamical systems and classical mechanics," in *International Mathematical Congress, Vol. 1* (Elsevier, Amsterdam), p. 315.

Kolmogorov, A. N., 1958, "A new invariant for transitive dynamical systems," Dok. Akad. Nauk SSSR **119**, 861 (in Russian).

Kolmogorov, A. N., and V. M. Tikhomirov, 1959, "ε-entropy and ε-capacity of sets in a function space," Usp. Mat. Nauk **14**, 4 [Russ. Math. Surv. **17**, 277 (1961)].

Korčak, J., 1938, "Deux types fondamentaux de distribution statistique," Bull. Inst. Int. Stat. **111**, 295.

Kraichnan, R. H., 1970, "Diffusion by a random velocity field," Phys. Fluids **13**, 22.

Kraichnan, R. H., and D. Montgomery, 1980, "Two-dimensional turbulence," Rep. Prog. Phys. **43**, 547.

Kravtsov, V. E., I. V. Lerner, and V. I. Yudson, 1986, "Classical diffusion in media with weak disorder," Zh. Eksp. Teor. Fiz. **91**, 569 [Sov. Phys. JETP **64**, 336 (1986)].

Krommes, J. A., 1978, "Plasma transport in stochastic magnetic fields. II. Principles and problems of test electron transport," Prog. Theor. Phys. Suppl. **64**, 137.

Krommes, J. A., C. Oberman, and R. G. Kleva, 1983, "Plasma transport in stochastic magnetic fields. Part 3. Kinetics of test particle diffusion," J. Plasma Phys. **30**, 11.

Laidlaw, D., J. MacKay, and N. Jan, 1987, "Some fractal properties of percolating backbone in two dimensions," J. Stat. Phys. **46**, 507.

Landauer, R., 1978, "Electrical conductivity of inhomogeneous media," in *Electrical Transport and Optical Properties of Inhomogeneous Media*, edited by J. C. Garland and D. B. Tanner (AIP, New York), p. 2.

Lanford, O. E., 1981, "Strange attractors and turbulence," in *Hydrodynamic Instabilities and the Transition to Turbulence*, edited by H. L. Swinney and J. P. Gollub (Springer, New York), p. 7.

Larichev, V. D., and G. M. Reznik, 1976, "On two-dimensional solitary Rossby waves," Dokl. Akad. Nauk SSSR **231**, 1077 (in Russian).

Larsson, T. A., 1987, "Possibly exact fractal dimensions from conformal invariance," J. Phys. A **20**, L291.

Laughlin, R. B., 1981, "Quantized Hall conductivity in two dimensions," Phys. Rev. B **23**, 5632.

Lawrie, I. D., and S. Sarbach, 1984, "Theory of tricritical points," in *Phase Transitions and Critical Phenomena*, edited by C. Domb, M. S. Green, and J. L. Lebowitz (Academic, London), Vol. 9, p. 1.

Lee, S. B., 1990, "Universality of continuum percolation," Phys. Rev. B **42**, 4877.

Levine, D., and P. Steinhardt, 1984, "Quasicrystals: A new class of ordered structures," Phys. Rev. Lett. **53**, 2477.

Lévy, Y. E., and B. Souillard, 1987, "Superlocalization of electrons and waves in fractal media," Europhys. Lett. **4**, 233.

Li, P. S., and W. Strieder, 1982, "Critical exponents for conduction in a honeycomb relation site lattice," J. Phys. C **15**, L1235.

Lichtenberg, A., and M. Lieberman, 1983, *Regular and Stochastic Motion* (Springer, New York).

Lifshitz, E. M., and L. P. Pitaevskii, 1981, *Physical Kinetics* (Pergamon, New York).

Longuet-Higgins, M. S., 1957a, "The statistical analysis of a random, moving surface," Philos. Trans. R. Soc. London, Ser. A **249**, 321.

Longuet-Higgins, M. S., 1957b, "Statistical properties of an isotropic random surface," Philos. Trans. R. Soc. London, Ser. A **250**, 157.

Longuet-Higgins, M. S., 1957c, "On the velocity of the maxima in a moving wave-form," Proc. Cambridge Philos. Soc. **52**, 230.

Longuet-Higgins, M. S., 1957d, "Statistical properties of a moving wave-form," Proc. Cambridge Philos. Soc. **52**, 234.

Longuet-Higgins, M. S., 1960a, "Reflection and refraction at a random moving surface. I. Pattern and paths of specular points," J. Opt. Soc. Am. **50**, 838.

Longuet-Higgins, M. S., 1960b, "Reflection and refraction at a random moving surface. II. Number of specular points in a Gaussian surface," J. Opt. Soc. Am. **50**, 845.

Longuet-Higgins, M. S., 1960c, "Reflection and refraction at a random moving surface. III. Frequency of twinkling in a Gaussian surface," J. Opt. Soc. Am. **50**, 851.

Lorenz, E. N., 1963, "Deterministic nonperiodic flow," J. Atmos. Sci. **20**, 130.

Lubensky, T. C., and A. M. J. Tremblay, 1986, "ε-expansion of transport exponents of continuum percolating systems," Phys. Rev. B **34**, 3408.

Ma, S.-K., 1976, *Modern Theory of Critical Phenomena* (Benjamin, London).

Machta, J., 1988, "Comment on the conductivity exponent in continuum percolation," Phys. Rev. B **37**, 7892.

Machta, J., R. A. Guyer, and S. M. Moore, 1986, "Conductivity in percolation networks with broad distributions of resistances," Phys. Rev. B **33**, 4818.

MacKay, G., and N. Jan, 1984, "Forest fires as critical phenomena," J. Phys. A **17**, L757.

Mandelbrot, B. B., 1967, "How long is the coast of Britain? Statistical self-similarity and fractional dimension," Science **155**, 636.

Mandelbrot, B. B., 1975a, *Les objects fractal: forme, hasarde et dimension* (Flammarion, Paris).

Mandelbrot, B. B., 1975b, "Stochastic models for the Earth's relief, the shape and the fractal dimension of the coastlines, and the number-area rule for islands," Proc. Natl. Acad. Sci. U.S.A. **72**, 3825.

Mandelbrot, B. B., 1975c, "On the geometry of homogeneous turbulence, with stress on the fractal dimension of the iso-sets of scalars," J. Fluid Mech. **72**, 401.

Mandelbrot, B. B., 1977, *Fractals: Form, Chance, and Dimension* (Freeman, San Francisco).

Mandelbrot, B. B., 1982, 1983, *The Fractal Geometry of Nature* (Freeman, San Francisco).

Mandelbrot, B. B., 1984, "Fractals in physics: squig clusters, diffusions, fractal measures, and the unicity of fractal dimensionality," J. Stat. Phys. **34**, 895.

Mandelbrot, B. B., 1985, "Self-affine fractals and fractal dimension," Phys. Scr. **32**, 257.

Mandelbrot, B. B., 1990, "New 'anomalous' multiplicative multifractals: left sided $F(\alpha)$ and the modelling of DLA," Physica A **168**, 95.

Mandelbrot, B. B., 1991, "Random multifractals: negative dimensions and the resulting limitations of the thermodynamic formalism," Proc. R. Soc. London, Ser. A **434**, 79.

Mandelbrot, B. B., and J. A. Given, 1984, "Physical properties of a new fractal model of percolation clusters," Phys. Rev. Lett. **52**, 1853.

Mandelbrot, B. B., and J. W. Van Ness, 1968, "Fractional Brownian motion, fractional noises and applications," SIAM Rev. **10**, 422.

Margolina, A., H. J. Herrmann, and D. Stauffer, 1982, "Size of largest and second largest cluster in random percolation," Phys. Lett. A **93**, 73.

Martin, J. L., 1974, "Computer techniques for evaluating lattice constants," in *Phase Transitions and Critical Phenomena*, edited by C. Domb, M. S. Green, and J. L. Lebowitz (Academic, London), Vol. 3, p. 97.

Martin, P. C., E. D. Siggia, and H. A. Rose, 1973, "Statistical dynamics of classical systems," Phys. Rev. A **8**, 423.

Maxwell, J. C., 1873, *A Treatise on Electricity and Magnetism* (Reprint: Dover, New York, 1954).

McLaughlin, D., G. C. Papanicolaou, and O. Pironneau, 1985, "Convection of microstructure and related problems," SIAM J. Appl. Math. **45**, 780.

Meakin, P., and F. Family, 1986, "Diverging length scales in diffusion-limited aggregation," Phys. Rev. A **34**, 2558.

Mehr, R., and A. Aharony, 1988, "Fractal geometry of electron orbits in random systems with strong magnetic field," Phys. Rev. B **37**, 6349.

Milton, G. W., 1982, "Bounds on the complex permittivity of a two-component composite material," J. Appl. Phys. **52**, 5286.

Mitescu, C. D., M. Allain, E. Guyon, and J. P. Clerc, 1982, "Electrical conductivity of finite-size percolation networks," J. Phys. A **15**, 2523.

Moffatt, H. K., 1981, "Some developments in the theory of turbulence," J. Fluid Mech. **106**, 27.

Moffatt, H. K., 1983, "Transport effects associated with turbulence with particular attention to the influence of helicity," Rep. Prog. Phys. **46**, 621.

Monin, A. S., and A. M. Yaglom, 1971, 1975, *Statistical Fluid Mechanics of Turbulence* (MIT, Cambridge, MA), Vols. I and II.

Montroll, E. W., and H. Scher, 1973, "Random walks on lattices. IV. Continuous-time walks and influence of absorbing boundaries," J. Stat. Phys. **9**, 101.

Mori, H., 1980, "Fractal dimensions of chaotic flows of autonomous dissipative systems," Prog. Theor. Phys. **63**, 1044.

Moser, J., 1962, "Perturbation theory for quasiperiodic solutions of differential equations," Nachr. Akad. Wiss. Göttingen Math. Phys. Kl 2 **1**, 15 [also published in *Bifurcation Theory and Nonlinear Eigenvalue Problem*, edited by J. B. Keller and S. Antman (Benjamin, New York, 1969)].

Moser, J., 1967, "Convergent series expansions of quasiperiodic motions," Math. Ann. **169**, 163.

Murat, M., S. Marianer, and D. J. Bergman, 1986, "A transfer matrix study of conductivity and permeability exponents in continuum percolation," J. Phys. A **19**, L275.

Murzin, S. S., 1988, "Conductivity of metals and semiconductors with defects with long- and short-range potentials in a magnetic field," Pis'ma Zh. Eksp. Teor. Fiz. **39**, 567 [JETP Lett. **39**, 695 (1984)].

Nagatani, T., 1986, "A Monte Carlo renormalization approach to fractal dimensions of infinite clusters, backbone, and cutting bonds for percolation," J. Phys. A **19**, L275.

Nakanishi, H., and P. J. Reynolds, 1979, "Site-bond percolation by position-space renormalization group," Phys. Lett. A **71**, 252.

Neishtadt, A. I., 1986, "Change of an adiabatic invariant at a separatrix," Fiz. Plazmy **12**, 992 [Sov. J. Plasma Phys. **12**, 568 (1986)].

Neishtadt, A. I., 1991, "Probability phenomena due to separatrix crossing," Chaos **1**, 42.

Newman, C. M., and L. S. Schulman, 1981, "Number and density of percolation clusters," J. Phys. A **14**, 1735.

Nicopoulos, V. N., and S. A. Trugman, 1990, "Complex quantum scattering and the breakdown of the quantum Hall effect," Phys. Rev. Lett. **65**, 779.

Nienhuis, B., 1982, "Exact critical point and critical exponents of $O(n)$ models in two dimensions," Phys. Rev. Lett. **49**, 1062.

Nienhuis, B., 1984, "Critical behavior of two-dimensional spin models and charge asymmetry in the Coulomb gas," J. Stat. Phys. **34**, 731.

Nienhuis, B., A. N. Berker, E. K. Riedel, and M. Schick, 1979, "First- and second-order phase transitions in Potts models: Renormalization-group solutions," Phys. Rev. Lett. **43**, 737.

Nycander, J., and M. B. Isichenko, 1990, "Motion of dipole vortices in a weakly inhomogeneous medium and related convective transport," Phys. Fluids B **2**, 2042.

Obukhov, A. M., 1941, "On the distribution of energy in the spectrum of turbulent flow," Izv. Akad. Nauk SSSR Ser. Geogr. Geofiz. **5**, 453 [C. R. Acad. Sci. U.R.S.S. **32**, 19 (1941)].

Onizuka, K., 1975, "Computer experiment on a 3D site percolation model of porous material—its connectivity and conductivity," J. Phys. Soc. Jpn. **39**, 527.

Onsager, L., 1944, "Crystal statistics. I. A two-dimensional model with an order-disorder transition," Phys. Rev. **65**, 117.

Orbach, R., 1984, "Dynamics of fractal structures," J. Stat. Phys. **34**, 735.

Orey, S., 1970, "Gaussian sample functions and the Hausdorff dimension of level crossings," Z. Wahrscheinlichkeitstheorie Verw. Geb. **15**, 249.

Osborne, A. R., and R. Caponio, 1990, "Fractal trajectories and anomalous diffusion for chaotic particle motions in 2D turbulence," Phys. Rev. Lett. **64**, 1733.

Osborne, A. R., A. D. Kirwan, Jr., A. Provenzale, and L. Bergamasco, 1986, "A search for chaotic behavior in large and mesoscale motions in the Pacific Ocean," Physica D **23**, 75.

Oseledec, V. I., 1968, "A multiplicative theorem. Lyapunov characteristic numbers for dynamical systems," Tr. Mosk. Mat. Obshch. **19**, 179 [Moscow Math. Soc. **19**, 197 (1968)].

O'Shaughnessy, B., and I. Procaccia, 1985a, "Analytical solutions for diffusion on fractal sets," Phys. Rev. Lett. **54**, 455.

O'Shaughnessy, B., and I. Procaccia, 1985b, "Diffusion on fractals," Phys. Rev. A **32**, 3073.

Osipenko, M. V., O. P. Pogutse, and N. V. Chudin, 1987, "Plasma diffusion in an array of vortices," Fiz. Plazmy **13**, 953 [Sov. J. Plasma Phys. **13**, 550 (1987)].

Ott, E., 1981, "Strange attractors and chaotic motions of dynamical systems," Rev. Mod. Phys. **53**, 655.

Ott, E., and T. M. Antonsen, 1988, "Chaotic fluid convection and the fractal nature of passive scalar gradients," Phys. Rev. Lett. **61**, 2839.

Ott, E., and T. M. Antonsen, 1989, "Fractal measures of passively convected vector fields and scalar gradients in chaotic fluid flows," Phys. Rev. A **39**, 3660.

Ottaviani, M., 1992, "Scaling laws of test particle transport in two-dimensional turbulence," Europhys. Lett., in press.

Ottino, J. M., 1989, *The Kinematics of Mixing: Stretching, Chaos, and Transport* (Cambridge University, Cambridge, England).

Paladin, G., and A. Vulpiani, 1987, "Anomalous scaling laws in multifractal objects," Phys. Rep. **156**, 147.

Pearson, R. B., 1980, "Conjecture for the extended Potts model magnetic eigenvalue," Phys. Rev. B **22**, 2579.

Peitgen, H.-O., and D. Saupe, 1988, Eds., *The Science of Fractal Images* (Springer, Berlin).

Penrose, O., J. L. Lebowitz, J. Marro, M. H. Kalos, and A. Sur, 1978, "Growth of clusters in a first-order phase transition," J. Stat. Phys. **19**, 243.

Perkins, F. W., and E. G. Zweibel, 1987, "A high magnetic Reynolds number dynamo," Phys. Fluids **30**, 1079.

Pettini, M., A. Vulpiani, J. H. Misguich, M. De Leener, J. Orban, and R. Balescu, 1988, "Chaotic diffusion across a magnetic field in a model of electrostatic turbulent plasma," Phys. Rev. A **38**, 344.

Petviashvili, V. I., and V. V. Yankov, 1989, "Solitons and turbulence," in *Reviews of Plasma Physics*, edited by B. B. Kadomtsev (Consultants Bureau, New York), Vol. 14, p. 1.

Pietronero, L., and E. Tosatti, 1986, Eds., *Fractals in Physics* (North-Holland, Amsterdam).

Pike, G. E., and C. H. Seager, 1984, "Percolation and conductivity: A computer study, I," Phys. Rev. B **10**, 1421.

Pike, R., and H. E. Stanley, 1981, "Order propagation near the percolation threshold," J. Phys. A **14**, L169.

Pippard, A. B., 1969, *Magnetoresistance in Metals* (Cambridge University, New York).

Polyakov, A. M., 1970, "Conformal symmetry of critical fluctuations," Pis'ma Zh. Eksp. Teor. Fiz. **12**, 538 [JETP Lett. **12**, 381 (1970)].

Polyakov, D. G., 1986, "Change, due to scattering-act correlation, of electron diffusion in a classically strong magnetic field," Zh. Eksp. Teor. Fiz. **90**, 546 [Sov. Phys. JETP **63**, 317 (1986)].

Pomeau, Y., A. Pumir, and W. R. Young, 1988, "Transitoires dans l'advection-diffusion d'impuretes," C. R. Acad. Sci. (Paris) **306 II**, 741.

Poston, T., and I. Stewart, 1978, *Catastrophe Theory and Its Applications* (Pitman, London).

Potts, R. B., 1952, "Some generalized order-disorder transformations," Proc. Cambridge Philos. Soc. **48**, 106.

Prange, R. E., 1990, "Effects of imperfections and disorder," in *The Quantum Hall Effect,* edited by R. E. Prange and S. M. Girvin (Springer, New York).

Prange, R. E., and S. M. Girvin, 1990, Eds., *The Quantum Hall Effect* (Springer, New York).

Procaccia, I., 1984, "Fractal structures in turbulence," J. Stat. Phys. **36**, 649.

Quinn, G. P., G. H. Bishop, and R. J. Harrison, 1976, "On the cluster size distribution for critical percolation," J. Phys. A **9**, L9.

Rammal, R., 1984, "Random walk statistics on fractal structures," J. Stat. Phys. **34**, 547.

Ramshankar, R., D. Berlin, and J. P. Gollub, 1990, "Transport by capillary waves. Part I. Particle trajectories," Phys. Fluids A **2**, 1955.

Ramshankar, R., and J. P. Gollub, 1991, "Transport by capillary waves. Part II. Scalar dispersion and structure of the concentration field," Phys. Fluids A **3**, 1344.

Rechester, A. B., and M. N. Rosenbluth, 1978, "Electron heat transport in a tokamak with destroyed magnetic surfaces," Phys. Rev. Lett. **40**, 38.

Rechester, A. B., M. N. Rosenbluth, and R. B. White, 1979, "Calculation of the Kolmogorov entropy for motion along a stochastic magnetic field," Phys. Rev. Lett. **42**, 1247.

Redner, S., 1989, "Superdiffusion transport due to random velocity fields," Physica D **38**, 287.

Reich, G. R., and P. L. Leath, 1978, "The ramification of large clusters near percolation threshold," J. Phys. C **11**, 1155.

Rendell, R. W., and S. M. Girvin, 1981, "Hall voltage dependence on inversion-layer geometry in the quantum Hall-effect regime," Phys. Rev. B **23**, 6610.

Rice, S. D., 1944, "Mathematical analysis of random noise," Bell Syst. Tech. J. **23**, 282; **24**, 46.

Richardson, L. F., 1926, "Atmosphere diffusion shown on a distance-neighbour graph," Proc. R. Soc. London, Ser. A **110**, 709.

Rose, H. A., and P.-L. Sulem, 1978, "Fully developed turbulence and statistical mechanics," J. Phys. (Paris) **39**, 441.

Rosenbluth, M. N., H. L. Berk, I. Doxas, and W. Horton, 1987, "Effective diffusion in laminar convective flows," Phys. Fluids **30**, 2636.

Rosenbluth, M. N., R. Z. Sagdeev, J. B. Taylor, and G. M. Zaslavsky, 1966, "Destruction of magnetic surfaces by magnet-

ic field irregularities," Nucl. Fusion **6**, 297.
Ross, B., 1975, Ed., *Fractional Calculus and Its Applications*, Lecture Notes in Mathematics No. 457 (Springer-Verlag, Berlin).
Ruelle, D., 1989, *Chaotic Evolution and Strange Attractors: The Statistical Analysis of Time Series for Deterministic Nonlinear Systems* (Cambridge University, Cambridge, England).
Ruelle, D., and F. Takens, 1971, "On the nature of turbulence," Commun. Math. Phys. **20**, 167.
Safran, S. A., I. Webman, and G. S. Grest, 1985, "Percolation in interacting colloids," Phys. Rev. A **32**, 506.
Sagdeev, R. Z., D. A. Usikov, and G. M. Zaslavsky, 1988, *Nonlinear Physics: From Pendulum to Turbulence and Chaos* (Harwood, New York).
Sahimi, M., 1987, "Hydrodynamic dispersion near the percolation threshold: scaling and probability densities," J. Phys. A **20**, L1293.
Saleur, H., 1987, "Conformal invariance for polymers and percolation," J. Phys. A **20**, 457.
Saleur, H., and B. Duplantier, 1987, "Exact determination of the percolation hull exponent in two dimensions," Phys. Rev. Lett. **58**, 2325.
Sapoval, B., M. Rosso, and J. F. Gouyet, 1985, "The fractal nature of a diffusion front and the relation to percolation," J. Phys. Lett. **46**, L149.
Scher, H., and R. Zallen, 1970, "Critical density in percolation processes," J. Chem. Phys. **53**, 3759.
Schulgasser, K., 1976, "On a phase interchange relationship for composite materials," J. Math. Phys. **17**, 378.
Schulgasser, K., 1983, "Sphere assemblage model for polycrystals and symmetric materials," J. Appl. Phys. **54**, 1380.
Schwägerl, M., and J. Krug, 1991, "Subdiffusive transport in stochastic webs," Physica D **52**, 143.
Seager, C. H., and G. E. Pike, 1974, "Percolation and conductivity: A computer study. II," Phys. Rev. B **10**, 1435.
Sen, P. N., J. N. Roberts, and B. I. Halperin, 1984, "Nonuniversal critical exponents for transport in percolating systems with a distribution of bond strengths," Phys. Rev. B **32**, 3306.
Shante, V. K. S., and S. Kirkpatrick, 1971, "An introduction to percolation theory," Adv. Phys. **20**, 325.
Shapiro, B., 1979, "Real-space renormalization in the percolation problem," J. Phys. C **12**, 3185.
Shklovskii, B. I., and A. L. Efros, 1984, *Electronic Properties of Doped Semiconductors* (Springer, New York).
Shlesinger, M. F., B. J. West, and J. Klafter, 1987, "Lévi dynamics of enhanced diffusion: Application to turbulence," Phys. Rev. Lett. **58**, 1100.
Shraiman, B., 1987, "Diffusive transport in a Rayleigh-Bénard convection cell," Phys. Rev. A **36**, 261.
Sinai, Ya. G., 1970, "Dynamical systems with elastic reflections," Russ. Math. Survey **25**, 137.
Skal, A. S., and B. I. Shklovskii, 1973, "Influence of impurity concentration on the hopping conduction in semiconductors," Fiz. Tekh. Poluprovodn. **7**, 1589 [Sov. Phys. Semicond. **7**, 1058 (1973)].
Skal, A. S., and B. I. Shklovskii, 1974, "Topology of an infinite cluster in the theory of percolation and its relation to the theory of hopping conduction," Fiz. Tekh. Poluprovodn. **8**, 1586 [Sov. Phys. Semicond. **8**, 1029 (1975)].
Skal, A. S., B. I. Shklovskii, and A. L. Efros, 1973, "Percolation level in a three-dimensional random potential," Pis'ma Zh. Eksp. Teor. Fiz. **17**, 522 [JETP Lett. **17**, 377 (1973)].
Smith, L. N., and C. J. Lobb, 1979, "Percolation in two-dimensional conductor-insulator networks with controllable anisotropy," Phys. Rev. B **20**, 3653.
Sokolov, I. M., 1986, "Dimensionalities and other geometric critical exponents in percolation theory," Usp. Fiz. Nauk **150**, 221 [Sov. Phys. Usp. **29**, 924 (1986)].
Solomon, T. H., and J. P. Gollub, 1988, "Passive transport in steady Rayleigh-Bénard convection," Phys. Fluids **31**, 1372.
Soward, A. M., 1987, "Fast dynamo action in a steady flow," J. Fluid Mech. **180**, 267.
Sreenivasan, K. R., and C. Meneveau, 1986, "The fractal facets of turbulence," Physica D **38**, 322.
Sreenivasan, K. R., and R. R. Prasad, 1989, "New results on the fractal and multifractal structure of the large Schmidt number passive scalars in fully turbulent flows," Physica D **38**, 322.
Sreenivasan, K. R., R. Ramshankar, and C. Meneveau, 1989, "Mixing, entrainment, and fractal dimensions of surfaces in turbulent flows," Proc. R. Soc. London, Ser. A **421**, 79.
Stachowiak, H., 1978, "Calculation of the magnetoresistance of polycrystalline metals," in *Electrical Transport and Optical Properties of Inhomogeneous Media*, edited by J. C. Garland and D. B. Tanner (AIP, New York), p. 156.
Stanley, H. E., 1968, "Dependence of critical properties on dimensionality of spins," Phys. Rev. Lett. **20**, 589.
Stanley, H.E., 1977, "Cluster shapes at the percolation threshold: an effective cluster dimensionality and its connection with critical-point exponents," J. Phys. A **10**, L211.
Stanley, H. E., 1984, "Application of fractal concepts to polymer statistics and to anomalous transport in randomly porous media," J. Stat. Phys. **34**, 843.
Stanley, H. E., and N. Ostrowsky, 1986, Eds., *On Growth and Form* (Martinus Nijhoff, Boston).
Stauffer, D., 1979, "Scaling theory of percolation clusters," Phys. Rep. **54**, 2.
Stauffer, D., 1985, *Introduction to Percolation Theory* (Taylor and Francis, London).
Steinhardt, P., and S. Ostlund, 1987, Eds., *The Physics of Quasicrystals* (World Scientific, Singapore).
Stiassnie, M., Y. Agnon, and L. Shemer, 1991, "Fractal dimensions of random water surfaces," Physica D **47**, 341.
Straley, J. P., 1977, "Critical exponents for the conductivity of random resistor lattices," Phys. Rev. B **15**, 5733.
Strenski, P. N., R. M. Bradley, and J.-M. Debierre, 1991, "Scaling behavior of percolation surfaces in three dimensions," Phys. Rev. Lett. **66**, 1330.
Suzuki, M., 1983, "Phase transition and fractals" Prog. Theor. Phys. **69**, 65.
Swerling, P., 1962, "Statistical properties of the contours of random surfaces," IRE Trans. Inf. Theory **IT-8**, 315.
Swinney, H., and W. Y. Tam, 1987, "Mass transport in turbulent Couette-Taylor flow," Phys. Rev. A **36**, 1374.
Sykes, M. F., and J. W. Essam, 1963, "Some exact critical percolation probabilities for bond and site problems in two dimensions," Phys. Rev. Lett. **10**, 3.
Sykes, M. F., and J. W. Essam, 1964a, "Critical probabilities by series methods," Phys. Rev. A **133**, 310.
Sykes, M. F., and J. W. Essam, 1964b, "Exact critical percolation probabilities for site and bond problems in two dimensions," J. Math. Phys. **5**, 1117.
Sykes, M. F., D. S. Gaunt, and M. Glen, 1976a, "Percolation process in two dimensions II. Critical concentrations and the mean size index," J. Phys. A **9**, 97.
Sykes, M. F., D. S. Gaunt, and M. Glen, 1976b, "Percolation process in two dimensions III. High density series expansions," J. Phys. A **9**, 715.
Sykes, M. F., D. S. Gaunt, and M. Glen, 1976c, "Percolation

process in two dimensions IV. Percolation probability," J. Phys. A **9**, 725.
Sykes, M. F., and M. Glen, 1976, "Percolation process in two dimensions I. Low-density series expansion," J. Phys. A **9**, 87.
Tatarinova, E. B., 1990, "Conductivity of a two-dimensional, two-phase system with the Hall effect," unpublished.
Tatarinova, E. B., P. A. Kalugin, and A. V. Sokol, 1991, "What is the propagation rate of the passive component in turbulent flows limited by?" Europhys. Lett. **14**, 773.
Taylor, G. I., 1921, "Diffusion by continuous movements," Proc. London Math. Soc., Ser. 2, **20**, 196.
Taylor, G. I., 1953, "Dispersion of soluble matter in solvent flowing slowly through a tube," Proc. R. Soc. London, Ser. A **219**, 186.
Taylor, G. I., 1954, "Conditions under which dispersion of solute in a stream of solvent can be used to measure molecular diffusion," Proc. R. Soc. London, Ser. A **225**, 473.
Taylor, S. J., 1955, "The α-dimensional measure of the graph and set of zeros of a Brownian path," Proc. Cambridge Philos. Soc. **51**, II, 265.
Tennyson, J. L., J. R. Cary, and D. F. Escande, 1986a, "Change of the adiabatic invariant due to separatrix crossing," Phys. Rev. Lett. **56**, 2117.
Tennyson, J. L., J. R. Cary, and D. F. Escande, 1986b, "Adiabatic invariant change due to separatrix crossing," Phys. Rev. A **34**, 4526.
Thompson, A. H., A. J. Katz, and C. E. Krohn, 1987, "The microgeometry and transport properties of sedimentary rock," Adv. Phys. **36**, 625.
Thouless, D. J., 1974, "Electrons in disordered systems and the theory of localization," Phys. Rep. **13**, 93.
Trugman, S. A., 1983, "Percolation, localization, and quantum Hall effect," Phys. Rev. B **27**, 7539.
Trugman, S. A., 1986, "General theory of inhomogeneous systems, based on maximum entropy," Phys. Rev. Lett. **57**, 607.
Trugman, S. A., 1989, "Complex classical and quantum scattering dynamics and the quantum Hall effect," Phys. Rev. Lett. **62**, 579.
Trugman, S. A., and S. Doniach, 1982, "Vortex dynamics in inhomogeneous superconducting films," Phys. Rev. B **26**, 3682.
Trugman, S. A., and V. N. Nicopolous, 1992, "Complex dynamics of the integer quantum Hall integer," in *Physical Phenomena at High Magnetic Fields*, edited by E. Manousakis *et al.* (Addison-Wesley, New York).
Trugman, S. A., and A. Weinrib, 1985, "Percolation with a threshold at zero: A new universality class," Phys. Rev. B **31**, 2794.
Városi, F., T. M. Antonsen, and E. Ott, 1991, "The spectrum of fractal dimensions of passively convected scalar gradients in chaotic fluid flows," Phys. Fluids A **3**, 1017.
Vassilicos, J. C., and J. C. R. Hunt, 1991, "Fractal dimensions and spectra of interfaces with application to turbulence," Proc. R. Soc. London, Ser. A **435**, 505.
Vicsek, T., and J. Kertész, 1981, "Monte Carlo renormalization-group approach to percolation on a continuum: test of universality," J. Phys. A **14**, L31.
Voss, R. F., 1984, "The fractal dimension of percolation cluster hulls," J. Phys. A **17**, L373.
Voss, R. F., 1989, "Random fractals: self-affinity in noise, music, mountains, and clouds," Physica D **38**, 362.
Vulpiani, A., 1989, "Lagrangian chaos and small-scale structure of passive scalars," Physica D **38**, 372.
Webman, I., J. Jortner, and M. H. Cohen, 1976, "Numerical simulation of continuous percolation conductivity," Phys. Rev. B **14**, 4737.
Weinrib, A., 1982, "Percolation threshold of a two-dimensional continuum system," Phys. Rev. B **26**, 1352.
Weinrib, A., 1984, "Long-range correlated percolation," Phys. Rev. B **29**, 387.
Weinrib, A., and B. I. Halperin, 1982, "Distribution of maxima, minima, and saddle points of the intensity of laser speckle patterns," Phys. Rev. B **26**, 1362.
Weinrib, A., and B. I. Halperin, 1983, "Critical phenomena in systems with long-range correlated quenched disorder," Phys. Rev. B **27**, 413.
Weinrib, A., and S. Trugman, 1985, "A new kinetic walk and percolation perimeter," Phys. Rev. B **31**, 2993.
White, R. B., 1989, *Theory of Tokamak Plasmas* (North-Holland, Amsterdam).
Wilson, K. G., 1971a, "Renormalization group and critical phenomena. I. Renormalization group and Kadanoff scaling picture," Phys. Rev. B **4**, 3174.
Wilson, K. G., 1971b, "Renormalization group and critical phenomena. II. Phase-space cell analysis of critical behavior," Phys. Rev. B **4**, 3184.
Wilson, K. G., 1975, "The renormalization group: critical phenomena and the Kondo problem," Rev. Mod. Phys. **47**, 773.
Yoon, C. S., and S.-I. Lee, 1990, "Measurements of the ac conductivity and dielectric constant in a two-dimensional percolation system," Phys. Rev. B **42**, 4594.
Young, L.-S., 1982, "Dimension, entropy and Lyapunov exponents," Ergodic Theory and Dyn. Syst. **2**, 109.
Young, L.-S., 1984, "Dimension, entropy and Lyapunov exponents of differentiable dynamical systems," Physica A **124**, 639.
Young, W. R., 1988, "Arrested shear dispersion and other models of anomalous diffusion," J. Fluid Mech. **193**, 129.
Young, W. R., and S. Jones, 1991, "Shear dispersion," Phys. Fluids A **3**, 1087.
Young, W. R., A. Pumir, and Y. Pomeau, 1989, "Anomalous diffusion of tracer in convection rolls," Phys. Fluids A **1**, 462.
Yushmanov, P. N., 1990a, "Diffusive transport processes caused by ripple in tokamaks," in *Reviews of Plasma Physics*, edited by B. B. Kadomtsev (Consultants Bureau, New York), Vol. 16, p. 117.
Yushmanov, P. N., 1990b, "Two-dimensional diffusion in a shear system," Pis'ma Zh. Eksp. Teor. Fiz. **52**, 848 [JETP Lett. **52**, 217 (1990)].
Yushmanov, P. N., 1992, "Neoclassical diffusion in a turbulent plasma," Comments Plasma Phys. Controlled Fusion **14**, 313.
Zabusky, N. J., and J. C. McWilliams, 1982, "A modulated point-vortex model for geostrophic, β-plane dynamics," Phys. Fluids **25**, 2175.
Zakharov, V. E., 1984, "Kolmogorov spectra of weak turbulence," in *Basic Plasma Physics*, edited by A. A. Galeev and R. N. Sudan (North-Holland, New York), Vol. II, p. 3.
Zallen, R., 1983, *The Physics of Amorphous Solids* (Wiley, New York).
Zallen, R., and H. Scher, 1971, "Percolation on a continuum and the localization-delocalization transition in amorphous semiconductors," Phys. Rev. B **4**, 4471.
Zaslavsky, G. M., 1991a, "Stochastic webs and their applications," Chaos **1**, 1.
Zaslavsky, G. M., 1991b, "Lagrangian turbulence and anomalous transport," Fluid Dyn. Res. **8**, 127.
Zaslavsky, G. M., 1992, "Anomalous transport and fractal kinetics," in *Topological Aspects of the Dynamics of Fluids and Plasmas*, edited by H. K. Moffatt, G. M. Zaslavsky, *et al.*

(Kluwer, Netherlands), in press.
Zaslavsky, G. M., R. Z. Sagdeev, and A. A. Chernikov, 1988, "Stochastic nature of streamlines in steady-state flows," Zh. Eksp. Teor. Fiz. **94**, 102 [Sov. Phys. JETP **67**, 270 (1988)].
Zeilinger, A., and K. Svozil, 1985, "Measuring the dimension of space-time," Phys. Rev. Lett. **54**, 2553.
Zeldovich, Ya. B., 1937, "Limiting laws for free upwelling convective flows," Dokl. Akad. Nauk SSSR **7**, 1466 (in Russian).
Zeldovich, Ya. B., 1982, "Exact solution of the problem of diffusion in a periodic velocity field, and turbulent diffusion," Dokl. Akad. Nauk SSSR **266**, 821 [Sov. Phys. Dokl. **27**, 797 (1982)].
Zeldovich, Ya. B., 1983, "Percolation properties of a random two-dimensional stationary magnetic field," Pis'ma Zh. Eksp. Teor. Fiz. **38**, 51 [JETP Lett. **38**, 57 (1983)].
Ziff, R. M., 1986, "Test of scaling exponents for percolation-cluster perimeters," Phys. Rev. Lett. **56**, 545.
Ziff, R. M., 1989, "Hull-generating walks," Physica D **38**, 377.
Ziff, R. M., P. T. Cummings, and G. Stell, 1984, "Generation of percolation cluster perimeters by a random walk," J. Phys. A **17**, 3009.
Ziff, R. M., and B. Sapoval, 1987, "The efficient determination of the percolation threshold by a frontier-generating walk in a gradient," J. Phys. A **19**, L1169.
Ziman, J. M., 1969, "The localization of electrons in ordered and disordered systems, I. Percolation of classical particles," J. Phys. C **1**, 1532.
Ziman, J. M., 1979, *Models of Disorder* (Cambridge University, New York).